LICENTIATE THESIS

Prefabricated Composite Bridges

- a Study of Dry Deck Joints

Robert Hällmark

LULEÅ UNIVERSITY OF TECHNOLOGY

LULEÅ
UNIVERSITY
OF TECHNOLOGY

Licentiate Thesis

Prefabricated Composite Bridges

- a Study of Dry Deck Joints

Robert Hällmark

Luleå University of Technology
Department of Civil, Mining and Natural Resources Engineering
Division of Structural and Construction Engineering
SE-971 87 Luleå
Sweden

Printed by Universitetstryckeriet, Luleå 2012

ISSN: 1402-1757
ISBN 978-91-7439-474-0

Luleå 2012

www.ltu.se

"Imagination is more important than knowledge"

(A.E. 1929)

Prefabricated Composite Bridges – a Study of Dry Deck Joints

Robert Hällmark
Avdelningen för byggkonstruktion och produktion

Institutionen för samhällsbyggnad och naturresurser

Akademisk avhandling

som med vederbörligt tillstånd av Tekniska fakultetsnämnden vid Luleå tekniska universitet för avläggande av teknologie licentiatexamen kommer att offentligt försvaras:

Sal F1031, Luleå tekniska universitet
Måndag den 24 september 2012, 14.00

Diskutant: Professor Ian May, Herriot-Watt University, Edinburgh, Scotland

Huvudhandledare:
Professor Peter Collin, Byggkonstruktion och produktion, Konstruktionsteknik, Luleå Tekniska Universitet

Biträdande handledare:
Professor Milan Veljkovic, Byggkonstruktion och produktion, Stålbyggnad, Luleå Tekniska Universitet
Lektor Martin Nilsson, Byggkonstruktion och produktion, Konstruktionsteknik, Luleå Tekniska Universitet

Front page: The picture shows the test specimen used in the large-scale tests of a composite bridge with prefabricated deck elements at LTU in year 2011.

Preface

The academic world and the real world are sometimes a bit contradictive, but they both share the very nice quality to always provide new paths and winding roads to explore and races to run. After a long a winding road, and moments of inspiration as well as perspiration, the Licentiate degree is now looming in the distance. But even if this voyage of discovery soon has come to an end, other journeys are waiting just behind the corner, and I hope that I am far from finished with my journey as a bridge designer, researcher and a human being.

I would like to take the opportunity to thank the people and who made this work come true.

First, I would like to thank my supervisor Peter Collin, for giving me the opportunity to perform this research at Luleå University of Technology and Ramböll. Your help, guidance and support have been very valuable to me.

I would also like to thank all my colleagues at the Bridge Department at Ramböll Luleå. You have all filled my working days with laughter and joy. Special thanks also to Ph.D. Martin Nilsson at LTU, Ph.D. Mikael Hallgren at KTH and the project partners within the ELEM-project, who all have contributed to the research within this thesis. The Complab staff also deserve a big thanks for their work and for their friendly reception.

I am also grateful for the financial support from the European research programme *RFCS* and the *Swedish Construction Industry´s Organisation for Research and Development* (*SBUF*). My employer, *Ramböll*, has also supported me both economically and by giving me time and space to dig a little bit deeper in the field of composite bridges.

Finally, greatest thanks to my family and friends for their support, help and belief in me. The list will be endless if I try to name each and every one of you that fill my life with joy and fruitful discussions. Some of you have spent

a lot of time listen to my thoughts and problems concerning this thesis and the everyday work. Lars, at this point after endless of hours in the ski- and running-tracks with me, you can surely apply for a job as a professional advisor. Thanks for the support! Thanks also to JJ who always make my world look a bit brighter, by painting the rest of the world in the darkest colours in a way that only Finns can.

Last but definitely not least, I would like to thank my beloved Alexandra for all the love, patience and support you have given me through the years. You are the best!

Luleå, August 2012

Robert Hällmark

Abstract

This thesis deals with prefabricated composite bridges in general, and prefabricated concrete deck elements with dry joints in particular.

As outlined in Paper I and Chapter 2 prefabrication has several advantages over in situ construction, and has hence been discussed for decades in the construction business. Further, the house building sector has taken large steps towards a more industrialized approach, in which prefabrication, lean thinking and Building Information Modelling (BIM) are all important components. Numerous studies have also examined the applicability of such an approach in the bridge sector, and several types of prefabrication techniques have been tested. Nevertheless, in many countries the bridge sector seems to lag far behind in the general shift towards more industrialized construction processes. One of the reasons for the relatively slow progress may be the fact that bridges are often unique objects with unique specifications and constraints. This hinders the standardisation that is often regarded as a key to industrialised construction.

Chapter 2-3 and Paper I, presents evidence from a literature review together with information gathered from a Workshop, attended by bridge designers and researcher in Europe and the US, that prefabricated deck elements are still quite rarely used in bridge construction. Deck elements with dry transverse joints are even rarer. Few examples have been reported. In addition, the degree of prefabrication and the rate of progress towards more industrialised construction processes seem to vary substantially from one country to another.

However, as described in Chapter 3 and Paper II, a prefabricated concrete deck element system with dry joints has been developed in Sweden for constructing composite bridges. The transverse joints are completely dry, and all forces are transferred by contact pressure between concrete surfaces. This implies that no tensional forces can be transferred over the transverse joints. Shear forces are transferred by overlapping concrete shear keys, designed as a series of male-female connections. The research presented in

this thesis is focused on the structural behaviour of this deck element system. In order to investigate this, laboratory tests have been performed as well as field monitoring.

Results of large-scale laboratory tests, presented in Chapter 4 and Paper V, show that a bridge of this type is less stiff than a similar bridge with an in-situ cast deck slab. The concrete elements' contributions to stiffness are negligible in sections with hogging moments, but make some contribution to global stiffness in sections with sagging moments. At moderate load levels, the interacting concrete area is much smaller than in a similar in-situ cast section. This is believed to be due to the combined effects of small gaps in the joints and continuous in-situ cast concrete in the injection channels. After the channels have been injected, existing gaps will be more or less permanent, since the in-situ cast concrete must be compressed up to a certain limit before the rest of the joint will be closed. Destructive testing showed that the differences in stiffness and stresses between a deck of this type and an in-situ cast bridge deck are much smaller in the ultimate limit state. In this case it could even be reasonable to design a cross-section according to Eurocodes, neglecting effects of the joints.

As shown in Chapter 5 and Paper III, the overlapping shear keys are a critical detailing in this deck system. Therefore, they were tested in the laboratory to determine how they fail and evaluate their load capacity. The tests revealed two failure modes. The first is a rather ductile failure, activating the shear reinforcement. This was the expected failure mode for shear keys of this design. The second failure mode observed was a quite brittle failure in the concrete covering layer. It has only been observed in small-scale tests, and might be related to the test set-up. Nevertheless, overlapping of the rebars in the male-female shear key connection is strongly recommended to assure the robustness of shear transfer if failure occurs in the concrete covering layer.

To complement the laboratory tests, a single span bridge was monitored in the field (Chapter 6 and Paper IV). The bridge was built in 2000, using the prefabricated deck system that this thesis is focusing on, and was tested in both 2001 and 2011. The tests, and subsequent Finite Element analyses, showed that under moderate loading the interacting concrete area is smaller than for a similar in-situ cast bridge. No significant long-term effects were observed, except that under eccentric loading the distribution of the deflection between the girders decreased slightly during the 10 years between tests. This indicates that the joint gaps may have narrowed and at least partly closed during this time.

Chapter 7 summarises the research and presents recommendations for dealing with general issues related to the design and construction of a

bridge of this type. The design methods are generally the same as for a conventional composite bridge with an in-situ cast deck slab. However, the Eurocodes require some modification for the design of prefabricated deck elements with dry joints, particularly regarding global analysis and the resistance of cross-sections.

Finally, conclusions, a general discussion and suggestions for further research are presented in Chapter 8.

Keywords: *prefabricated composite bridges, concrete deck elements, dry joints, large-scale tests, field monitoring*

Sammanfattning

I denna avhandling studeras ämnet prefabricerade samverkansbroar i allmänhet och prefabricerade betongelementfarbanor med torra fogar i synnerhet

Prefabricering är ett ämne som har diskuterats i byggbranschen under de senaste decennierna. Husbyggnadsbranschen har gjort stora framsteg i riktning mot ett mer industriellt tänkande, i vilket prefabricering, Lean och BIM är viktiga pusselbitar. Även i brobranschen har mängder med forskningsprojekt utförts runt om i världen och ett flertal olika prefabriceringslösningar har testats genom åren. Trots detta förefaller brobranschen ligga långt efter i utvecklingen mot en mer industrialiserad byggprocess. Den långsamma utvecklingstakten kan till viss del förklaras av att varje bro ofta är ett unikt objekt med unika förutsättningar. Detta utgör ett hinder mot standardisering vilket ofta är beskrivet som nyckeln till industrialiserat byggande.

En litteraturstudie kompletterad med en Workshop, för insamling av information och erfarenheter från brokonstruktörer och forskare i Europa och USA, visar att prefabricerade farbaneelement fortfarande är ganska ovanliga i brosammanhang runt om i världen. Farbaneelement med torra fogar förefaller vara extremt ovanliga, enbart ett fåtal exempel har påträffats i litteraturstudien. Prefabriceringsnivån och utvecklingstakten mot ett mer industriellt byggande varierar mycket från ett land till ett annat. (Paper I och Kapitel 2-3)

För samverkansbroar har ett prefabricerat farbanesystem med torra fogar mellan betongelementen utvecklats i Sverige. De tvärgående fogarna är helt torra och all kraft överförs genom kontakttryck mellan olika betongytor. Detta medför att inga dragkrafter kan överföras genom fogen. Tvärkrafterna överförs genom överlappande betongklackar som är utformade som en serie av hane-hona kopplingar. Forskningen som presenteras i denna avhandling är fokuserad på konstruktionens statiska beteende. Detta beteende har

undersökts via såväl labbtester som genom fältförsök. (Paper II och Kapitel 3)

Storskaliga labbtester visar att en bro av denna typ är mindre styv än en liknande bro med en plastgjuten farbaneplatta. I områden med negativt böjmoment är betongelementens bidrag till styvheten försumbart. I områden med positivt böjmoment bidrar betongelementen till den globala styvheten. Vid måttlig belastning är dock den medverkande betongarean avsevärt mindre än i en motsvarande platsgjuten konstruktion. Denna skillnad orsakas förmodligen av de små glipor som finns i fogarna, i kombination med det faktum att de injekterade kanalerna är kontinuerliga över elementskarvarna. Detta medför att de initiala fogöppningarna mer eller mindre blir permanenta då kanalen injekteras, eftersom den injekterade betongen i kanalen måste tryckas samman till en viss gräns innan den resterande delen av fogen stängs. Förstörande provningar visar dock att skillnaderna i spänningar och styvhet är avsevärt mindre i brottgränstillståndet. Det är därför rentav rimligt att utföra tvärsnittskontroller, i brottgränstillstånd, i enlighet med de regler som anges i Eurokoderna och därmed försumma de effekter som fogarna ger upphov till. (Paper V och Kapitel 4)

De överlappande betongklackarna är en väsentlig detalj i det aktuella prefabriceringssystemet. Dessa klackar har därför testats i ett laboratorium för att för utreda hur de går i brott samt vilken lastkapacitet som de har. Testerna resulterade i två olika typer av brott. Den första typen av brott aktiverade skjuvarmeringen, vilket resulterade i ett tämligen duktilt brott. Detta var även det förväntande brottscenariot och tämligen i linje med de dimensioneringsmetoder som föreslås för denna typ av betongklackar. Den andra typen av brott som observerades var ett tämligen sprött brott i betongens täckskikt. Denna typ av brott har enbart observerats i dessa labbtester och är möjligen relaterad till utformningen av testriggen. Det rekommenderas dock att utforma armeringen i klackarna så att armeringsjärnen i hona-hane överföringen överlappar varandra. Detta för att säkerhetsställa erforderlig bärförmåga för skjuvöverföringen även efter ett eventuellt brott i betongklackarnas täckskikt. (Paper III och Kapitel 5)

Som ett komplement till labbtesterna har fältförsök utförs på en enspannsbro. Den aktuella bron byggdes år 2000 med den prefabriceringsteknik som denna avhandling behandlar och har instrumenterats såväl år 2001 som 2011. Även dessa tester och de efterföljande FE-analyserna visar att den medverkande betongarean, under måttlig belastning, är klart mindre än den medverkande arean för en platsgjuten betongfarbana. Inga väsentliga långtidseffekter har kunnat observeras. Enbart nedböjningsfördelningen mellan balkarna, vid excentrisk last, har minskat en del efter 10 år. Denna skillnad kan indikera

att fogöppningarna var större år 2001, dessa kan åtminstone delvis ha stängts under den tid som förlöpt mellan testen. (Paper IV och Kapitel 6)

Denna avhandling mynnar ut i ett kapitel som summerar den utförda forskningen genom att presentera råd och förslag på hur det går att hantera generella konstruktions- och produktionsfrågor för en bro av denna typ. Dimensioneringsmetoderna är i regel de som används för konventionella samverkansbroar med platsgjutna farbanor. För denna typ av prefabricerade farbaneelement finns det dock vissa områden där dimensioneringsreglerna i Eurokoderna bör modifieras eller rentav ändras. Systemanalys och tvärsnittskontroll är två av de dimensioneringssteg där reglerna i Eurokoderna bör modifieras en del. (Kapitel 7)

Avhandlingen avslutas med slutsatser, diskussion och förslag till framtida forskning. (Kapitel 8)

Nyckelord: *prefabricerade samverkansbroar, betongfarbaneelement, torra fogar, storskaliga tester, fältmätningar*

Table of Contents

Notations, symbols and abbreviations

Roman upper case letters

A	Area
A_{S0}	Bending reinforcement area in the tensile part
A_{S0}	Shear reinforcement area
A_{conc}	Effective concrete area
E	Modulus of elasticity
E_{steel}	Modulus of elasticity for constructional steel
E_{conc}	Modulus of elasticity for concrete
F	Force
F_{max}	Maximum value of the measured force
I	Moment of inertia
I_2	Moment of inertia for the equivalent steel cross-section
L	Length
L_e	Equivalent length for shear-lag calculations
$L_{element}$	Element length
M	Bending moment
M_{mean}	Mean value of bending moment
M_{dim}	Dimensioning bending moment
N	Normal force
N_{dim}	Dimensioning normal force
V	Vertical force/Shear force
$V_{Rd,c}$	Concrete shear resistance, without any reinforcement
$V_{Rd,s}$	Shear resistance governed by shear reinforcement
V_{max}	Maximum value of the measured shear force
W	Elastic section modulus
$W_{top,fl}$	Elastic section modulus at the upper side of the top flange
$W_{bot,fl}$	Elastic section modulus at the bottom side of the bottom flange
$W_{w,t}$	Elastic section modulus at the top of the web
$W_{w,b}$	Elastic section modulus at the bottom of the web
Ø	Diameter

Roman lower case letters

b_{eff}	Effective width of the interacting concrete deck slab
b_w	The smallest concrete width within the effective height
d	Effective height
e_{CG}	Vertical position of the neutral bending axis
f_{ct}	Concrete tensile strength
f_{ct}	Concrete shear strength
f_{ywd}	Yield strength for the shear reinforcement
h	Height
h_{conc}	Concrete thickness
s	Rebar spacing
z	Internal lever arm for bending moments

Greek letters

α	Factor for traffic loads/Inclination of the shear reinforcement
δ	Deflection or displacement
δ_{joint}	Theoretical Joint opening
$\delta_{meas.}$	Measured Joint opening
ε	Strain/elongation
η	Ratio between measured value and predicted value (meas./pred.)
θ	The angle of the shear crack
σ	Stress
σ_{tfl}	Stress on the upper side of the top flange
σ_{bfl}	Stress on the bottom side of the bottom flange

Abbreviations

AASHTO	American Association of State Highway and Transportation Officials
ABC	Accelerated Bridge Construction
ASCE	American Society of Civil Engineers
BIM	Building Information Modelling
FE	Finite Element
FHWA	Federal Highway Administration (USA)
FLS	Fatigue Limit State
KTH	Royal Institute of Technology (Stockholm, Sweden)
LF	Load Factor
LMn	Traffic load model n in Eurocode
LTU	Luleå University of Technology
LVDT	Linear Variable Differential Transformer
NCHRP	National Cooperative Highway Research Programme (USA)
NYSDOT	New York State Department of Transportation
SCC	Self Compacting Concrete
SKn	Shear Key type n
SLS	Serviceability Limit State
RFCS	Research Fund for Coal and Steel
RQ	Research Question
RWTH	Rheinisch-Westfaelische Technische Hochschule
UDoT	Utah Department of Transportation
UHPC	Ultra High Performance Concrete.
ULS	Ultimate Limit State
VFT	Verbundfertigtträger

Part I

1 Introduction

1.1 Background

The construction industry is often described in media as a very conservative market, with a high resistance towards changes in methods, materials etc. On top of that, the bridge sector has probably been the most conservative sector within the construction industry.

Prefabrication, lean-thinking and BIM are all starting to gain momentum in the house building sector. The bridge sectors in Sweden and Europe have tried to implement prefabrication during recent decades and there are several examples of successful projects involving prefabrication of both steel and concrete. Still, the bridge sector always seems to fall back into old habits and conventional construction methods. In order to get an impact of new building technologies there must be a change in the behaviour of contractors, designers and last but not least the bridge owners.

These changes in behaviour of the market actors are the incentive for this thesis but at the same time without the scope.

This thesis is focusing on the construction and the design of prefabricated steel-concrete composite bridges in general and dry deck joints in particular.

In the rest of the thesis, when the denomination "*composite bridge"* is used it shall be regarded as a synonym for "*steel-concrete composite bridge*".

This licentiate thesis is a part of the outcome from the European R&D-project "ELEM – Composite Bridges with Prefabricated Decks", RFSR-CT-2008-00039, which has been carried during the years 2008-2011. The project has been carried out within the financial grant of the Research Programme of the Research Fund for Coal and Steel.

1.2 Objectives and research questions

The main objective of this thesis is to study the structural behaviour of prefabricated bridge superstructures, consisting of two steel I-girders and prefabricated full depth concrete elements with dry joints.

Another objective is to present rational ways to perform design calculations, for this type of structure, in real design situations.

The questions raised are:

RQ1: What is the state of the art in this field?

RQ2: How does a superstructure with dry deck joints behave under different load situations?

- hogging moment
- sagging moment

RQ3: How do the shear keys fail under a static load?

RQ4: How should a rational design calculation of the shear keys be done?

RQ5: How is the long-term behaviour of the bridge, compared to a composite bridge with a conventional in-situ cast deck slab?

RQ6: What is necessary to check in a detailed design of this kind of bridges?

- Resistance in ULS/SLS/FLS
- Tolerances
- Waterproofing

1.3 Limitations

First, this thesis is only focusing on the structural behaviour of superstructures.

Second, the type of superstructure is limited to a composite superstructure, consisting of two steel I-girders and a deck made of prefabricated concrete elements. The transverse joints between the elements are dry, and forces are transferred from one concrete surface to another by contact pressure only. In order to gain composite action between the steel girders and the prefabricated concrete elements, in-situ cast concrete is used. Figure 1.1 illustrates a typical cross-section of such a superstructure.

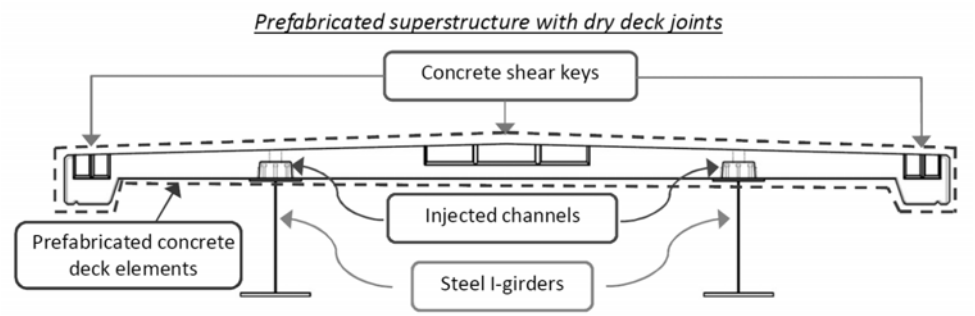

Figure 1.1 *Cross-section of the type of superstructure that this thesis is limited to.*

1.4 Scientific approach

To achieve the objectives and answer the research questions of this thesis, the following scientific approach has been used.

Step 1: Information about the status of the research and practice concerning prefabricated bridge construction has been gathered. This has been done generally by performing a literature survey.

Step 2: Critical details have been identified, and the focus have been set on these details.

Step 3: Experimental methods have been used to study the identified details. The behaviour of the critical parts of the bridge has been tested in the laboratory and by field measurements.

Step 4: The experimental results have been evaluated and compared to FE-analyses and mathematical models, aiming for design criteria for different parts.

Step 5: The results from steps 1 to 4 are summarised by this thesis and areas for further research are pointed out.

1.5 Structure of the thesis

Part I summarizes the work that has been done during the research project. It spans from an introduction of this specific subject to the final conclusion and recommendation for further research.

Chapter 1 gives a brief introduction to the subject. The objectives, research questions as well as the limitations are all presented. The chapter also describes how this thesis is composed and the included components.

Chapter 2 is an overview over the research topic in general. It also presents the state of the art in this field. This part is based on a literature review as well as on experiences gathered directly from bridge designers in Europe and the US.

Chapter 3 presents different types of full depth concrete deck elements, and the advantages and disadvantages related to these. The Swedish concept with dry deck joints is also described.

Chapter 4 describes the structural behaviour of the type of superstructure this thesis is limited to. Large-scale tests done at LTU are together with FE-analyses the main sources to this chapter. Other tests done by partners within the "ELEM"-project are also briefly reviewed in this chapter.

Chapter 5 deals with the capacity of the concrete shear keys. Results from laboratory tests on shear keys are presented. Based on these results and FE-analyses, a rational approach for the design of the shear keys is suggested.

Chapter 6 summarises experiences from field monitoring of the Rokån Bridge. This bridge has been monitored in year 2001 and 2011. This makes it possible to evaluate if there are any long-term effects, due to deterioration of the concrete in the dry joints.

Chapter 7 discusses specific design issues related to this type of bridge and recommendations for bridge designers are given. The recommendations that are given are based on experiences from the literature survey, test results, monitoring and design of pilot objects.

Chapter 8 closes Part 1, by presenting the conclusions from the previously presented research together with suggestions for further research.

Appendix A is a complement to Chapter 4 and gives a more detailed presentation of the large-scale laboratory tests.

Part II contains five papers. Paper I-III are all published in different journals, and paper IV-V were submitted to journals at the time when this thesis was written. Section 1.6 gives a more detailed presentation of the different papers.

Figure 1.2 shows a graphical scheme of how the different papers fit into the major research topic and relates to the research questions.

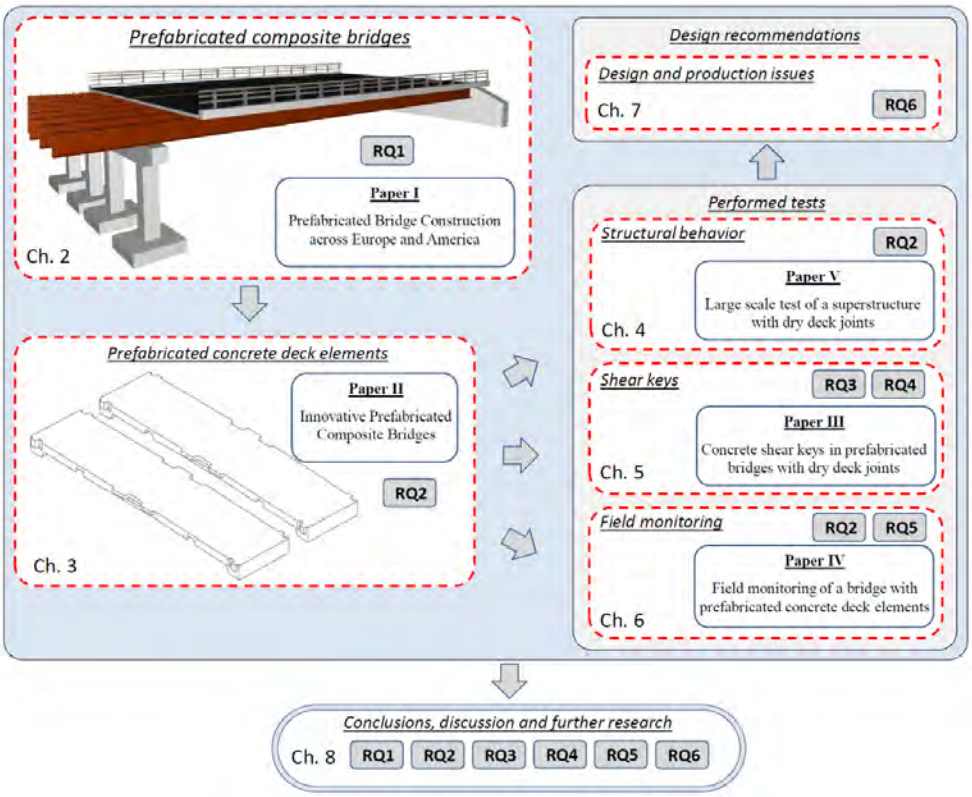

Figure 1.2 *Schematic illustration of how this thesis is composed.*

1.6 Summary of appended papers

Paper I "Prefabricated Bridge Construction across Europe and America" by Robert Hällmark, Harry White and Peter Collin was published in 2012 in *Practice Periodical on Structural Design and Construction (ASCE)*, Vol.17, No.3.

This paper summarises the state of the art in the field of prefabricated bridge design. The paper is based on experiences from researchers and bridge designers. The information has been gathered by a literature review and by arranging an international Workshop in Stockholm 4th March 2009.

Paper II "Innovative Prefabricated Composite Bridges" by Robert Hällmark, Peter Collin and Anders Stoltz was published in 2009 in *Structural Engineering International*,19 (1): 69-78.

Paper II summarises the previous done research in Sweden on this type of superstructures. The paper presents the results from laboratory fatigue tests of shear keys as well as shear studs. Some experiences from the construction process of a real bridge built in Sweden, in 2002, are also presented together with an economic analysis of prefabricated concrete decks vs. conventional in-situ cast concrete decks.

Paper III "Concrete shear keys in prefabricated bridges with dry deck joints" by Robert Hällmark, Martin Nilsson and Peter Collin was published in 2011 in *Nordic Concrete Research*, 44 (2/2011): 109-122.

Paper III is focused on the capacity of the shear keys in the dry joints. Laboratory tests of shear keys in scale 1:1 have been performed. This paper presents the tests, the results and an analysis aiming for a rational way to design the shear keys.

Paper IV "Field monitoring of a bridge with prefabricated concrete deck elements" by Robert Hällmark, Peter Collin and Mikael Möller was submitted to *Structural Engineering International* in June 2012.

Paper IV presents the results from field monitoring of a single span bridge with a prefabricated concrete deck with dry joints. This bridge was constructed in 2000 and has been in service since that. The field monitoring performed in 2011, is compared to a monitoring performed in 2001, shortly after the opening of the bridge. This is done in order to study the long-term behaviour of the bridge, and if there are some deterioration of the joints.

Paper V "Large-scale tests of a composite bridge with a prefabricated concrete deck with dry deck joints" by Robert Hällmark, Martin Nilsson and Peter Collin was submitted to *Bridge Engineering* in August 2012.

Paper V describes large-scale laboratory tests of a composite bridge with prefabricated deck elements with dry joints. The structural behaviour of such a cross-section has been studied in case of both sagging and hogging moments. The effective width of the interacting concrete, which corresponds to the test results, has been compared to the model given in EN 1994-2. Recommendations of how this type of bridges should be modelled in global analysis are given, together with recommendations for cross-sectional design.

1.7 Additional publications

In addition to the appended papers, some other papers have been published by the author within the field of bridge design.

Journal papers

Thulstrup M, Nielsen J P, Nilsson M & Hällmark R (2011) "Railway bridge over Södertälje Canal, Sweden" *Institution of Civil Engineers, Engineering Sustainability*, 163 (3) 123-132

Hällmark R, Collin P and Nilsson M (2010) "Prefabricated composite bridges", World Bridge Construction no:2 2010*, AMOST Foundation*, Moscow, Russia, 71-80 (in Russian)

Conference papers

Hällmark R, Collin P, Pétursson H & Johansson B (2007) Simulation of low-cycle fatigue in integral abutment piles. IABSE Symposium – Improving Infrastructure Worldwide, September 19-21, 2007, Weimar, Germany

Hällmark R, Collin P and Nilsson M (2009) Prefabricated composite bridges. IABSE Symposium – Sustainable Infrastructure, September 9-11, 2009, Bangkok, Thailand, Proceedings (96) 282-283

Thulstrup M, Nilsson M, Hällmark R & Nielsen J P (2009) Design, fabrication and construction of railway bridge over Södertälje Canal. Nordic Steel Construction Conference, September 2-4 2009, Malmö, Sweden. Proceedings (181) 128-137

Hällmark R, Nilsson M & Collin P (2011) Concrete shear keys in prefabricated bridges with dry joints. XXIth Symposium on Nordic Concrete Research & Development May 30 – June 1 2011, Hämeenlinna, Finland.

Technical reports

Breisand S & Hällmark R (2012) Tidig samverkan gav bättre samverkansbroar. Samhällsbyggaren nr:3 2012, pp: 12-15 (in Swedish)

Möller F, Hällmark R et al. (2012) ELEM-Composite Bridges with Prefabricated Decks. RFSR-CT-2008-00039, Final report – Technical report No: 6.

Möller F, Hällmark R et al. (2012) ELEM-Composite Bridges with Prefabricated Decks. RFSR-CT-2008-00039, Design Guide.

International Workshop on prefabricated composite bridges. Edited by: Collin P, Hällmark R & Nilsson M (2009) Technical report, Division of Construction and Structural Engineering, Luleå University of Technology, Luleå, Sweden, ISBN: 978-91-7439-003-2
http://pure.ltu.se/portal/files/3112371/ELEM_Seminar_4_Mars_2009.pdf

International Workshop on EC 4-2 - Swedish experience from EC4-2, Edited by: Collin P, Nilsson M & Häggström J (Hällmark R, pp 133-144) (2011), Technical report, Division of Construction and Structural Engineering, Luleå University of Technology, Luleå, Sweden, ISBN: 978-91-7439-285-2
http://pure.ltu.se/portal/files/33167428/Workshop.Collin_Nilsson_H_ggstr_m.pdf

2 *Prefabricated composite bridges*

Today, the total cost of a bridge is no longer limited to the money spent on labour and material. In an urban environment, there are several other factors that should be taken into account when new bridges are constructed or existing bridges are replaced, widened, strengthened or repaired. Construction activities that disrupt the ordinary traffic flow will result in increased road user costs, since the road users have to wait in queues or taking detours around the roads disturbed by the construction site. Finding ways to shorten the time spent on construction sites will give positive effects for contractors, bridge owners and the road users.

2.1 Industrial bridge construction

The time spent on a bridge site can be shortened by using a more industrial approach to the construction process. The definition of the term "industrial", in the construction industry, seems to vary from one author to another. Simonsson (2008) gives some examples of different interpretations, and defines also his own definition as: "a modernisation process of the construction industry for a smarter and more sustainable production". One philosophy that often is mentioned together with industrialised construction is *lean production*.

Lean production is an approach that was started by Toyota in the middle of the 20th century. Womack et al. (1990, 2003) describes the lean thinking concept in detail. Briefly, it is all about eliminating *waste* (Muda) from the production process, and to do "more and more with less and less" as Womack et al. writes.

If *lean production* is applied on a bridge construction process, the waste activities are tried to be minimized. The first step might be to prefabricate reinforcement cages to the supports or to use rebar carpets, which are rolled out on site as deck reinforcement. Another waste activity is the concrete compaction activities. If traditional vibrated concrete can be replaced by

self-compacting concrete, it would be possible to eliminate a work task. These examples can all be classified as industrial in-situ construction.

In order to shorten the time spent on the construction site even more, industrial prefabrication can be applied. This means that construction elements are produced in a controlled workshop environment. In some instances, entire structures have been fabricated off-site under strict environmental and quality controls and then shipped to the site and erected in a matter of days instead of months.

Concerning prefabrication, composite bridges have a large benefit compared to in-situ cast concrete bridges. The prefabricated steel girders are capable of carrying the weight of the formwork and the fresh concrete, and can be launched out in the right position without affecting the activities on the ground below. Due to this aspect, this type of bridge is superior in situations where it is hard, or even impossible, to find space for temporary supports. Examples of such situations are bridges over water, roads, railways etc. Figure 2.1 illustrates the benefits of composite bridges, during the constructions stage, compared to in-situ cast concrete bridges. The left picture shows a lot of temporary formwork that are often needed in case of in-situ cast concrete bridges. The right picture shows the launching of a steel box girder over highway E4 close to Kista, Sweden (January 2012). In this case, the traffic is running unaffected on the highway below, when the steel section and the formwork are launched into the final position.

Figure 2.1 *One concrete bridge and one composite bridge under construction.*

There are different levels of prefabrication. From small-scale prefabrication, in which only the steel girders are prefabricated and the rest of the structure constructed on site, up to complete prefabrication of the entire bridge structure. Figure 2.2 illustrates different levels of prefabrication. **Paper I** gives a more detailed description of different bridge prefabrication techniques.

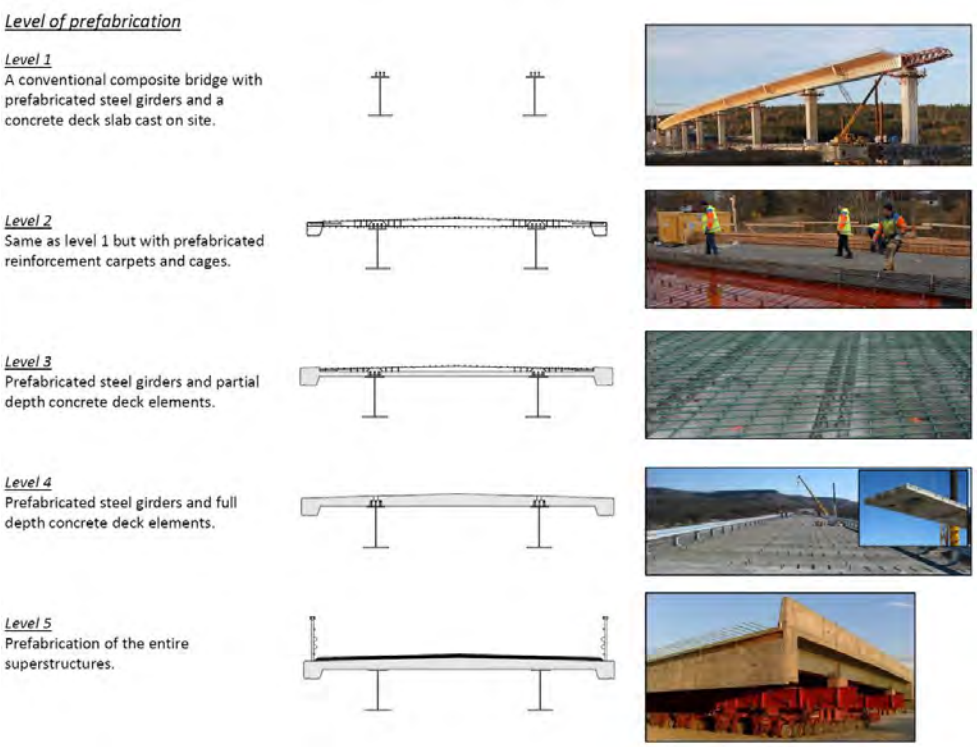

Figure 2.2 *Different levels of prefabrication for composite bridge superstructures.*

Although prefabrication is possible for all structural parts of a bridge structure, the superstructure tends to be the bridge component that is most suitable for prefabrication, according to a survey performed in the USA. (NCHRP 2003)

2.2 Advantages and disadvantages

Prefabricated composite bridge solutions have several advantages but also some disadvantages. The main advantages and disadvantages of using prefabricated concrete deck elements are presented in **Paper II** and are also listed below. (Culmo 2009a, Hällmark et al. 2009, NCHRP 2003)

Advantages

The construction time can be reduced in comparison to a conventional composite bridge with on-site reinforcement work and concreting.

⇒ Reduced traffic disturbance and environmental impact

⇒ Lower road user costs

⇒ Minimised construction delay on-site

The deck elements are cast indoors.

⇒ This is believed to result in high quality.

⇒ Improved working environment and safety.

Disadvantages

Tighter tolerances

⇒ Increases the need of extra control programs.

⇒ Can be time consuming in the production.

Lack of experience, from constructing prefabricated bridges, among the contractors

⇒ Gives higher bids at the tender stage.

No standardisation in the design of the prefabricated elements. The prefabrication industry has to deal with new details and new geometries all the time, and gains only small benefits from repetition. Standardisation of details and girder spacing would be beneficial.

2.3 Economy

When comparing the costs of constructing a prefabricated structure instead of an in-situ cast, it is important to not only consider the initial costs of the construction, such as the monetary costs of labour and materials. One should also keep in mind that there are other costs for the society, due to traffic disruptions, bad working environment etc.

Unfortunately, road user costs are often neglected when different design alternatives are compared. A study done in the USA, shows that the initial monetary costs of prefabricated bridges often are a bit higher or comparable with the costs for bridges constructed with traditional on-site techniques (NCHRP 2003). Culmo (2009a) indicates however that the traffic agencies, in the USA, that use prefabrication more frequently can lower the initial costs significantly. If the road user costs are taken into account, the traditional construction technique tends to be more expensive. Studies done in Sweden by Nilsson (2001) and Degerman (2002) present similar results.

The lack of standardisation is highlighted as one of the most important reasons to why prefabricated bridges have higher initial costs than conventional bridges (NCHRP 2003). Going forward, prefabricated bridges should consistently result in lower initial construction costs and produce higher quality of the final products once the prefabricated elements, connection details, construction procedures, and other details are

standardized and become more familiar. Today, sometimes even when it is obvious that prefabrication gains some advantages, typical construction techniques seem to be the first choice due to familiarity and habit.

Paper I and **II** are both dealing with economic issues concerning prefabricated bridge construction. This issue is also discussed in the Final Report from the RFCS-project "ELEM" (Möller, Hällmark et al. 2012a).

2.4 International experiences

International experiences have been gathered by a literature review and by arranging an international workshop with the topic *Prefabricated Composite Bridges*. The workshop took place in Stockholm, Sweden, on 4th March 2009. The workshop was free to attend and gathered 55 persons from 9 different countries. The proceedings from the workshop are available for free on the internet (Collin et al. 2009).

Paper I is a summary of the state-of-the-art in this particular field. Similar studies have also been performed by Collin et al. (1998), Ralls et al. (2005), and Gordon & May (2007) among others.

2.4.1 USA

In the US a lot of time and effort have been invested in order to improve the safety during and after construction, reduce the congestions due to the construction work and to improve the quality of the highway infrastructure. A part of this work have been done within the FHWA-project (Federal Highway Administration) *"Highways for LIFE"*, where LIFE stands for ***L****onger-lasting highway infrastructure using* ***I****nnovations to accomplish the* ***F****ast construction of* ***E****fficient and safe highways and bridges* (FHWA 2011). Within this project different technologies have been studied from prefabrication systems to innovative performance contracting.

One thing that is highlighted by FHWA is Accelerated Bridge Construction (ABC). ABC is defined as *"bridge construction that uses innovative planning, design, materials, and construction methods in a safe and cost-effective manner to reduce the onsite construction time"* (FHWA 2011). This type of construction technique is described more in detail by Culmo (2009a) and Hällmark et al. (2012). The ABC approach spans from prefabricated deck elements to total bridge prefabrication, the latter has been proved very efficient in several states. The Utah department of transportation (UDOT) is using ABC as the standard way of building bridges within the state, and provides several guidelines for ABC (UDoT 2012). One of the most interesting guidelines, for this thesis, is the Full

Depth Precast Concrete Deck Panel Manual, which is available for free (UDoT 2010). Design manuals and guidelines for prefabricated bridge construction have also been developed at a federal level. Culmo (2009b) provides a national review of connection details for prefabricated bridge elements and systems, and NCHRP (2009) gives some guidelines for Best Practice in Accelerated Construction Techniques. A brief introduction to prefabricated bridge projects in the US is given in the document Prefabricated Bridges (AASHTO 2009).

Concerning the concrete deck panels, the detailing varies a lot between the different states. Several different details have been tested during the years. A few of the more recently and innovative details are presented in **Paper I** (Hällmark et al. 2012).

2.4.2 Korea

In recent years several bridges have been constructed in Korea by using prefabricated concrete deck elements. At the same time, several research projects have been going on in the field of prefabricated bridges. Shim et al. (2010) presents experimental studies, FE-analyses and implementation of precast decks for composite bridges. Figure 2.3 illustrates a typical Korean design of a prefabricated steel-concrete composite superstructure. As shown in the figure, pre-stressing tendons are often used in order to keep the joints in compression during the lifetime of the deck, and preventing cracking and leakage at the joints.

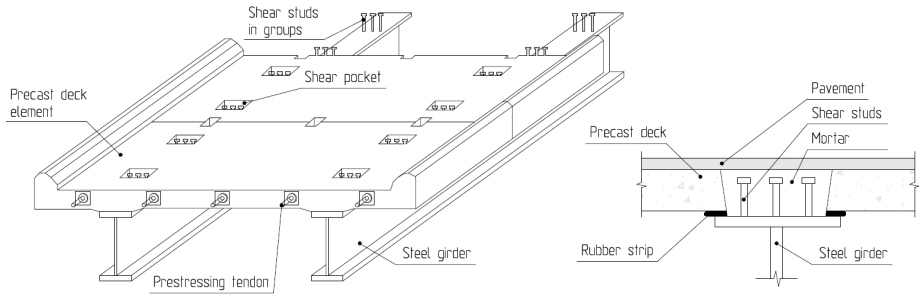

Figure 2.3 *Typical Korean deck panels for steel girders (after Shim et al. 2010).*

One example of a large composite bridge in Korea, where prefabricated full depth deck elements have been implemented, is the Secheon Bridge near Seoul. About 1000 deck elements were used on the approach bridges with a total length of 1.56 km. The width of the deck varies between 14.6 – 28 m. Figure 2.4 illustrates the erection of the concrete deck elements.

Figure 2.4 *Erection of deck panels on the Secheon Bridge (Shim et al. 2010).*

2.4.3 Germany

Bridges with prefabricated concrete deck elements are rare exceptions in Germany. However, in recent years different types of prefabricated superstructure have been developed by bridge designers and researchers.

The VFT-girders in the outcome of a RFCS-project named *PreCoBeam (Prefabricated Composite Beam)*. In this construction method, the steel girders are integrated into precast deck slabs by using concrete dowels for the transfer of shear flow from the steel web to the concrete web. Figure 2.5 shows a VFT-girder prior and after the prefabricated concrete parts have been cast. (Seidl 2009a, b)

Figure 2.5 *VFT-girder at different production stages (Seidl 2009b)*.

Another concept with a high degree of prefabrication is the VTR-concept. Möller et al. (2012) presents this technique more in detail. The basic concept is to prefabricate different concrete modules, such as cross girders and carriageway slabs. In-situ cast concrete is only used to create composite action between the prefabricated elements. Figure 2.6 is a illustration of the concept.

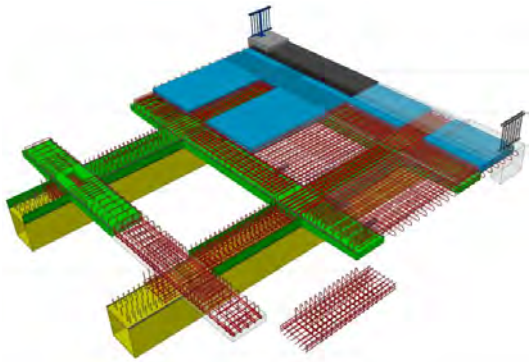

Yellow - Steel girder level
Steel girder + shear studs

Green - Cross girder level
Cross-girders + first in-situ concrete

Blue - Carriageway level
Carriageway slabs + second in-situ concrete

Red - Reinforcement level
Reinforcement of all constructional elements

Figure 2.6 *Illustration of the VTR-concept (Möller et al. 2012).*

2.4.4 UK

Prefabricated deck elements have been used in UK for many years. Gordon & May (2007) present some of the bridges where prefabricated elements have been used. An extensive research on the capacity of the transverse in-situ joints has also been performed (Gordon & May 2006).

One of the largest bridge projects in Europe at the moment is the Forth Replacement Crossing outside Edinburgh, Scotland. The bridge will be 2.7 km long, and consists of two large cable stayed main spans and approach viaducts up to the main spans. The superstructure is a steel-concrete composite section along the whole bridge, with a total width of about 40 m. In the south approach viaducts, length 540 + 540 m, partial depth element will be used as a collaborating formwork, reducing the need of temporary formwork significantly. Only the edge beams will be cast with temporary formwork. The tender design of the approach viaducts was performed by the author and his colleagues at Ramböll Luleå (2009-2010). Figure 2.7 illustrates how the final bridge will look like and Figure 2.8 shows a section through one of the two composite girders, which the approach viaducts will consist of. The black areas are the in-situ cast parts, and the hatched areas are the prefabricated parts. The concrete cross-girders, in the prefabricated elements, are hidden in the figure by the in-situ cast concrete.

Figure 2.7 *Illustration of the Forth Replacement Crossing.*

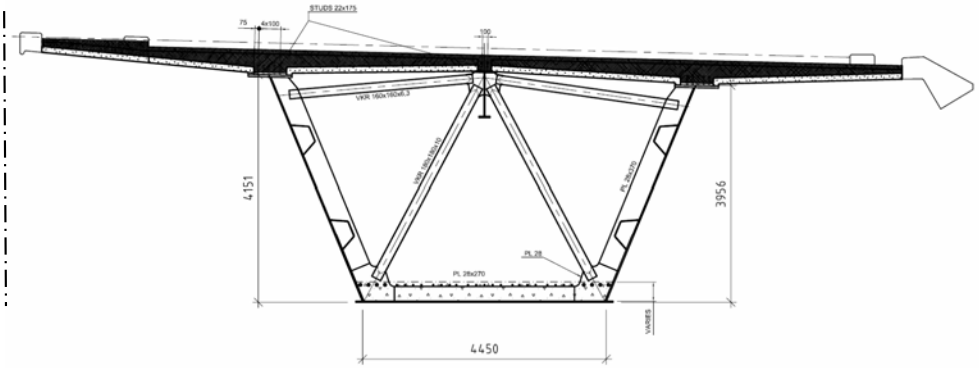

Figure 2.8 *Cross-sectional drawing of one half of the south approach viaduct on the Forth, with the symmetry line to the left.*

2.4.5 Finland

Composite bridges are not that common in Finland, and composite bridges with prefabricated elements are even rarer. In 2006, the Steel Bridge Development Group of Finnish Constructional Steelwork Association (TRY) started an R&D-project aiming for a bridge with shortest possible installation time. The outcome of this project was a composite bridge with prefabricated concrete deck element, the Laisentianjoki Bridge. This project is described in detail by Möller et al. (2012) and Hällmark et al. (2012).

2.4.6 France

France has been using prefabricated concrete decks panels for decades, and there are experiences from wet-joints as well as dry joints. Berthellemy (2001, 2009) summarises the experiences from France within the field of prefabricated composite bridges. One of the more innovative solutions is presented below.

A French company has developed their own patented system for a continuous in-situ prefabrication of the deck slab, which might be described as a hybrid between conventional in-situ techniques and prefabrication. The deck is cast in segments of a few meters at the time. When one segment is finished it is pushed out of the formwork and onto the steel girders by hydraulic jacks, see Figure 2.9. Next segment are then reinforced and cast with a continuous connection to the previous segment. In this way the bridge deck can be prefabricated in the end of the bridge and just launched out in the final position. Composite action is achieved by in-situ cast concrete that is injected through opening above the steel girders. Figure 2.10 illustrates the principle of this construction technique.

Figure 2.9 *Launching of the first segment (Berthellemy 2009).*

Figure 2.10 *Illustrations of the French technique (Berthellemy 2009).*

2.4.7 Sweden

Sweden has in line with France, tested many types of prefabricated deck elements with wet-joints as well as dry joints. Collin et al. (1998, 2009) and Hällmark et al. 2012 present some experiences from Sweden.

The majority of the Swedish composite bridges with prefabricated deck elements have been constructed with wet joints, in the transverse direction, and with overlapping longitudinal reinforcement bars. Only a few bridges have been designed with dry joints. One of these bridges is the Rokån Bridge which was a successful pilot project back in year 2000. In this Bridge not only the deck was prefabricated, the retaining walls and the foundation plinths were also prefabricated. The bridge was constructed parallel to the old one and sideways launched into the final position. Table 2.1 presents the

time schedule of the bridge replacement, and the working process. Figure 2.11 shows one of the deck elements under the erection of the deck.

Table 2.1 *Timetable for the bridge replacement across Rokån.*

Day	Time	Activity
Day 1	19:00	The old road was closed.
	22:00	The old bridge was removed using two mobile cranes. The dismantling works continued until 6 p.m. the next day
	00:00	The old back walls and wing walls were removed, and the ground behind the abutments was excavated. New gravel fill was placed up to the correct level.
Day 2	09:00	The prefab plinths were placed on the new gravel bed.
	10:00	The lifting contractor temporarily placed the new bridge on launching girders, which took 4 hours. The sideways launching took only 10 minutes.
	18:00	Installation of bearings and filling behind the retaining walls.
Day 3	01:00	The new bridge was opened to traffic.

Figure 2.11 *Deck element in final position.*

3 Prefabricated concrete deck elements

A further step to improve the competitiveness of composite bridges is not only to reduce the amount of formwork for the superstructure, but to eliminate it. This can be done by using prefabricated concrete deck elements on top of the steel girders.

Prefabricated concrete deck elements can be used for different types of bridge girders from concrete girders to steel girders. This section deals with prefabricated concrete deck panels in general.

Roughly speaking, there are two types of prefabricated deck elements, partial depth elements and full depth elements. Partial depth elements are used as a collaborating formwork, always requiring on-site reinforcement work and in-situ concreting of the upper part of the deck slab. In contrast to partial depth element, full depth elements are prefabricated up to a level that requires only on site concreting in the joints between the steel girders and the concrete deck panels in order to create a composite structure. Some reinforcement work and in-situ concreting is often also needed in the transverse joint between the elements (wet-joints).

3.1 Longitudinal deck joints

Examples of different longitudinal joints are presented in Table 3.1. This table is based on the state of the art study presented in the final report from the RFCS-project ELEM, Möller et al. (2012)

***Table 3.1** Different types of longitudinal joints in steel-concrete composite bridges.*

Open joints

- continuous reinforcement

The elements are placed on top of the steel girders, as one unit from edge-beam to edge-beam.

+ easy to erect
+ traditional vibrated concrete can be used
+ no problems with air entrapment
- Shear reinforcement might be necessary in the joints.
- Cracks can occur at the surface in the bonding area between prefabricated concrete and in-situ concrete.
- Relatively slow work progress, since the concrete surface must dry out/harden before the work with the waterproofing/ pavement can start.

- overlapping reinforcement

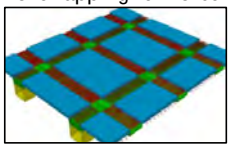

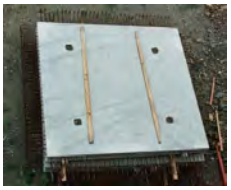

The elements are placed on top of the steel girders and the cross-beams, giving linear supports on at least 3 sides of each element.

+ easy to assemble
+ traditional vibrated concrete can be used
+ no problems with air entrapment
+ smaller/lighter elements to handle during erection
- Cross-beams are needed at every transverse joint.
- Cracks can occur at the surface in the bonding area between prefabricated concrete and in-situ concrete.
- Relatively slow work progress, since the concrete surface must dry out/harden before the work with the waterproofing/ pavement can start.

Pocket joints

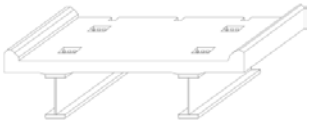

The shear studs are placed in groups on the steel girders, and pockets are made in the prefabricated concrete elements.

+ Less in-situ concreting necessary, compared to open joints
+ Higher transverse bending moment/shear force capacity during the construction stage ⇒ the elements can be made bigger
- Stricter tolerances for the positioning of the shear studs

Channels

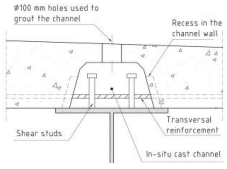

The composite action is created by injecting concrete in a channel above the steel girders.

+ Fast work progress, since the work with the waterproofing can start almost immediately after the channels are injected.
+ Relatively high transverse bending moment/shear force capacity during the construction stage.
- Stricter tolerances for the positioning of the shear studs

Studs in recesses

The studs are welded on-site in individual recesses, which are injected later on.

+ No problems with positioning of the studs
- On-site welding must be used

Open joints seems to be the most common solution, examples can be found from Sweden, Finland, USA, France etc. (Collin et al. 1998, 2009) (Hällmark et al. 2012) (Culmo 2009a,b).

Reports from experiences with pocket joints can be found in Collin et al. (1998), Ralls et al. (2005) and Shim et al. (2010).

Injection channels have been used successful in several countries. Sweden and USA are two countries that have tested this solution, but with slightly different approaches. (Hällmark et al. 2009, 2012, Stoltz 2001, FHWA 2009, 2010)

Experiences from bridges with shear studs that have been welded on site, through recesses in the concrete, have only been found from one country France. (Berthellemy 2009, Ralls et al. 2005)

3.2 Transverse deck joints

The literature review indicates that the common solution, worldwide, is in-situ reinforced transverse wet joints (Collin et al. 2009). To shorten the time spent on the constructions site even more, a system with dry joints can be used. Such a system has been developed in Sweden during the last 15 years. Chapter 4-7 is only dealing with this Swedish system, while this chapter deals with prefabricated deck elements from a more general perspective.

Examples of different transverse joints are presented in Table 3.2. This table is based on the state of the art study presented in the final report from the RFCS-project ELEM, Möller et al. (2012)

Table 3.2 *Different types of transverse joints.*

	Wet joints		***Injection joints***	***Dry joints***
Joint material	Concrete	Cement mortar	Epoxy mortar	-
Thickness	≥ 100 mm	≤ 30 mm	< 3 mm	~ 0 mm
Tensile coupling by reinforcement bars	Possible	Not possible	Not possible	Not possible
Hardening time	Long	Long	Fast	None
Joint surface tolerances	Moderate	Moderate	Limited	Strictly limited

3.2.1 Wet joints

Wet joints are by far the most common way to design transverse deck joints in prefabricated composite bridge decks, and the number of different types of wet-joints is enormous. Each bridge designer seems to have their own way to solve the same problem. In Figure 3.1 some examples of wet joints are presented.

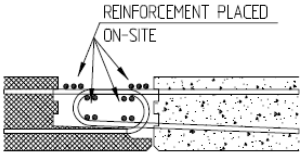

(a) In-situ reinforced joint Sweden. [1]

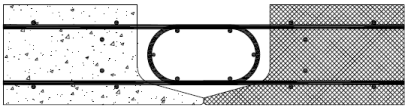

(b) In-situ reinforced joint, Japan. [2]

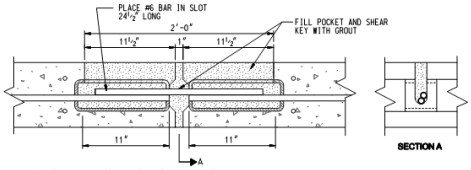

(c) "Slot-in" reinforced joint USA. [3]

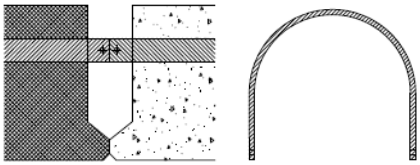

(d) Welded joint, and the geometry of the flat steel profile embedded in the concrete. [4]

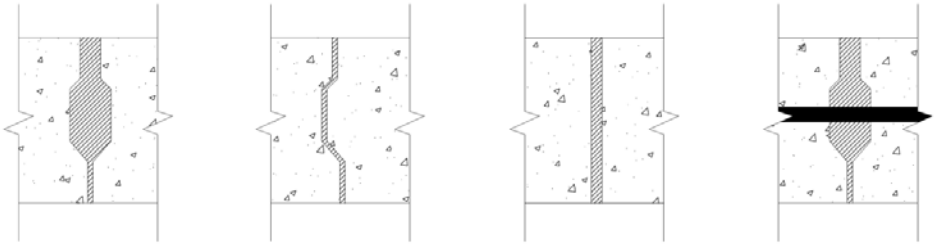

1. Female-Female-joint 2. Female-Male-joint 3. Butt-joint 4.Post-tensioned F-F-joint.

(e) In-situ cast concrete shear keys [5]

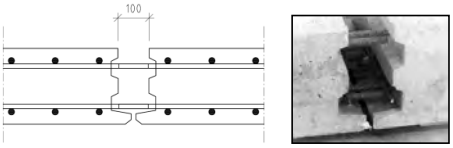

(f) CRC-joint with High-Performance–Concrete. [6]

[1] Ingbo Bridge, Sweden (Collin et al. 1998).
[2] After Ralls et al. (2005)
[3] Live Oak Creek Bridge, Texas (Culmo 2009b)
[4] Idijokki Bridge, Sweden (Collin et al. 1998)
[5] After Markowski (2005)
[6] Harryson (2008)

Figure 3.1 *Examples of wet joints.*

In-situ reinforced wet-joints have been studied and tested in several countries. Culmo (2009b) presents several different examples of joints from the USA, from in-situ reinforced joints to in-situ cast shear keys. In the research field, Gordon & May (2006) have performed extensive testing on in situ cast joints.

In Sweden, wet joints have been reinforced and made continuous by butt-welding steel profiles connected in the adjacent elements, as shown in Figure 3.1 (d). This type of welded joint has only been used in one Swedish bridge, since the welding procedure was quite time consuming and made this solution expensive.

Markowski (2005) summarizes the US experiences from in-situ cast concrete shear keys, Issa et al. (1995) and Chi (1985) are the main sources. The female-male joint is reported to perform badly, and this solution in not recommended since it is difficult to get a good result of the grouting and since major spalling and extensive leakage is very common. Also the butt-joints are reported to perform quite badly in tension. In cases where the deck is kept in compression, by longitudinal pre-stressing, the solution with butt-joint is satisfactory. The female-female joint is probably the most common in-situ cast shear key joint, and also the joint that performed best among joint (e) 1-3 in Figure 3.1. However, also in this case leakage is common in areas where the deck is in tension. Therefore, the recommended solutions for in-situ cast shear keys is post-tensioned female-female joints. The capacity of such joints, for different grouting materials, has been studied by Issa et al. (2003). A more recent source on this type of joints is Culmo (2009b).

Harryson (2008) has performed some research on a new type of high-performance joint for concrete bridge decks, with a very short overlapping length of the longitudinal rebars, 100 mm. A high strength fibre reinforced concrete, f_{cc} = 150 MPa, made this type of joint possible. The joint, shown in Figure 3.1 (f), has still not been tested in any real bridge deck. However, laboratory tests as well as FE-analyses indicate a satisfactory behaviour.

3.2.2 Dry joints

Dry joints have been used in different type of superstructures, from pre-tensioned segmental concrete bridges to composite bridges without any pre-stressing tendons.

A dry transverse joint must be able to transfer the vertical and the horizontal shear forces from one side of the joint to the other. If the deck elements are pre-stressed by a clamping force, it would be possible to make use of the friction between the elements. However, creep and shrinkage must be considered during the technical life time of the bridge. Another possible solution is to use overlapping concrete shear keys to transfer the shear forces. This thesis is focused on the latter one.

Segmental bridges

In segmental bridges, shear keys can be used to transfer the shear forces during the erection stage or permanently. If dry joints are used, without even epoxy, the shear keys must be designed for the permanent load situation. The design of shear keys in segmental bridges varies a lot. One extreme is to use a few large reinforced shear keys and the other extreme is to use many small shear keys without any reinforcement. It is quite common to provide additional shear keys in segmental bridges, in order to avoid problems if one or a few shear keys are damaged during storage or erection. (Hewson 2003)

Pre-stressed prefabricated concrete decks

One example of a bridge with pre-stressed concrete deck elements, with dry joints, is a 160 m long four span composite bridge on the A51 motorway in France, built in 1991. The joints were designed to transfer shear forces by carefully fitted shear keys. The elements were match-cast in order to achieve good tolerances. All joints were glued during the erection and longitudinal pre-stressing was used. Inspections, made during the first 20 years after the opening of the bridge, reports no signs of any cross-cracking, and the state of the bridge is regarded as good. A similar type of prefabricated bridge deck, but without any glue in the joints, has been used more recently in the VINCI overpass system, also developed in France. Figure 3.2 shows a concrete element from this system. The shear keys/recesses can be seen at the joint surface. (Berthellemy 2009)

Figure 3.2 *Prefabricated deck element with dry joints, France. (Berthellemy 2009)*

In Germany, a new type of prefabricated deck element with dry joints has been developed during the last years. The elements are connected to each other by a dry key and slot joint, which are pre-stressed in the longitudinal direction. The joint, which is illustrated in Figure 3.3, has been developed in order to accelerate the bridge erection on long bridges with many elements. Möller et al. (2012) gives a well-detailed presentation of the Greisselbach Bridge built with this technique.

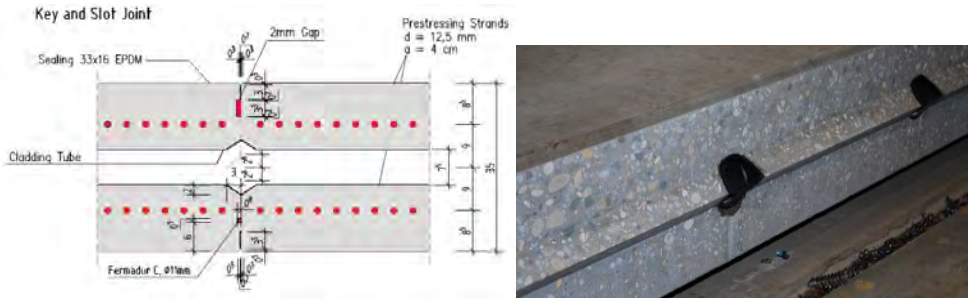

Figure 3.3 *Dry joints with linear shear keys (Möller et al. 2012).*

<u>Prefabricated concrete decks without external pre-stressing</u>

In Sweden, three single span composite bridges have been built with dry joints, and without any pre-stressing tendons. However, the deck elements have been clamped together by bolting the prefabricated back walls to the end plate on the steel girders. This gives a form of pre-stressing in the concrete, but is mainly used to minimise the joint gaps before the in-situ cast channels are injected. The design of the shear keys has varied from stainless steel rods to concrete shear keys. Figure 3.4 shows the different type of shear keys that have been used in Sweden.

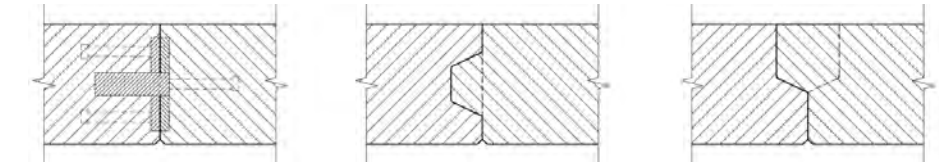

(a) Stainless steel stud, Ø50mm. *(b) Internal shear key.* *(c) Concrete tongues.*

Figure 3.4 *Example of different types of dry joints tested in Sweden.*

The Swedish research and development on dry joints has been summarized by Collin et al. (1998), Stoltz (2001) and Hällmark et al. (2009, 2012). The Swedish experiences from dry joints are summarized in **Paper I** and **II**.

3.3 Tolerances

In general, prefabrication increases the demand on tighter tolerances. In theory, the tolerances might appear sufficient, but the reality and the theory do not always go hand in hand. An example from France (Berthellemy 2009), shows how the theory sometimes can differs from the reality, see Figure 3.5.

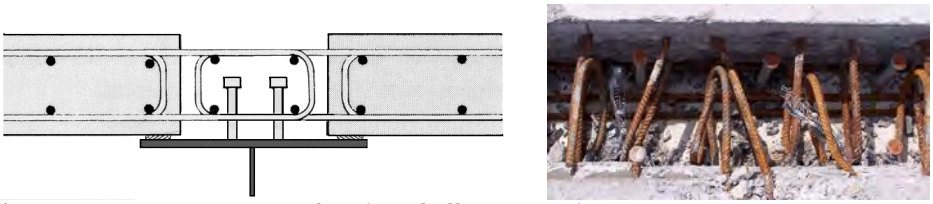

Figure 3.5 *Drawing vs. reality (Berthellemy 2009).*

If dry joints are used the demand of tight tolerances is increased even more.

Generally speaking, there are two ways of dealing with problems concerning tight tolerances.

Alt. 1 Use additional controls and control plans

Alt. 2 Avoid the intersections/collisions ⇒ increased tolerances

If a prefabricated concrete deck with dry joints is chosen, it is strongly recommended to match-cast the element in order to get a sufficient precision. The first element can be cast in an ordinary formwork, but from the second element and further, the previous cast element should be used as formwork on one side of the next element. By using this match-casting technique, and by numbering the elements, is has been shown that it is possible to keep the mean joint-gap ≤ 0.4 mm (Hällmark et al. 2009).

The Swedish solution, with overlapping shear keys, implies that the elements must be erected with a longitudinal displacement larger than the depth of the concrete shear keys. The transverse rebars in the bottom of the elements can easily collide with the shear studs if the demanded tolerances cannot be achieved. Figure 3.6 illustrates the tight tolerances during the erection stage.

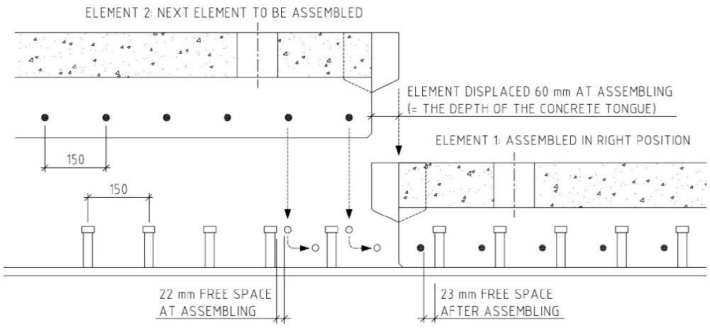

Figure 3.6 *Illustration of the tight tolerances at erection (Hällmark et al. 2009).*

In Sweden, the technique described above has proved successful on single span bridges with a length up to 30 m. Additional control plans have been used in the steel workshop, in the concrete prefabrication workshop and for the on-site erection (Alt.1 on previous page). (Hällmark et al. 2009)

In USA, the same problem has been solved by re-designing the connection between the steel girders and the concrete deck panels. The modified detail implies that the intersection plane between the shear studs and the transverse rebars has been avoided (Alt.2 on previous page). Figure 3.7 shows a longitudinal joint detail developed by the New York State Department of Transportation (NYSDOT). By using Ultra-High-Performance-Concrete it is possible to achieve composite action by using shear studs with a height of as low as 75 mm. Combined with a concrete haunch above the steel-girders, it is possible to achieve a cross-section in which the transverse rebars never can collide with the shear studs. (FHWA 2010, Hällmark et al. 2012)

In chapter 7 the tolerances are discussed even more.

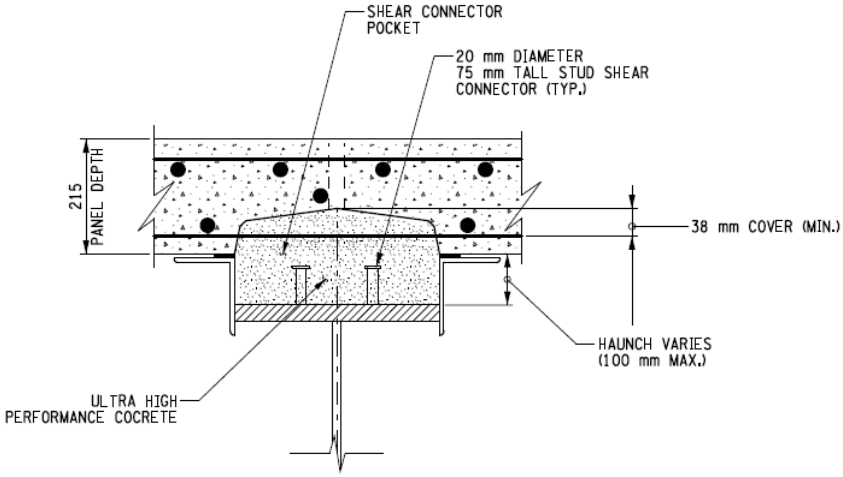

Figure 3.7 *Connection details using UHPC (FHWA 2010).*

3.4 The prefabricated concept studied in this thesis

The Swedish prefabricated concept with dry joints is briefly summarised in this section by describing the concept from the manufacturing process to the final assembly. The described concept is suitable for bridges up to ~40 m, without using any wet-joints. For longer bridges, the tight tolerances could make it necessary to use some wet joint in order to zero cumulative errors.

This type of prefabricated concrete deck stands out, since it has totally dry joints between the elements and transfers the shear forces by concrete shear keys. Figure 3.8 shows the erection of one of the bridges that has been built.

Figure 3.8 *Erection of a bridge deck.*

The elements must be produced with very tight tolerances regarding both the geometry of the element and the positions of the rebars. The production of the elements has so far been done in concrete prefabrication workshops. The elements are always match-cast, with the previous cast element as formwork on one side and a steel form work on the other sides. This procedure makes in necessary to cast the element in the order in which they shall be erected, and to number the elements to assure that the elements fits into each other.

The upper surface of the element is almost completely finished already in the prefabrication stage. Longitudinal injection channels are used above the steel girders in order to create the necessary composite action between the steel girders and the concrete deck. The channels are done with concrete injection holes (Ø100 mm) as well as air release holes (Ø16 mm). The transverse reinforcement bars, together with the recesses in the channel walls, transfer the shear forces from the in-situ cast concrete, in the channel, to the prefabricated concrete. See Figure 3.9.

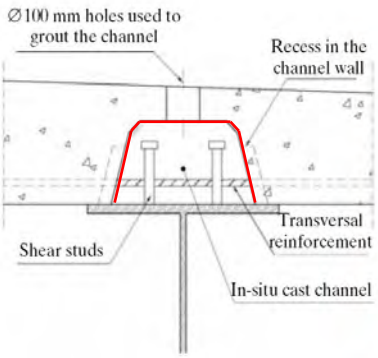

Figure 3.9 *The in-situ cast channel.*

During the erection of the deck, the elements must be placed with a longitudinal displacement larger than the depth of the shear keys, as described in Figure 3.6 and the text above. Also in this step the tolerances are tight.

When all elements are in their final positions the elements are pushed together. This can be done by pulling the end-screen elements against the deck elements, by prestressing threaded bars that go through the end-screens, creating a clamping force, see Figure 3.10. After the elements have been pushed together, the channels are injected with Self Compacting Concrete through the injection holes. In order to avoid air pockets, air release holes are used every 300-400 mm.

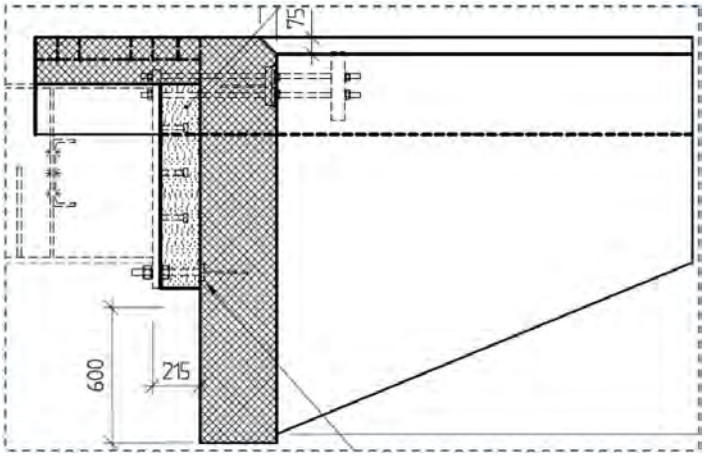

Figure 3.10 *Illustration of how the clamping force is created.*

After the channels have been injected, the waterproofing can be installed almost immediately, since the concrete top surface is made of prefabricated concrete, except at the injection holes. Next step is to put pavement on the bridge and then take it into service.

In order to fulfil the tight tolerances, additional control programs have been used on all steps from the manufacturing to the assembly stage.

4 Structural behaviour

In order to investigate the behaviour of a composite superstructure with dry deck joints, large-scale tests were performed at Luleå University of Technology, by the staff at the Complab-laboratory. The results from these tests were compared to FE-models and suggested design models, in order to evaluate if the general design rules given in Eurocode can be used also for this type of bridges.

Figure 4.1 illustrates the large-scale test specimen and defines also the co-ordinate system that has been used in all tests. Figure 4.2 shows a picture from the laboratory during one of the tests. Appendix A gives details of the test programme and the results.

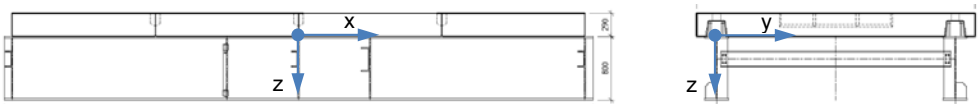

Figure 4.1 *Illustration of the test specimen and the local coordinate system.*

Figure 4.2 *Large-scale tests specimen in the laboratory.*

This chapter summarises the structural behaviour of the type of bridge this thesis deals with. This is done by presenting results from the large-scale tests, previous tests and tests performed by research partners at other universities.

Paper V describes the test set-up in detail and summarises the results. This paper is mainly focused on the degree of composite action between the steel and the concrete, based on the measured deflections and the steel-stress distribution. Section 4.1 – 4.2 gives a brief summary of this paper.

At the same time as the deflections and the steel stresses were investigated in the large-scale tests, other measurements were also performed. These measurements and their results are briefly presented in Section 4.3 – 4.5. Some of these quite extensive tests are still under evaluation and will be presented in a research paper in the future.

A more complete description of the large-scale tests and their results is given in Appendix A. The structure of this appendix is presented below.

Appendix A – Large-scale tests

A.1 Test specimen
A.1.1 Geometry
A.1.2 Tolerances

A.2 Test set-up

A.3 Results
A.3.1 Deflections
A.3.2 Steel strains
A.3.3 Concrete strains
A.3.4 Reinforcement strains
A.3.5 Joint openings

4.1 Deflections - Stiffness

The results from the laboratory tests, as well as the results from the field monitoring presented in Chapter 7, indicates that a composite section of the bridge system studied in this thesis, has a lower stiffness than a composite section with an in-situ cast deck.

A detailed presentation of the deflection measurements and the results is given in Appendix A.3.1, and the analyses are presented in **Paper V**.

Areas with hogging moments
In sections with hogging moments, the contribution to the stiffness from the concrete elements is negligible. The interacting concrete area is very limited, since the forces carried by the composite section must enter and leave an element within the length of the distance between the outermost shear studs within the element. This behaviour is confirmed by the FE-analyses. Figure 4.3 illustrates how the longitudinal stresses vary within the web plate in the FE-analyses.

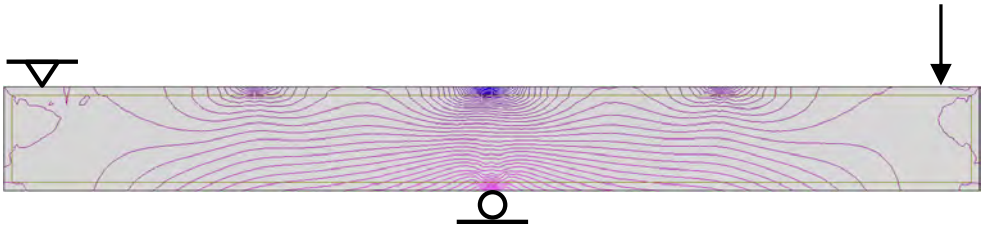

Figure 4.3 *Longitudinal stress iso-lines.*

The neutral bending axis of the composite section will be very close to the neutral bending axis of the steel girder. In the global analysis it would be reasonable to assume no interaction at all in areas with tension stresses in the upper flanges, in other words near internal supports if no pre-stressing is used.

Areas with sagging moments
In sections with sagging moments, the concrete elements will contribute to the global stiffness. However, results from both laboratory tests and field monitoring show that the interacting concrete area is smaller than the interacting area in a corresponding in-situ cast section. This indicates that the joint gaps, together with the in-situ cast channels, will influence the stiffness even if the gaps are very small.

In the tests described by Hällmark et al. (2012b), the initial joint gap was ≤ 0.5 mm, in similar tests at RWTH (Aachen, Germany) the joint gaps were 1-5 mm (Möller et al. 2012a). The deflection measurements in the latter tests indicated global stiffnesses that were equal to the stiffness of a composite

section with an effective concrete width that equals the width of the in-situ cast concrete channels. However regarding the stress calculations, the same tests indicate that the width of the interacting concrete, in SLS and FLS, on the safe side can be described by assuming a distance between points of zero bending moment, L_e, which equals the longitudinal distance between the outermost shear studs within an element (1.5 m in this case). This statement is also verified by the Swedish tests. These tests, with smaller gaps, indicate that this is valid also for the calculation of the deflections. This is a bit contradictive to the German results, where large gaps in the joints might have affected the deflections.

The Swedish tests were non-destructive tests, which mean that there are no data showing the interacting concrete area in the ULS. However, the tests in Aachen were destructive tests, more focused on the behaviour in ULS. These tests show that the gap width will influence the ultimate capacity of the composite section, since the stress concentration in the contact areas will increase with an increasing gap width. These stress concentrations are also governing the initial concrete failure. However, even then the measured ultimate capacity was lower than for the reference specimen, with an in-situ cast deck slab. The tests still reached the ultimate limit capacity according to EN 1994-2, calculated with real material parameters and neglecting the safety factors. This indicates that there is no significant reduction of the effective width of the interacting concrete compared to the model suggested by EN 1994-2. Figure 4.4 shows the load-displacement curves from the test by RWTH. The deck slab in test specimens VT1 – VT3 were made of prefabricated concrete deck element, gap widths ≤ 5 mm, and VT4 was a reference test with an in-situ cast deck slab. These tests are described in detail by Möller et al. (2012).

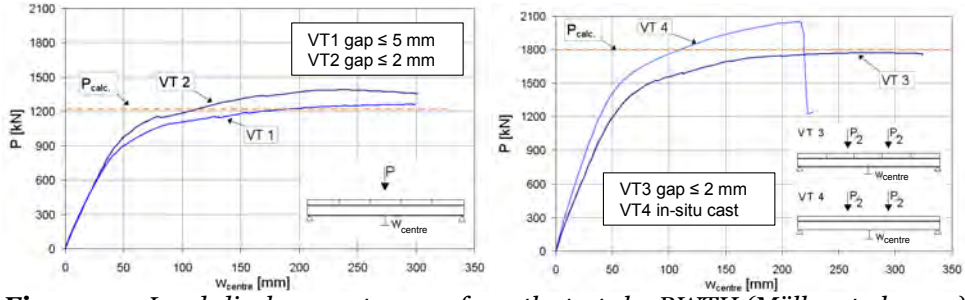

Figure 4.4 *Load-displacement curves from the tests by RWTH (Möller et al. 2012).*

Conclusions

The concrete elements in the specimens tested by RWTH were all cast with a steel-formwork along all sides. This is not recommended, since it is very hard to get a good accuracy of fit in the contact areas between the elements. The elements tested at LTU were match-cast and had, roughly speaking, joint gaps that were 10 times smaller than the gaps on the similar elements

at RWTH. Therefore, it is strongly recommended to use match-casting for this type of element, and to erect the elements with the same configuration as in the match-casting. The problems with concrete spalling, near the joint contact surfaces, will probably be reduced significantly if the joint gap is reduced.
If the elements are match-cast, the stiffness of sections in areas with sagging moments can be estimated by assuming an effective concrete width based on an equivalent length, L_e, equal to the maximum distance between the outermost shear studs. This conclusion is valid for moderate loading, in other words SLS and FLS. In the ULS, the results from the tests by RWTH indicate that it might be ok to use the effective concrete width for an ordinary deck slab given in EN 1994-2. This should however be verified by more tests, and in order to be on the safe side it might be better to assume an interacting concrete width that is 20% smaller than the width given in EN 1994-2.

In areas with hogging moments the influence from the concrete is negligible, and only the stiffness of the steel section should be taken into account. This could be compared with the global analysis according to EN 1994-2 were 15% of the span lengths on each side of the internal supports is considered as having no composite action between the steel and the concrete, only the reinforcement is taken into account.

4.2 Steel strains

In Appendix A section A.3.2 the steel strain measurements are presented more detailed, and the analyses are presented more in detail in **Paper V**.

In this section the steel strains have been transformed into stresses, according to Hooke´s law, assuming E_{steel} = 210 GPa.

Areas with hogging moments

In areas with hogging moments, the vertical stress distribution within the steel girders will be rather close to the case with no interacting concrete at all. There is an enormous shear-lag in the concrete deck, since the stresses enters and leaves the element over a very short distance (1.5 m in the tests). However, a part of the sectional forces will be carried by the concrete. This can be observed in Figure 4.5 - Figure 4.7, which presents the measured steel stresses in different sections from Test 4, which is described in **Paper V**.

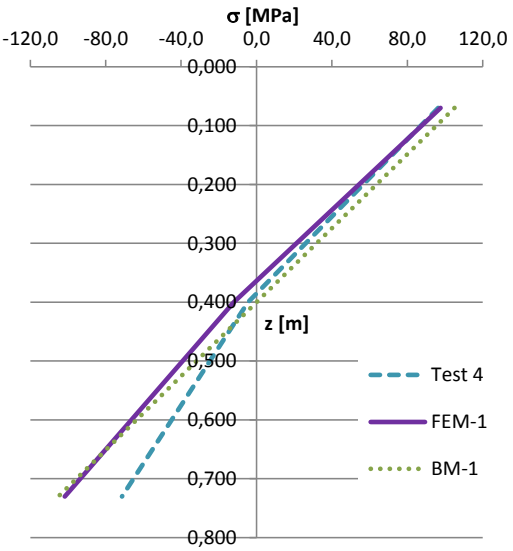

Figure 4.5 *Longitudinal stresses in the web plate, x = 0.050 m Test 4.*

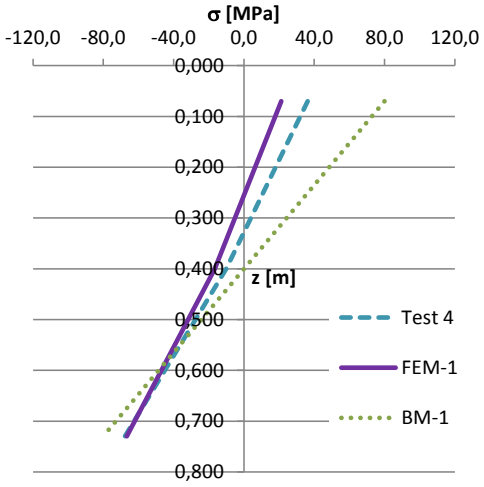

Figure 4.6 *Longitudinal stresses in the web plate, x = 0.850 m, Test 4.*

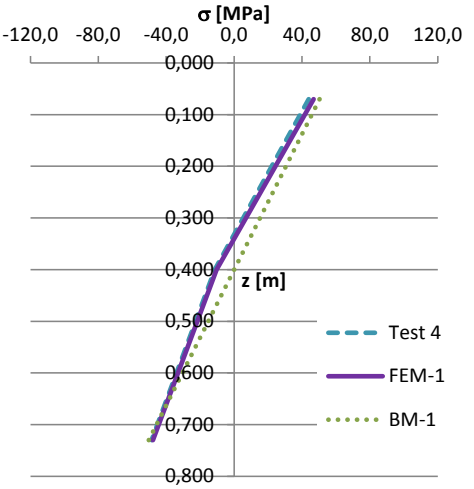

Figure 4.7 *Longitudinal stresses in the web plate, x = 1.800 m, Test 4.*

The relative stress level in the upper part of the web is lower in the middle of the element (x = 0.850 m) compared to the joint sections (x = 0.050 and 1.800 m). The top of the steel girder will profit from the concrete in the middle of the element, but might even be disadvantaged by it near the joints. This phenomenon indicates that the forces carried by the concrete, is unevenly distributed over the steel cross-section, in other words the vertical steel stress distribution is non-linear.

The stiffness measurements, in section 4.1, indicate that it is a reasonable assumption to only use the steel section in the global analysis. This assumption seems applicable also for the stress calculations. In Figure 4.5 - Figure 4.7 the stress distribution in the steel-section is plotted assuming no composite action at all, BM-1. All tests indicate that this assumption is on the safe side, also in the upper flanges near the joints, even if there are stress-concentrations in these areas.

Figure 4.5 - Figure 4.7 also shows the results from a FE-analysis, assuming no longitudinal interaction at all in the joints. The stresses according to the FE-model corresponds rather well to the measured stresses, if the stresses in the bottom flange in section x = 0.050 m is excluded. In this area a thick load distribution plate was used, which probably has interacted with the bottom flange due to friction, and resulted in lower stresses in the bottom of the web. In the FE-model the support was modelled along a single line at x = 0.000 m. Figure 4.8, illustrates the longitudinal stresses from the FE-analysis in the web-plate for the test presented in Figure 4.5 - Figure 4.7.

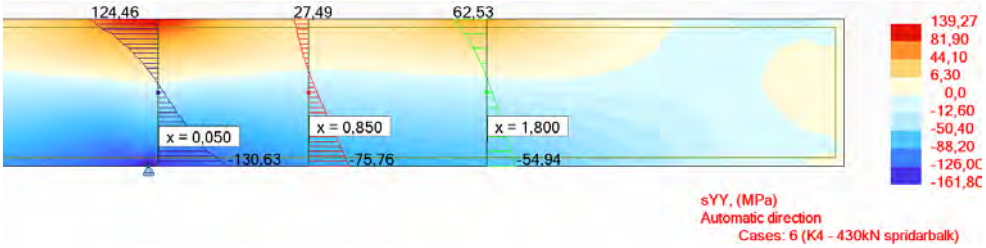

Figure 4.8 *Longitudinal stresses in web-plate, Test 4, FEM-1.*

Areas with sagging moments

In line with the deflection measurements, the steel strain measurements indicate that the effective width of the concrete is less than the effective width according to EN 1994-2. This means that the dry joints will influence the steel-stresses even in sections where the joints are in compression. Figure 4.9 - Figure 4.11 present the measured steel stresses from one of the tests, Test 9.

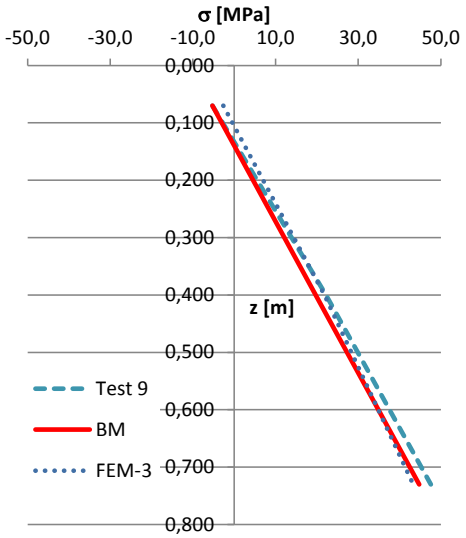

Figure 4.9 *Longitudinal stresses in the web plate, x = 0.050 m, Test 9.*

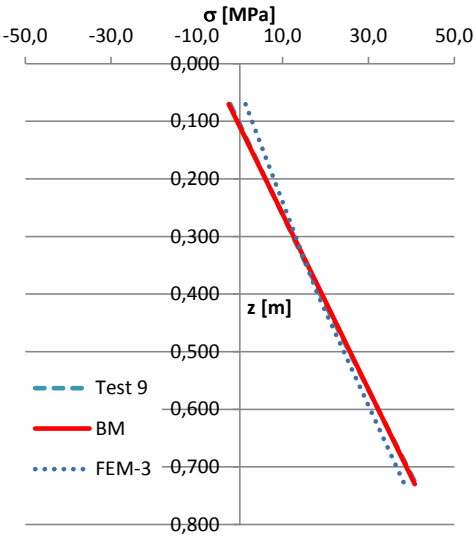

Figure 4.10 *Longitudinal stresses in the web plate, x = 0.850 m, Test 9.*

The measured stress distribution within the steel girder is almost linear, which makes it possible to adapt a beam model to the test results. Together with the test results in Figure 4.9 - Figure 4.11, the results are also plotted for a beam model and a FE-model. The effective concrete width in the beam model has been adjusted to fit the tests results. For section x = 0.850 – 1.800 mm the mean value is 470 mm. This is rather close to the concrete width (513 mm) that is achieved by assuming an equivalent length, L_e, equal to the maximum longitudinal distance between the outermost shear studs within an element (1.5 m). This observation is in line with the results from the deflections measurements.

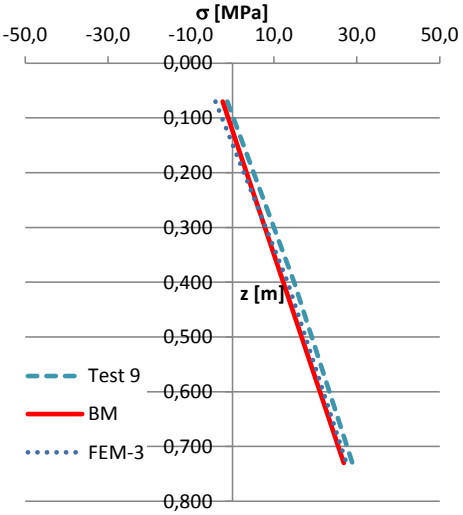

Figure 4.11 *Longitudinal stresses in the web plate, x = 1.800 m, Test 9.*

However, the section x = 0.050 m shows stress levels that indicates a smaller effective concrete width ~330 mm. The stress distribution in this section might however be disturbed by the load that is applied over the distance x = 0.200 – 0.550 m.

In the FE-model, that has been used to simulate these tests, open gaps (0.4 mm) that close under an increasing load have been used. This model describes the measured deflections quite good, but is not better than a simple beam model regarding steel stresses. However, the FE-model indicates that the steel stresses might not be linear in the top of the web, see Figure 4.12. No steel stresses have been measured in the top flange and 50 mm down in the web, it is therefore hard to verify the observation from the FE-model.

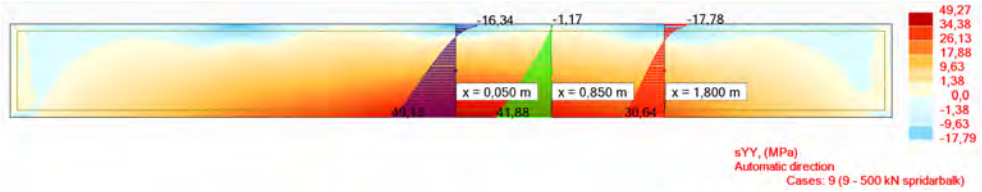

Figure 4.12 *Longitudinal stresses in web-plate, Test 9, FEM-3.*

Conclusion

The steel strain measurements indicate that the conclusions from the previous section about deflections also are valid for the calculations of steel stresses. This means that the steel stresses in sections with sagging moments can be estimated by assuming an effective concrete width based on an equivalent length, L_e, equal to the maximum distance between the outermost shear studs. In areas with hogging moments the influence from the concrete is negligible, and only the steel section should be taken into account when the steel stresses are calculated.

The conclusions above should be ok, as long as the stresses in the outermost fibre are studied. However, if there are some critical fatigue details along the height of the web it might be necessary to perform a FE-analysis, which takes the joint gaps into consideration in order to assure that stress concentrations will not increase the local stress amplitudes around the critical detail.

When the ultimate capacity of a cross-section is studied, the test by RWTH, described in previous section, indicates that it is reasonable to design a composite section according to the rules given in the Eurocodes and neglect the effects from the joints. However, to be on the safe side it might be better to reduce the effective concrete width 20%.

4.3 Joint openings

The joint openings were measured at two joints in the large-scale tests. In the joint between Element 2 and 3, five LVDT´s measured the longitudinal joint opening at the top of the concrete deck. In the joint between Element 3 and 4, three LVDT´s were used in the same way. The test set-up, the measurement equipment and the test results are all presented more in detail in Appendix A section A.3.5.

Areas with hogging moments

The measured joint openings in test set-up 1, at the maximum load in Test 1-8, are presented in Figure 4.13 and Figure 4.14.

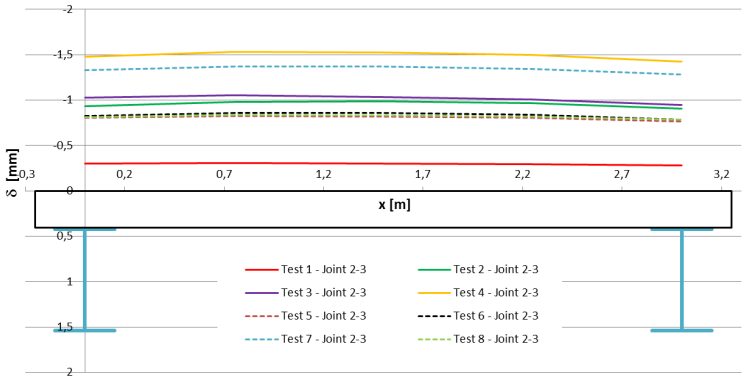

Figure 4.13 *Measured joint openings at Joint 2-3, test set-up 1.*

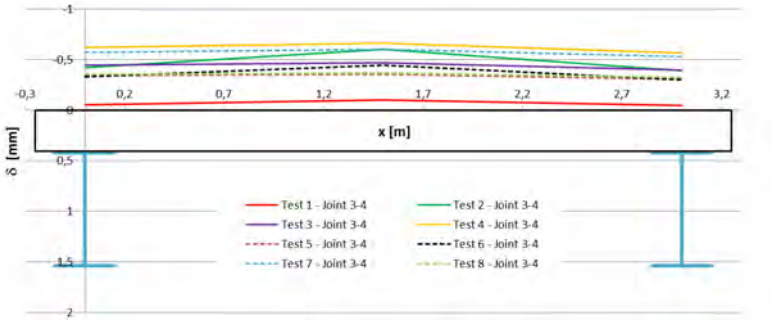

Figure 4.14 *Measured joint openings at Joint 3-4, test set-up 1.*

If the waterproofing layers are fixed to the concrete deck slab, a hogging moment will cause an elongation of the layers over a very short length near the joints. This may result in a rupture of the waterproofing layers and lead to leakage through the joints. Therefore, it is of highest importance to distribute the elongation over a longer distance, which means that the waterproofing layers cannot be fixed to the concrete deck slab near an opening joint. Fatigue tests at KTH (The Royal Institute of Technology, in

Stockholm) have been performed to investigate the durability of different water sealing solutions. The results and the conclusions from these tests are presented in Chapter 7.

The magnitude of the joint openings is of interest as a design criterion for the waterproofing and for the pavement. Therefore, a model to estimate the joint openings has been suggested and compared to the joint openings that were measured during the large-scale tests.

The theoretical joint openings will have a maximum at the internal supports, and can be estimated by Equation 1.

$$\delta_{joint} = \frac{\left(M_{mean} / W_{top.fl}\right)}{E_{steel}} \cdot \frac{\left(e_{CG} + h_{conc}\right)}{e_{CG}} \cdot L_{element} \qquad (1)$$

M_{mean} = mean value of the moment along the length of one element, in this case 50% of the length of the elements on each side of the internal support.

$W_{top.fl}$ = elastic section modulus at the upper side of the top flange, $W_{top.fl} = I/e_{top.fl}$.

e_{CG} = vertical position of the neutral bending axis, 0.400 m in this case with e = 0 at the upper side of the top flange.

h_{conc} = concrete thickness, in this case 0.290 m.

$L_{element}$ = element length, in this case 1.800 m.

E_{steel} = the elastic modulus for steel, 210 GPa.

The results presented in section 4.1, show that it is reasonable to assume no interaction at all between the concrete deck slab and the steel girders. Therefore the joint openings are calculated with a section modulus representing only the steel cross-section. In Table 4.1 the calculated joint openings are presented together with the measured joint openings.

Table 4.1 *Theoretical joint openings vs. measured joint openings, in Joint 2-3.*

	F [kN]	M_{mean} [kNm]	δ_{joint} [mm]	$\delta_{meas.}$ [mm]
Test 1	100	147	-0.38	-0.30
Test 2	280	412	-1.08	-0.95
Test 3	310	456	-1.19	-1.02
Test 4	430	633	-1.65	-1.49
Test 5	250	368	-0.96	-0.80
Test 6	250	368	-0.96	-0.83
Test 7	400	589	-1.54	-1.33
Test 8	250	368	-0.96	-0.81

The measured joint openings are 10-20% smaller than the calculated joint openings. The differences in absolute values are less than 0.2 mm.

Areas with sagging moments

The measured joint openings in test set-up 2, at the maximum load in Test 9-13, are presented in Figure 4.15 and Figure 4.16.

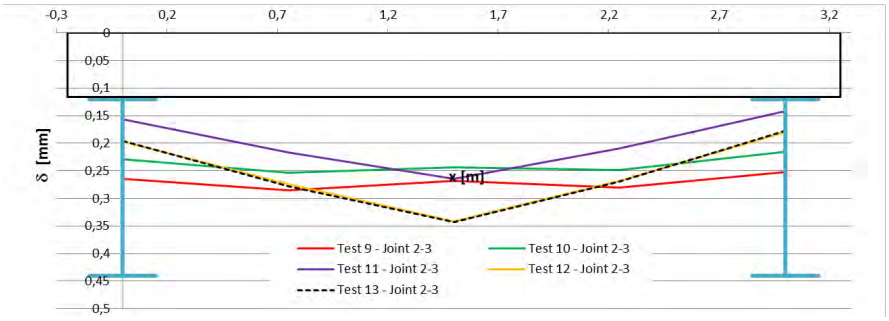

Figure 4.15 *Measured joint openings at Joint 2-4, test set-up 2.*

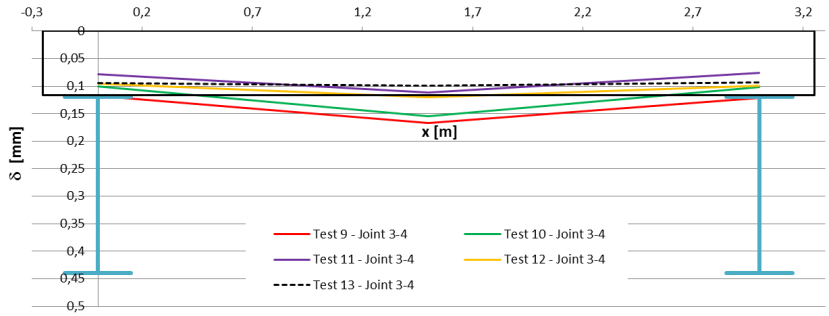

Figure 4.16 *Measured joint openings at Joint 3-4, test set-up 2.*

If the elements are match-cast and the initial joint openings are small, ≤0.5 mm, the joint openings in areas with sagging moment are not believed to be that important for the water insulation layer. The joint openings are however more interesting for the global stiffness behaviour, since the deflection measurements and the steel stress measurements indicate that the effective width of the concrete is far below the effective width for an in-situ cast deck slab.

Conclusions

The test results indicate that a joint opening at an internal support can be estimated by Equation 1, on the safe side. At the design stage, it is therefore suggested that the waterproofing layers are designed to resist the calculated joint opening according to the suggested formula. The design of the waterproofing is a bit out of the scope for this Thesis, but is described briefly in Chapter 7.

4.4 Concrete strains

During the large-scale tests, the concrete strains have been measured at the surfaces of the deck element. How these measurements were done is presented in Appendix A section A.3.3. Below, results from two of the thirteen tests are presented.

Figure 4.17 shows the measured concrete strains for a case with hogging bending moment, test set-up 1 and Test 7, and Figure 4.18 presents the strains for a case with sagging bending moment, test set-up 2 and Test 9. The rest of the results are in line with these two tests, but with some differences depending on how the specimen is loaded (one point load or two point loads). In Appendix A section A.3.3 the concrete strains from all tests are presented.

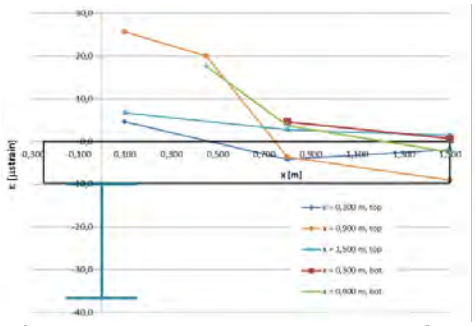

Figure 4.17 *Concrete strains at the max load in Test 7, F_{max} = 400 kN.*

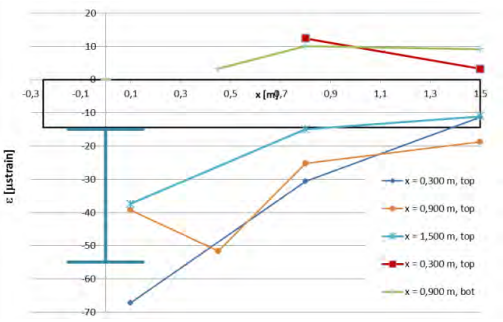

Figure 4.18 *Concrete strains at the max load in Test 9, F_{max} = 500 kN.*

The concrete strain measurements indicate very low concrete stresses both in tension and compression. The maximum tensile stress measured in the concrete was 1.6 MPa in test set-up 1, and the maximum compressive stress was less than 2.5 MPa in test set-up 2. All strains have been transformed into stresses using the mean value of the measured concrete E-modulus, E_{conc} = 35.0 GPa

All test-results from set-up 1, with hogging moments, indicate that the composite action between the steel and concrete is very limited. If the measured stresses in the concrete surface are plotted in a 3D-diagram, see Figure 4.19, it is quite obvious that there is a significant difference in the composite action within an element, along the longitudinal axis. The shear-lag is also very large, since the distance between the outermost shear studs within an element is very short. The very small strains measured at the concrete surface in the middle between the steel girders are actually compressive strains. However, the contribution from the concrete to the global stiffness and to the cross-sectional capacity is negligible in all

sections with hogging moment. Therefore there is no need of a model that describes the shear-lag in these sections perfectly.

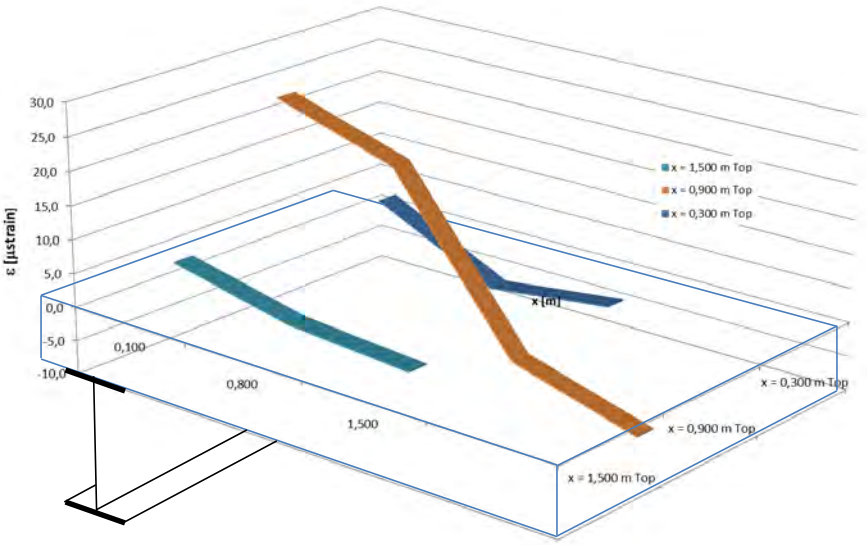

Figure 4.19 *3D-diagram of the measured concrete strains in Element 3, Test 7.*

The test results from test-set up 2 shows a more normal distribution of the shear-lag. The area of interacting concrete is however a lot smaller than a similar section in an in-situ cast bridge, which is in line with the results presented in previous sections.

In the cases with a point load (Test 11-13) very high strains have been measured in the bottom of the concrete slab, see Figure A.40 - Figure A.42 in Appendix A. These strains indicate that there were tensile stresses in the bottom of the deck element that exceeded the tensile strength of the concrete. This effect has only been discovered directly below the loading point.

4.5 Reinforcement strains

The results from the strain measurement on the reinforcement bars are presented in Figure 4.21 and Figure 4.22. The strain gauge named FA3 did not work properly during the test. Therefore, this measuring point has been excluded from the test results. When the strain distribution are plotted over the cross-section of the bridge, the value of FA4 have been used also in the position of FA3, in order to make it easier to see if the other results are symmetric or not. FA3 and FA4 are located on the neighbouring rebars, with only 150 mm distance between them, see Figure 4.20. In Appendix A section A.3.4 a detailed description of the tests is given, together with a presentation of the results.

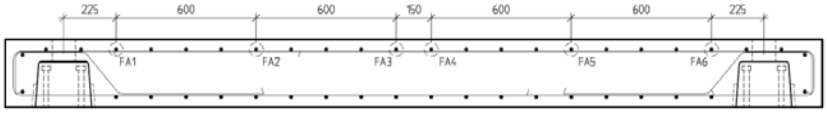

Figure 4.20 *Positions of the strain gauges FA1-6, located in x = 0.900 m.*

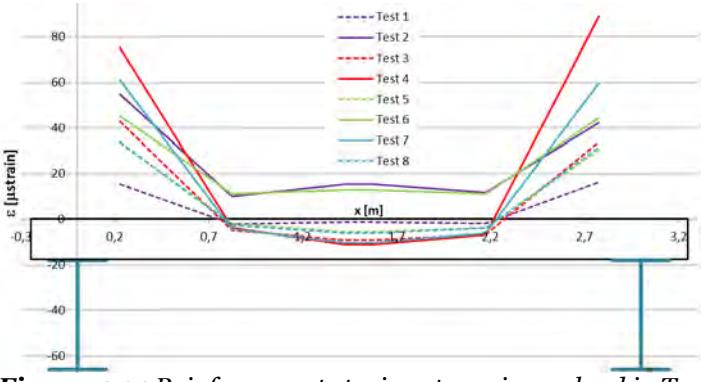

Figure 4.21 *Reinforcement strains at maximum load in Test 1-8, test set-up 1.*

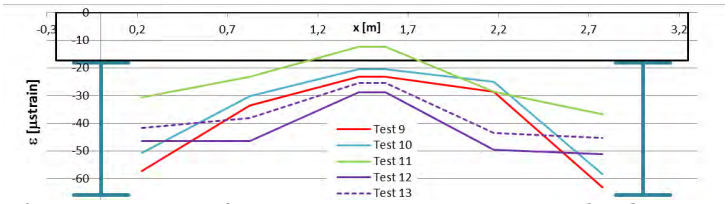

Figure 4.22 *Reinforcement strains at maximum load in Test 9-13, test set-up 2.*

The results from the reinforcement strain measurements are in line with the results from the concrete strain measurements.

It can be noted that the longitudinal strain distribution over the cross-section is a bit disturbed when a point load is used in the middle of an element (Test 1, 2, 6, 11-13). This could be compared to the cases with two point loads on top of the steel girders (Test 3-5, 7-10).

4.6 Shear studs

In the large-scale test performed in year 2011, the shear transmission was not investigated. Previous tests performed at LTU in year 2001, have however been focused on the fatigue of the shear studs. The results from these tests are given in Stoltz (2001) and have also been studied and summarised by Hällmark et al. (2009).

In areas with hogging moment it is strongly suggested that the concrete deck slabs are properly connected to the steel girders, by shear studs, even if the transmission of shear forces between the steel and the concrete are very limited.

In areas with sagging moments, no differences are made between an in-situ cast bridge and a bridge of the type studied in this thesis.

The shear transmission in this type of bridges is a recommended area for future research, since the performed large-scale tests show that even joints in compression interferes the assumed stress trajectories and increases the stresses in the upper part of the steel girders. The joints will most likely increase the shear forces transferred by the adjacent shear studs. To which extent this will influence the design in SLS and FLS has not been investigated yet. In ULS, tests shows that the cross-section behaves very similar to a cross-section with an in-situ cast deck slab, which makes it reasonable to believe that the shear studs can be designed assuming an in-situ cast deck in the ULS.

5 Shear keys

In the studied joint, shear keys are used to transfer vertical and lateral forces through the transverse joint, and to prevent vertical displacements between the deck elements at the joints. The shear keys are designed as a series of overlapping male-female connection along the transverse joint, see Figure 5.1.

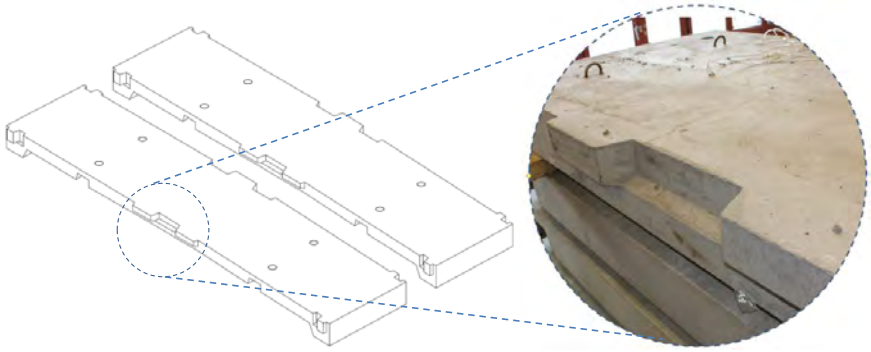

Figure 5.1 *Dry joints with shear keys.*

In order to better understand how the shear key fails statically and to be able to predict their static capacity with a rational design rule, laboratory tests have been performed.

Paper III describes these tests in detail, and the following sections give a summary of the tests and some discussions about the outcome.

The fatigue capacity of the shear keys have been tested in large-scale tests by Stoltz (2001). The fatigue test results are also presented by Hällmark et al. (2009) in **Paper I**.

5.1 Design criterion

In order to be able to establish whether or not the shear keys have a sufficient capacity to transfer the shear forces over the dry joints, the maximum force in the shear key must be estimated. This can be done by using a simple FE-model representing the studied superstructure. Below an example is given for the element type used in Sweden so far.

The studied bridge has a free width of 7.0 m and a superstructure made of 1.8 m long prefabricated concrete deck elements, on top of two steel I-girders with a spacing of 4.0 m. The deck elements are made of C40/50 concrete with a varying thickness, 300 mm in the centreline and 216 mm in the thinness parts near the edge beams, see Figure 5.2.

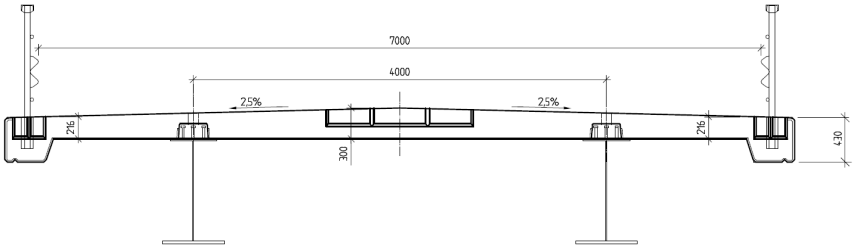

Figure 5.2 *Geometry of the studied superstructure.*

The suggested FE-model is kept as simple as possible, in order to be able to be useful in real bridge design situations. A series of deck element (5 in this case) are modelled as simply supported by the steel girders in the transverse direction. The steel girders are just modelled as linear supports for the concrete elements. In the transverse joints, the elements are connected only in the position of the shear keys. This is done by rigid elements that only transfer vertical forces over the joints.

In Figure 5.3 the middle element is loaded. The elements to the left are modelled with a single shear key in the middle, while the elements to the right are modelled with two shear keys. This is in line with the Swedish design of dry joints, which has been illustrated in Figure 5.1. All elements have also rigid links in the edge beams, since there is a male-female key in each edge beam.

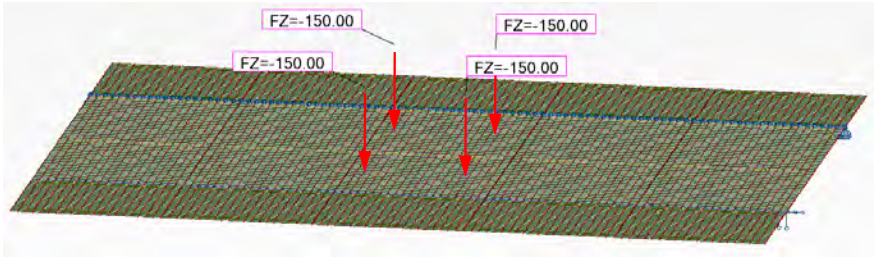

Figure 5.3 *FE-model for estimation of the force transfer over a dry joint.*

Table 5.1 presents the shear force transferred by the shear keys, when the middle element is loaded with traffic load 1 and 2 (LM1 and LM2) given in EN 1991-2. The characteristic values have been used, which means that all α-factors are set to 1.0. Figure 5.4 shows the worst load situation for the large shear keys.

Table 5.1 *Shear forces transferred by the shear keys [kN].*

		Large shear key		*Small shear keys*	
		LM1	LM2	LM1	LM2
Axle loads	2x300 kN	109.8	-	73.6	-
Axle load	400 kN	-	104.2	-	75,4
Lane load 1	9.0 kPa	9.5	-	5.5	-
Lane load n	2.5 kPa	0.2	-	0.1	-
	V_{Sd} =1.5 x Σ =	**179.1**	156.3	**118.8**	113.0

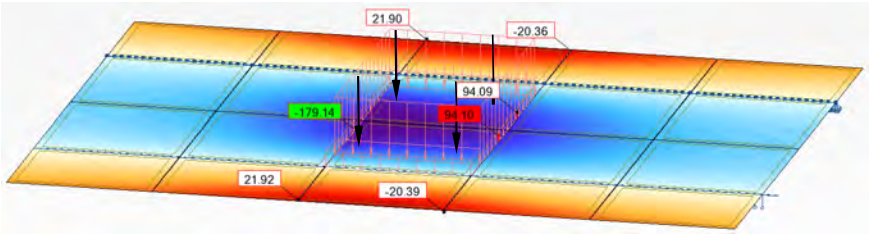

Figure 5.4 *Illustration of the worst load situation for the large shear key, LM1.*

This means that the shear key capacity, for the studied bridge, must be higher than 180 kN.

5.2 Laboratory tests

The tests presented in this chapter were performed by Complab at Luleå University of Technology in 2010.

5.2.1 Test specimens

The test specimens were designed in order to get results that were representative to the shear failure capacity. In an early stage it was discussed how to perform a small-scale test only focusing on the shear key capacity. As a first approach, punch-out tests were considered, see Figure 5.5:a. However, in order to assure that the load is not transferred directly into the supports, by inclined compressive struts, the specimen must be made longer. But if the specimens are made longer, it was believed to be better to skip the punch-out test, and instead perform a test on a simply supported strip of a real deck slab. Therefore, the test specimens were designed for a test set-up as shown in Figure 5.5:b. This design makes it possible to test two shear keys on each specimen, by using an extra vertical support.

The expected failure was a shear failure, activating the SX-rebars (blue) and the C-rebars (green) in Figure 5.6.

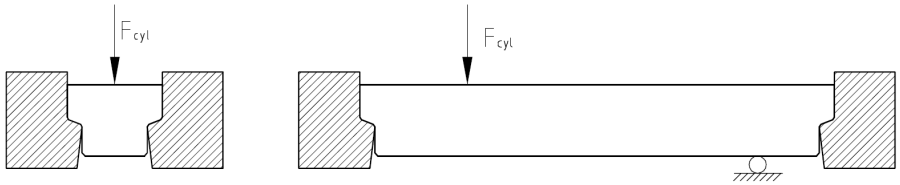

(a) Punch-out test. (b) Final design of the test.

Figure 5.5 *Different kind of tests that were evaluated.*

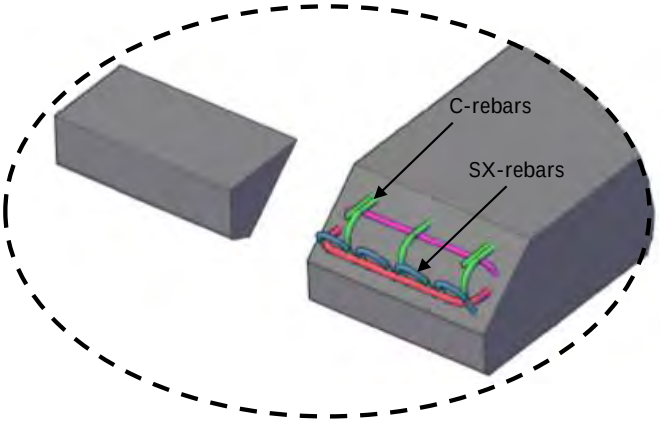

Figure 5.6 *Expected shear failure showing the reinforcement in the crack plane.*

In order to avoid discussions about scale effects, the shear keys in the test specimens were made in scale 1:1, compared to a real bridge element. The studied shear key has a width of 540 mm, and the first approach was to use a specimen with the same width as the shear key, Figure 5.7:a. In order to not underestimate the load distribution effect, it was decided to widen the specimens to a total width of 1 300 mm, Figure 5.7:b. The recesses for the shear keys from the adjacent element, was however believed to affect the result. Therefore the recesses were included in the final design, Figure 5.7:c.

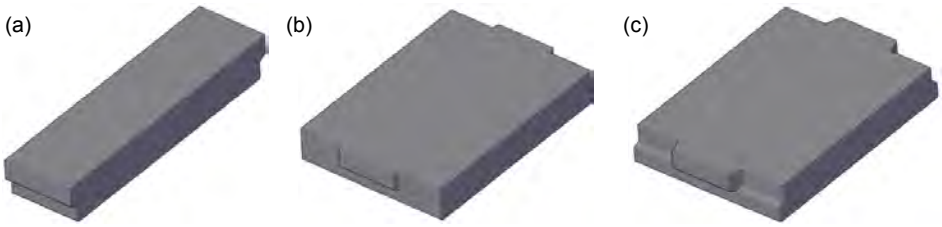

Figure 5.7 *Different types of specimens evaluated before the tests started.*

Three of six specimens were made according to the design in Figure 5.7:b, since the concrete prefabrication workshop had already started their production before the final drawings were delivered. The remaining three specimens were made with the design shown in Figure 5.7:c. The geometry and the reinforcement drawings of the test specimens are presented in detail in **Paper III**. Table 5.2 summarises the varied parameters of the test specimens.

Table 5.2 *Parameters of the shear key test specimens.*

	Shear key 1	Shear key 2	Shear key 3
Number of tests	4	4	4
Element type no:	1	2	2
Recesses	No	No/Yes	Yes
Materials			
Concrete	C30/37	C30/37	C30/37
Reinforcement	B500B	B500B	B500B
Varied parameters			
Ø -SX1 [mm]	12	8	-
Ø -E2 [mm]	16	12	-

SX and E – Swedish labels for the type of looped rebars that are used in the shear key.
These two types of rebars are illustrated in Figure 7.2 and also in Paper III, Figure 10 and 11.

5.2.2 Test set-up

The test specimens were placed in a rig that consisted of two concrete supports on top of a steel frame. Since each specimen had two shear keys, the first test must be performed without affecting the second shear key. Therefore, an extra vertical support was added to the test rig. Then, the first shear key was loaded until failure. After that the vertical support was moved to the other side of the specimen, which was adjusted to fit properly to the support at the tested side. Figure 5.8 shows a schematic illustration of the test set-up.

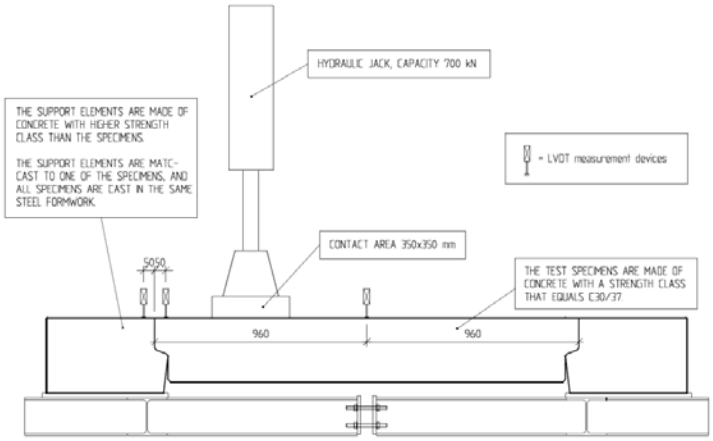

Figure 5.8 *Schematic illustration of the test set-up.*

Despite the load and the stroke in the jack, deformations were measured in 10 points. This was done in order to see how the element deflected under the load, and to be able to filter out the undesired deflections, in the floor and the test rig, from the test results. All tests were deformation controlled with a stroke of 0.02 mm/s.

5.2.3 Results

Two different kinds of failures were observed in the tests. The first type of failure was ductile, with crack planes that crossed the shear reinforcement (SX-bars). This type of failure was observed in 5 of 8 reinforced shear keys. The other type of failure was more brittle and the concrete covering layer in the shear key was separated from the concrete by crack planes. This type of failure was observed in 3 of 8 reinforced shear keys.

Figure 5.9 and Figure 5.10 show the load-deformation curves for the tests of the reinforced shear key type 2 and the unreinforced shear key type 3.

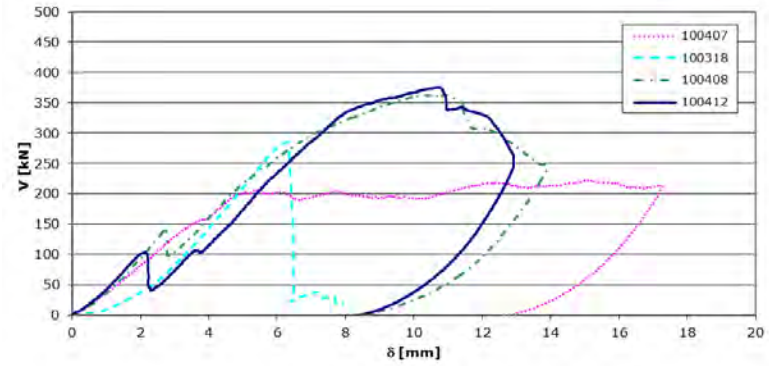

Figure 5.9 *Load-deformation curve for shear key type 2.*

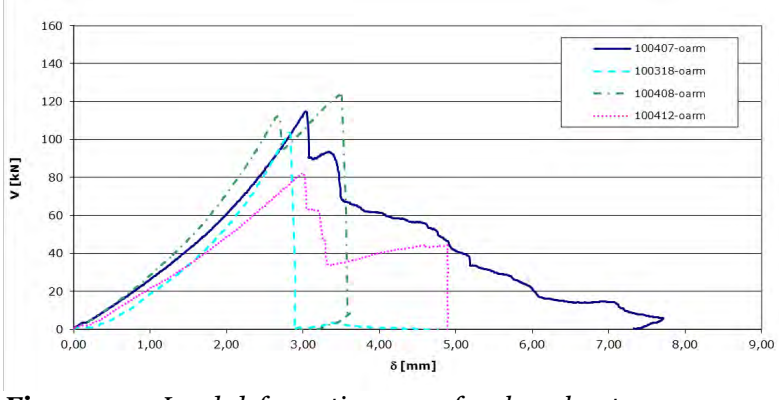

Figure 5.10 *Load-deformation curve for shear key type 3.*

Two of the shear keys of type 2 failed in the concrete covering layer, SK2:1 and SK2:2. The failure load was higher than the failure load for an unreinforced concrete shear key, but far below the capacity of the shear keys that failed more ductile. In the case with SK2:1, the test rig was not fixed properly, and there were some undesired lateral movements, which can explain why the load-deformation curve has a wide plateau after the failure.

From the tests of the unreinforced shear keys it can be noted that three of four tests indicate a post failure capacity, while the fourth shear key failed in a very brittle mode.

Figure 5.11 shows pictures of the shear keys, type 2 and 3, after the tests.

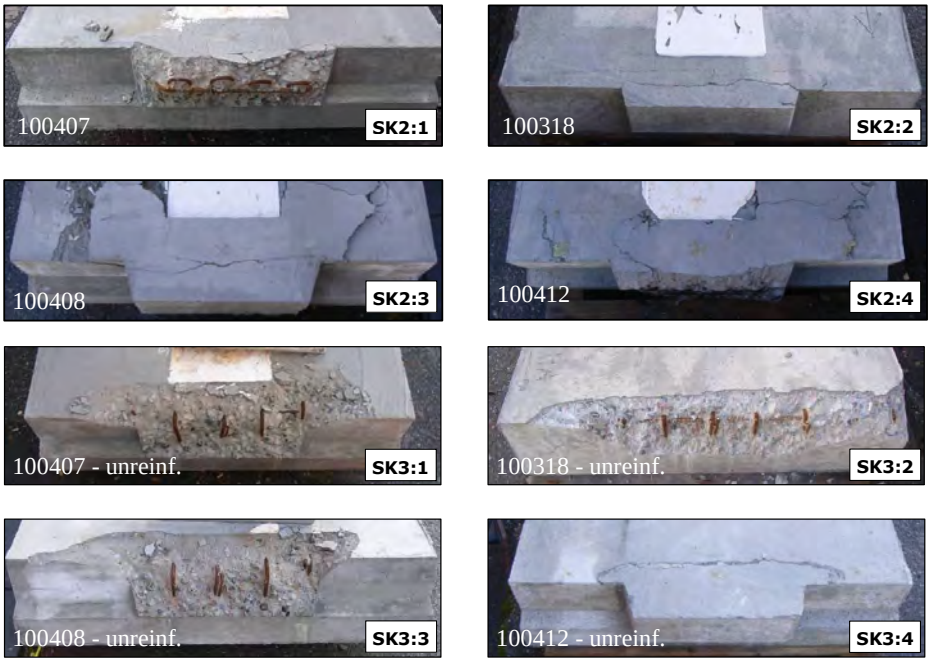

Figure 5.11 *Picture of shear keys of type 2 and 3, after the tests.*

5.2.4 Analysis

One of the aims of the tests was to find a rational design model for the shear keys. Below, the hour different models have been compared.

1. Classic beam linear elastic analysis – SK3 (concrete capacity)

This model is based on models from a Swedish concrete design guidebook, *Betonghandboken* (1990).

$$V_{Rd,c} \le \frac{1}{3} b_w h f_{ct} \quad (2)$$

b_w = the smallest width of the cross-section within the effective height

h = the height of shear key

f_{ct} = is the splitting tensile strength of the concrete

2. EN 1992 – SK1 and 2 (concrete capacity)

$$V_{Rd,c} = b_w d f_v \quad (3)$$

$$f_v = 0.3 \cdot \xi \cdot (1 + 50\rho) f_{ct} \quad (4)$$

$$\rho = A_{s0} / (b_w \cdot d) \le 0{,}02 \quad (5)$$

ξ = 1.4 when d ≤ 0.2 m

b_w = the smallest width of the cross-section within the effective height

d = effective height

f_v = shear strength of the concrete

f_{ct} = tensile strength of the concrete

A_{s0} = bending reinforcement area in the tensile part of the studied cross-section

3. EN 1992 – SK1 and 2 (reinforcement capacity)

$$V_{Rd,s} = \frac{A_{sw}}{s} z f_{ywd} (\cot\theta + \cot\alpha) \sin\alpha \quad (6)$$

A_{sw} = the area of the shear reinforcement

f_{yw} = the yield strength of the shear reinforcement

s = the rebar spacing

z = internal lever arm for bending moments

θ = the angle of the shear crack

α = the inclination of the shear reinforcement

When shear reinforcement is used locally, with inclined rebars in one line, the equation above can be simplified to:

$$V_{Rd,s} = A_{sw} f_{ywd} \sin\alpha \quad (7)$$

4. Force equilibrium model.

A force equilibrium model has also been evaluated. This model includes both the reinforcement bars and the compressive struts in the concrete.

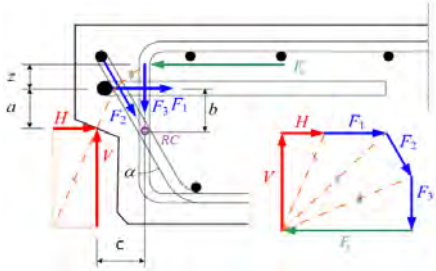

Figure 5.12 *Illustration of the force equilibrium model.*

Table 5.3 presents the results from the different design models compared to the test results.

Table 5.3 *Test results vs. calculations models.*

Cast date	Test results V_{max} [kN]			Model 1 V_{max} [kN]				Model 2 V_{max} [kN]				Model 3 V_{max} [kN]				Model 4 V_{max} [kN]			
2010-	SK1	SK2	SK3	SK1	SK2	SK3	η^*	SK1	SK2	SK3	η^*	SK1	SK2	SK3	η^*	SK1	SK2	SK3	η^*
03-15	449	-	-	80	-	-	*5.61*	*84*	-	-	*5.36*	392	-	-	*1.15*	561	-	-	*0.80*
03-15	337	-	-	80	-	-	*4.21*	*84*	-	-	*4.03*	392	-	-	*0.86*	561	-	-	*0.60*
03-16	532	-	-	83	-	-	*6.41*	*88*	-	-	*6.07*	392	-	-	*1.36*	561	-	-	*0.95*
03-16	370	-	-	86	-	-	*4.30*	*88*	-	-	*4.22*	392	-	-	*0.94*	561	-	-	*0.66*
03-18	-	285	-	-	68	-	*4.19*	-	*73*	-	*3.88*	-	174	-	*1.64*	-	344	-	*0.83*
03-18	-	-	104	-	-	68	*1.53*	-	-	73	*1.42*	-	-	0	-	-	-	0	-
04-07	-	222	-	-	63	-	*3.52*	-	67	-	*3.30*	-	174	-	*1.28*	-	344	-	*0.65*
04-07	-	-	114	-	-	63	*1.81*	-	-	67	*1.70*	-	-	0	-	-	-	0	-
04-08	-	363	-	-	77	-	*4.71*	-	82	-	*4.42*	-	174	-	*2.09*	-	344	-	*1.06*
04-08	-	-	123	-	-	77	*1.60*	-	-	82	*1.50*	-	-	0	-	-	-	0	-
04-12	-	376	-	-	68	-	*5.53*	-	71	-	*5.30*	-	174	-	*2.16*	-	344	-	*1.09*
04-12	-	-	82	-	-	68	*1.21*	-	-	71	*1.16*	-	-	0	-	-	-	0	-

* η = test result divided by the predicted value for the given calculation model.

When the test results were compared to the calculations model, the following were noted.

- Model 1 and 2 can be useful for estimating the strength of shear keys without reinforcement.
- Model 3 gives results on the safe side, except when the failure occurs in the concrete covering layer.
- Model 4 gives often results on the unsafe side. This indicates that the vertical reinforcement bars, which are included in this model, do not influence the load carrying capacity as much as assumed in the model.

5.3 FE-analyses

The tests of the shear keys have been complemented by non-linear FE-analyses. This has been done in order to study different types of reinforcement layouts, and in order to get a better understanding of how the forces are distributed between the rebars.

During year 2012, Professor Mikael Hallgren (KTH) has supported this research project by performing non-linear FE-analysis of the tested shear keys. The analyses have been made in the software ATENA, using a smeared crack approach in a model that includes the individual reinforcement bars. The measured concrete parameters have been used as input to the model. Figure 5.13 illustrates the model, which is made as a half of the tested element, making use of the symmetry axis.

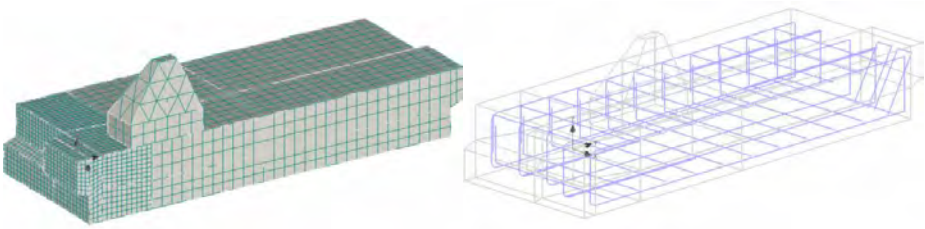

Figure 5.13 *FE-model of the shear key tests.*

At the moment when this thesis is written, the FE-analyses of the tested shear keys have just been finished. The first results from the modelling of the unreinforced shear keys, indicates a good agreement between the tests and the FE-model. The ultimate load capacity in the FE-model is 124 kN, which shall be compared to the test results 82 – 123 kN. The analysis indicates also that the shear keys have a post failure capacity of ~100 kN. Figure 5.14 shows the load-deformation diagram from the FE-model.

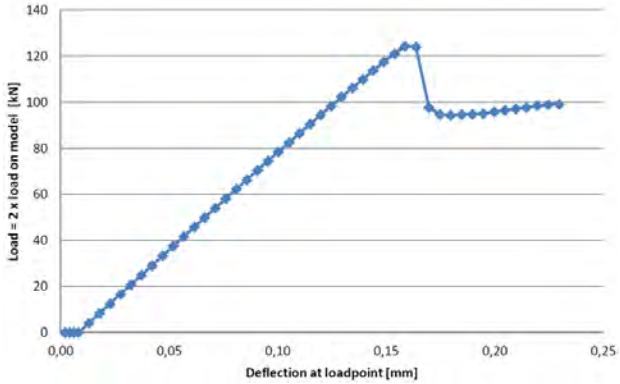

Figure 5.14 *Load-deformation diagram from the FE-analysis.*

Despite the ultimate capacity of the shear key, the crack pattern has also been compared to the test results. It can be noted that the final failure in the FE-model is very similar to the failure observed in the tests. In Figure 5.11 photos of the unreinforced shear keys are presented, SK3. These photos can be compared to the crack pattern at the ultimate load in Figure 5.15:a and the crack pattern at the final failure in Figure 5.15:b.

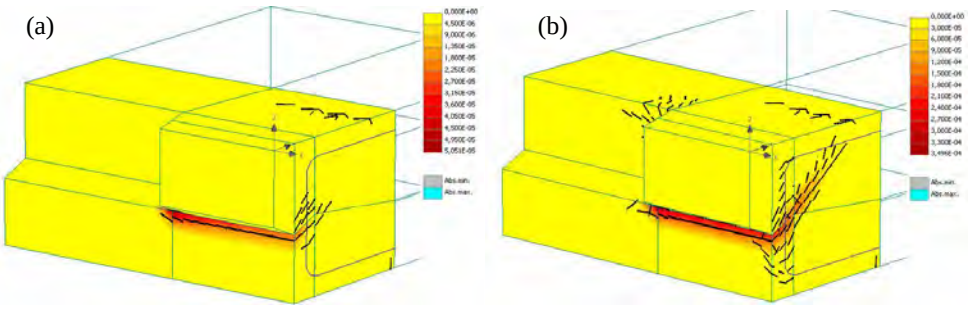

Figure 5.15 *Crack pattern at the ultimate load (a) and at final failure (b).*

The FE-analyses will continue and a new reinforcement layout will hopefully be presented in a paper later and also tested in the laboratory.

5.4 Discussion

The test results show a considerable scatter, which makes it hard to establish any general design rule. Still there are some interesting points that can be noted.

It is obvious that unreinforced shear keys is not strong enough to transfer the traffic loads given in EN 1991-2 and in section 5.1. This is in line with all design models, and the expected results.

Concerning the reinforced shear keys, all shear keys show a sufficient capacity compared to forces that is expected due to the loads given in EN 1991-2 and section 5.1. With the knowledge available today, it is recommended to design the shear keys according to the formulas for inclined shear reinforcement in EN 1992-1-1, presented in Equation 7.

Another interesting thing is the fact that all shear keys that failed in the concrete covering layer transferred forces a lot higher than the concrete capacity. Thus, the reinforcement must have been activated, and should be included in the design formula in some way. It is also obvious that it is of highest importance that failures in the concrete covering layers can be avoided.

When a whole joint has been tested in the laboratory (Stoltz 2001, Hällmark et al. 2009) the failure of the shear keys has never involved cracking of the concrete covering layer. The cracks have been developed from the bottom of the shear keys and up to the concrete surface, and have always activated the reinforcement. After the large-scale tests, described in Chapter 4 and Appendix A, were finished, a joint was loaded until a final failure in the shear keys. Also in this test there were no sign of cracking in the concrete covering layer.

In the reality, at least for single span bridges, it is most likely so that the shear key capacity will be higher than the test results in this chapter indicate. This statement is based on the fact that the surrounding elements, in a real case, will deflect together with the loaded element. This behaviour should result in longitudinal clamping forces which would counteract the tensile stresses that occur due to the shear forces. Figure 5.16 illustrates some differences between the test set-up and the reality.

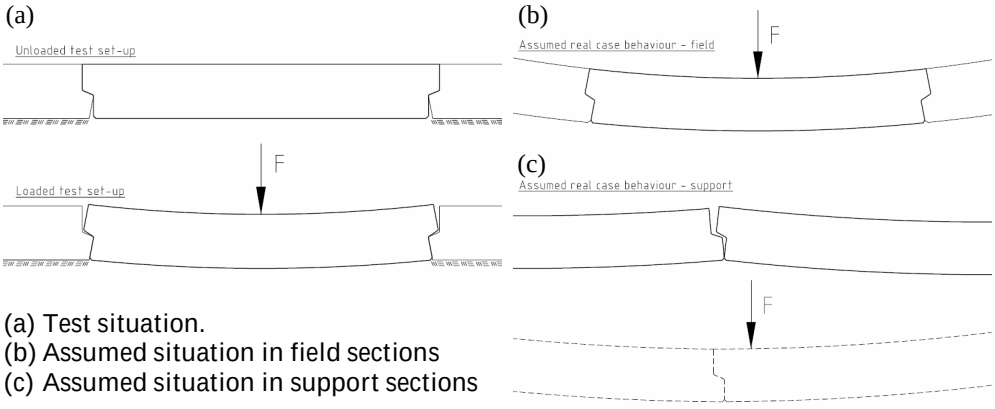

(a) Test situation.
(b) Assumed situation in field sections
(c) Assumed situation in support sections

Figure 5.16 *Differences in the structural behaviour between the test set-up and real situations.*

The behaviour in (a) and (b) is rather easy on understand. But the behaviour in (c) is more complex. If dry joints above internal supports shall be open, there must be a load in the field section of the bridge. However, this load case involves only a very small load transfer through the shear key. The shear keys in the open joint will only experience a significant load when the elements adjacent to the joint, or the nearest elements, are loaded. This means that a local action must be superposed on the global action. The real situation will probably be somewhere between the two illustrations given in Figure 5.16:c.

To assure the robustness of the shear transfer in a situation with a failure in the shear key, it is very important to assure that the rebars in the shear keys are overlapping the rebars in the supporting element, see Figure 5.17. If the rebars are not overlapping, one should assure that a failure in the concrete covering layer cannot occur. Longitudinal compressive stresses in the joints will be beneficial. This is always achieved in single span bridges and in midspan sections in multi span bridges. If necessary, compressive forces could be achieved near the internal supports by longitudinal pre-stressing tendons.

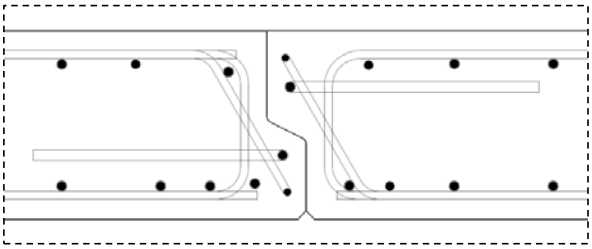

Figure 5.17 *Illustration of a joint with overlapping reinforcement bars.*

The previously performed fatigue tests and the static tests in this section show that the previously used shear keys, SK1, has sufficient capacity to transfer the forces given in EN 1992-1. The static tests also indicates that it would be possible do decrease the amount of shear reinforcement in the shear keys. However, if the shear reinforcement bars are changed from Ø12 mm to Ø8 mm, the saving will be less than 20 kg/element, for an element of the type previously used in Swedish bridges.

Further research will focus on how to optimize the reinforcement. Section 5.3 gives a brief view of the work that has already started.

6 Field monitoring – Rokån Bridge

Back in year 2000 a single span bridge was built in Northern Sweden, with the prefabricated deck system described in this thesis. In order to study the structural behaviour of this system, this bridge was monitored in 2001. This field monitoring together with several laboratory tests have all been focused on the short-term behaviour, except the fatigue test (by Stoltz) presented in **Paper II**. Therefore, a second field monitoring was performed in year 2011 in order study if there are any significant long-term effects that have been missed, since the other tests all have been focused on short-term effects.

Paper IV describes the field monitoring in detail, and the following sections gives a brief summary of the tests and discuss the results. Figure 6.1 shows one of the load positions during the field monitoring in year 2011.

Figure 6.1 *Picture from the field monitoring in year 2011.*

6.1 Rokån Bridge

The monitored bridge, Rokån Bridge, was built in year 2000 as a pilot object for the prefabricated concrete deck system with dry joints. In this case, not only the deck elements were prefabricated. The wing-walls as well as the supports were prefabricated. Stoltz (2001) and **Paper I** describes the erection of this bridge, which was actually performed in 30 hours.

The superstructure of this bridge is made of prefabricated concrete deck elements on top of two steel I-girders, see Figure 6.2. This is the typical layout for the superstructure that this thesis is limited to. The bridge has a free width of 7.0 m and a span length of 16.2 m.

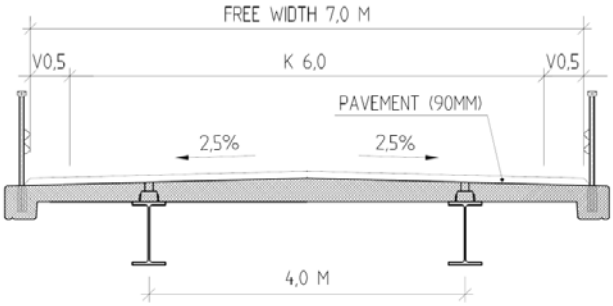

Figure 6.2 *Cross-section drawing of the Rokån Bridge.*

6.2 Test set-up

The monitoring was focused on two specific things, the deflections and the steel strains. In order to make it easier to compare the test results, from year 2001 and 2011, the LVDT-sensors as well as the strain gauges were all placed in the same positions in both tests. The deflections were measured at the supports and in midspan on both girders, and the steel strains were measured in three sections along one of the girders and in two sections on the other. Figure 6.3 shows a schematic sketch of how the bridge was monitored.

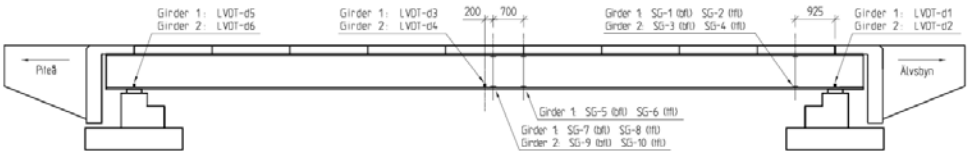

Figure 6.3 *Elevation drawing presenting the measurement equipment.*

6.3 Tests

The new field tests were performed in the early summer of year 2011 by the staff at the Complab Laboratory, LTU. Before the tests started the truck was scaled and the aimed load positions were marked on the pavement in both longitudinal and transverse direction. The truck was driven along three longitudinal lines over the bridge, the centre line of the deck and the centre line of each girder, making two stops along each line. The first stop was when the front axle was in the middle of the span, and the second stop was when the bogie was centred at midspan. A similar load pattern was used in year 2001.

6.4 Results

The test results from 2011 indicate a very symmetric behaviour when the bridge was loaded along the centreline. Unevenly distributed deflections and stresses, due to varying contact in the transverse joints, have not been found. The same goes for the eccentric loading above each girder. One test result is almost the mirror image of the other.

Concerning the stress distribution within the steel, all tests indicate that the neutral bending axis is located about 100 mm below the top of the upper flange.

6.5 Analysis

The test results have been compared to a simple beam model, which is the way that this bridge originally was designed, and to FE-models. All models are made with a continuous concrete deck with no gaps.

The analyses have been focused on the deflections as well as the interacting concrete area, and are presented in **Paper IV**. In the next section, the most important results from the analysis and the measurements are discussed.

6.6 Discussion and conclusion

The general conclusion is that all models that do not include the soil pressure behind the back walls overestimates the deflections and steel stresses in midspan a lot. This conclusion is general for all composite bridges of this type, and not specific for the studied prefabricated deck system. For eccentric loading the beam model gives deflections and steel stresses that are more than 50% higher than the measured values. It is

quite obvious that the back walls and the warping/torsional stiffness of the superstructure distribute the load effects between the girders.

Another interesting thing is the fact that all design models, beam model or FE-models, have their neutral bending axis positioned about 100 mm higher than the measured position on the bridge. This indicates that all design models, that assume a continuous deck with no gaps, overestimate the interacting concrete area. This is believed to be caused by the gaps in the joints, in combination with the continuous in-situ cast concrete in the injection channels. After the channels have been injected, existing gaps will be more or less permanent, since the in-situ cast concrete must be compressed up to a certain limit before the rest of the joint will be closed. This effect will however be counteracted by higher concrete creep in the most loaded parts of the joint. Still, after 11 years in service, the interacting concrete area is about 50% of the interacting area in the beam model. Therefore it is reasonable to recommend a reduction of the interacting concrete for design in SLS (Serviceability Limit State) and FLS (Fatigue Limit State). This is discussed more in Chapter 7.

Concerning the long-term effects, it has been noticed that the distribution of the deflection between the loaded girder and the passive girder have changed from year 2001 to 2011. In the earlier tests the relative deflection of the passive girder was about 0.4 and in the latter tests 0.3. The measured scatters in these distributions are very small, with magnitude of +/- 0.01. This difference might indicate that there were larger joint gaps back in year 2001, that have been at least partly closed during the time elapsed between the tests (10 years). One possible explanation is that there has been an abrasion of irregularities at the concrete contact surfaces, giving a better distribution of forces over the joint. If this is the case, the deflection of the unloaded bridge should be a bit higher today. Since the absolute vertical position of the girders, has not been measured in 2001, it is hard to verify this effect. And even if all data was available, it would be hard to distinguish this effect among the ordinary concrete creep that increases the deflection due to the dead load.

7 Design and production issues

This chapter gives a resume of the rest of the thesis by giving some suggestions of how to deal with general design and production of composite bridges with prefabricated concrete deck elements with dry joints. The suggested models and advices are based on the results from laboratory tests, field monitoring and the design of three single span bridges of this type.

The design methods are in general the same as for a conventional composite bridge with an in-situ cast deck slab. Therefore, this section deals only with the design steps where differences have been discovered. Parts of this chapter have also been added to a design guide regarding *"Design of Composite Bridges with Prefabricated Decks"*, which is an outcome of the European research project ELEM, RFSR-CT-2008-00039.

7.1 Global analysis

The global analysis should be performed according to EN 1994-2. However, some parts need to be modified to better describe the behaviour of this type of construction. Below, some of the most important modifications are described.

EN 1994-2 5.4.1.2
Considering sagging bending moment, bridges of this kind behave rather similar to composite bridges with in-situ cast decks.

ULS – sagging moments
In the ULS it is suggested to use the formulas given in EN 1994-2 for calculating the effective width of the interacting concrete and the equivalent span length, L_e, see Figure 7.1. This behaviour has been verified in tests by RWTH, Möller et al. (2012). This should however be verified by more tests, and in order to be on the safe side it might be better to assume a concrete width that is 80% of the width according to EN 1994-2.

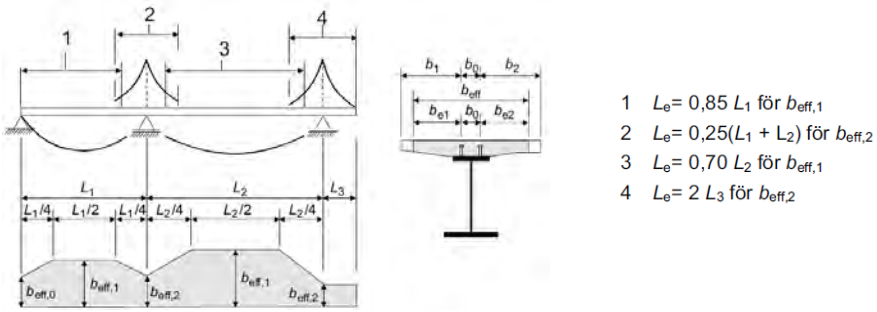

Figure 7.1 *Equivalent length for calculation of effective concrete width, EN 1994-2.*

SLS and FLS – sagging moments

Laboratory tests, field monitoring and FE-analyses, all indicate that a bridge of this type, under moderate loading, has a lower stiffness than a bridge with an in-situ cast deck. This implies that the steel stresses will be a bit higher compared to an in-situ cast bridge. This is believed to be caused by a combination of initial joint gaps that need to be closed, and the existences of the in-situ cast channel that tries to resists the closing of the joint. This leads to a significant reduction of the effective concrete width for a beam model in SLS and FLS.

Based on the work presented in this thesis, it is suggested that the effective concrete width is calculated according to EN 1994-2 5.4.1.2, assuming an equivalent length, L_e, equal to the maximum longitudinal distance between the outermost shear studs within an element.

However, if it is likely that the joint gap will be big > 0.5 mm, it is strongly recommended to perform a FE-analysis simulating the gaps in the joints that are closing under an increasing load. Special care has to be paid on the edges of the concrete elements, which can crush in the contact areas when the large gaps are closing. In Sweden, tolerances allowing an average gap of 0.4 mm have been used successfully.

ULS, SLS and FLS – hogging moments

In case of hogging bending moments, the model described in EN 1994-2 is not suitable for defining the effective width of concrete flanges. The distance between the points of zero bending moment, L_e, cannot be approximated in the same way. L_e can never be longer than the maximum longitudinal distance between the shear studs within the element, since the concrete element itself cannot transfer any longitudinal tensional forces over a joint. Laboratory tests, as well as FE-analyses, indicate that the structural stiffness over an internal support (hogging moment) is rather close to the stiffness of the steel section itself. Therefore, it is a quite good approximation to only use the stiffness of the steel cross-section in the

global analysis. If there are doubts whether this approximation can be used on a specific bridge or not, it is recommended to perform a sensitivity analysis studying the effect on the moment distribution, where a part of the concrete is included.

EN 1994-2 5.4.2.3 (3)

The simplified method that is described in this paragraph should be good enough also for a global analysis of multi span composite bridges with dry deck joints. But the stiffness in the support regions, 15% of the span length at each side of an inner support, must be changed. Eurocode provides a stiffness for composite sections with cracked concrete, that is based on the moment of inertia for the equivalent effective steel cross-section (I_2), including reinforcement bars but excluding concrete in tension. Since there is no longitudinal reinforcement that crosses the joints, only the steel girder cross-section should be used to model the superstructure in the global analysis. It is also recommended to perform a small sensitivity analysis of the assumption that 15% of the span length from the inner support should be treated as cracked.

7.2 Resistance of cross-sections

When the resistance of the superstructure is studied, the following approach is suggested.

If the concrete deck is in tension, both bending moments and normal forces taken into consideration, the steel cross-section should be designed to take the whole load. This approach will of course add some steel to the support sections of a composite bridge, approximately replacing the area of the longitudinal reinforcement, with a minor addition due to the smaller distance to the neutral bending axis.

If the concrete deck is in compression, both bending moments and normal forces taken into consideration, then the resistance is checked according to the rules given in EN 1994-2.

For the latter case, it is assumed that the concrete elements in compression behave as an in-situ cast deck. In the ULS this should be ok, but regarding SLS and FLS one should have in mind that the effective width of the interacting concrete is less under moderate loading. Tests have showed that and approximation of the effective concrete width can be achieved by using an equivalent length, L_e, equal to the distance between the outermost shear studs within an element.
If the mean value of the gaps between the elements are assumed to be large (>0.5 mm), one should consider doing a non-linear FE-analysis simulating gaps in the joints that closes under an increasing load. Such an analysis will give an estimation of the impact from the joints gaps on the stress

distribution in the composite cross-section. In most cases the neutral bending axis will be close to the upper flange in sections with sagging moments. Therefore, the bottom flange will often be the critical part of the steel girder, together with the details attached to the bottom flange that has to be checked for fatigue. The percental influence on the stresses, from joint gaps, is quite small in the bottom flange and quite high in the upper flange. This is beneficial since the stress levels generally are low in the upper part of the steel when the concrete is in compression.

7.3 Concrete element design

The concrete element design is performed according to EN 1994-2 and EN 1992. There are some differences compared to the design of an in-situ cast deck slab, some of these are listed below.

The shear keys are of course a critical detail in the design of the elements. This thesis describes one type of shear key that has been tested and evaluated, with varying reinforcement layout. This type of shear key, Figure 7.2, has been proven to be suitable for bridges with a girder spacing ≤ 5.0 m. The shear keys are designed as a series of overlapping male-female connections, always with one large shear key that distributes the load in one direction, and two smaller shear keys in the other direction, see Figure 5.1.

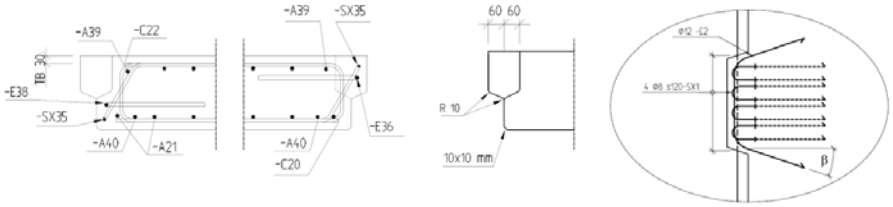

Figure 7.2 *Type of shear key tested in laboratory and in single span bridges.*

Since the design of bridge decks tends to vary a lot due to varying road profiles and due to different design traditions in different countries, the design of the shear keys will also vary. The dimensions of the elements will vary with respect to height, length and width. The distance between the steel girders will also vary, as well as the reinforcement layout in the element. This section shall be seen as a summary of recommendations and advices of how shear keys can be designed, rather than rules. If a new type of shear key is invented or the reinforcement layout is changed a lot, it is recommended to perform some tests.

The forces transferred through the shear keys from one element to another must be checked. Since the design of the deck slab will vary from one bridge to another, it is strongly suggested that a simple FE-analysis is made for each bridge, giving the information needed to design the shear keys, the

transverse/longitudinal reinforcement etc. In an early design stage a simple model, like the one shown in Figure 7.3 is often accurate enough to investigate the force distribution between the elements. This model can also be used for the design of the slab reinforcement.

The elements can be modelled as simply supported by the steel girders, with no interaction at all in the joints between the elements, despite in the location of the shear keys. In these points rigid elements are used to transfer forces from one side of the joint to another. In the model below, see Figure 7.3, the element in the middle is loaded. On one side of this element all joints are modelled with one shear key, and on the other side with two shear keys. The rigid links between the elements are placed in the middle of each shear key, and illustrated in Figure 7.3 by the element numbers (25-38).

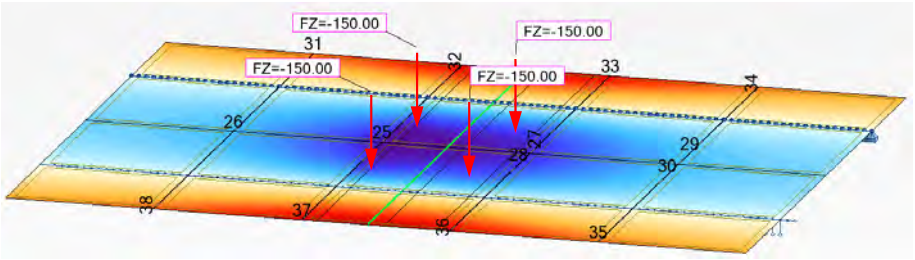

Figure 7.3 *FE-model for estimation of shear key forces. [kN]*

Tests have shown that an approach assuming that only the inclined rebars carries the whole load gives results on the safe side. The capacity to transfer shear forces through the shear key, is suggested to be calculated according to the formulas for inclined shear reinforcement in EN 1992-1-1 (6.13),

$$V_{Rd,s} = A_{sw} f_{ywd} \sin\alpha \qquad (8)$$

A_{sw} = the area of the shear reinforcement

f_{ywd} = the yield strength of the shear reinforcement

α = the inclination of the shear reinforcement

As already mentioned in the conclusions of Chapter 5, it is strongly recommended that the shear reinforcement in the shear keys male-female connection are overlapping, see Figure 5.17. This gives a more robust construction in the ultimate limit state, since the shear keys will have a post failure capacity to transfer forces even if the concrete cover has been separated from the rebars.

The concrete elements must be handled carefully during the transport and assembly, in order to avoid damages. It is strongly recommended to avoid right-angled corner wherever possible. This can for example be done by using splines (45°) in the formwork.

The elements are often handled by a crane, that lowers the element in the displaced position (> the depth of the shear key), before the element is slided into the final position, see Figure 7.4. In order to make sure that the joint gaps have been closed as good as possible, it is recommended that the elements are pushed together in one way or another. Different techniques have been tested. Small portable jacks can be supported by the shear studs and be used to push the elements together. In short bridges, where the steel girders often are cast into the back walls at the abutment, bolts can be used to pull the back walls against the deck elements, clamping them together, before the steel girders are cast into the back walls and the channels are injected

Figure 7.4 *Erection of deck elements.*

It is hard to perform a good compaction of the concrete in the in-situ cast channels, by using concrete vibrators. Therefore, it is recommended to use Self-Compacting Concrete (SCC) for the in-situ cast channels.

The concrete can be injected through injection holes. In the tests as well as in the real bridges, Ø100 mm injection holes have been used, with a spacing of 0.6 – 1.2 m. When the channels are injected it is important to make sure that the air can escape. Therefore, in addition to the injection holes, air release holes with smaller diameters are recommended, Ø16 mm s300 mm have been successfully used. The filling ability of the injected concrete should be established by full scale tests.

7.4 Steel design

The steel is designed according to EN 1994-2 and EN 1993. Essentially the steel is designed as in an ordinary composite bridge. The shear studs spacing can however give a lot of problems if it is not done in a proper way.

The distance between the shear studs is governed by the spacing of the transverse rebars in the bottom of the prefabricated element. In the bridges

constructed so far, the stud spacing has been 150 mm and the shear key depth has been 60 mm. In the assembling stage, the new element must be longitudinally displaced ≥ 60 mm in order to pass the shear keys on the former element, see Figure 3.6. If the shear studs spacing is 150 mm, as well as the spacing of the transverse rebars in the bottom of the deck element (Ø12 mm), the tolerances will be about ± 22 mm (the rebar ribs taken into account). If possible it is strongly suggested to increase the shear studs spacing and the spacing of the transverse rebars, in order to increase the tolerances.

The tolerance of a single shear studs is recommended to be set to ± 5 mm. But it is of highest importance that the same mistake is not repeated again and again. Therefore, the absolute position of the first shear studs in each group shall be checked, as well as the distance between the first and the last shear stud within the group, see Figure 7.5.

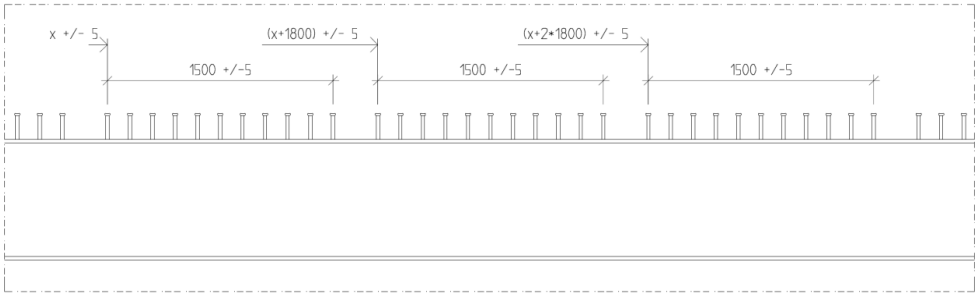

Figure 7.5 *Shear studs tolerances.*

Today, almost all drawings are made in computer programs, which makes it quite easy to preassemble the bridge virtually, and making sure that there will be no collisions between the shear studs and the rebars. Such a preassembly is strongly recommended.

The alignment of the steel girders is also very important. Experiences from real bridges have shown that there is no idea focusing on the alignment, before the steel girders are in their final position (after launching/lifting). Laterally adjustable cross stays can be used to adjust the position of the girders. Attachment points for such cross stays should be considered in the design stage.

To make it easier to align the girders, measurement points can be marked and checked already in the workshop. One the bridge site, the distances between these points can be measured and used to adjust the girders into the right positions. Figure 7.6 shows an example of how an alignment control can be done. Theoretical distances and a formula for calculating the necessary displacement of girder B is presented. The formula is only valid for the specific bridge, and not general.

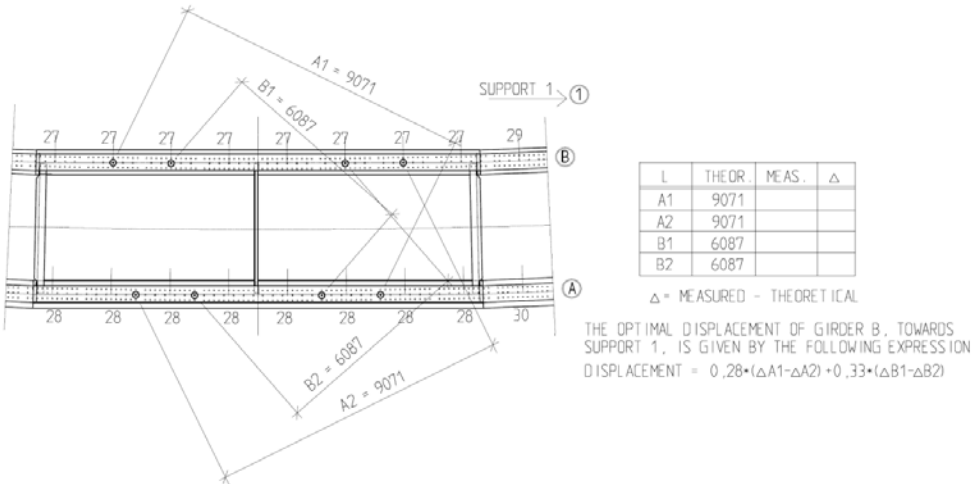

Figure 7.6 *Plan for steel girder alignment controls.*

7.5 Joint gaps

The initial gap in each joint should be measured at the concrete workshop, by doing a test assembly. In this stage, without any pre-stressing forces on the elements, the mean value of the gaps has so far been allowed to be 1.0 mm, in Sweden. The gaps can be measured by using feeler gauges. If a feeler gauge of 0.30 mm cannot be pushed into the joint, the joint gap has been considered as 0.0 mm. The gaps should be measured at several positions along the joint, both from the top and the bottom side. Figure 7.7 presents the measurements points used on one of the single span bridges that has been built in Sweden.

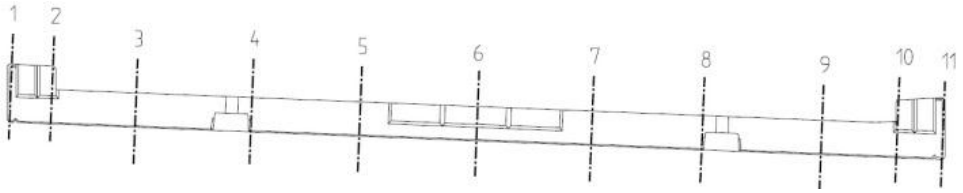

Figure 7.7 *Measurement positions for joint gaps.*

The joint gaps should also be measured after the assembly. In this case the gaps can often only be measured from above, since it can be quite hard to get access to the bottom of the joints under the bridge. At this stage after the element have been pushed together during the assembly, the mean value of the joint gap should be ≤ 0.40 mm. So far in Sweden, the maximum allowed gap has been ≤ 1.5 mm locally over a maximum distance of 1.0 m.

7.6 Waterproofing

The research done on this specific part has been performed by researchers at KTH (Stockholm, Sweden), under the lead of Bert Norlin. Since the waterproofing is essential for the sustainability of a bridge of this kind, this section summarises the results from their research and highlights the problems related to the waterproofing. The tests are described more in detail by Möller et al. (2012a).

In multi-span bridges, the joint gaps in areas with hogging moments will increase when the moment increases. The waterproofing must be able to withstand the elongation it will be subjected to, without cracking. The joint openings can be quite big (1-2 mm) especially near internal supports.

In order to test the long-term behaviour of the waterproofing, fatigue tests were performed in the test rig presented in Figure 7.8. The tests were performed with different layouts of the water insulation layers and with mastic asphalt on top of the membranes. During the tests the temperature was decreased by a freezer unit down to -20°C, if failure did not occur before. The final failure was defined as the moment when leakage occurred through the joint. To be able to simulate a leakage, the surface of the test specimens were covered with 1 cm of a water/antifreeze mixture.

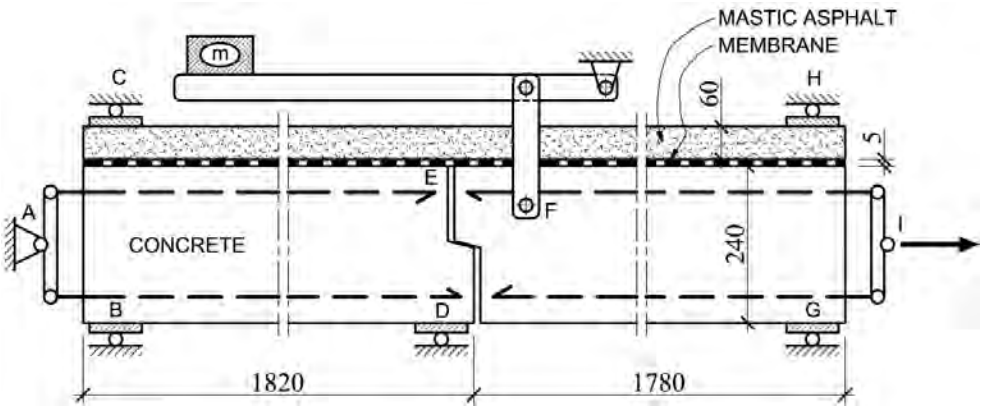

Figure 7.8 *Schematic illustration of the test rig and the specimen.*

Six tests were performed with four different types of waterproofing. The different waterproofing layouts are presented in Table 7.1, Figure 7.9 and Figure 7.10.

Table 7.1 *Waterproofing used in Test 1-6.*

	Membranes	De-bonding downwards	De-bonding upwards	Pavement
Test 1	1 layer	none	none	Mastic asphalt
Test 2	1 layer	140 + 140 mm*	none	Mastic asphalt
Test 3	3 layers	150 + 150 mm*	200 mm	Mastic asphalt
Test 4	2 layers	150 + 150 mm*	200 mm	Mastic asphalt
Test 5	2 layers	150 + 150 mm*	200 mm	Mastic asphalt
Test 6	2 layers	150 + 150 mm*	200 mm	Mastic asphalt

* = symmetric above the joint

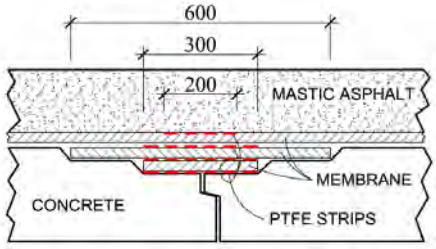

Figure 7.9 *Waterproofing in Test 3.*

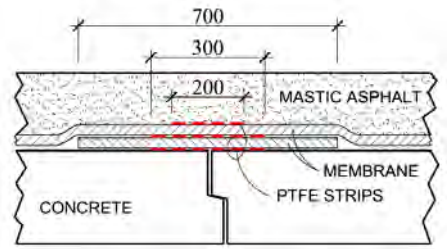

Figure 7.10 *Waterproofing in Test 4-6.*

The conclusions from the tests show that it is not possible to allow bonding between the membranes and the concrete/asphalt, as in Test 1 and 2. The failure occurs already at moderate temperatures (-5°C) and low displacement amplitudes (0.5 mm).

The waterproofing layers in Test 3 withstand the joint openings, under a low temperature, a lot better than Test 1 and 2. Up to 2.0 million cycles the displacement was increased stepwise up to 2.0 mm, at a temperature of -19°C. From 2.0 million cycles, until the leakage occurred at 3.05 million cycles, the amplitude was kept constant at 2.0 mm. The leakage occurred before a crack had propagated through all membranes, due to a membrane-weld that was not properly done.

In test 4-6 the welding were properly done, and the fatigue resistance was a lot higher. The amplitude of the joint opening was increased up to 2.0 mm in a faster rate than in the earlier test, and the temperature was -20°C in all tests. In test 4 and 5, no leakage had occurred when 5.0 million cycles were passed. The amplitudes were therefore increased in steps of 0.2 mm. Leakage occurred after 5.9 respectively 5.3 million cycles, and at an amplitude of 2.6 mm respectively 2.4 mm. Test 6 failed after 4.4 million cycles at the amplitude of 2.0 mm.

The results from these test lead to the recommendations presented below. These recommendations are directly cited from a section written by Bert Norlin, in the Design Guide by Möller et al. (2012b).

"If just one single waterproofing membrane is used, some kind of artificial de-bonding between the membrane and concrete as well as between the membrane and asphalt must be present to substantially improve the fatigue resistance. The total width of such regions must be about 20 cm. For this solution to work it is probably also necessary to artificially control the cracking of the asphalt layer such that it is more or less located over the deck joint opening rather than over the edge of the de-bonded region. Otherwise, the de-bonding strip cannot prevent the crack from growing into the membrane.

If two or more water proofing membranes are used the above statement holds but the de-bonded regions must increase in width when going from the top towards the concrete surface. Otherwise, the de-bonded region will not be able to stop a crack in an upper layer from growing into an underlying one. This reasoning holds as long as the cracks are formed and propagates from the top and downwards, which is the most likely scenario over an intermediate support of a bridge deck. The width increase should not be less than 5 cm, even if these regions can be placed with great accuracy.

One cannot rely on natural de-bonding between the material layers. De-bonding will not occur, not even between the concrete and the membrane, before the asphalt layer cracks right through at the deck-to-deck joint. Best practice is to artificially ensure that the asphalt cracks in line with the deck-to-deck joint such that the already de-bonded region below can stop the crack from propagating into the membrane. This can, for instance, be achieved by putting some kind of rubber based product in the asphalt layer right above the joint and towards the top membrane, see Figure 7.11. In combination with mastic asphalt, which in itself is water tight, this rubber can act as a fist seal preventing water an dust from penetrating into the de-bonded region below.

The actual de-bonding can be achieved by any practical means. But in order to promote rapid assembly and sufficient quality it should preferably be built into the membranes themselves. Here, product development in collaboration with some membrane manufacturer might be needed. The means used for de-bonding must in all cases ensure that the materials does not stick or bond to each other as time passes.

Mastic asphalt is preferred in contrast to traditional asphalts, as this product in itself is water tight, which will effectively localise the water proofing problem to each deck joint. This will also make it easier to protect the de-bonded regions as stated above.

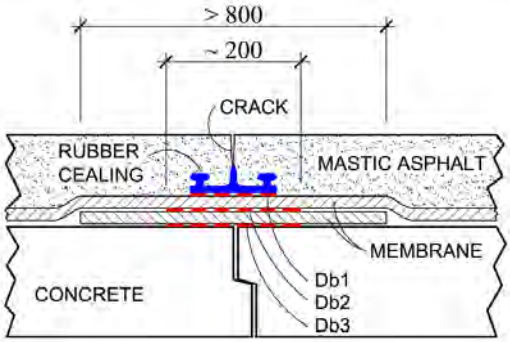

Figure 7.11 *Arrangement of water proofing membranes and de-bonded regions (denoted Db1, Db2 and Db3) over a deck-to-deck joint at an intermediate support.*

For a joint, produced following the above recommendations, the expected life time is more than 2 million cycles of 2.0 mm joint displacement at -20°C. If the temperature is higher than -20°C, the traffic induced joint opening is smaller than 2 mm and/or the de-bonded regions are longer than 20 cm the number of cycles to failure will be much greater.

There are two major drawbacks with the above solution. The first is that deliberate de-bonding is not allowed in the present regulations of some European countries. It is suspected that the de-bonded region may grow in size when for instance passed by heavy vehicles. The second is that water, dust and all kinds of pollutions may penetrate down to the membrane as soon as the asphalt cracks. Especially the water may increase the de-bonded region if it repeatedly freezes to ice. The first problem can be counteracted by using a thicker asphalt layer than usual, and the second by using some kind of rubber sealing as described above."

The test by KTH, indicate that is it possible to find a waterproofing solutions, which can resists the expected joint openings even in very low temperatures. The test shows also that this is an area for further research and product development.

7.7 Design example

To summarise this chapter a design example is given. In order to cover most of the issues that this chapter deals with, a section over an internal support is checked.

Example – Design of a section with hogging moment

In this example a 265 m long five span bridge is studied, Forsjösjön Bridge. This bridge was constructed in year 2011 as an ordinary composite bridge, with an in-situ cast concrete deck. Cut outs from the general drawing can be seen in Figure 7.12 and Figure 7.13. The steel cross-section is a hybrid girder, with S460/S420 in the flanges and S355 in the web plates.

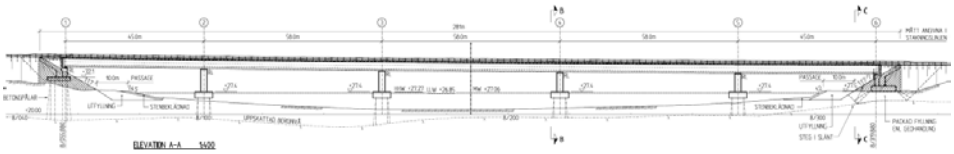

Figure 7.12 *Forsjösjön Bridge elevation.*

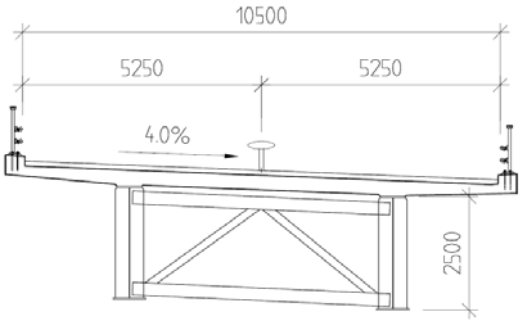

Figure 7.13 *Typical cross-section of the superstructure.*

In order to illustrate the differences in the design at internal supports, and to give an indication of how the steel weight is affected, a comparative design has been done with a prefabricated deck with dry joints.

Global analysis

The stiffness of the superstructure in the support sections (15% out in the spans) are modelled as the steel section only. This implies that the support moment will decrease in comparison to an in-situ cast deck (~5% in this case), in which the reinforcement area is included in the stiffness in the support sections. However, the sectional modulus will also decrease (~25% for the upper flange). This results in steel stresses that are far higher than in a similar in-situ cast bridge. This implies that the bending moment capacity of the steel girders must be increased.

Cross-sectional capacity

In the case with an in-situ cast concrete deck, the deck is casted in 9 stages, giving step wise composite action in different part of the bridge. In case of a prefabricated deck, the total load from the deck slab is acting on non-composite cross-sections. Since no composite action is assumed in the support sections, moments and normal forces can just be summed up from the different loads. In Table 7.2 the sectional forces in support section 3 are summarised.

Table 7.2 *Cross-sectional forces at support 3, for the prefabricated alternative.*

Section	Characteristic loads		ULS		Dim. Loads
x = 103.169 m	M [MNm]	N [MN]	LF	M_{dim} [MNm]	N_{dim} [MN]
Steel	-2.43	0	1.2	-2.92	0
Conc. deck	-14.23	0	1.2	-17.08	0
Railing + walkway	-0.40	0	1.2	-0.49	0
Pavement	-3.28	0	1.32	-4.33	0
Shrinkage	-2.74	0	1.2	-3.29	0
Temp. grad -	-2.22	0	0.9	-2.00	0
Support settl.	-0.72	0	1.1	-0.79	0
LM1	-12.84	0	0	0	0
Special vehicle	-14.44	0	1.5	-21.66	0
Breaking load	-0.01	1.2	0.68	-0.01	0.81
				-52.55	***0.81***

Below, the cross-section in the in-situ cast bridge is compared to the cross-section in the prefabricated alternative. In the in-situ cast alternative 1% reinforcement is assumed in the concrete deck slab. In order to get a similar utilization ratio in both alternatives, the thickness of the upper flange has been increased from 50 mm to 64 mm, in the case with a prefabricated deck.

Section	ELEM-
x = 103.169 m	Bridge
web t [mm]	22
web h [mm]	2386
b.flange t [mm]	50
b.flange w [mm]	1000
t.flange t [mm]	64
t.flange w [mm]	750
web.red.	
A [mm^2]	-1543
I [mm^4]	-6.3E+05
CG [mm]	1967
conc.	
n_L or n_0	
A_{conc} [m^2]	
I [m^4]	
CG [mm]	
e_{CG} [mm]	1264
Area [mm^2]	0.1489
I_x [mm^4]	0.17035
W_{tfl} [m^3]	-0.1348
$W_{w.t}$ [m^3]	-0.1420
$W_{w.b}$ [m^3]	0.1436
W_{bfl} [m^3]	0.1378

⇒ σ_{tfl} = 396 MPa
σ_{bfl} = 387 MPa

Section	In-situ cast
x = 103.169 m	deck
web t [mm]	22
web h [mm]	2400
b.flange t [mm]	50
b.flange w [mm]	1000
t.flange t [mm]	50
t.flange w [mm]	750
web.red.	
A [mm^2]	-595
I [mm^4]	-3.6E+04
CG [mm]	1990
conc.	
n_L or n_0	100.0
A_{conc} [m^2]	1.565
I [m^4]	0.0120
CG [mm]	-195
e_{CG} [mm]	1200
Area [mm^2]	0.1554
I_x [mm^4]	0.18875
W_{tfl} [m^3]	-0.1573
$W_{w.t}$ [m^3]	-0.1641
$W_{w.b}$ [m^3]	0.1510
W_{bfl} [m^3]	0.1452

⇒ σ_{tfl} = 395 MPa
σ_{bfl} = 379 MPa

Joint openings

The steel girders are precambered for the weight of the concrete and the steel. In theory, there will be no joint openings from these loads if the elements can be pushed together after installation. All loads that are applied after the injection of the channels will however contribute to the rotations.

The theoretical joint openings at the internal supports are estimated by Equation 1 given in section 4.3, and also presented once again below.

$$\delta_{joint} = \frac{\left(M_{mean} / W_{top.fl}\right)}{E} \cdot \frac{\left(e_{CG} + h_{conc}\right)}{e_{CG}} \cdot L_{element} \qquad (1)$$

When the maximum joint opening is calculated for ULS all moments are summarized, except the moments due to steel and concrete dead loads. In the FLS, only the moment caused by the fatigue vehicle is taken into account (FLM-3 from EN 1991-2).

With the highest point of the concrete surface 350 mm above the upper flange of the steel girder, and with an element length of 1.8 m, the following joint openings are calculated.

Maximum joint opening – ULS

$$\delta_{joint} = \frac{\left(-32.6 / -0.1348\right)}{210 \cdot 10^3} \cdot \frac{\left(1264 + 350\right)}{1264} \cdot 1.8 \text{ = 0.0027 m}$$

Maximum joint opening – SLS

$$\delta_{joint} = \frac{\left(-21.8 / -0.1348\right)}{210 \cdot 10^3} \cdot \frac{\left(1264 + 350\right)}{1264} \cdot 1.8 \text{ = 0.0018 m}$$

Maximum joint opening – FLS

$$\delta_{joint} = \frac{\left(-4.7 / -0.1348\right)}{210 \cdot 10^3} \cdot \frac{\left(1264 + 350\right)}{1264} \cdot 1.8 \text{ = 0.0004 m}$$

The joint openings are most interesting for the sustainability of the water insulation as well as the pavement. Fatigue tests performed at KTH indicates that the waterproofing can be designed to resists at least 2 million cycles with a displacement amplitude of 2.0 mm at -20°C. If the recommendations given in 7.6 are followed, it should definitely be possible to design a waterproofing that resists the fatigue it will be exposed to during its technical lifetime of 40 years. However, it is probably also necessary to define a ULS and SLS criterion.

Conclusions

The general conclusion is that it will be necessary to add some steel in the upper flanges near the internal supports, if a bridge is designed with prefabricated deck elements with dry joints instead of a concrete deck cast on site. For this specific bridge, the total steel weight of the solution with an in-situ cast deck is 465 ton, and the additional steel needed in the solution with a prefabricated deck is approximately 21 ton.

The assembly joints in the steel girders are in this case optimized for an in-situ cast bridge. It is possible to lower the amount of additional steel for the alternative with a prefabricated deck, if the joints instead are optimized for this type of construction.

The waterproofing can be designed to withstand the fatigue caused by the joint openings due to the cross-sectional rotations.

8 Discussion and conclusions

This chapter summarises the conclusions of the research this thesis is based upon, then provides a brief general discussion and finally gives suggestions for future research.

8.1 Conclusions

Clearly, the time spent on-site when constructing a bridge can be shortened by using a more industrial process. However, a number of issues must be addressed to assure that pre-fabrication designs and procedures are robust. Some of the key issues were formulated in the research questions (RQs) expressed in Chapter 1, and the main findings related to these questions are summarised and briefly considered in this section.

RQ1: What is the state of the art in this field?

The need to construct bridges in urban areas with high traffic flows has necessitated the development of new methods and designs to reduce the time spent on their construction sites. Thus, accelerated bridge construction techniques are gaining ground around the world. Procedures for prefabricating bridge elements have been intensively researched, and numerous ways of designing prefabricated deck elements have been described. This thesis focuses on elements with dry transverse joints, which are currently very rare. Currently, prefabricated decks are generally continuous, and constructed using wet joints with in-situ cast concrete surrounding overlapping rebars from the adjacent deck elements.

This research question is addressed in detail in Chapters 2 and 3, together with Paper I.

RQ2: How does a superstructure with dry deck joints behave under different load situations?

The structural behaviour of a composite superstructure with dry deck joints was investigated by performing large-scale laboratory tests in combination with field monitoring of a single span bridge constructed using this deck system.

The results from the tests indicate that in many cases a bridge of this type can be treated as an in-situ cast bridge, as long as the deck is in compression. This is at least valid for the ULS, which is often most relevant in the design of this type of bridge. Under moderate loading (SLS and FLS), the stiffness is significantly reduced due to the dry joints. The superstructure appears to be less stiff under moderate loading due to the combined effects of the initial joint gaps and in-situ cast channels. As long as the joints are open, no longitudinal forces can be transferred by contact pressure, thus any such forces exerted on the concrete deck must be transferred down to the steel girders before they reach an open joint. This results in a huge shear-lag, since the equivalent length is reduced to the longitudinal distance between the outermost shear studs within an element. In addition, the in-situ cast channels may be disadvantageous in this respect, since they cross the open joints and must be compressed before the rest of the joints can start transferring forces. It might therefore be necessary to take this into consideration when the steel is checked for fatigue and the deflection is checked against allowed values.

When a concrete bridge deck in a superstructure of this type is in tension, the stiffness or cross-sectional resistance of the superstructure can be modelled using solely the corresponding parameters of the steel section.

This research question is covered by Chapters 4 and Paper V.

RQ3: How do the shear keys fail under a static load?

The shear keys are vital parts of the construction, since they ensure that vertical forces are distributed between the elements. The ultimate capacity of the shear keys was studied in laboratory tests and by FE-analysis, as described in detail in Chapter 5 and Paper III.

Two contrasting failure modes were observed in the tests.

The first failure mode was the expected shear failure, where cracking starts in the bottom of the shear keys then cracks extend at an inclination of ~45° until they reach the upper surface. Such cracks will cross the shear reinforcement, the SX-rebars, and the dimension of the rebars will govern the ultimate capacity of the shear keys.

The second failure mode was cracking through the concrete covering layer. If the shear keys are properly reinforced with overlapping reinforcement in the male-female concrete tongues, this type of failure will not govern their ultimate capacity. They will continue to transfer forces even if the cracks cut through the concrete covering layer. However, this type of failure is undesirable, since it will affect the long-term sustainability of the bridge.

The second type of failure has only been observed in the laboratory tests with a very stiff supporting element. When whole joints have been tested in the laboratory, only the first failure mode has been observed. Chapter 5 discusses possible reasons why this failure occurred only in the small-scale tests.

RQ4: How should a rational design calculation of the shear keys be done?

The scatter of the test results was quite high, making it difficult to establish any general design rule. The scatter was mainly caused by the fact that two totally different failure modes were observed, as mentioned before.

With current knowledge, based on the observations and measurements presented in Chapter 5 and Paper III, it is recommended to design the shear keys according to the formulas for inclined shear reinforcement in EN 1992-1-1, presented in Equation 7 in this thesis.

RQ5: How is the long-term behaviour compared to a composite bridge with a conventional in-situ cast deck slab?

The long-term behaviour of the deck system described in this thesis was mainly investigated by testing a 10-year-old single span bridge constructed using the system. The most recent field monitoring of this bridge was performed in year 2011 and has been compared to a similar monitoring in year 2001. The procedure and findings are described in detail in Chapter 6 and Paper IV.

Only one long-term effect was observed from a comparison of the results from the two field monitoring occasions. When the bridge was loaded unsymmetrically the load distributions between the girders were more extensive in 2001 than in 2011, possibly because the joint gaps were larger in 2001, and at least partly closed during the time between the tests. A possible explanation for this is that abrasion of irregularities at the concrete contact surfaces occurred during the intervening time, resulting in better distribution of forces over the joints.

This bridge was inspected in 2011 by the Swedish Road Administration, and no comments on the superstructure related to the joints were made in the subsequent report.

RQ6: What is necessary to check in a detailed design of this kind of bridges?

Design and production issues that should be addressed for a bridge of the type described in this thesis are discussed at in Chapter 7. Briefly, such a bridge has many similarities to a conventional composite bridge with an in-situ cast concrete deck. However, the findings show that it may sometimes be necessary to modify the Eurocode design rules. Modifications suggested in Chapter 7 are summarised in the list below. Some experience-based recommendations, arising from considering the design and construction of three single-span bridges, are also included in this list.'

Global analysis

- Sagging moments
  - In ULS, L_e can be calculated according to EN 1994-2.
  - In SLS and FLS, L_e can be approximated as the distance between the outermost shear studs within an element.
  - If it is likely that the final joint gaps will exceed 0.5 mm, one should consider performing an FE-analysis with closing joints.
- Hogging moments
  - In ULS, SLS and FLS it is a good approximation to only use the stiffness of the steel section in the global analysis.
  - The longitudinal reinforcement in all sections can be neglected, since no reinforcements cross the joints, see EN 1994-2 5.4.2.3 (3).

Resistance of cross-sections

- Sagging moments
  - In ULS, FLS and SLS the steel section should be designed to take the whole load.
- Hogging moments
  - In ULS, the resistance can be checked according to the rules given in EN 1994-2.

- In SLS and FLS, the effective concrete width can be approximated by assuming that Le is equal to the distance between the outermost shear studs within an element.

Shear keys

- The capacity to transfer shear forces through the shear key, is suggested to be calculated according to the formulas for inclined shear reinforcement in EN 1992-1-1 (6.13)

Joint gaps / Waterproofing

- Tests performed at KTH show that it is possible to create a waterproofing system capable of resisting the joint openings that a deck of the considered type will be subjected to during its technical lifetime.

- The joint opening can be estimated using Equation 1 in Chapter 4.

Tolerances

- It is crucial to ensure that all elements have the allowed tolerances, and to apply rigorous checks to detect any mistakes before the prefabricated elements reach the bridge site. Hence:
  - The deck elements should always be match cast.
  - The joint openings should be tested both in the concrete workshop, by preassembly to the previous cast element, and at the bridge site after the elements have been pushed together.
  - The positions of the shear studs must checked, in both longitudinal and transverse directions. It is very important to check the tolerances between the studs both within elements and in different elements, to avoid repetitive errors. Therefore, it is recommended to check the absolute position of the first shear stud in each element.

8.2 Discussion and further research

The prefabricated deck system presented in this thesis is generally most suitable for short bridges with dry joints. If the technique is to be used for longer bridges, it will be essential to use wet joints to zero cumulative errors. In order to design longer bridges without wet-joints, it would of course be beneficial if the tolerances could be increased or the deck system

could be redesigned to avoid collisions. One way of doing this is by applying the technique shown in Figure 3.7, which has been tested in the US.

A prefabricated bridge deck of this type will definitely contain more steel in its superstructure than a corresponding bridge of conventional prefabricated design. Therefore, this type of prefabricated deck will not be the optimal choice for a new bridge that can be built without disturbing the traffic or environment. However, if work at the bridge site will excessively disturb traffic, the neighbouring area etc., or if the client and contractor would benefit sufficiently from a short construction time, this solution will be competitive. Two major alternatives are composite bridges with prefabricated deck elements incorporating wet joints and prefabricated concrete bridges. If elements with wet-joints are used it will not be possible to install the waterproofing almost immediately after the erection, since the concrete will have to dry out. Hence, the bridge will not be able to carry traffic as quickly as a bridge with dry joints. However, if the geometry of the bridge is complex, with varying curvature, deck widths etc., it might be better to use elements with wet joints, since such elements can be adjusted a slightly at each joint.

One of the most critical details in this type of construction is the waterproofing, which must be durable to avoid damage due to water penetration and leakage in the joints. This is beyond the scope of the thesis, but it is probably the most important issue to address in further research, since it must be confirmed that applied solutions do not fail in the field. There is also a need to involve the manufacturers of the waterproofing systems in further research and development concerning this issue.

The shear studs also require further research. The outermost shear studs within an element will probably transfer higher shear forces than those in the middle of an element. Previous tests have shown that the fatigue resistance of studs near internal supports is sufficient, if they are designed for composite action, in contrast to the steel sections which is designed assuming no composite action. Nevertheless, further research would be beneficial to ensure that all of the studs provide sufficient resistance under field conditions.

In order to advance development of this type of prefabricated deck system it would also be very beneficial to use it to construct a multi-span pilot bridge and examine its properties in detail.

References

AASHTO (2002) *Prefabricated Briges*, AASHTO – Technology Implementation Group, Washington DC, USA

Berthellemy J (2001) Composite construction – Innovative solutions for road bridges, *Proceedings: 3rd International Meeting on Composite Bridges*, Madrid, Spain

Berthellemy J (2009) French bridge experiences from prefabricated deck elements, In: *Proceedings from Workshop on Composite Bridges with Prefabricated Deck Elements*, March 4th 2009, Stockholm, Sweden, ISBN: 978-91-7439-003-2

Betonghandoken (1990) *Betonghandboken konstruktion – utg. 2*, Svensk Byggtjänst, Stockholm, Sverige, ISBN: 91-7332-533-3 (in Swedish)

Chi M (1985) *Precast Concrete Modular Bridge Deck Case Studies,* FHWA-TS-85-232, Office of Engineering, Bridge Division, Washington DC, USA

Collin P, Hällmark R & Nilsson M (editors) (2009) International Workshop on Prefabricated Composite Bridges, Technical Report, Luleå University of Technology, Sweden, pp 180, ISBN: 978-97-7439,
Also available at: http://pure.ltu.se/portal/files/3112371/ELEM_Seminar_4_Mars_2009.pdf

Collin P, Johansson B & Pétursson H (1998) *Samverkansbroar med elementbyggda farbanor*, SBI - Publication 165 : 1998, Swedish Institute of Steel Construction, Stockholm, Sweden, pp 66, ISBN: 91-7127-022-1

Culmo M P (2009a) Prefabricated Composite Bridges in the United States – including total bridge prefabrication, In: *Proceedings from Workshop on Composite Bridges with Prefabricated Deck Elements*, March 4th 2009, Stockholm, Sweden, ISBN: 978-91-7439-003-2

Culmo M P (2009b) *Connection Details for Prefabricated Bridge Elements and Systems*, FHWA Publication no: FHWA-IF-09-010, Office of Engineering, Bridge Division, Washington DC, USA

Degerman H (2002) *Samhällsekonomisk analys av hastighetsnedsättning vid bro söder om Norrfors,* Internal Report – Banverket norra regionen, Sweden (in Swedish)

EN 1991-2 (2005) *Eurocode 1- Actions on structures – Part 2: Traffic Loads on Bridges*, CEN – European Committee for Standardisation, Brussel, Belgium

EN 1992-1-1 (2004) *Eurocode 2- Design of concrete structures – Part 1: General rules and rules for buildings*, CEN – European Committee for Standardisation, Brussel, Belgium

EN 1994-2 (2005) *Eurocode 4- Design of composite steel and concrete structures– Part 2: General rules and rules for bridges*, CEN – European Committee for Standardisation, Brussel, Belgium

FHWA - Federal Higway Adminstration (2010) *Field cast UHPC connection for modular bridge deck elements*, FHWA-HRT-11-022, Office of Engineering, Bridge Division, Washington DC, USA

FHWA - Federal Higway Adminstration (2011) Highways for Life
Available at: http://www.fhwa.dot.gov/hfl/ (May 29, 2012)

Gordon S & May I (2006) Development of in situ joints for pre-cast bridge deck units*, Prodeedings of the ICE – Bridge Engineering, Vol* 159 (1): 17-30

Gordon S & May I (2007) Precast deck systems for steel-concrete composite bridges*, Prodeedings of the ICE – Bridge Engineering, Vol* 160(1): 25-35

Hällmark R, Collin P & Stoltz A (2009) Innovative Prefabricated Composite Bridges, *Structural Engineering International,*19 (1): 69-78.

Hällmark R, White H & Collin P (2012) Prefabricated Bridge Construction across Europe and America, *Practice Periodical on Structural Design and Construction – ASCE, Vol. 17, No.3.*

Harrysson P (2008) *Industrial Bridge Engineering – Structural developments for more efficient bridge construction*, Ph.D. Thesis, Chalmers University of Technology, Göteborg, Sweden. ISBN: 978-91-7385-129-9

Hewson N R (2003) *Prestressed Concrete Bridges: design and construction*, Tomas Telford,London, UK, ISBN: 0-7277-3233-4

Issa et al. (2003) Performance of Transverse Joint Grout Materials in Full-Depth Precast Concrete Bridge Deck Systems*, PCI Journal, Vol* 48 (4): 92-103

Issa M et al. (1995) Field Perfomance of Full Depth Precast Concrete Panels in Bridge Deck Reconstruction*, PCI Journal, Vol* 40 (3): 83-108

Markowski S (2005) *Experimental and Analytical Study of Full-Depth Precast/Prestressed Concrete Deck Panels for Highway Bridges*, Master Thesis, University of Wisconsin-Madison, USA

Möller F, Hällmark R, Seidl G et al. (2012a) Final Report – ELEM - Composite Bridges with Prefabricated Decks, RFSR-CT-2008-00039, Technical report No: 6.

Möller F, Hällmark R, Seidl G et al. (2012b) Design Guide – ELEM - Composite Bridges with Prefabricated Decks, RFSR-CT-2008-00039.

NCHRP (2003) *NCHRP Synthesis 324 – Prefabricated Bridge Elements and Systems to Limit Traffic Disruption During Construction*, Transportaion Research Board, Washington DC, USA, ISBN: 0-309-06972-6

NCHRP (2009) *NCHRP Project 20-68A – Best Practice in Accelerated Construction Techniques*, Scan Team Report, Scan Management, Lawrencville, USA

Nilsson M (2001) *Samverkansbroar ur ett samhällsekonomiskt perspektiv*, Master Thesis, Luleå University of Technology, Sweden (in Swedish)

Ralls et al. (2005) *Prefabricated Brige Elements and Systems in Japan and Europe*, FHWA Publication no: FHWA-PL-05-003, pp 64, Office of Engineering, Bridge Division, Washington DC, USA

Seidl G & Braun A (2009b) VFT-WIB-Brücke bei Vigaun – Verbundsbrück mit externer Bewehrung, *Stahlbau, Vol* 78 (2): 86-93 (in German)

Seidl G (2009a) Composite Element Bridges, In: *Proceedings from Workshop on Composite Bridges with Prefabricated Deck Elements*, March 4th 2009, Stockholm, Sweden, ISBN: 978-91-7439-003-2

Shim et al. (2010) Development and Application of Precast Decks for Composite Bridges, *Structural Engineering International,* 20 (2): 126-133.

Simonsson P (2008) *Industrial Bridge Construction with Cast in Place Concrete*, Licentiate Thesis 2008:17, Luleå, Sweden, pp 163

Stoltz A (2001) *Effektivare samverkansbroar – Prefabricerade farbanor med torra fogar*, Licentiate Thesis 2001:41, Luleå, Sweden, pp 188 (in Swedish)

UDoT (2010) *Full Depth Precast Concrete Deck Panel Manual*, Utah Department of Transportation

Available at: http://www.udot.utah.gov (May 29, 2012)

UDoT (2012) Utah Department of Transportation

Available at: http://www.udot.utah.gov (May 29, 2012)

Womack J & Jone D (2003) *Lean Thinking – Banish waste and create wealth in your corporation*, Simon and Schuster, New York, USA, ISBN: 0-7432-4927-5

Womack J, Jone D & Roos D (1990) *The Machine that Changed the World*, Simon and Schuster, New York, USA, ISBN: 1-4165-5452-1

Appendix A
Results from the large-scale tests

This appendix presents the large-scale tests performed at LTU, in the summer of year 2011.

The test specimen was designed to make it possible to use two different test set-ups. The first test set-up was used to simulate the behaviour in a field section of a bridge, and the second was used to simulate the behaviour at an internal support, see Figure A.1.

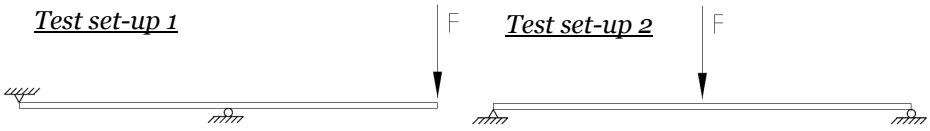

Figure A.1 *Schematic illustration of test set-up 1 and 2.*

The test schedule is presented in Table A.1 below.

Table A.1 *Test Schedule.*

Test no:	*Type of load situation*	*Force*	*Number of cycles*
Test 1	Set-up 1 - one point load	100 kN	-
Test 2	Set-up 1 - one point load	280 kN	-
Test 3	Set-up 1 - two point loads	310 kN	-
Test 4	Set-up 1 - two point loads	430 kN	-
Test 5	Set-up 1 - two point loads	5-250 kN	50 cycles
Test 6	Set-up 1 - one point load	250 kN	-
Test 7	Set-up 1 - two point loads	400 kN	-
Test 8	Set-up 1 - two point loads	5-250 kN	50 cycles
Test 9	Set-up 2 - two point loads	500 kN	-
Test 10	Set-up 2 - two point loads	5-450 kN	100 cycles
Test 11	Set-up 2 - one point loads	300 kN	-
Test 12	Set-up 2 - one point loads	450 kN	-
Test 13	Set-up 2 - one point loads	5-400 kN	100 cycles

A.1 Test specimen

The test specimen consisted of prefabricated concrete deck elements as well as prefabricated steel elements. In order to get an insight in which tolerances that can be expected from steel workshops and concrete factories, both the concrete and the steel parts were ordered from two large actors on the construction market in the Nordic countries. The results, the precision of the delivered products, were very satisfying, see section A.1.2.

The laboratory test specimen had the dimension 7.2 x 3.5 x 1.1 m, and consisted of four prefabricated concrete deck elements, two welded steel I-girders and three cross-beams, see Figure A.2. Composite action was achieved by shear studs.

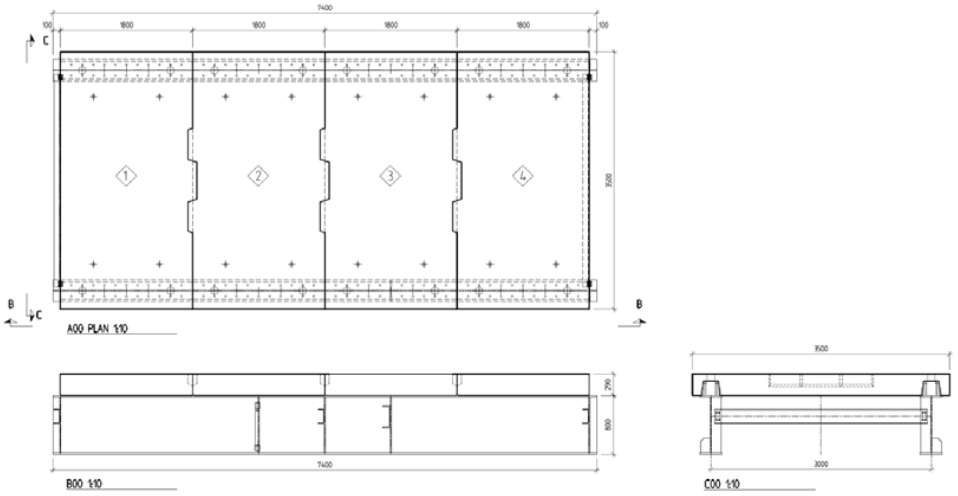

Figure A.2 *Drawing of the test specimen [mm].*

A.1.1 Geometry

Steel
The theoretical dimensions of the main girders and the cross beams are presented in Figure A.3 - Figure A.6. All figures are taken from the final construction drawings. In the table in Figure A.5 the measured geometry of the steel, at a temperature of 20 °C, is presented.

Position number 5 and 6, in Figure A.3, are cross-beams used in tests that are out of scope for this report. These cross-beams were removed during the tests described in this report.

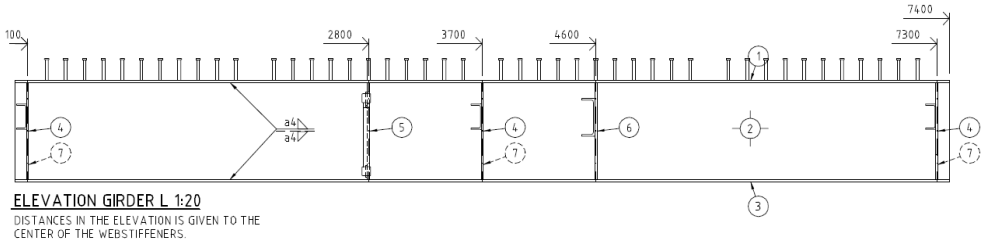

Figure A.3 *Elevation drawing of the steel girders [mm].*

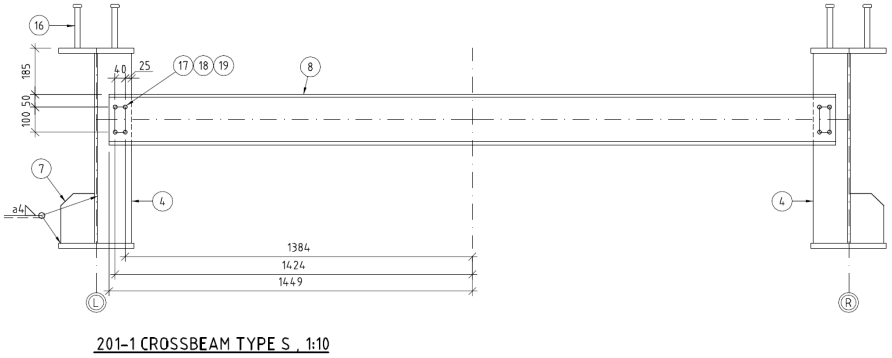

Figure A.4 *Cross-beam drawing [mm].*

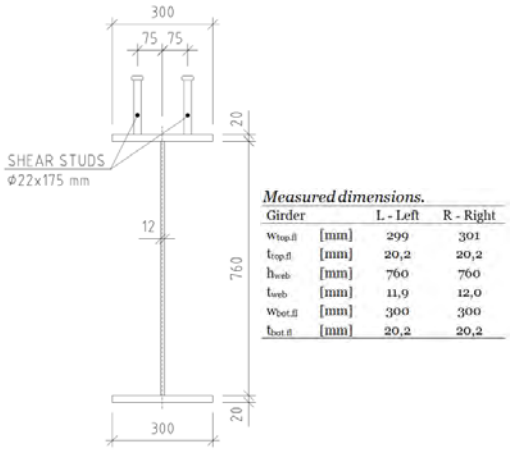

Measured dimensions.

Girder		L - Left	R - Right
$w_{top.fl}$	[mm]	299	301
$t_{top.fl}$	[mm]	20,2	20,2
h_{web}	[mm]	760	760
t_{web}	[mm]	11,9	12,0
$w_{bot.fl}$	[mm]	300	300
$t_{bot.fl}$	[mm]	20,2	20,2

Figure A.5 *Steel girder dimensions [mm].*

Figure A.6 *Picture of steel girder.*

Concrete and reinforcement

The theoretical dimensions of the prefabricated elements are presented in Figure A.7, together with the reinforcement drawing of deck element no: 3 in Figure A.8.

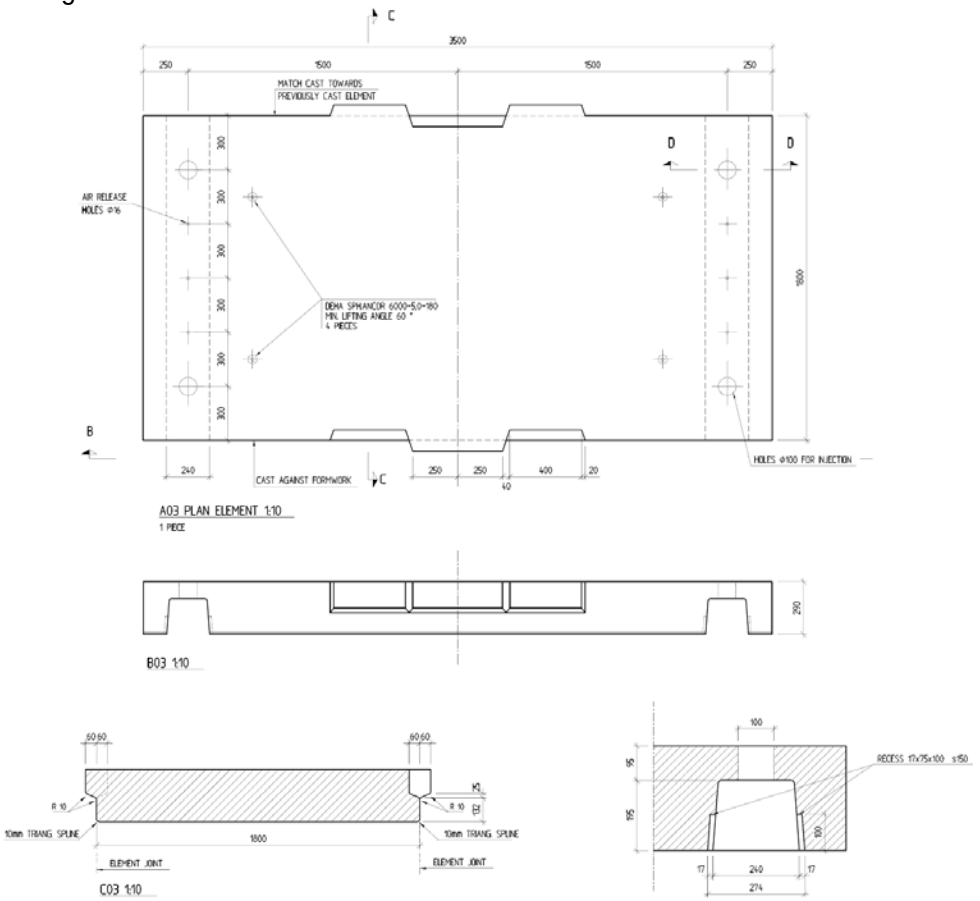

Figure A.7 *Concrete element dimensions [mm].*

A.1.2 Tolerances

Steel

The tolerances of the steel girders were mainly the same as for conventional composite bridge girders. The big differences were the importance of the location and the spacing of the shear studs. The shear studs had a longitudinal spacing of 150 mm and needed to be placed with an absolute tolerance of +-5 mm for a single stud, giving a total tolerance of +-10 mm for a group of studs. One group of studs is defined as the number of studs within the length of an element. In this case there were 11 x 2 studs in each group. The alignment of the studs was also important. The transverse tolerance of the shear studs was +-5 mm from the theoretical line.

To avoid summing up errors from one group to another, it was of highest importance that the first stud in each group was measured from a fixed position. In this case the end of the beam.

The precision of the steel work was excellent. All measurements made were within the tolerances. The only thing that had to be corrected was the alignment of a few studs. Some studs had been bent during the handling or transport, and a few others had been bent by purpose. The latter is done due to a demand in the Swedish bridge code. For every 500 stud one shear stud shall be beat 45° slant and one bend 45° slant. These studs were bent back in their vertical position, before the erection of the elements.

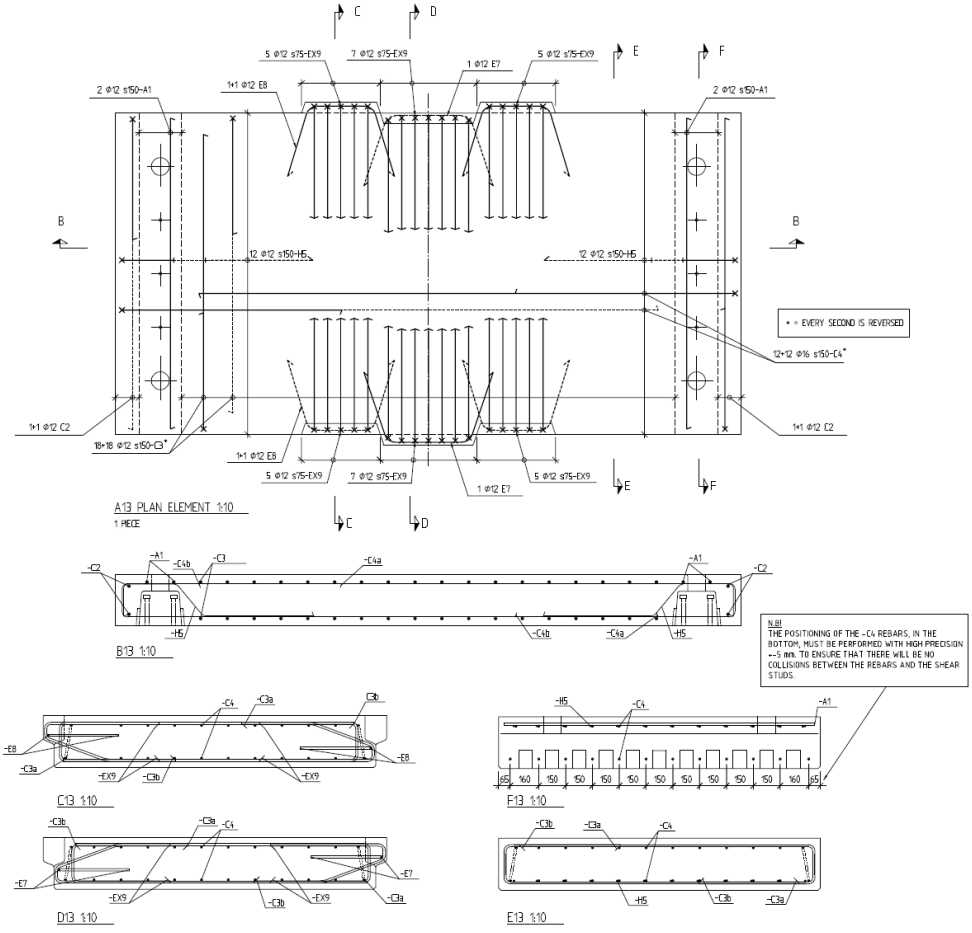

Figure A.8 *Reinforcement drawing, Element no:3 [mm].*

Concrete and reinforcement

All elements were cast in the same formwork made of steel, and with one side match-cast against the previously cast element. This formwork was checked carefully before the casting started. The tolerance of the length was +-2 mm, and the tolerance of the diagonal distance was +-4 mm.

The location of the reinforcement bars named C4 were very important, since the tolerances between the rebars and the shear studs were very limited. The C4 rebars should be positioned with a precision of +-5 mm for each rebar and +-5 mm for the length between the first and the last rebar. Figure A.9 illustrates the installation of an element. There is a tolerance between the rebars and the studs of only +-22 mm, for the total length of the prefabricated bridge deck.

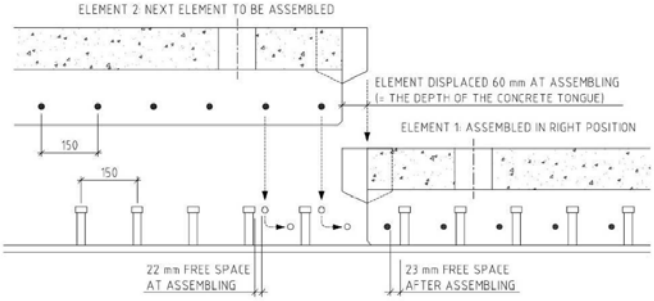

Figure A.9 *Illustration of the tight tolerances at the assembling stage [mm].*

In order to ensure that the tolerances were fulfilled, a fixed rig was produced for the reinforcement that crosses the injection channel, see Figure A.10.

The concrete elements were examined and measured when they arrived to the laboratory. All measurements, both concrete dimensions and reinforcement locations, were satisfying and within the tolerances.

Figure A.10 *Picture of the formwork where the rebars crosses the injection channels.*

A.2 Test set-up

Test set-up no: 1
Figure A.11 shows the load situation in test set-up 1.

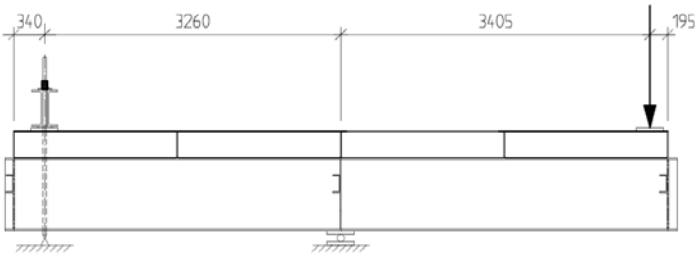

Figure A.11 *Detailed illustration of test set-up no:1.*

The internal support was achieved by using two steel rolls between the bottom flange and the concrete floor in the laboratory. Thick steel plates were also used as distances, both to the steel and to the floor, in order to distribute the point load. The negative support consisted of two post-tensioning bars, Ø36 mm. Two holes, Ø50 mm, were drilled through the concrete slab, and the post-tensioning bars were thread through these holes and down through similar holes in the floor. In the bottom, the bars were anchored beneath the 1.0 m thick concrete floor. In the top, a load distributing steel beam was used in order to get the support reactions straight above the steel girders. The bars were post-tensioned with approximately 300 kN in each bar. The bars can be seen in Figure A.12.

Figure A.12 *Picture of the negative support.*

Test set-up no: 2

Figure A.13 shows the load situation in test set-up 2.

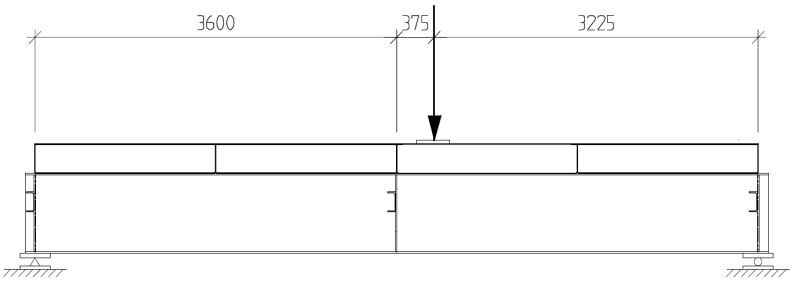

Figure A.13 *Detailed illustration of test set-up no:2.*

In both test set-ups the load was applied in two different ways. First as a point load, 350x350 mm, acting in the centreline of the bridge, then as two point loads acting straight above the steel girders. The latter was achieved by using a load distribution beam. The two different ways of applying the load are shown in Figure A.14.

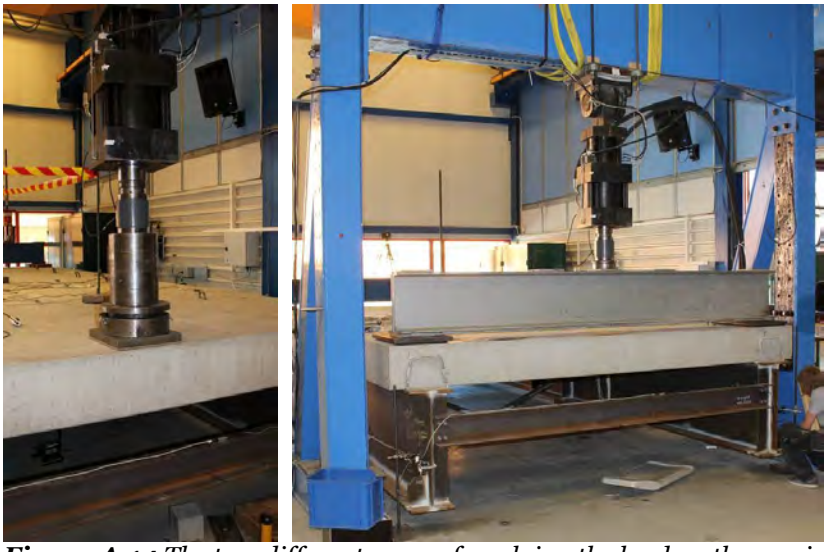

Figure A.14 *The two different ways of applying the load on the specimen.*

The hydraulic jack that was used in all tests had a maximum capacity of 700 kN. During the static tests it was deformation controlled with a stroke rate of 0.02-0.03 mm/s during the loading sequence and 0.05 mm/s during unloading. In the case of cyclic loading the jack was load controlled with a frequency of 0.0333 Hz.

A.3 Results

In section A.3.1 – A.3.5 the large-scale tests results are presented together with descriptions of the measurement devices.

Throughout this appendix, the x-axis is defined with its origin in the joint between Element 2 and 3 (in midspan) and is defined as positive in the direction of increasing element numbers. Figure 4.1 defines the co-ordinate system used in the tests.

A.3.1 Deflections

Deflections were measured in the middle and at the ends of each girder. The equipment used was six LVDTs (Linear Variable Differential Transformer), named LU1-LU6. The LVDTs were mounted vertically, and measured the deflections on top of the low stiffeners. Figure A.15 shows a plan over the deflection measurements, and Figure A.16 shows a picture of one of the LVDTs that were used.

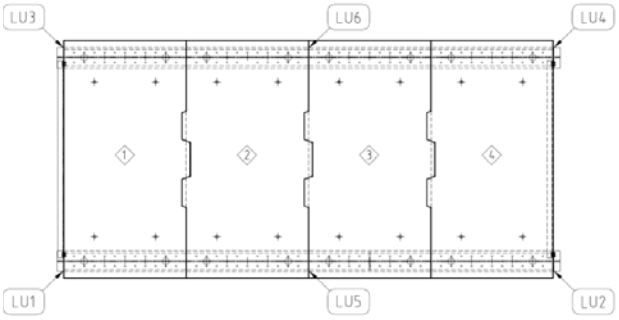

Figure A.15 *Deflection measurement plan.*

Figure A.16 *Picture of LVDT.*

The deflections that are presented are the deflections caused by pure bending. It means that the support settlements have been taken into consideration in the case of a simply supported beam, test set-up no:2 (test 9-13). In test set-up no:1 (test 1-8) the support settlements have been taken into consideration as well as the rotation due to the settlements at the negative support, see Equation 1-4

$$LU2_{bend} = LU2 - LU5 + (LU1-LU5) \quad (1)$$

$$LU4_{bend} = LU4 - LU6 + (LU3-LU6) \quad (2)$$

$$LU5_{bend} = LU5 - (LU1 + LU2)/2 \quad (3)$$

$$LU6_{bend} = LU6 - (LU3 + LU4)/2 \quad (4)$$

The vertical deformations, $LU2_{bend}$ and $LU4_{bend}$, from Test 1-8 are all plotted in the same load-deformation diagram see Figure A.17, and the vertical deformations, $LU5_{bend}$ and $LU6_{bend}$, from test 9-13 are shown in Figure A.18.

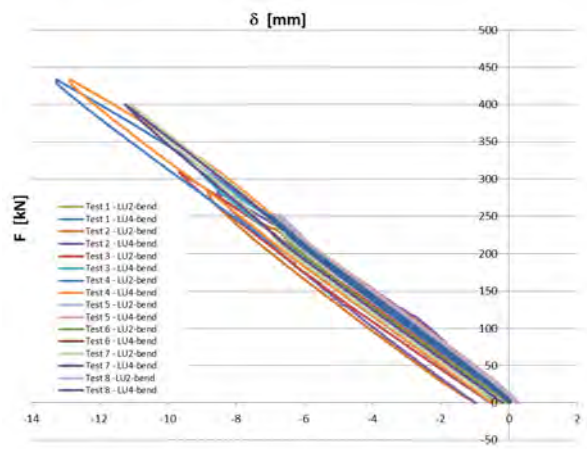

Figure A.17 *Load-deformation diagram for Test 1-8, $LU2_{bend}$ and $LU4_{bend}$.*

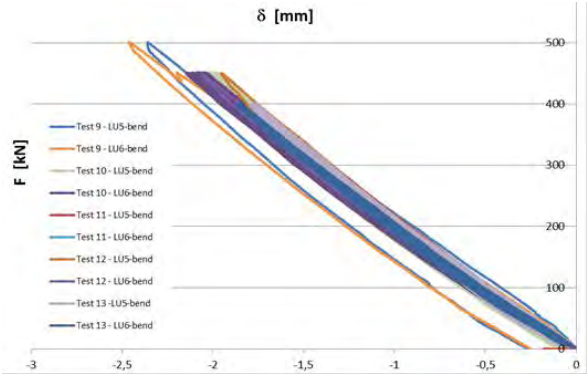

Figure A.18 *Load-deformation diagram for Test 9-13, $LU5_{bend}$ and $LU6_{bend}$.*

In general, the results indicate a quite linear behaviour in the loading and unloading sequence, but a part of the deformation is remaining. Test 2 and Test 5 are used to illustrate the differences in deflection during the first large load cycle in comparison to the deflections when a similar load is repeated, see Figure A.19.

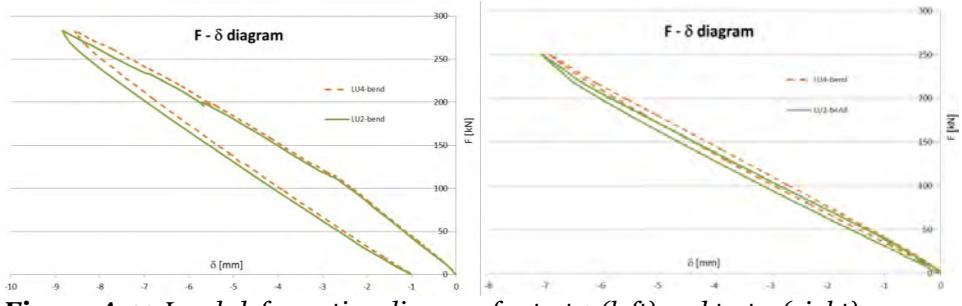

Figure A.19 *Load-deformation diagram for test 2 (left) and test 5 (right).*

A.3.2 Steel strains

The steel strains were measured in the top respectively the bottom of the web in three sections. Figure A.20 shows a picture of the strain gauges, and Figure A.21 gives their positions.

In order to get a third reference point, an extra strain gauge was used in the middle of the web in each section. The strain gauges were all located over the length of Element 3.

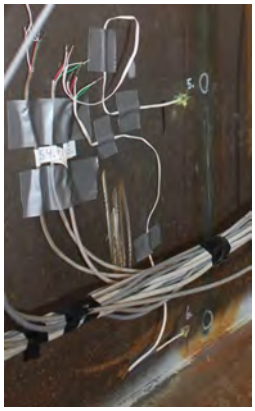

Figure A.20 *Steel stain gauges.*

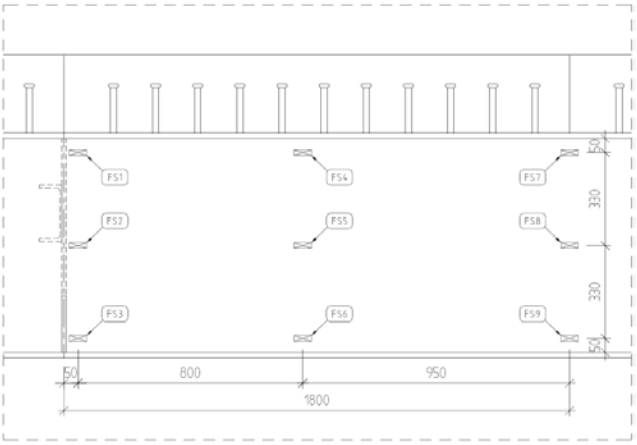

Figure A.21 *Installation scheme for the steel strain gauges.*

The results from the strain measurements in test 1 to 13 are presented in Figure A.22 - Figure A.27. All strains have been transformed into stresses according to Hooke's law, assuming E_{steel} = 210 GPa

$$\sigma = E \cdot \varepsilon \tag{5}$$

The first section is located at x = 0.050 m, which means 0.050 m from the joint between Element 2 and 3.

The second section is located at x = 0.850 m, which means 0.050 m from the middle of Element 3.

The third and last section is located at x = 1.800 m, which means right at the joint between Element 3 and 4.

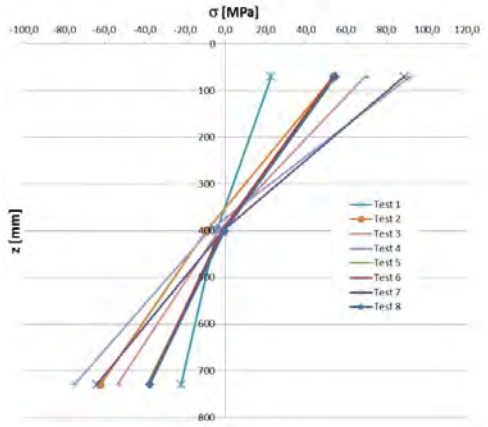

Figure A.22 *Measured steel stresses in section x = 0.050 m, test set-up 1.*

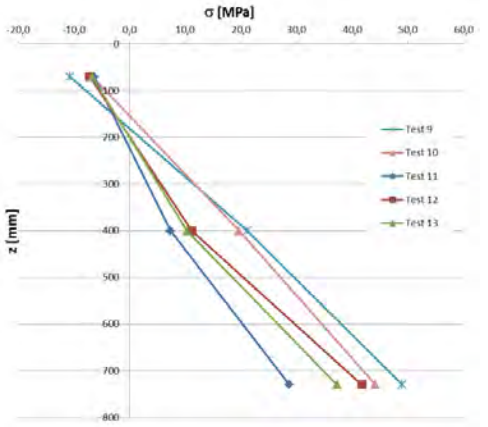

Figure A.23 *Measured steel stresses in section x = 0.050 m, test set-up 2.*

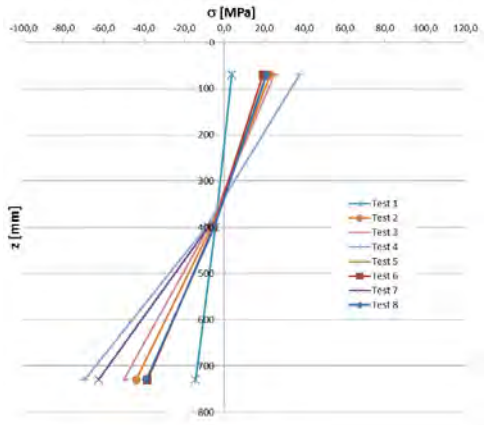

Figure A.24 *Measured steel stresses in section x = 0.850 m, test set-up 1.*

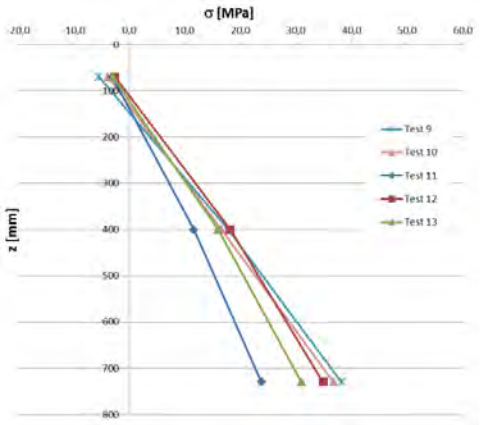

Figure A.25 *Measured steel stresses in section x = 0.850 m, test set-up 2.*

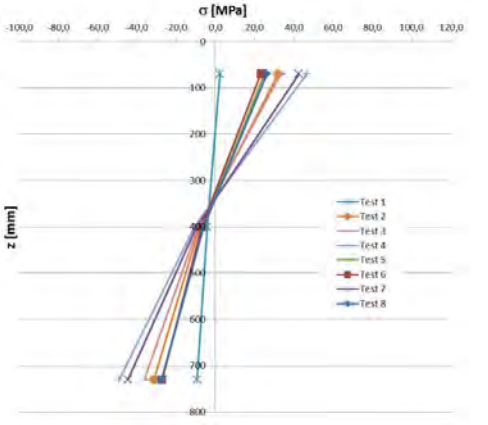

Figure A.26 *Measured steel stresses in section x = 1.800 m, test set-up 1.*

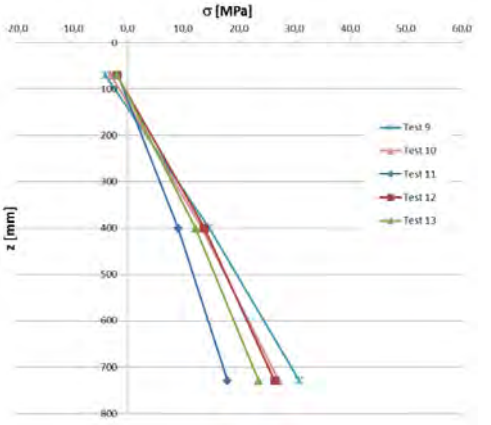

Figure A.27 *Measured steel stresses in section x = 1.800 m, test set-up 2.*

A.3.3 Concrete strains

Concrete strains were measured by strain gauges glued onto the concrete surface, see Figure A.28. During the first tests, concrete strains were measured in 9 points on top of Element 3, FB1-9. Half way through the test schedule, these points were complemented by 6 additional points. Figure A.29 shows the name of the measurement points, and the location of the strain gauges.

Figure A.28 *Strain gauge on top of the concrete.*

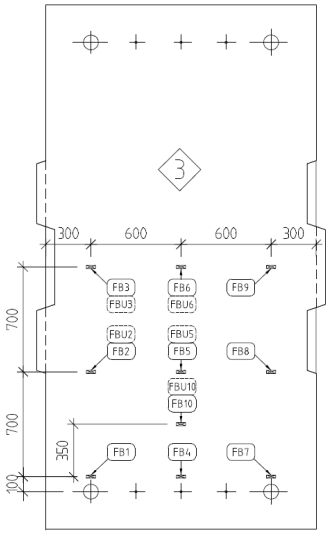

Figure A.29 *Concrete strain measurement points.*

Figure A.30 - Figure A.42 summarise the results from the concrete strain measurements. The maximum strains are plotted on the vertical axis and the locations of the strain gauges are plotted along the horizontal axis.

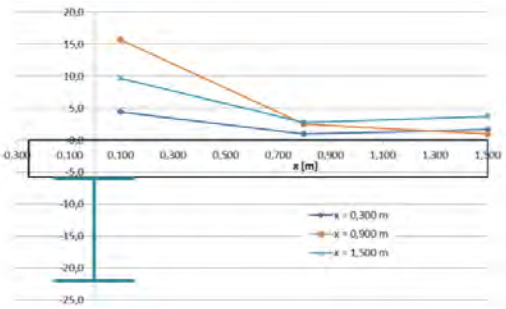

Figure A.30 *Concrete strains at maximum load in test 1, F_{max} = 100 kN.*

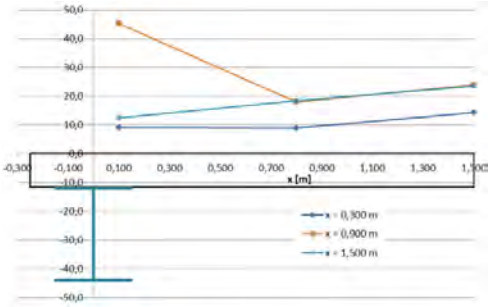

Figure A.31 *Concrete strains at maximum load in test 2, F_{max} = 280 kN.*

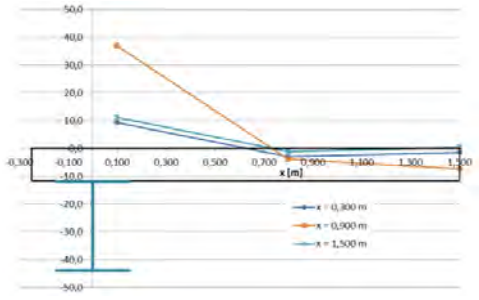

Figure A.32 *Concrete strains at maximum load in test 3, F_{max} = 310 kN.*

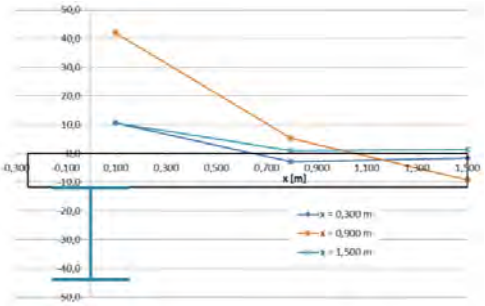

Figure A.33 *Concrete strains at maximum load in test 4, F_{max} = 430 kN.*

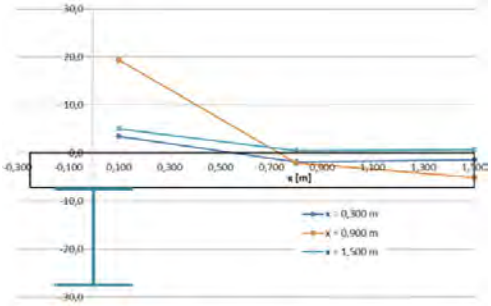

Figure A.34 *Concrete strains at maximum load in test 5, F_{max} = 250 kN.*

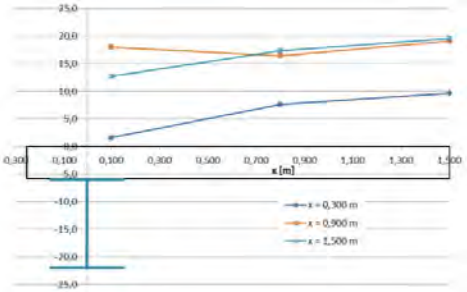

Figure A.35 *Concrete strains at maximum load in test 6, F_{max} = 250 kN.*

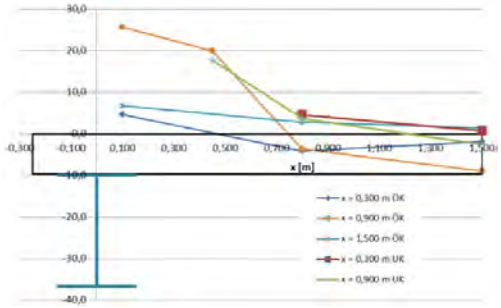

Figure A.36 *Concrete strains at maximum load in test 7, F_{max} = 400 kN.*

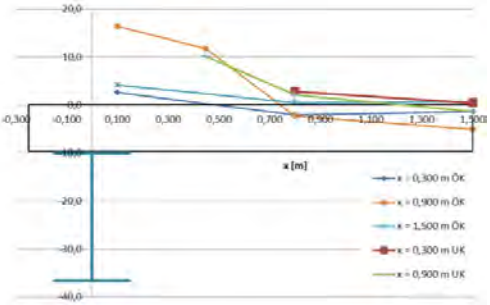

Figure A.37 *Concrete strains at maximum load in test 8, F_{max} = 250 kN.*

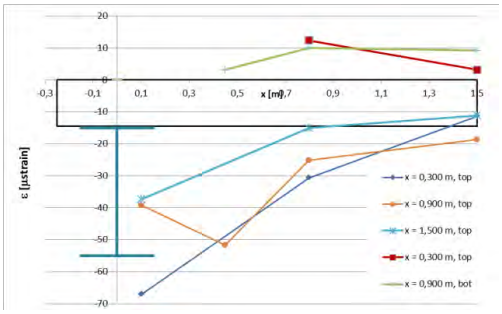

Figure A.38 *Concrete strains at maximum load in test 9, F_{max} = 500 kN.*

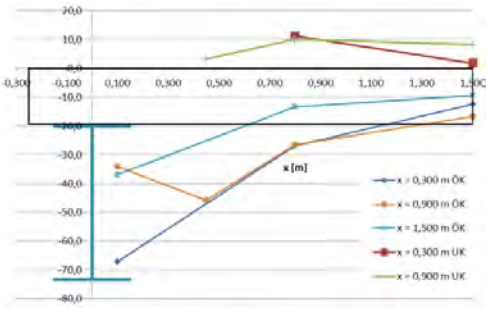

Figure A.39 *Concrete strains at maximum load in test 10, F_{max} = 450 kN.*

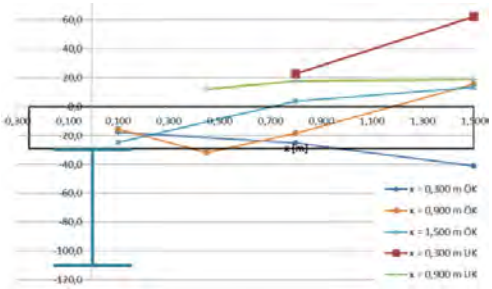

Figure A.40 *Concrete strains at maximum load in test 11, F_{max} = 300 kN.*

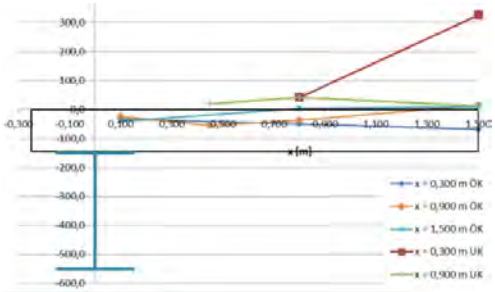

Figure A.41 *Concrete strains at maximum load in test 12, F_{max} = 450 kN.*

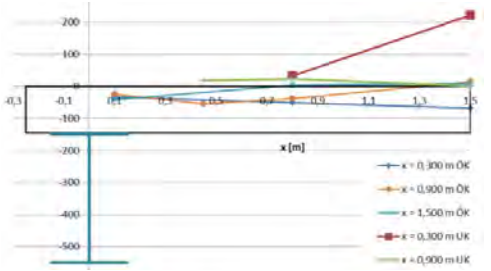

Figure A.42 *Concrete strains at maximum load in test 13, F_{max} = 400 kN.*

A.3.4 Reinforcement strains

In Element 3, 10 strain gauges were mounted on the reinforcement bars. The ribs were grinded down before the strain gauges were glued on smooth surfaces. This was done in the concrete workshop just prior to the casting. The location of the strain gauges, and their labels, are presented in Figure A.43

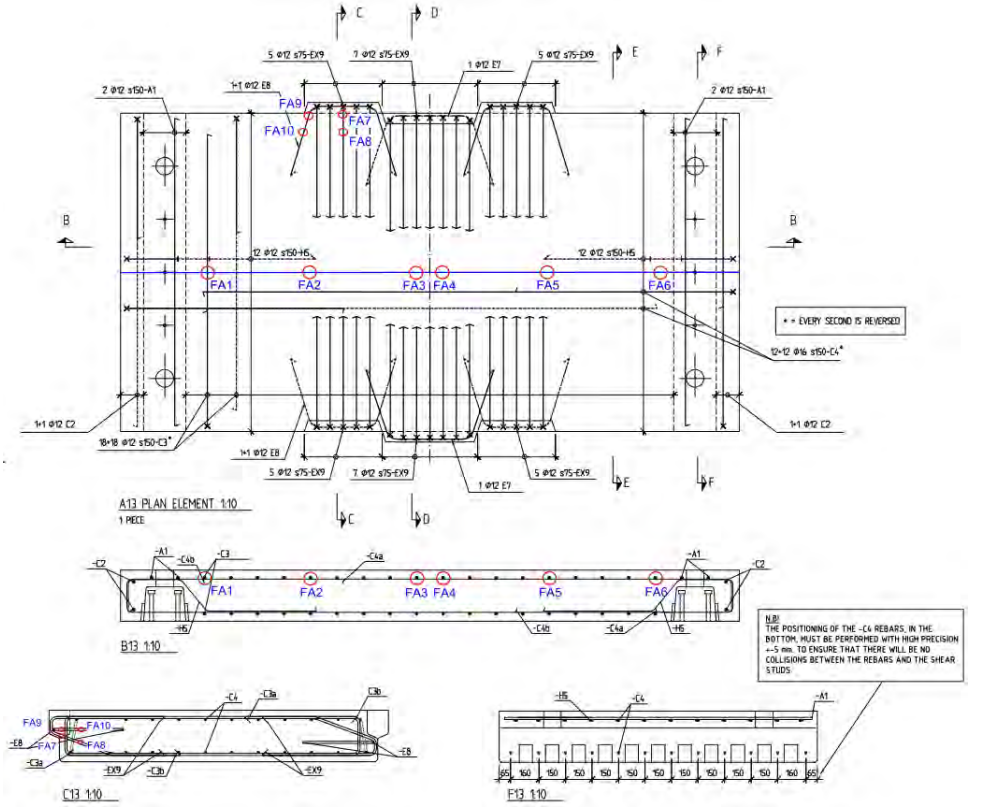

Figure A.43 *Installation scheme for the reinforcement strain gauges.*

The results from the strain measurement on the reinforcement bars are presented in Figure A.44 - Figure A.56. All strains are given in μstrain.

One thing that can be noted is that the strain gauge named FA3, did not work properly during the tests. Therefore, this measuring point has been excluded from the test results. In order to make it easier to see if the other results are symmetric or not FA3 is presented with the same value as FA4. These strain gauges are located on the neighbouring rebars, with only a distance of 150 mm between them.

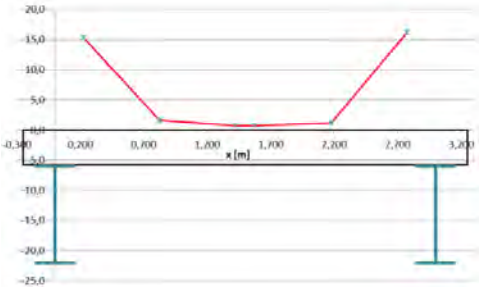

Figure A.44 *Reinforcement strains at maximum load in test 1, F_{max} = 100 kN.*

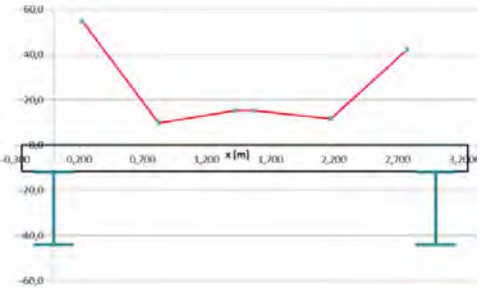

Figure A.45 *Reinforcement strains at maximum load in test 2, F_{max} = 280 kN.*

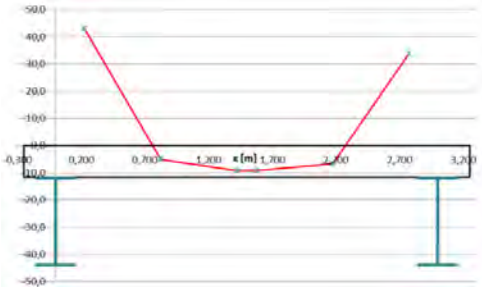

Figure A.46 *Reinforcement strains at maximum load in test 3, F_{max} = 310 kN.*

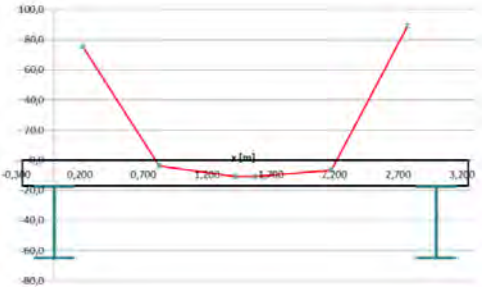

Figure A.47 *Reinforcement strains at maximum load in test 4, F_{max} = 430 kN.*

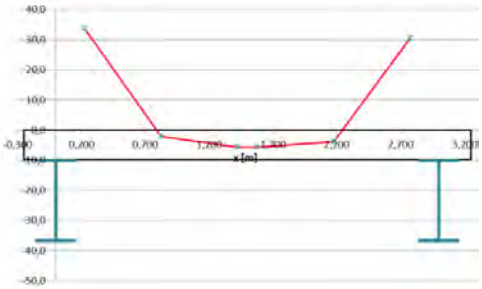

Figure A.48 *Reinforcement strains at maximum load in test 5, F_{max} = 250 kN.*

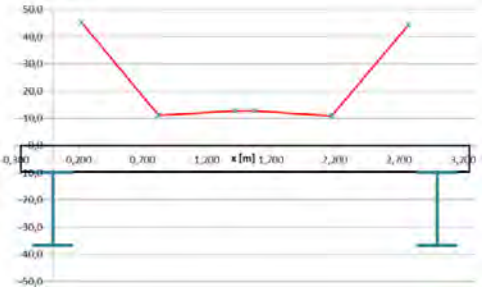

Figure A.49 *Reinforcement strains at maximum load in test 6, F_{max} = 250 kN.*

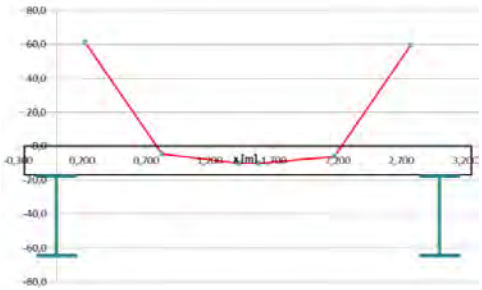

Figure A.50 *Reinforcement strains at maximum load in test 7, F_{max} = 400 kN.*

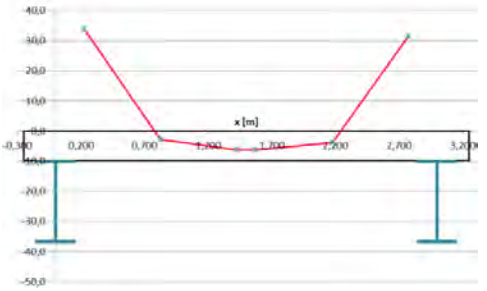

Figure A.51 *Reinforcement strains at maximum load in test 8, F_{max} = 250 kN.*

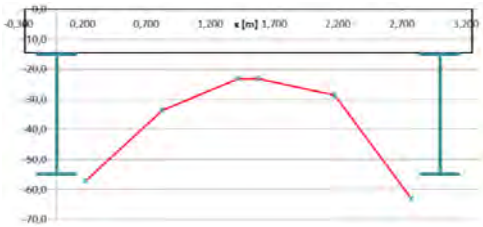

Figure A.52 *Reinforcement strains at maximum load in test 9, F_{max} = 500 kN.*

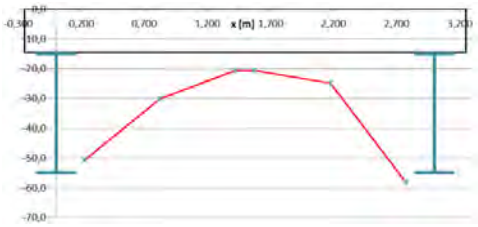

Figure A.53 *Reinforcement strains at maximum load in test 10, F_{max} = 450 kN.*

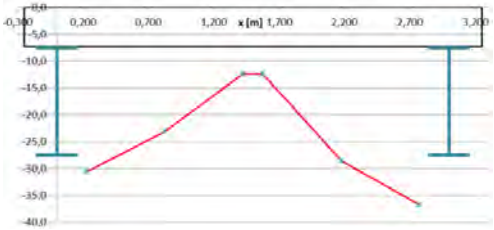

Figure A.54 *Reinforcement strains at maximum load in test 11, F_{max} = 300 kN.*

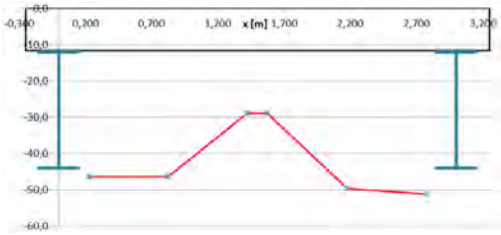

Figure A.55 *Reinforcement strains at maximum load in test 12, F_{max} = 450 kN.*

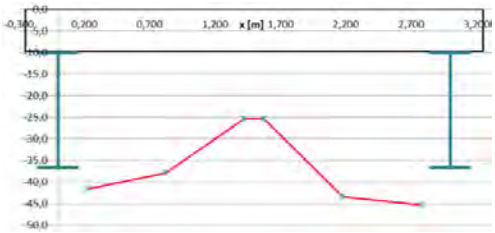

Figure A.56 *Reinforcement strains at maximum load in test 13, F_{max} = 400 kN.*

A.3.5 Joint openings

The joint openings were measured in eight points. At five points along the joint between Element 2 and 3, and at three points along the joint between Element 3 and 4. Eight LVDTs were used as measurement devices, LS1-LS8. Figure A.57 shows how these were fixed by glue, on top of the concrete. The plan and the name of the measurement points are presented in Figure A.58.

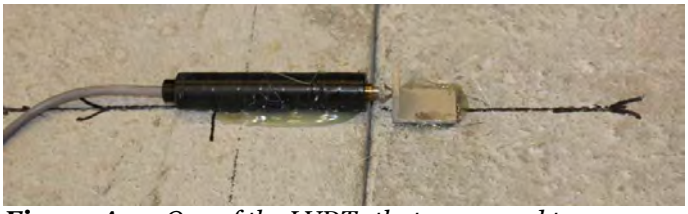

Figure A.57 *One of the LVDTs that were used to measure the joint openings.*

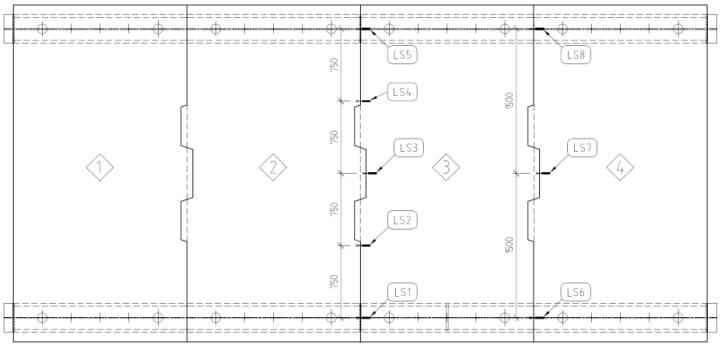

Figure A.58 *Joint opening measurement points.*

The results from the measurements of joint openings are presented below. The joint opening is defined as negative when the gap between the elements increases. The measured joint openings are presented graphically by F-δ diagrams, in Figure A.59 - Figure A.71. All movements are given in millimetres.

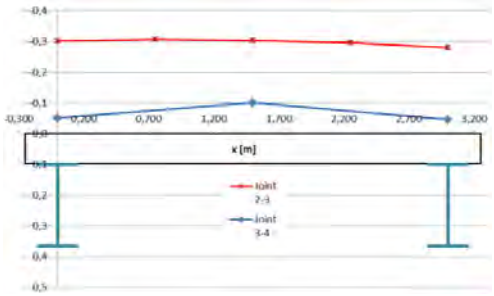

Figure A.59 *Joint opening at maximum load in test 1, F_{max} = 100 kN.*

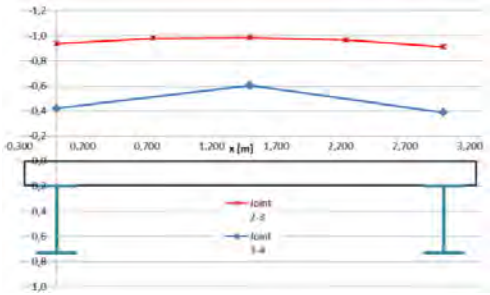

Figure A.60 *Joint opening at maximum load in test 2, F_{max} = 280 kN.*

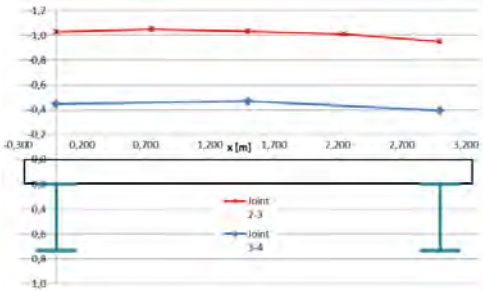

Figure A.61 *Joint opening at maximum load in test 3, F_{max} = 310 kN.*

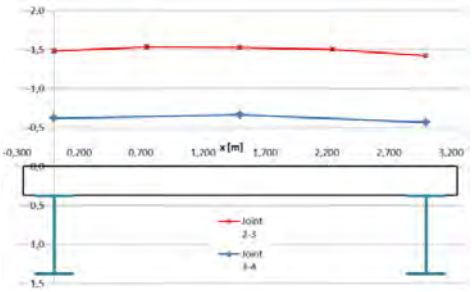

Figure A.62 *Joint opening at maximum load in test 4, F_{max} = 430 kN.*

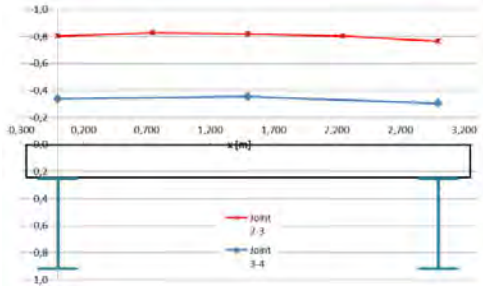

Figure A.63 *Joint opening at maximum load in test 5, F_{max} = 250 kN.*

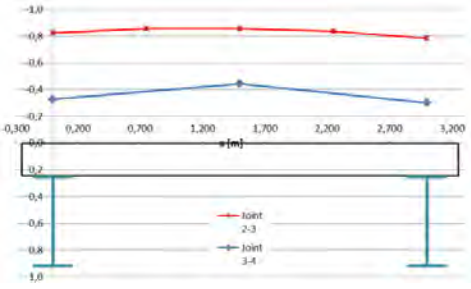

Figure A.64 *Joint opening at maximum load in test 6, F_{max} = 250 kN.*

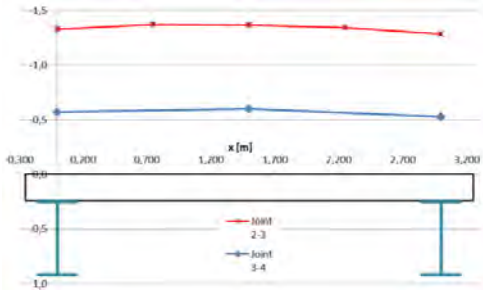

Figure A.65 *Joint opening at maximum load in test 7, F_{max} = 400 kN.*

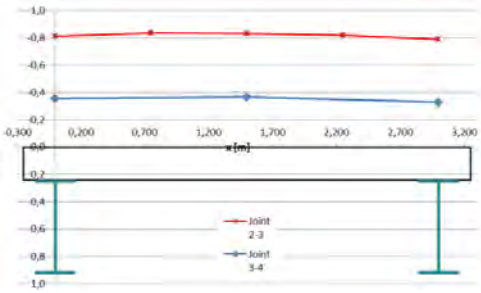

Figure A.66 *Joint opening at maximum load in test 8, F_{max} = 250 kN.*

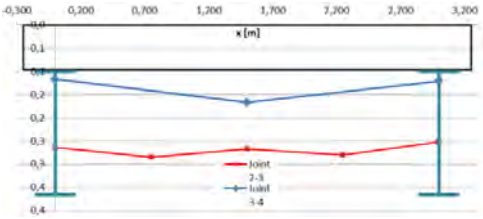

Figure A.67 *Joint opening at maximum load in test 9, F_{max} = 500 kN.*

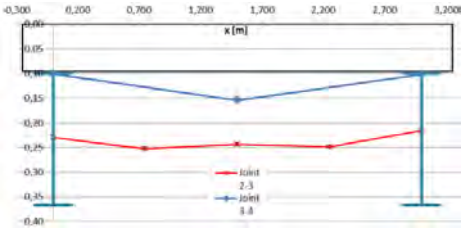

Figure A.68 *Joint opening at maximum load in test 10, F_{max} = 450 kN.*

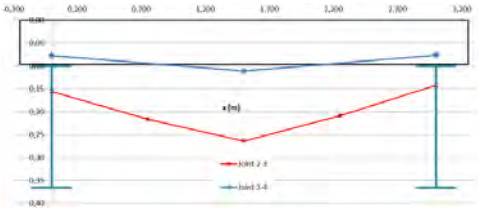

Figure A.69 *Joint opening at maximum load in test 11, F_{max} = 300 kN.*

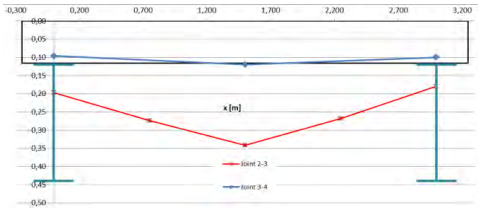

Figure A.70 *Joint opening at maximum load in test 12, F_{max} = 450 kN.*

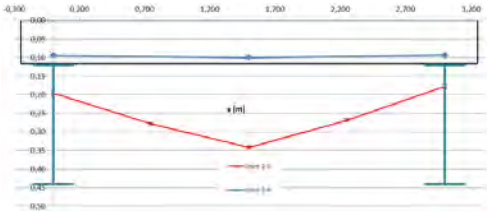

Figure A.71 *Joint opening at maximum load in test 13, F_{max} = 400 kN.*

Part II
Appended papers

Paper I

Prefabricated Bridge Construction across Europe and America

Robert Hällmark, Harry White and Peter Collin

Published in:
Practice Periodical on Structural Design and Construction, Vol. 17, No. 3, August 2012.

The majority of this paper is written by Hällmark, and has been edited by White. The latter has also added some sections about the state of art in the US. Collin has contributed with his views and opinions about the content of the paper.

Prefabricated Bridge Construction across Europe and America

Robert Hällmark[1]; Harry White[2]; and Peter Collin[3]

Abstract: Determining the most efficient and economical way to build a new or replacement bridge is not as straightforward a process as it once was. The total cost of a bridge project is not limited to the amount spent on concrete, steel, and labor. Construction activities disrupt the typical flow of traffic around the project and results in additional costs to the public in the form of longer wait times, additional mileage traveled to get around the work zone, or business lost attributable to customers avoiding the construction. The risk of injury to workers because of traffic interactions or construction activities increase with each hour spent at the construction site. Finding a way to shorten the time spent on the jobsite is beneficial to the contractor, the owner, and the traveling public. Prefabricating certain bridge elements reduces the time spent at the construction site and reduces the effects on the road users and the surrounding community. For example, steel beams with composite concrete decks reduce the construction time over cast-in-place concrete superstructures. In some instances, entire structures have been fabricated off-site under strict environmental and quality controls and then shipped to the site and erected in a matter of days instead of months. The total cost of using prefabricated bridge elements (PBE) depends greatly on the scale of the prefabrication. The more that prefabrication is used, the lower the costs. Even under limited use, however, prefabrication is usually comparable to traditional construction techniques. However, when durability and user costs are taken into account, the overall cost may be significantly less than traditional piece-by-piece construction. To improve the competitiveness of prefabricated composite bridges, a European research and development project, ELEM RFSR-CT-2008-00039, was started in 2008. The overall objective of the project is to make prefabricated bridges more competitive through development of new cost-effective, time-efficient, and sustainable bridge structures. The project has started with a knowledge extension, in the form of the workshop on "Composite Bridges with Prefabricated Deck Elements." This workshop was held in Stockholm, Sweden, in March 2009 to share the knowledge and experience gained by agencies around the globe. During the workshop, experiences from Europe and the United States were presented in an effort to promote the use of accelerated bridge construction (ABC) and prefabricated bridge elements. **DOI: 10.1061/(ASCE)SC.1943-5576.0000116.**

CE Database subject headings: Prefabrication; Bridges; Construction; Europe; United States.

Author keywords: Prefabricated bridge elements; PBE; Accelerated bridge construction; ABC; ELEM.

Introduction

Congestion is a growing problem in urban areas across the globe. The mobility needs of an increasing population demand that new roads and bridges be built even while existing infrastructure is maintained, widened, or reconstructed. Therefore, the total cost of a bridge or roadway project is not limited to the amount spent on concrete, steel, and labor: user costs must be considered.

Transportation construction, especially reconstruction of an existing roadway, disrupts the typical flow of traffic around the project area and results in additional user costs to the public in the form of longer wait times, additional mileage traveled to get around the work zone, inefficient movement of goods and services, and business lost attributable to customers staying away from the construction.

[1]M.Sc. Civil Engineering, LTU/Ramböll Sverige AB, Luleå, Sweden. E-mail: Robert.Hallmark@ramboll.se

[2]New York State Dept. of Transportation, Albany, NY (corresponding author). E-mail: hwhite@dot.state.ny.us

[3]Professor, LTU/Ramböll Sverige AB, Luleå, Sweden. E-mail: Peter.Collin@ramboll.se

Note. This manuscript was submitted on May 16, 2011; approved on August 29, 2011; published online on July 16, 2012. Discussion period open until January 1, 2013; separate discussions must be submitted for individual papers. This paper is part of the ***Practice Periodical on Structural Design and Construction***, Vol. 17, No. 3, August 1, 2012. ©ASCE, ISSN 1084-0680/2012/3-0–0/$25.00.

In recent years, transportation agencies around the globe have begun to use accelerated construction techniques (ACT) that incorporate prefabricated bridge elements (PBE). Prefabricating certain bridge elements reduces the time spent at the construction site and reduces the effects on the road users and the surrounding community.

For example, steel beams with composite concrete decks reduce the construction time over cast-in-place concrete structures. Additional time savings can be achieved by prefabricating the riding deck and the substructure. In some instances, entire structures have been fabricated off-site under strict environmental and quality controls. The fabricated components are then shipped to the site and erected in a matter of days instead of months.

Unfortunately, road user costs are often neglected when comparing design alternatives. The total expense of using a prefabricated bridge is usually comparable to traditional construction techniques. However, the overall cost may be significantly less than traditional construction when durability and user costs are taken into account (Culmo 2009). Even where there are advantages to using prefabrication, typical construction techniques are still often used out of familiarity and habit.

In some countries, prefabrication seems to be gaining momentum (Culmo 2009; Seidl 2009), but it is far from a common procedure everywhere. The workshop on Composite Bridges with Prefabricated Deck Elements was held in Stockholm, Sweden, in March 2009 to share the knowledge and experiences from Europe

and the United States concerning prefabricated bridge elements (PBE).

Costs of Bridges Using Prefabricated Bridge Elements

When looking at costs, it is important to consider not only the initial costs of a structure, which consist of the monetary cost of the materials and labor required to design and construct the structure, but also the societal costs associated with the construction noise and traffic disruption A U.S. study (Ralls 2008) states that, for agencies that use prefabrication infrequently, the initial cost of a structure built using PBE is slightly higher than for traditional piecemeal construction procedures. However, it is the overall, or life-cycle, costs of PBE structures that must be compared with traditional construction to determine which provides the best value.

A cost-benefit analysis (Degerman 2002) of a single-span railway crossing bridge in Norrfors, Sweden, that used PBE showed a dramatic positive effect on cost and schedule. The cost to prefabricate the bridge was presumed by the designers to be higher than the cost to cast the concrete deck on-site. However, a bidding contractor indicated that the prefabricated deck was actually less expensive, as the additional costs attributable to prefabrication is overcome by the savings achieved by eliminating formwork and other activities required when building a bridge over an operating railway.

Time spent on-site often causes disturbance of the local traffic patterns. Prefabrication can be used to shorten this time considerably, which indicates that the delay-related road user costs would be reduced. A study of a Swedish road bridge (Nilsson 2001), called the Rokan Bridge, compared the cost of constructing a prefabricated composite bridge, a conventional composite bridge with a temporary detour bridge, and a conventional composite bridge with the traffic directed to the nearest bypass roads. The conclusion from the study was that the most economical alternative, from a societal perspective, was to construct a prefabricated bridge and eliminate the need for the long-term detours.

Agencies that use prefabrication more consistently find that project bid prices are in line with, or sometimes lower than, traditional construction as contractors become more familiar with the methods. Once the prefabricated elements, connection details, construction procedures, and other details are standardized and become more familiar, prefabricated bridges should consistently result in lower initial construction costs and produce higher-quality final products.

To capitalize and on this theory, the Massachusetts Dept. of Transportation (MassDOT) has begun to bundle multiple accelerated bridge construction (ABC) projects along a travel corridor into a single contract (Commonwealth of Massachusetts 2010). This way, the designs on similar projects can be produced more efficiently and the construction methods become repetitive. Bundled design projects, as opposed to having separate contracts for each project, save procurement time and take advantage of the contractor's progress along the learning curve of ABC projects. MassDOT has already solicited bids on 13 bundled contracts that will address repairs to several hundred substructures and bridge decks, primarily located on interstate highways and major arterials across the commonwealth.

United States—Accelerated Bridge Construction

Accelerated bridge construction can be defined as "building the bridge first before setting up the traffic control cones, and then move it quickly into place, like in hours or a weekend." (Mistry 2008). Different prefabrication concepts have been used in the United States. The prefabrication level varies from prefabricated components in the superstructure to totally prefabricated bridges. A variety of design solutions have been proposed and tested during the years. The Federal Highways Administration (FHWA) publication titled *Connection Details for Prefabricated Bridge Elements and Systems* outlines the state of practice in the United States for ABC (FHWA 2009). The publication breaks down the details into three levels. Level 1 is for details that have become standard practice in at least one agency. Level 2 details have been used once and found to be practical to construct. Level 3 details are conceptual or experimental and have not been placed in field service. The Federal Highway Administration has also prepared two documents to assist decision makers on implementing ABC technologies in bridge projects.

The Utah Dept. of Transportation (UDOT) is just one example of a U.S. agency that believes accelerated bridge construction is the future, and it intends to include this concept in all future bridge projects. So far, UDOT has constructed bridges with precast deck panels, precast abutments, and precast approach slabs, and it has moved entire superstructures into place using self-propelled modular transports (SPMT) (UDOT 2004).

Prefabricated Bridge Girders and Decks

Prefabricated steel or prestressed concrete girders are the overwhelming choice in the United States and cast-in-place concrete girders are very rare. Prefabricated bridge decks are less commonly used, but are typically made of prestressed concrete panels, although there has been limited use of orthotropic decks, prefabricated aluminum decks, and fiber reinforced polymer (FRP) panels.

The prefabricated deck elements are almost always designed to provide composite action between the deck element and the girders. The composite action between steel girders and precast deck elements is primarily achieved by welded shear studs.

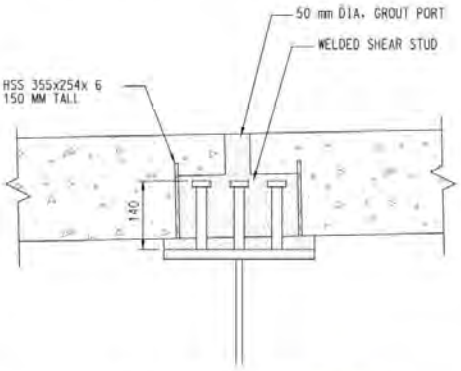

Fig. 1. Composite connection (FHWA 2009)

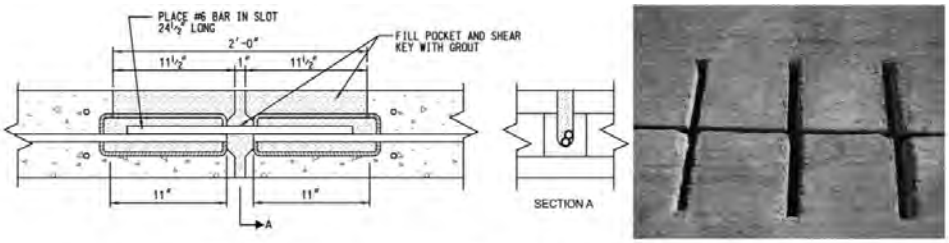

Fig. 2. Transverse connection at Live Oak Creek Bridge, Texas (FHWA 2009)

Composite action between prestressed concrete girders and deck elements can also be achieved by using headed studs cast into girder, as well as extended reinforcement. The prefabricated deck elements can either be made with full thickness pockets or with blind pockets with grouting ports, as shown in Fig. 1. There has been a tremendous amount of research in the area of prefabricated decks and their associated connections.

The design of the transverse joint between precast panels varies significantly between U.S. transportation agencies. Many states do not use waterproofing membranes and prefer to apply posttensioning force to the panels to ensure a crack free deck. Non-post-tensioned transverse joints are also used. For example, the bridge over Live Oak Creek in Texas uses blind pocket details with dowel bar connections at the joints and no posttensioning, as shown in Fig. 2. This solution works best on single spans where the deck is always in compression, but it has also been used in multi-span bridges where the areas over the piers are in tension.

Recently, the New York State Dept. of Transportation has developed a detail that uses full width precast Portland cement concrete panels that are connected using ultra-high-performance concrete (UHPC), as shown in Fig. 3. UHPC has compressive strengths exceeding 30 ksi (200 MPa) and postcracking tensile strengths of 1.5 ksi (10 MPa) while simultaneously being nearly impenetrable to chloride ions (FHWA 2010). Given these exceptional properties, composite action can be obtained using only 3-in. (75-mm)-tall shear studs. This eliminates possible interference between the more traditional 6-in.-tall shear studs and the transverse reinforcement. Also, the high postcracking tensile capacity indicates that the costs and time involved in posttensioning are not necessary to assure water tightness, even in areas of negative, or hogging, moment.

Prefabricated Superstructures

In 2004, a U.S. transportation team conducted an international scan to gather worldwide information about prefabricated bridge elements and systems (FHWA 2005). One of the top implementation recommendations was to introduce the concept of completely assembling bridge components off-site and then moving them into final position using different movement systems.

Self-propelled modular transports (SPMT), and similar types of vehicles, enable the superstructure to be prefabricated in pieces that weigh up to several thousand tons and are transported to the construction site for a rapid installation. The build-and-slide-into-place concept of building bridges has started to gain ground in the United States, and it has been used successfully by several agencies. For example, the Graves Avenue Bridge in Florida was

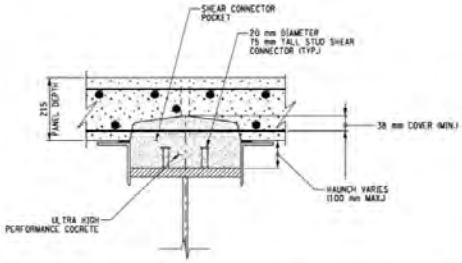

Fig. 3. Connection detail of precast panel and steel girder using UHPC (Reprinted with permission from NYSDOT)

Fig. 4. SPMT transportation of 4500 South Bridge, Utah (Reprinted with permission from Mammoet USA South, Inc.)

Fig. 5. Grouted reinforcing splice-sleeve connector (Reprinted with permission from Splice Sleeve North America, Inc.)

replaced in 2006 using SPMTs to remove the old bridge and install the new bridge. The new spans were built alongside the existing bridge to avoid traffic disturbance. The 59-ft (18-m)-wide superstructure had a span of 144 ft (44 m) and a weight of 1,430 tons (1,300 metric tons). A similar procedure was used in Utah when in October 2007 the single-span superstructure of the 4500 South Bridge, which weighed 1,650 tons (1,500 metric tons) and had a longitudinal inclination of 10%, was replaced in only 53 h, as can be seen in Fig. 4.

Complete Bridge Prefabrication

Prefabricated substructures are not common in the United States, although the concept has been used and is gaining in popularity. One method of prefabrication is to precast segments of the piers, abutments, walls, etc. at an off-site fabrication facility. Splice-sleeve connectors, as shown in Fig. 5, are cast into the segment during fabrication. The segments are then transported to the construction site, where they are rapidly assembled. The segments are

Fig. 6. Prefabricated substructures (FHWA 2009)

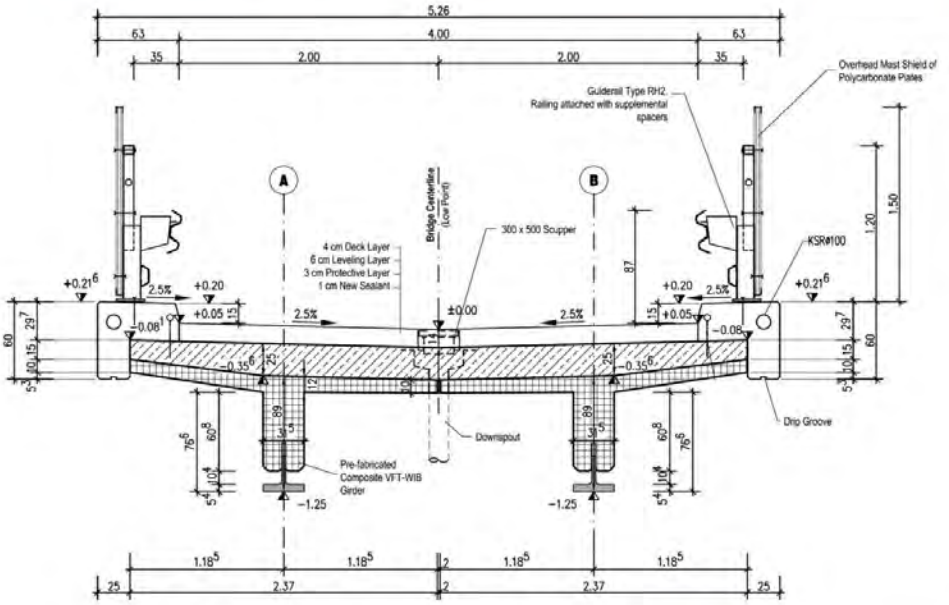

Fig. 7. VFT-bridge cross section (Reprinted with permission from Seidl and Braun 2009)

rigidly connected together by grouting the overlapping reinforcing bars within the splice-sleeve connector. There are many potential uses for prefabricated substructures with these connections, as can be seen in Fig. 6. Combined with prefabricated superstructures, it is possible to achieve complete bridge prefabrication.

Germany—Prefabricated Deck

In Germany, as well as many other countries, cast-in-place concrete decks are almost obligatory, and prefabricated decks are rare exceptions. However, prefabricated composite girders have begun to gain ground. A new construction method, called VFT, has been developed to achieve a high level of prefabrication and, therefore, shorten the on-site construction time. The VFT construction method indicates that composite steel girders are prefabricated with precast partial depth slabs, as shown in Figs. 7 and 8. This method has been developed in Germany and tested on railway bridges in Austria. (Seidl 2009; Seidl and Braun 2009)

Prefabricated full-depth slabs have also been tested in Germany. The Bahretal viaduct is an example of such a bridge. It is a six-span bridge with a length of 1,155 ft. (352 m). The composite superstructure is made of a steel box girder with transversal cantilever cross beams every fourth meter; see Fig. 9. Precast deck slabs, which are almost square shaped, are placed in the cantilever portion of the superstructure. Fresh concrete is cast between the precast elements in the longitudinal direction of the bridge. The concrete deck on top of the upper flange of the box girder is also cast in place.

Fig. 8. Prefabricated VFT-girder (Reprinted with permission from Seidl and Braun 2009)

France—Prefabricated Decks

In France, bridges with prefabricated deck slab elements have been used for quite a long time. Two kind of transverse joints that have been used are match-cast joints and reinforced joints. Several bridges have been built using one of these two joints.

The first composite bridges with dry joints were erected in 1988 in Manosque on Escota Highway A51. These bridges were the first two built with the technique of prestress assembling of elements with carefully fitted keys in the joint faces that are simply glued to one another. The longest bridge was a four-span twin girder bridge with a length of 160 m and a maximum span of slightly more than 50 m. A detailed inspection carried out in 1995 showed no sign of cross-cracking of the slab element. Later inspections gave the same results, with the joints seeming to perform well (Berthellemy 2001, 2009).

A more recently used technique of dry joints is the VINCI overpass system with high-strength concrete. Because the deck is precast, high-strength concrete can be used without getting problems with large shrinkage. The durability of the slab will be better in many aspects, for example, better anticorrosion protection and better fatigue durability, because the prestressed concrete will remain in compression. The building process, as illustrated in Fig. 10, typically proceeds as follows (Berthellemy 2001, 2009):

1. Steel girders and match-cast deck elements are prefabricated off-site.
2. Elements are placed onto the girder, which has no shear studs at this stage.
3. The precast concrete elements are prestressed together, without connection to the steel.
4. Shear studs are welded to the steel beam through holes in the concrete.
5. The holes are filled with fresh concrete, which results in composite action between the deck and the girder.

United Kingdom (U.K.)—Precast Bridge Deck Systems

There are several examples of bridges with prefabricated deck elements in the U.K. Partial-depth precast deck elements have been used in several bridges all over the U.K. These elements act as a formwork to the cast-in-place concrete. There are, however, disadvantages to the use of these elements. For example, a large amount

Fig. 9. Bahretal viaduct with prefabricated full-depth slab elements (Reprinted with permission from Seidl 2009)

Fig. 10. The VINCI assembling process (Reprinted with permission from Berthellemy 2009): (a) elements are lifted and placed on girders without studs; (b) elements are prestressed; (c) studs are welded through holes in the deck

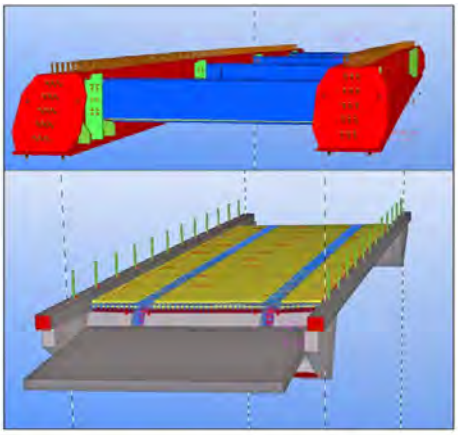

Fig. 11. 3D model of Laisentianjoki bridge (Reprinted with permission from Harju 2009)

of reinforcement is required to achieve a moment capacity large enough to withstand the crane lift operations. Another disadvantage, compared with full-depth elements, is the need of in situ cast concrete, which reduces the speed of construction. Full-depth precast concrete decks would provide faster construction, but there has been some reluctance to use them in the U.K. (Gordon and May 2007).

In Scotland, much research has been conducted in the field of in situ cast joints between the precast deck elements, and different joints have been laboratory tested (Gordon and May 2006).

Finland—Case Study: Laisentianjoki Bridge

In 2006, the Steel Bridges Development Group of Finnish Constructional Steelwork Association (TRY) started the development work for a new type of cantilever composite steel-concrete bridge. The targets for the study were to develop a composite bridge according to following criteria:

- Shortest possible installation time;
- Easy to build—Even in difficult conditions; and
- Extensively utilize 3-D design tools.

The outcome of the development project was the Laisentianjoki bridge, which was built in 2007. The bridge is 24.6 ft (7.5 m) wide with spans that are 6.5 ft + 59.0 ft + 6.5 ft (2.0 m + 18.0 m + 2.0 m). The superstructure consists of two main steel girders, 72 ft (22 m) each, and four cross beams. Both steel and concrete drawings were modeled in 3D, as shown in Fig. 11. The installation of the main girders and cross beams took approximately 6 h. Cross beam joints were bolted connections, so there was no need to treat the surface of the joints on-site. The bridge deck, wing walls, and end beam were constructed of prefabricated concrete elements. The panel joints and edge beams were cast in place so that the concrete and steel elements form a monolithic structure. The placement of the prefabricated elements was completed in approximately four days. The installation of the steel reinforcement, casting of the fresh concrete, and construction of the edge beams, as shown in Figs. 12 and 13, took eight additional working days (Harju 2009).

Sweden—Deck Elements with Dry Joints

Although Sweden has been building bridges using prefabricated deck elements for decades (Collin and Johansson 1999), the techniques are still rarely used. Different types of precast deck joints have been tried from reinforced cast-in-place wet joints to the latest solution with completely dry joints. The wet joints are similar to the techniques used in France, Scotland, the United States, etc. Wet joints require that some of the reinforcement be placed on-site

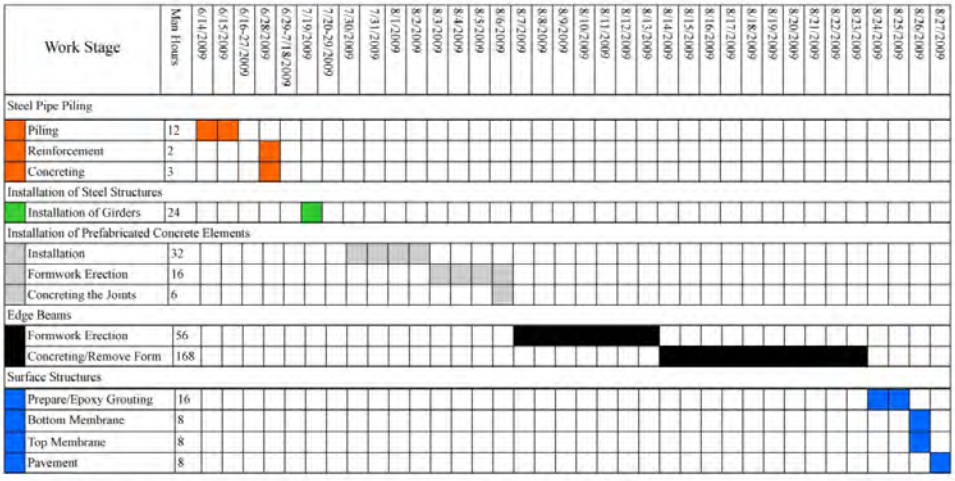

Fig. 12. Realized erection times for Laisentianjoki bridge (Reprinted with permission from Harju 2009)

Fig. 13. Construction sequence for the Laisentiajoki bridge (Reprinted with permission from Harju 2009): (a) large diameter steel piles being driven into the soil; (b) concrete filled piles with bearings in place; (c) steel girders being lifted into place; (d) completed steel structure; (e) prefabricated concrete end beams and wing walls being placed into final position and cast to the steel girders; (f) erection of prefabricated concrete deck elements; (g) prefabricated deck placed and awaiting concrete closure pour; (h) composite action is achieved by in situ cast concrete in the open channels

and that fresh concrete will be exposed as a part of the surface above the joints. Both of these items have associated time and durability concerns. Field placing reinforcement is yet another time-consuming procedure that must be done on-site. Any exposed field placed concrete provides an easier path for water and chlorides to permeate the concrete deck and begin attacking the reinforcing bars. Even if a waterproofing membrane is used, any field placed concrete must have time to mature before the waterproofing membrane can be installed. These are but a few of the items that increase construction time until the bridge can become operational and shorten the life of the final structure. To avoid these problems, a concept with dry joints has been developed in Sweden.

In a dry joint, match-cast overlapping concrete keys are used to transfer both lateral and vertical forces through the transverse joints and, thus, prevent vertical displacement between the deck elements at the joints. These keys are designed as a series of overlapping male-female connections along the joints, as given in Fig. 14.

The overlapping concrete keys require a longitudinal displacement of the elements during assembly. The tolerances for the deck slabs can be demanding because the distance between the transverse reinforcement bars in the slab and the shear studs on the steel girder is rather short. The required displacement is at least the depth of the overlapping concrete keys plus the tolerances, as indicated in Fig. 15. This technique has been used successfully on single-span

(e)

(f)

(g)

(h)

Fig. 13. (*Continued*).

bridges and is now developed to be used on multispan bridges. One key factor in multispan bridges will be the ability of the waterproofing system to withstand the negative moments and joint openings above an intermediate support.

European Research Project—ELEM

Studies conducted in the United States and Europe show the advantages of prefabrication in the field of bridge construction. To improve the competitiveness of prefabricated composite bridges, a European research and development project, ELEM RFSR-CT-2008-00039, was started in 2008. Four countries are represented in the research group: Sweden, Germany, Finland, and Poland. The success of the project relies on the cooperation between universities, engineering consultants, and steel producers. The overall objective of the project is to make prefabricated bridges more competitive through development of new cost-effective, time-efficient, and sustainable bridge structures. Both wet and dry joints between the slabs are investigated, with particular attention given to the opening of dry joints above internal supports. To avoid leakage, suitable waterproofing and paving systems must be developed and thoroughly tested in the laboratory. The project also aims to determine how shear forces transfer through the concrete keys to each slab, and examine the actual design of the concrete keys. The project started with a knowledge extension, in form of an international workshop held in Stockholm, Sweden, in March 2009 and literature studies. The project has also included improvement of the details in element bridges, testing of the solutions in laboratories, and field monitoring on a one span bridge with dry joints.

Fig. 14. Deck elements with dry joints (Reprinted with permission from Hällmark et al. 2009; first published in *Structural Engineering International SEI*, Vol. 19, Nr. 1, 2009, pp. 69–78, IABSE, Zurich, Switzerland, www.iabse.org)

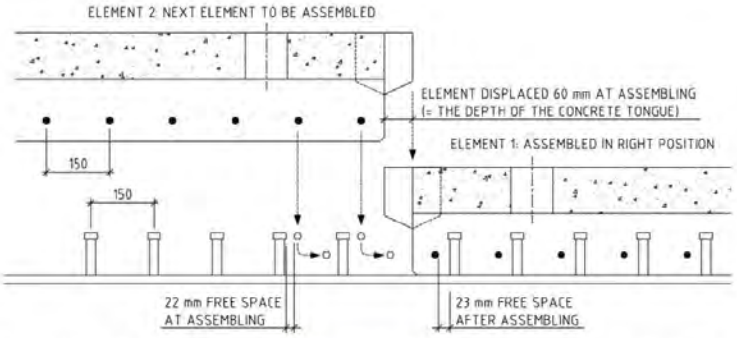

Fig. 15. Tolerances at assembling (Reprinted with permission Hällmark et al. 2009; first published in *Structural Engineering International SEI*, Vol. 19, Nr. 1, 2009, pp. 69–78, IABSE, Zurich, Switzerland, www.iabse.org)

Discussion and Conclusion

High-traffic pressure on an aging infrastructure network gives rise to demands from the traveling public for construction techniques that have as little effect on traffic as possible. Conventionally, bridges are built with cast-in-place concrete decks on girders that are cast-in-place concrete, precast concrete, or prefabricated steel. Accelerated construction techniques that use prefabricated elements lower road user costs by reducing traffic disturbance, lessening time spent on construction sites, and making the working environment safer. Prefabrication, especially of concrete decks, is a spreading methodology worldwide, but examples of prefabricated piers, abutments, walls and combined steel girders and partial concrete decks can be found.

Composite action between the girders and prefabricated deck elements is desirable and typically achieved by casting concrete into preformed pockets that surround shear studs attached to the girder flanges. The transverse joints between the elements must be carefully designed, depending on the demand for water tightness and ability to transfer loads between elements. Posttensioning offers good performance, but is not required to achieve satisfactory results. Blind pocket details with dowel bar connections promise composite action without exposing cast-in-place concrete to the elements.

The most thrilling and challenging technique is the idea of using completely dry joints. Overlapping male-female concrete keys are used to transfer both lateral and vertical forces through the joints and prevent vertical displacements between the deck elements. This solution has been used on single-span bridges but is now being further developed to be used on multispan bridges as well.

References

Berthellemy, J. (2001). "Composite construction—Innovative solutions for road bridges." *Proc., 3rd Int. Meeting on Composite Bridges*, Madrid, Spain.

Berthellemy, J. (2009). "French experiences from prefabricated deck elements." *Proc., Workshop on Composite Bridges with Prefabricated Deck Elements*, Stockholm, Sweden.

Collin, P., and Johansson, B. (1999). "Wettbewerbsfähige Brücken in Verbundbauweise." *Stahlbau*, 68(11), 908–918 (in German).

Commonwealth of Massachusetts. (2010). "Laboratory for Innovation." ⟨http://www.eot.state.ma.us/acceleratedbridges/pr_lab.htm⟩ (Jun. 21, 2011).

Culmo, M. P. (2009). "Prefabricated composite bridges in the United States including total bridge prefabrication." *Proc., Workshop on Composite Bridges with Prefabricated Deck Elements*, Stockholm, Sweden.

Degerman, H. (2002). "Samhällsekonomisk analys av hastighetsnedsättning vid bro söder om Norrfors." *Internal Rep.*, Banverket, Norra Regionen, Sweden (in Swedish).

Federal Highway Administration (FHWA). (2005). "Prefabricated bridge elements and systems in Japan and Europe." *FHWA-PL-05-003*, Office of Engineering, Bridge Division, Washington, DC.

Federal Highway Administration (FHWA). (2009). "Connection details for prefabricated bridge elements and systems." *FHWA-IF-09-010*, Office of Engineering, Bridge Division, Washington, DC.

Federal Highway Administration (FHWA). (2010). "Field cast UHPC connections for modular bridge deck elements." *FHWA-HRT-11-022*, Office of Engineering Bridge Division, Washington, DC.

Gordon, S., and May, I. (2006). "Development of in situ joints for pre-cast bridge deck units." *Proc. ICE—Bridge Eng.*, 159(1), 17–30.

Gordon, S., and May, I. (2007). "Precast deck systems for steel-concrete composite bridges." *Proc. ICE—Bridge Eng.*, 160(1), 25–35.

Harju, T. (2009). "CASE—Laisentianjoki Bridge." *Proc., Workshop on Composite Bridges with Prefabricated Deck Elements*, Stockholm, Sweden.

Hällmark, R., Collin, P., and Stoltz, A. (2009). "Innovative prefabricated composite bridges." *Struct. Eng. Int.*, 19(1), 69–78.

Mammoet USA. (2009). ⟨http://www.mammoet.com⟩ (Aug. 4, 2011).

Mistry, V. (2008). "Need for prefabricated bridge elements and systems for accelerated bridge construction." *WASHTO-X Webinar*, June 17, 2008.

Nilsson, M. (2001). "Samverkansbroar ur ett samhällsekonomiskt perspektiv." Master's thesis, Luleå Univ. of Technology, Sweden (in Swedish).

Ralls, M. L. (2008). "Benefits and costs of prefabricated bridges."*Accelerated Bridge Construction Study*, Utah Dept. of Transportation, Salt Lake City, UT.

Seidl, G. (2009). "Composite Element Bridges." *Proc., Workshop on Composite Bridges with Prefabricated Deck Elements*, Stockholm, Sweden.

Seidl, G., and Braun, A. (2009). "VFT-WIB-Brücke bei vigaun—Verbundsbrücke mit externer bewehrung." *Stahlbau*, 78(2), 86–93 (in German).

Splice Sleeve North America. (2009). ⟨http://www.splicesleeve.com⟩ (Aug. 4, 2011).

Utah Dept. of Transportation (UDOT). (2004). *"Utah Dept. of Transportation,"*⟨www.udot.utah.gov⟩ (Mar. 27, 2009).

All presentations from the Workshop on Composite Bridges with Prefabricated Deck Elements are published in a Technical Report available at: ⟨http://pure.ltu.se/portal/files/3112371/ELEM_Seminar_4_Mars_2009.pdf.⟩.

Paper II

Innovative Prefabricated Composite Bridges

Robert Hällmark, Peter Collin and Anders Stoltz

Published in:
Structural Engineering International, Vol. 19, No. 1, February 2009, pp 69-78.

This paper is written by Hällmark. Collin has contributed with his views and opinions about the content. Stoltz has performed the tests and provided the data presented in this paper.

Innovative Prefabricated Composite Bridges

Robert Hällmark, MSc, Ramböll, Luleå, Sweden; **Peter Collin,** Prof., Luleå University of Technology and Ramböll, Luleå, Sweden and; **Anders Stoltz,** Lic. of Technology, Skanska, Kalix, Sweden. Contact: Robert.Hallmark@ramboll.se

Summary

The competitiveness of composite bridges depends on different circumstances such as site conditions, local costs of material and staff, and the experience of the contractor. Two major advantages of composite bridges compared to concrete bridges are the ability of the steel girders to carry the weight of the formwork and the fresh concrete, and the shorter construction time which not only saves money for the contractor but even more for the road users. A further step is to prefabricate not only the steel girders, but also the concrete deck. In this paper, a new concept for composite bridges is described, with dry joints between the prefabricated concrete elements. The principal of the technique is presented, as well as some laboratory test simulating the load situation at an internal support in a multi-span bridge. Also, some experiences from an already built single span composite bridge with dry joints are presented.

Keywords: composite bridges; prefabricated decks; deck elements; dry joints.

Introduction

Composite bridges have become more popular in many countries.[1,2] The cost effectiveness of composite bridges is governed by different factors such as site condition, local cost of material and staff, and the experience of the contractor. In comparison to concrete bridges, one major advantage is that steel girders can carry the weight of the formwork and the fresh concrete, which means that the need for temporary structures is reduced, as indicated in *Fig. 1*.

In comparison with concrete bridges, in most cases less time is spent on the construction site if a composite structure is chosen. A shorter construction time saves money not only for the contractor but often even more for the road user. Unfortunately, the road-user costs tend to be neglected when alternative bridge designs are evaluated and compared.

The concrete deck is usually cast on-site, which means that the work with the formwork, reinforcement as well as the casting most often takes places outdoors. This work can be problematic and expensive during wintertime in countries with a cold climate.

A further step to improve the competitiveness of composite bridges is to prefabricate not only the steel girders, but also the concrete deck. The main advantages of precast concrete deck slabs, compared to conventional bridges with concrete decks cast onsite, are:

- A less number of man-hours outdoors at the construction site.
- A shorter construction time onsite, giving lower road-user costs.
- The deck elements are cast indoors, which is believed to result in high quality.
- An improved working environment for the workers while erecting formwork, placing re-bars and casting concrete.

It is also clear that some problems need to be solved in connection with prefabricated deck slabs in order to make the concept cost efficient. This will be discussed in the current paper, in addition to presenting some new solutions.

Deck Elements with Dry Joints

Concrete deck elements acting compositely with steel girders have been used in many countries around the world, e.g. Germany, USA, Russia, France and Sweden.[2–4] When dealing with prefabricated deck elements, two main questions should be answered.

(a) How should the horizontal shear forces be transmitted between steel and concrete?
(b) How should the vertical shear forces be transmitted between the deck elements?

Different technical solutions have been used to transfer the vertical shear forces from one deck slab to another. Post-stressed cables have been used to press the elements together. This system was, for example, used on a three-span bridge in Sweden,[2] but it turned out to be rather expensive. Many countries have used different kinds of reinforced site-cast joints in order to transfer the forces between the elements. Site-cast joints mean, however, that some re-bars must be placed onsite, and that fresh concrete will be exposed on the surface at each joint. These two processes are activities which increase the time spent at the construction site until the bridge can become operational, and should be avoided if possible. In order to avoid these problems a system with dry joints has been developed in Sweden.

A research and development project was carried out at Luleå University of Technology during 1998–2001. Within the framework of this project, a new concept for dry joints between roadway slab elements was developed. In order to transfer both lateral and vertical forces through the transverse joints, and to prevent vertical displacements between the deck elements at the joints, overlapping concrete keys were used. These keys were designed as a series of overlapping male-female connections along the joints, see *Fig. 2*.

The connections between the deck slab and the steel girders are achieved at the channels above the girders. These channels are filled with concrete when all elements are in their final positions, and the prestressing force has been applied. Transverse reinforcement bars from the bridge deck elements pass through the channel between the shear studs, which provide the interaction between the girders and the concrete after the channels have been cast, as shown in *Fig. 3*.

Peer-reviewed by international experts and accepted for publication by SEI Editorial Board

Paper received: January 18, 2008
Paper accepted: October 28, 2008

Fig. 1: One concrete bridge and one composite bridge during construction

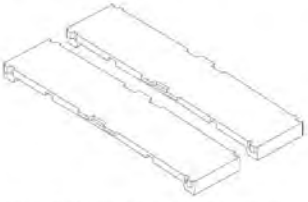

Fig. 2: Prefabricated deck slab units with dry joints

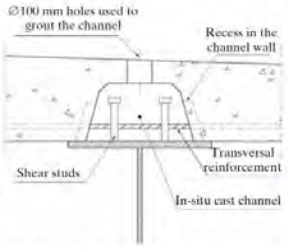

(a) The in-situ cast channel

(b) The channel in one slab element used in laboratory testing

Fig. 3: Site-cast channel in slab element right above the girders

The theoretical distances between the transversal reinforcement bars and the shear studs are rather short, and the tolerances can be demanding since the overlapping concrete keys require a longitudinal displacement of the elements at the assembling. The displacement has to be at least the depth of the overlapping concrete keys plus the tolerances (see section on Concrete Deck Elements and *Fig. 19*). Limited tolerances put higher demands on the steel workshop and the manufacturer of the concrete deck elements. In a bridge project involving prefabricated elements, it is a key factor that the demanded tolerances are fulfilled, since the possibilities of carrying out any last minute changes at the construction site are limited.

In the summer of 2000, an old bridge across Rokån outside Piteå in Sweden (Bridge 1883) was replaced using the concept of prefabricated deck slab elements with dry joints. Since many heavily loaded timber trucks use this bridge, the alternative would have been an expensive bypass road. Instead, a bridge with prefabricated retaining walls, girders, deck slab elements and foundation plinths, was chosen. Furthermore, the new bridge was temporarily erected next to the old bridge, which carried the traffic as usual. Then the old bridge was removed and the new bridge was launched sideways and placed on top of the prefabricated supports. After only 30 hours, the road was reopened and the new bridge was commissioned into use. *Table 1* shows the timetable for the project, and *Fig. 4* illustrates the work.

Laboratory Testing of Dry Joints

A laboratory testing of a prefabricated composite bridge was carried out and is described in detail in Ref. [5]. The aim of the test was to study the behaviour of a composite bridge with dry joints in the concrete element deck that open when negative bending moment is present. All the tests are made on elements with dry joints, and no epoxy is used.

The test setup was designed to imitate the load situation in an internal support of a multi-span bridge. The test specimen consisted of two steel girders and four deck slab elements (200 ×

Day	Time	Activity
Day 1	19:00	The old road was closed.
	22:00	The old bridge was removed using two mobile cranes. The dismantling work continued until 6 p.m. the next day.
	00:00	Old back walls and side wings were removed. The ground behind the abutments was excavated. New gravel fill was added up to the correct level.
Day 2	09:00	The prefab plinths were placed on the new gravel bed.
	10:00	The lifting contractor temporarily placed the new bridge on launching girders, which took 4 hours. Then the bridge was launched sideways, which took only 10 minutes.
	18:00	Installation of bearings and filling behind the retaining walls.
Day 3	01:00	The new bridge was opened to traffic.

Table 1: Timetable for the bridge replacement across Rokån

(a) Two more deck elements to go

(b) Sideways launch

(c) Bridge deck element in final position

Fig. 4: Bridge BD1883 over Rokàn

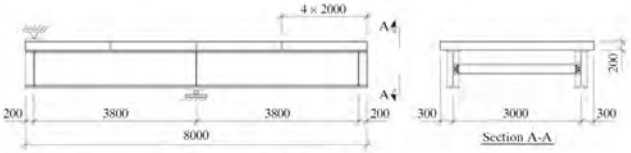

Fig. 5: Laboratory test specimen (Units: mm)

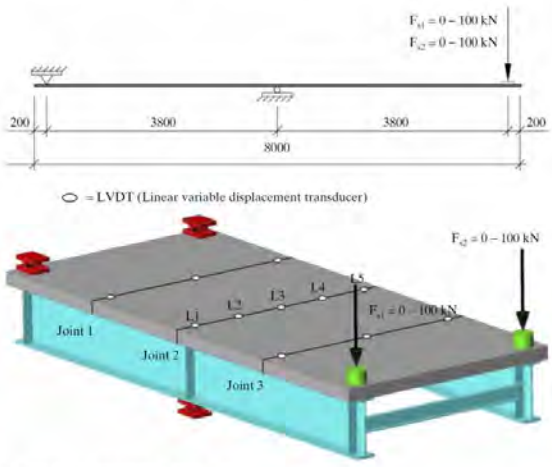

Fig. 6: Static load test setup (Units: mm)

2000 × 3600 mm), with dry joints. The deck slab elements had been match cast, and were mounted on the girders in the same order as they had been cast. Hydraulic jacks were used to move the elements towards each other. A compressive longitudinal lateral force of 400 kN was applied at the time when all the elements were in the right position and the channels were grouted with concrete. The force was then kept constant for 2 weeks, during the hardening of the concrete.

The steel girders used were HEA 900 S460, and the concrete was classified as C55/65. The laboratory tests of the compression strength gave f_{cc} = 73–75 MPa. Shear connectors, ∅22 × 100 mm, introduced the composite action between the deck slabs and the steel girders. The scale of the test specimen was approximately 2 : 3 of a real bridge section. An illustration of the test specimen is shown in *Fig. 5*.

Four types of tests were performed on the specimen. In these tests, vertical and lateral displacements were monitored on the concrete surface at the joint above the internal support, as well as tensions in the steel girders and the deck slabs. The tests were as follows:

(1) Static load test: Static loads, increased in stages of 20 kN up to 100 kN, were applied at the unsupported end of the steel girders, see *Fig. 6*.
(2) Fatigue test of concrete keys: Fatigue loads of 5 to 140 kN were applied on opposite sides of the internal support, Joint 2 in *Fig. 6*. This test was performed in order to simulate the fatigue of the concrete keys, when a vehicle wheel crosses the joint at the same time as a load is acting in midspan giving a negative moment at the joint.
(3) Fatigue test of shear studs: Fatigue loads were applied at the unsupported ends of the steel girders in order to investigate how the shear studs are affected by fatigue loads. The test setup was the same as in (1), but the applied load was cyclic, see *Fig. 6*.
(4) Static load test of concrete keys until failure: Finally, a test was performed to find the failure load of the overlapping concrete keys.

Static Load Test—Joint Displacements

During the static load test, the element gaps as well as the vertical deflections at each joint were measured. The vertical deflections were also measured under the hydraulic jacks and at the supports, in order to make sure that the specimen was behaving symmetrically in the test setup.

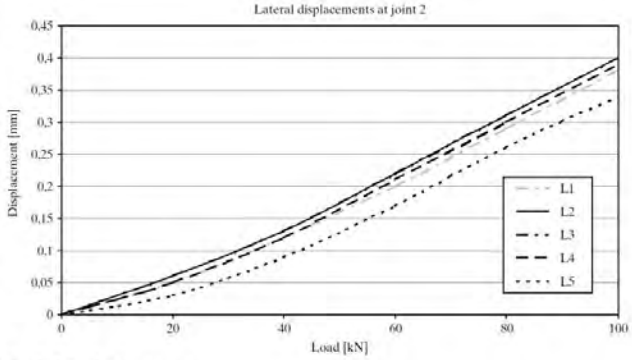

Fig. 7: Static load test setup

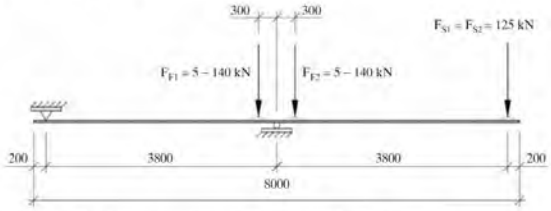

Fig. 8: Test setup for fatigue resistance test of concrete keys (Units: mm)

Fig. 9: Photography of the test setup (the dry joints have been highlighted)

Static loads, F_{S1} and F_{S2}, were applied at the unsupported ends of the steel girders, as shown in *Fig. 6*. Only one of the loads was acting at the time, giving an unsymmetrical load situation. The load was increased in stages of 20 kN, from 20 to 100 kN.

The test results showed that the test specimen behaved more or less perfectly symmetrically and as predicted. A combination of this and the rest of the test results from the static load test, led to the conclusion that possible deviations in the arrangement of supports and loading rig did not affect the results.

The lateral displacement at Joints 1 and 3 varied rather identically during the whole test. The largest difference in lateral displacement between the two joints was 0,04 mm, which is about 20% of the total displacement. The lateral displacements measured at Joint 2 were, as expected, about twice as large as the displacement at Joints 1 and 3 at the same time. *Figure 7* shows the relationship between the lateral displacements, at Joint 2, and the static load. Only four of the five lines are visible in *Fig. 7*, since the sensors L2 and L3 gave the same values.

Fatigue Test of Overlapping Concrete Keys

The fatigue resistance test of the concrete keys was conducted in order to simulate a situation when a vehicle wheel crosses a joint at an internal support, at the same time that a load is acting in mid-span giving a negative bending moment over the support. A fatigue load of 5 to 140 kN was applied in 1 million cycles with a frequency of 1,5 Hz. Two hydraulic jacks, with a phase difference of 180°, were placed at opposite sides of the joint above the internal support. The fatigue loads were transferred to the specimen by steel plates with a size of 200 × 200 × 50 mm. The size is less than that recommended according to EC 1-3 (400 × 400). The reason for using smaller plates was to concentrate the load to the overlapping concrete keys. During the whole test, a static load (2 × 125 kN) was applied at the unsupported ends of the steel girders, in order to open the joint between the elements, as shown in *Figs. 8* and *9*.

The test of the overlapping concrete keys indicated good results when subjected to fatigue load. The lateral opening of the joint at the internal support remains almost constant during the test of 1 million load cycles. The joint over the internal support had an opening of 1,06 mm due to the fact that the specimen was subjected to a global negative moment. The increase of the lateral opening of the joint, at the internal support, due to the fatigue load was 0,073 mm. The initial opening was determined by using feeler gauges before the test started. The average initial opening of the joint at the internal support was 0,15 mm. The total opening in the lateral direction caused by the loads was 1,13 mm. For the other

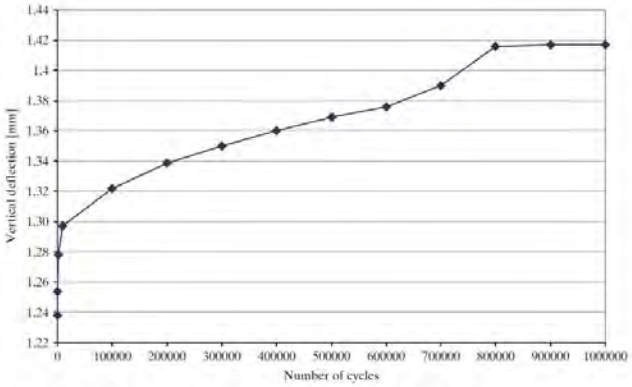

Fig. 10: The relative vertical deflection at the joint over the internal support

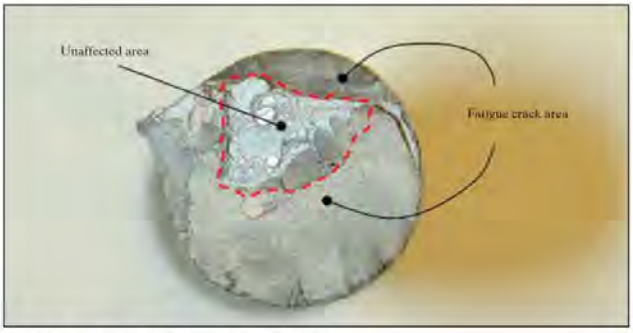

Fig. 11: Shear stud which has suffered from fatigue

two joints the lateral deflection was constant throughout the test.

The relative vertical deflection between the two concrete slabs on each side of the joint at the internal support caused by the pulsating loads was initially 1,24 mm. At the end of the test, after one million load cycles, this value was 1,42 mm (see *Fig. 10*). The vertical movement increased by 0,18 mm during the fatigue test. This vertical movement is a potential problem for the waterproofing and the surfacing, especially since joints over internal supports will experience tensile- and shear forces at the same time.

There were no indications that the concrete keys had suffered from fatigue decay during the test. No visible cracks of the concrete keys or dramatic change of behaviour was found during the test.

Fatigue Test of Shear Studs

In the setup for the fatigue test of the shear connectors, the cyclic loads were moved from mid-support to the cantilevering end of the test specimen. The test setup was the same as in the static load test (1), but the applied load was cyclical. The two jacks were synchronised and applied a load of 245 kN in one million load cycles. The load resulted, according to a FE-analysis, in a shear force of 44 kN on the shear connectors in the region closest to mid-support. At this stress range, the estimated number of cycles until fatigue failure are 262 000, according to Ref. [6].

For this part of the test, the lateral opening of the joints as well as the vertical deflection of the cantilevering end of the specimen were almost constant during the test. If many shear studs had suffered from fatigue, an increase of the lateral joint was expected as well as the vertical deflection. The relative vertical movement between the concrete slabs was measured at the internal support from 100 000 to 1 million load cycles. Due to technical limitations it was not possible to apply the LVDT-gauge until after 100 000 load cycles, and it was only possible to measure the slip between one of the concrete slabs and the steel girders. The relative vertical movement increased with 0,05 mm, during the 900 000 registered load cycles. This was the only displacement parameter that indicated that some of the studs might suffer from fatigue. As a complement to the displacement measurements, two other techniques were used to detect the crack propagation of individual shear studs: acoustic emission (AE) technology and strain measurements. These measurements were not a main purpose of the test. Therefore, the results are only described briefly.

The AE measuring devices were applied at the upper flange in each end of one of the girders. The measuring devices were two microphones which were fixed by magnets. Two devices were used on each end of the girder. They were applied in the transversal direction in the middle between the edge of the flange and the web. The equipment that was used is described in detail in Ref. [7] and the test setup is described in Ref. [5].

The data from the AE-measurement indicated, after about 400 000 cycles, that there was a specific zone on the girder which gave acoustic emission during the cycles. Such a tendency is typical for a propagating crack. Cracks which are just opening and closing without propagating, do not give any acoustic emissions of the kind that has been registered. The measurement shows that the fatigue cracks are growing faster and faster when the number of cycles are increasing. The AE-signal is about 30 times higher after 1 015 000 cycles, than after 400 000 cycles.

The presumed propagating crack was traced by the AE-measurement to a position 200 mm from the internal support (Joint 2), at the cantilevering part. The margin of error was estimated at ±100 mm. When all the tests were completed, concrete was removed at the zone where fatigue failures of the studs were expected. In this zone, it was visually confirmed that two studs had large fatigue cracks. The remaining areas of these studs were about 25%, as shown in *Fig. 11*. These two studs were located 250 mm from the internal support, which is inside the margin of error from the AE-measurement. Thus, this test shows that it is possible to detect cracks in a composite structure by using acoustic emission technology.

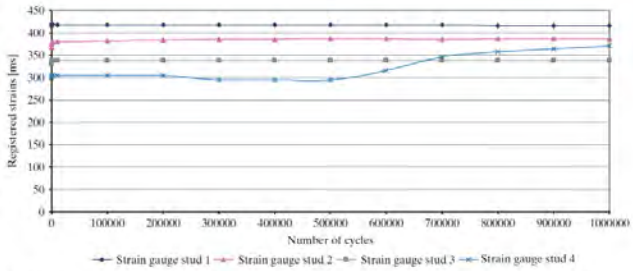

Fig. 12: Strains registered by the four strain gauges at the upper flange, representing four studs

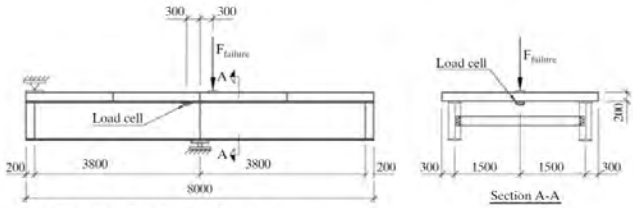

Fig. 13: Static load test setup (Units: mm)

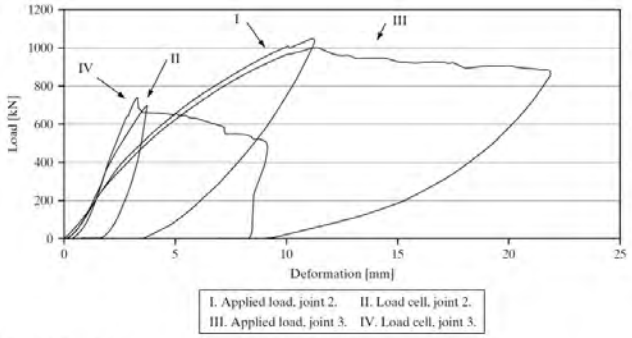

Fig. 14: Load deformation diagram at Joints 2 and 3

No AE-measurements were performed on the other girder. The strains in the upper flange, due to the bending of the shear studs, were however also measured by strain gauges. These were mounted underneath the upper flange, located below the studs and displaced 15 mm along the longitudinal axis. The result could be used to find out if some of the shear studs suffered from fatigue. The strain measurements indicated that two studs might have failed on this girder as well. One was at the same distance from the end of the girder as the stud that failed on the first girder. The surrounding concrete was removed and the failure was visually confirmed. By studying the crack area, of the same kind as shown in *Fig. 11*, the remaining area of that stud was estimated to be 50%. The second stud which might have failed was not uncovered from the surrounding concrete, and the failure was not visually confirmed.

Figure 12 shows the strains registered by strain gauges at four studs in a row at the middle joint in the test setup, two studs on each side of the joint. Three of the studs show a constant behaviour throughout the fatigue test, while the fourth one shows a deviant behaviour. The conclusion drawn from the measured strains, in *Fig. 12*, is that stud number four has suffered from fatigue, since the measured strain is increasing during the test. The surrounding concrete has probably been crushed and the resulting force acting on the bolt has been transferred upwards along the stud shank. The consequence of this is an excessive bending moment in the stud, and the observed rising strain is a result of the rising moment. The bending moment causes bending stresses, which result in a propagating fatigue crack. Similar strain behaviours were registered for another three studs, and the fatigue cracks were visually confirmed at three of the four studs which had suffered from fatigue according to the strain measurements.

Static Load Test of Overlapping Concrete Keys

After the fatigue test, an additional test was performed to check the resistance to the static load of the concrete keys. The joint at the internal supports that have been subjected to fatigue load, was tested, as well as an additional joint that had not been subjected to fatigue load as a reference. The test setup is shown in *Fig. 13*. It resembles the test setup used in section Concrete Deck Elements. Instead of using two jacks at each side of the joint, only one jack was used. The other jack is substituted to a load cell, which registers the force that is transferred directly through the concrete key.

The results confirm that Joint 2 at the internal support had not suffered from fatigue. The maximum static load capacity was about the same for the two tested joints. The maximum load applied was 1046 kN at Joint 2, and 1001 kN at Joint 3. These loads can be compared to the highest design vehicle wheel load in the Swedish Bridge Code [14], which is 163 kN.

Figure 14 shows a load deformation diagram, illustrating deformations caused by the forces applied at the concrete keys. The registered forces that have been transferred directly through the keys are plotted in the same diagram. At Joint 2, about 66% of the force is transferred through the keys, and about 73% in Joint 3.

Summary of Laboratory Tests

- The overlapping concrete keys can withstand the static load as well as the fatigue load, according to EC 1-3.

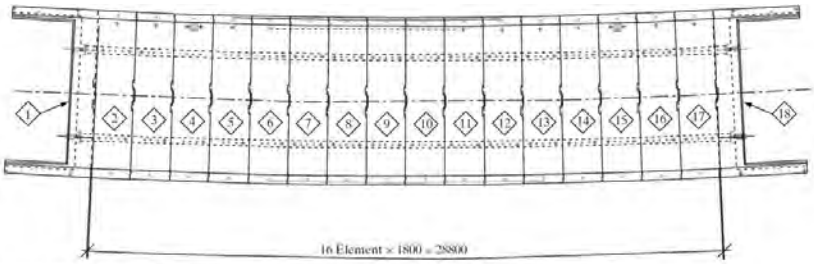

Fig. 15: General arrangement of the prefabricated bridge deck in road bridge AC1684 (Units: mm)

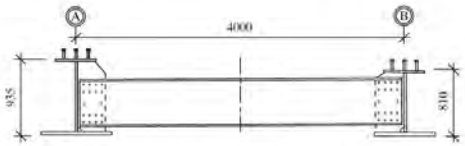

Fig. 16: Cross-section of the steel structure, c/c cross-girders 7,0 m (Units: mm)

- For a continuous girder bridge, the joint tends to open over intermediate supports. The total horizontal opening during the fatigue test was 1,1 mm. The relative vertical movement of the adjacent concrete slabs, caused by a passing wheel over an intermediate support, was stated to be 1,4 mm during the key fatigue test. This movement of the joint is a problem for the waterproofing and surfacing, thus it has to be investigated.
- Even if the slab elements under tension, near the intermediate support, are not included in the design calculations, it is strongly recommended that they should be properly connected to the steel girders. The connection should be as strong as possible without exceeding the tensile strength of the concrete. The force on the shear studs will vary with the traffic load and may cause fatigue failure. The laboratory test with 1 million load cycles caused at least three studs, but probably four, to fail from fatigue. The calculated force on the studs of 44 kN is high compared to the expected resistance to fatigue according to [12] and [13] for 1 million cycles. At the estimated number of stress-range cycles until failure, according to Eurocode 262 000 cycles, no signs of fatigue was observed. At 5 to 600 000 cycles, some studs seem to suffer from fatigue.
- Although not the main purpose of the test, acoustic emission was adopted, and it was possible to detect the propagation of cracks in the headed shear connectors. The first indication of a propagating crack was registered after 400 000 cycles.

Experience from Bridge AC 1684

In 2002, the Swedish road bridge AC 1684 was built over a railway in Norrfors, replacing an old narrow bridge in bad condition. It was designed as a single span composite bridge with a span width of 28 m. The bridge deck was designed to be prefabricated, in 16 concrete deck elements and two prefabricated abutments (see *Fig. 15*), and assembled with dry joints. The construction costs were presumed to be a bit higher than for a conventional concrete bridge, but since the disturbance of the railway traffic could be minimized it was worth trying the new concept. One of the demands which the bridge designer had to deal with was the requirement of a bridge which could be assembled in less than 24 h. The time limit was governing by how long time the electricity on the railroad must be switched off. During this period, girders would be lifted in place, deck slab elements assembled, and bridge rails, as well as safety roof and safety net mounted. The elements were also prestressed with a force of 600 kN, in order to ensure that there would not be any gap between the elements.

This bridge project has been evaluated in Ref.[8] in order to gather experiences and the opinions about this type of prefabricated element bridges. It also states that the most important experience is that all the participants must be aware of the aim of the project and their responsibilities. It is necessary that all partners realise the importance of the required precision.

Steel Girders

The bridge has a rather complex geometry, as shown in *Figs. 15* and *16*, and the lack of vertical and lateral surfaces requires an extra amount of information for the steel workshop. The extra information is needed in order to avoid small mistakes which may not be discovered before the units reach the construction site. If there is a mismatch between the studs and the transversal reinforcement in the grouting channel, the time benefits of a prefabricated bridge might be wasted.

During the assembling of the bridge, some tasks appeared to be a bit unpredictable and some proposals for improvement were raised. First, the two girders were not in the right positions. Measurement showed that they had a longitudinal displacement in relation to each other. A decision was taken to adjust the girders positions after they had been lifted in place. However, the measurements after the lift showed that the girders had gone back to the right position. In order to avoid these uncertainties, laterally adjustable cross stays could be mounted on the upper flanges. Displacements could then be adjusted by these. They will also give an extra lateral stiffness to the steel girders during the assembling of the deck elements. Another observation was the lack of reference points on the steel structure. This caused some problems when the first element was lifted in place, since it was not obvious where

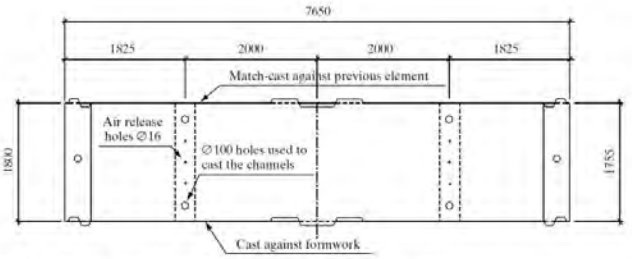

Fig. 17: Plan of a prefabricated bridge deck element (Units: mm)

Fig. 18: Bridge deck element is lifted in place

the right position was. This problem can be solved if the steel workshop adds some marks on the outside of the upper flange. These marks must be deep enough to be visible after the painting work is done.

Concrete Deck Elements

Each element had a dimension of 1800 × 7650 × 280 mm (see *Fig. 17*), giving an element weight of about 10 t. Experiences from previous projects have shown that the lifting devices should not be anchored in the grouting holes for the concrete channel. This conclusion was based on the observation of longitudinal cracks near the channels, caused by the bending moment due to the element's weight. Therefore, four spherical head lifting anchors were used to lift the elements at AC 1684. These anchors were cast in recesses in the concrete surface, outside the channels. The channels were filled with concrete when the elements were fixed at the right position. The new positions of the lifting anchors gave a significant decrease of the bending moment in the channels, and cracks were avoided. *Figure 18* shows an element during the lifting.

The concrete keys transfer the shear forces from one element to another and are designed to transfer high axle loads. The keys in this bridge might be slightly larger than necessary, compared to the results from full-scale laboratory testing.[9] In order to get larger tolerances, the concrete keys could be designed slightly smaller. Such a change would require further studies of the concrete cover and the shear reinforcement in the key areas. *Figure 19* shows the principle of the element assembling, and the limited tolerances associated with this application.

Tolerances

One of the experiences gained from this bridge is that the tolerances are limited and very demanding. If possible, larger tolerances should be used in order to minimize the risk of problems during the bridge assembling. As shown in *Fig. 19*, the theoretical tolerances between the channel reinforcement and the studs are about 22 to 23 mm. The positions of the studs and the reinforcement, as well as the width of the element, are very important. If the same error is repeated on each element it will soon lead to a fault larger than the tolerances at the assembling. This must be avoided if this method is to be competitive. The advantages of the method are the shorter construction time and the possibility of minimizing traffic disruption when replacing an old bridge. These advantages are lost if the prefabricated elements and the steel girders do not fulfil their tolerances[8], which are summarized in the following key factors in each phase of the bridge construction process, in order to ensure that all components are within their limits of tolerance:

Design phase:

- Detailed manufacture drawings, in which important distances are given with appropriate tolerances.
- Detailed and well-considered assembling instructions on the construction drawings and in the assembling plan.
- Plans for additional inspections and checking of own work during all phases of the bridge construction.

Manufacturing phase:

- Checking of own work, in order to fulfil the required tolerances.
- Be in agreement with the additional controls and the purpose of these.

Assembling phase:

- Be in agreement with the assembling instructions and the purpose of these.
- Preparation before the assembling.
- Coordination of the different participants during the assembling phase.

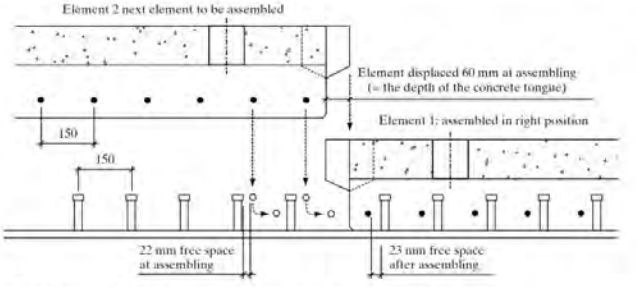

Fig. 19: Illustration of the narrow tolerances at assembling (Units: mm)

Extra Control Program

In order to achieve the demanded tolerances, extra control programs were developed for each phase of the bridge construction. In this section, the extra control program will be briefly described to illustrate how precisely the work has to be executed. The following items are checked by the manufacturer of the prefabricated concrete deck elements.

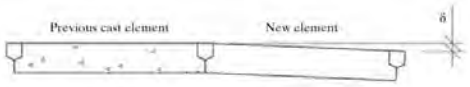

Fig. 20: Levelling tolerances for element formwork

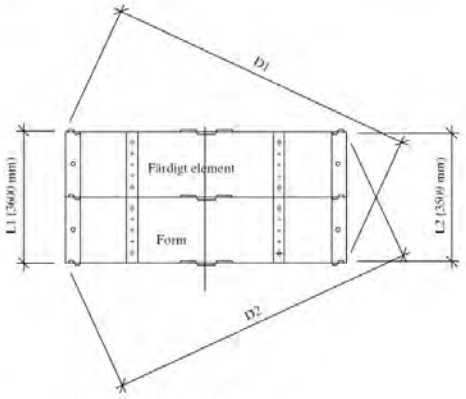

Fig. 21: Geometry checks of deck slab and formwork

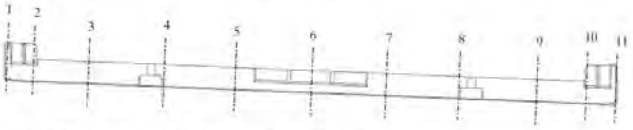

Fig. 22: Positions where the joint opening is checked

Checking the levelling of the formwork

The previous cast element is used as formwork on one side of the next element. The formwork for the new element was levelled with a precision of ±2 mm. The desired value of δ, shown in *Fig. 20*, was 2 mm (due to the vertical radius). It was checked before and after the concrete was cast, to ensure that there were no undesired deformations.

Checking of the geometry

It is very important that the elements in prefabricated bridges have the right geometry. This becomes even more important in Bridge AC1684, since it has both a horizontal and a vertical radius. Before the elements are cast, the formwork is measured together with the previous element, as shown in *Fig. 21*. The tolerances for L1, L2, D1 and D2 are ±3 mm.

Checking the concrete cover and effective cross-section

The desired concrete cover over the whole structure is 35 mm, and the tolerance is set at ±5 mm. The concrete cover and the effective cross-section is checked by measuring the position of the reinforcement before the element is cast. Tolerances for the effective cross-section vary, depending on which part of the structure is checked.

Initial opening of the joint

After formwork removal, the initial opening of the joints is checked by the manufacturer of the elements. It is checked at 11 positions along the joint (see *Fig. 22*), on both top and bottom surfaces of the element. The average opening is not allowed to exceed 1,0 mm at this stage.

The joint opening is also checked by the contractor when the bridge deck has been assembled and prestressed by a force of 600 kN. The joint opening after prestressing should be 0 mm on the upper or lower side of the joint. This is checked by using a feeler gauge. The joint is considered as 0 mm if a feeler gauge of 0,3 mm cannot be pushed through the joint, at the same time as the joint does not exceed 1,0 mm at the opposite side (upper/lower side). Locally, a 1,5-mm joint opening is allowed over a maximum distance of 1 m. The average opening of the joint is not allowed to exceed 0,4 mm, when all the measured values on the upper and lower side of a joint are taken into consideration.

Economy

The construction costs of the prefabricated bridge were presumed to be higher than the cost for a bridge with a concrete deck cast onsite. However, according to information received from the contractor, the cost of the prefabricated deck was the same as that of a deck cast onsite. Another contractor states that the prefabricated deck was less expensive according to their cost estimations. The extra costs due to the prefabrication is compensated by the saving achieved in formwork and other costs that appear when a bridge is built over an operating railway.[10]

Analyses made by the Swedish National Railway Administration (SNRA), estimate the costs to society if the bridge had been constructed in a conventional way.[10] The highest speed allowed on the railroad would then have to be decreased from 100 to 70 km/h over a two-km-long distance, during the construction time of the bridge. The cost for changes in signal equipment and signs was estimated at 16 500 €, and the cost due to the loss of capacity was estimated at 22 000 €.

The fee to the bridge designer is one of the costs that will be a bit higher for a prefabricated bridge, partly due to the lack of experience from similar construction projects. This cost is however low compared to other costs, and can probably be lowered when the bridge designers get some experience from this type of bridge.

For bridge BD1883, a study made in Ref. [11] compares the cost of constructing (A1) a prefabricated composite bridge (the system under study), (A2) a conventional composite bridge with a temporary bridge, and (A3) a conventional composite bridge with the traffic directed to the nearest bypass roads. The construction costs and the road-user costs for the three alternatives are shown in *Fig. 23*. The construction costs are inclusive of profit to the contractor, and some indirect taxes.

The most economical alternative in the social aspect, according to the study in Ref. [11] was to build a prefabricated composite bridge (A1). The construc-

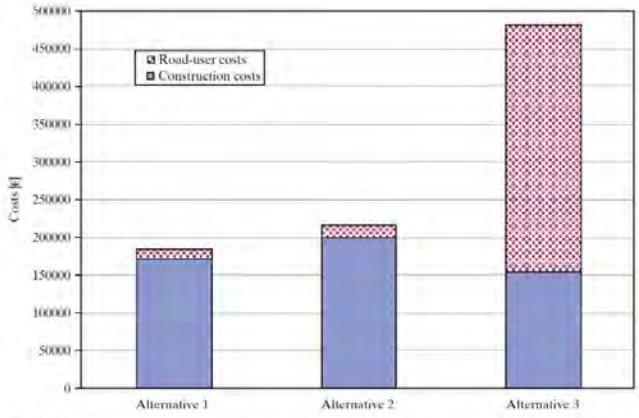

Fig. 23: Construction costs and road-user costs for concerned construction type 1 to 3

tion cost of a conventional bridge (A3) is lower, but the need for a temporary bypass road, or the indirect costs of directing the traffic to nearby roads are making the prefabricated composite bridge the most economical solution for society. The main reason why alternative 3 gets very high road-user cost is the fact that the nearest bypass roads resulted in a quite long pass for the road-users in this particular case.

Conclusions

Composite bridges are a well-established alternative to concrete bridges. The new concept for composite bridges with prefabricated decks described in this paper offers several advantages compared to concrete bridges and conventional composite bridges. Some of the advantages are the shorter erection time, better working environment, a dry bridge deck surface and a possibly higher quality.

Laboratory tests carried out on precast slab elements showed excellent abilities to withstand both static and fatigue loading. Pilot projects in northern Sweden erected in 2000 and 2002 showed that this design concept works well onsite.

Experiences from bridges constructed according to this concept show that it is possible to fulfil the demanded tolerances, even if the tolerances are limited. It is necessary that all partners involved are aware of the aim of the project and their responsibilities. Every step must be checked carefully since there is no time or possibilities for last minute changes at the construction site.

In a newly started European R&D project (ELEM), the concept of prefabricated deck elements will be studied by researchers and designers from Sweden, Finland, Germany and Poland. The estimated cost of the project is 1,5 million €. The project aims at building a multi-span bridge with dry joints, and monitoring the movements of these. This also includes experimental studies of whether the waterproofing can withstand these movements. Furthermore, the possibilities to allow larger longitudinal tolerances at the assembling stage, by placing the shear connectors in concentrated groups will be investigated.

References

[1] Collin P. Some trends in Swedish Bridge Construction. In *International Conference on welded Structures*, Budapest, 2-3 September 1996, 1996, 163–172.

[2] Collin P, Johansson B. Wettbewerbsfähige Brücken in Verbundbauweise. *Stahlbau* 1999; **68** Heft 11: 908–918.

[3] Biswas M. Precast bridge deck design systems. *PCI J. V.41, No.2,* . 1986; pp. 40–94.

[4] ARBED. *Innovative Composite Design of Motorway Overbridges*. Europrofil ARBED: Luxembourg.

[5] Stoltz A. Effektivare samverkansbroar. Licentiate Thesis 2001:141, Luleå University of Technology, Sweden, 2001, (in Swedish).

[6] EN 1993-1-9. *Eurocode 3 – Design of Steel Structures – Part 1-9: Fatigue*. CEN, European Committee for Standardization: Brussels, 2005.

[7] Boström S. Crack location in steel structures using acoustic emission techniques. Doctoral Thesis. Department of Civil Engineering, Division of Steel Structures. Luleå University of Technology, Sweden, ISSN: 1999, 1402–1544.

[8] Fahleson C. *Projektering, tillverkning och montage av elementbyggd samverkansbro*, Internal report Ramböll Sverige AB (former Scandiaconsult), Luleå, Sweden, 2003, (in Swedish).

[9] Lundmark R, Mikaelsson F. Elementbyggda samverkansbroar. Master's Thesis 1997:038, Luleå University of Technology, Luleå, Sweden, 1997, (in Swedish).

[10] Degerman H. Samhällsekonomisk analys av hastighetsnedsättning vid bro söder om Norrfors, Internal report Banverket, Norra regionen, 2002, Sweden, (in Swedish).

[11] Nilsson M. Samverkansbroar ur ett samhällsekonomiskt perspektiv – En jämförelse mellan platsgjutna och förtillverkade samverkansbroar. Master Thesis, Luleå University of Technology, Sweden, 2001, (in Swedish).

[12] EN 1991-2. *Eurocode 1 – Actions on Structure – Part 2: Traffic Loads on Bridges*. CEN, European Committee for Standardization: Brussels, 2003.

[13] EN 1994-2. *Eurocode 4 – Design of Composite Steel and Concrete Structures – Part 2: General Rules and Rules for Bridges*. CEN, European Committee for Standardization: Brussels, 2005.

[14] Bro 2004. *Swedish Regulations for Bridges*. Swedish National Road Administration: Borlänge, 2004, (in Swedish).

Paper III

Concrete shear keys in prefabricated bridges with dry deck joints

Robert Hällmark, Martin Nilsson and Peter Collin

Published in:
Nordic Concrete Research, Vol. 44, No. 2, December 2011, pp 109-122.

This paper is based on tests planned and evaluated by Hällmark, who has also been the author of this paper. The co-authors have contributed with their experiences, views and opinions through the whole process, from the planning of the test set-up to the final report of the tests.

1

Concrete shear keys in prefabricated bridges with dry deck joints

Robert Hällmark
M.Sc./Bridge Designer
LTU/Ramböll
Kyrkogatan 2, Box 850
SE – 971 26 Luleå
robert.hallmark@ramboll.se

Martin Nilsson
Ph.D.
Luleå University of Technology
SE – 971 87 Luleå
martin.c.nilsson@ltu.se

Peter Collin
Professor/Bridge Manager
LTU/Ramböll
Kyrkogatan 2, Box 850
SE – 971 26 Luleå
peter.collin@ramboll.se

ABSTRACT

A prefabricated concrete deck with dry joints between deck elements has been developed to make prefabricated bridges even more competitive. This type of bridge deck has been used on single span bridges in Sweden, and is now under development for multi span bridges. This paper describes how the deck system works. Results from laboratory tests of shear keys between deck elements are also presented together with an analysis comparing the predicted capacity with the measured failure load.

Key words: Bridge, prefabrication, element, dry joints, shear keys, laboratory tests.

1. INTRODUCTION

There is always a need to widen, build or rebuild bridges. To reduce the construction time and to minimize the impact on the traffic situation, prefabricated bridges can be used. Prefabricated steel girders are rather common but prefabricated concrete deck elements are still a rare exception. In order to make prefabricated bridges even more competitive, a deck of prefabricated concrete elements with dry joints between the elements has previously been developed. This system has been used on a few single span bridges in Sweden and is now under development for multi span bridges. The aim of the R&D project is to enable the use of dry joints between elements in multi span bridges without pre-tensioning. Particular attention has been paid to the ease of manufacturing, [1][2][3].

To transfer both lateral and vertical forces through the transverse joints, and to prevent vertical displacements between the deck elements at the joints, overlapping concrete keys are used. These keys are designed as a series of overlapping male-female connections along the joints, see Figure 1 and 2. In order to ensure a good accuracy of fit in the dry joint, the elements are match cast.

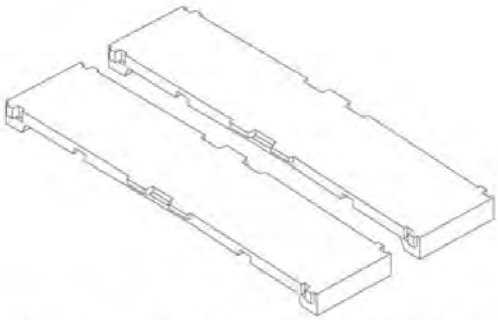

Figure 1 – 3D-sketch of two elements, illustrating the joint.

Figure 2 – Element during assembly

The theoretical distance between the transversal reinforcement bars in the concrete deck elements and the shear studs on the steel girders is limited, and the tolerances can be demanding since the overlapping concrete keys require a longitudinal displacement of the elements at the assembling. The displacement has to be at least the horizontal depth of the overlapping concrete keys plus the tolerances in the longitudinal direction of the bridge, see Figure 3. [2]

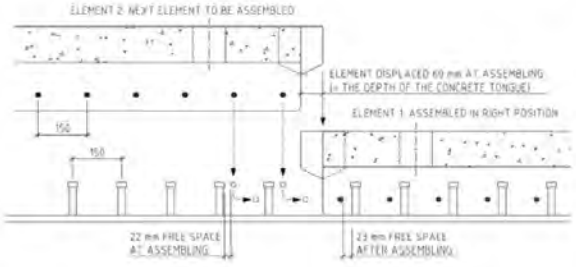

Figure 3 – Illustration of the limited tolerances. [2]

If possible, it would be preferable to use shear keys with smaller depth. However, the shear keys must be able to transfer the forces given in the design codes [4]. By using a FE-model of the bridge it can be shown that a maximum of about 40% of the traffic load acting on a single element is transferred through one of the joints. The rest of the load is transferred directly to the steel girders, or through the dry joint at the opposite side of the element. Therefore, the shear keys must be able to resist a load that is at least 40% of the design load given in the codes.

In order to find out how the shear keys transfer forces, and to be able to predict their strength and verifying the FE-model, laboratory tests have been performed.

2. Laboratory tests

Twelve static tests with three different layouts of the shear keys have been tested. The test set-up and the specimens are briefly described in the following sections.

2.1 Test set-up

The tests were focusing on pure shear capacity of the concrete keys. This means that no positive or negative effects were simulated, such as prestressing from the steel girders, or any misfit between the elements. A schematic and simplified sketch of the test set up is shown in Figure 4.

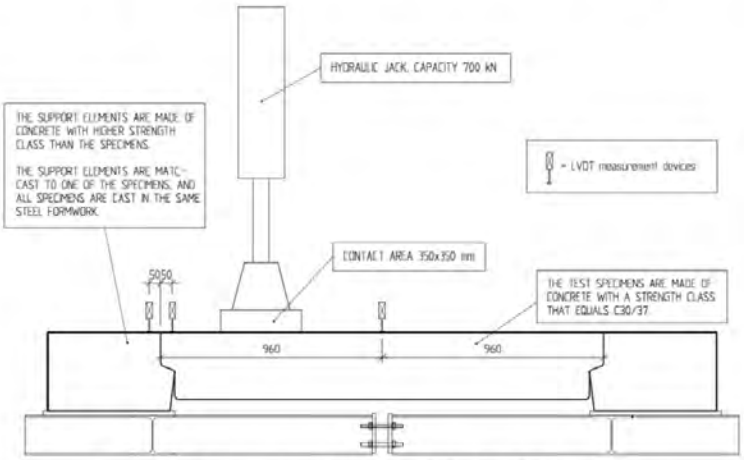

Figure 4 – Schematic and simplified sketch of the test set up.

The test specimens were placed in a test rig that consists of two concrete supports on top of a steel frame. The concrete support elements was match cast to one of the test specimens. All test specimens were made in the same steel formwork, and fitted well to the match cast supports. The supports were made in concrete with higher strength class (C40/50) than the specimens (C30/37). They were also heavily reinforced to avoid any failure in the support elements, and to make it possible to reuse them. The steel frame was used to keep the supports in the right positions and to make the demounting easier. The frame was constructed of HEA180 profiles. Figures 5 and 6 below show more detailed drawings of the support elements and the steel frame.

Before each the test was started, the bolt connections in the steel frame was tightened so that the frame could take care of the horizontal tensional forces that occurs due to the inclined contact surface in the shear keys. The bolts were tightened gently, aiming to get a remaining horizontal gap of ~0.5 mm at each shear key. The bolt connections were not used to clamp the specimen and the support elements together, giving a horizontal compressive force in the concrete.

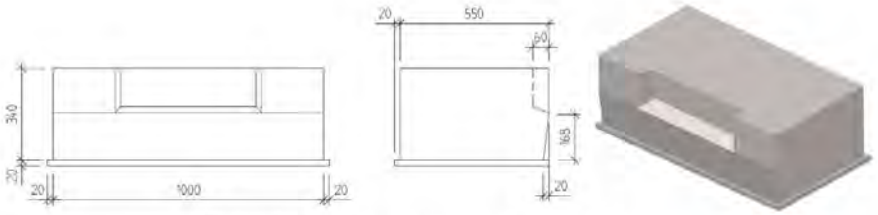

Figure 5 – Geometry drawings of support elements.

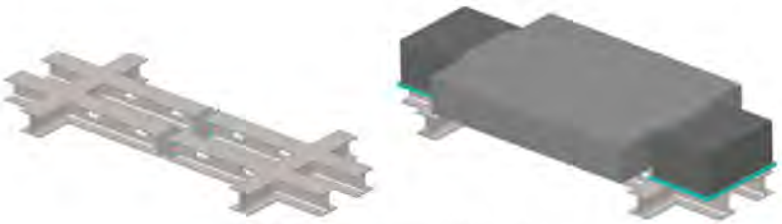

Figure 6 – Illustration of test rig.

Each specimen had two shear keys that were tested under static load. The first shear key was tested until failure. After that, the hydraulic jack was moved to the opposite side of the specimen, and the second key was tested. When the second shear key was tested an extra vertical support was used, to make sure that the specimen was levelled horizontally and that the support area was uncracked, see Figure 7.

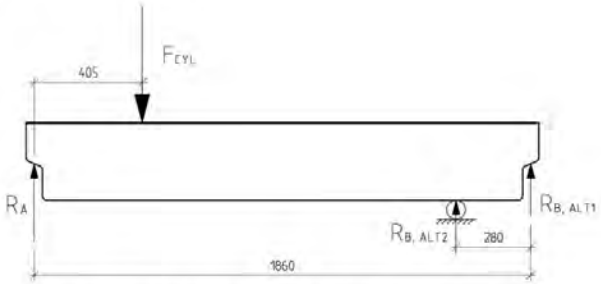

Figure 7 – Load situation with the extra support.

During the tests, data were recorded on 12 channels. Two channels were used to record the time elapsed and the load from the cylinder. The remaining ten channels were used to record deformations. Six measurement points were placed on top of the specimen. Three were placed on top of the support element and the last one was placed towards the floor measuring the reference deformation. The test set-up and the measurement devices are shown in Figure 8.

Figure 8 – Picture of test set-up.

2.2 Test specimens

The general geometry of the test specimens were 1.8 × 1.3 m, with a concrete shear key depth of 60 mm and a length of 540 mm, see Figure 9. The concrete strength in the specimens was aimed to be equal to strength class C30/37. For each specimen, six concrete cube tests were performed: 3 compressive and 3 tensile. The material test results are presented in Chapter 3.

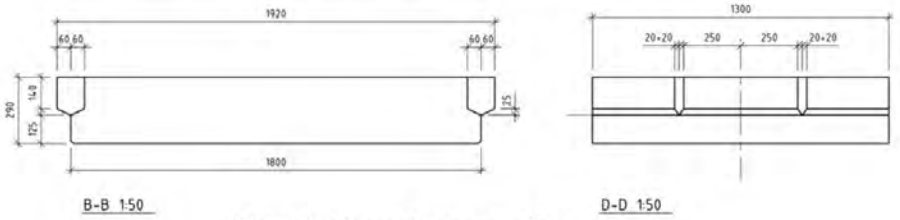

Figure 9 – General geometry of test specimens.

The first specimens (2 elements) were reinforced with exactly the same amount of reinforcement as used in deck elements in previously constructed single span bridges. In these specimens the shear keys were the same in both ends, shear key type 1. The second type of specimens (4 elements) had reduced shear key reinforcement in one of the shear keys, shear key type 2, compared to the first specimens. The other shear key, shear key type 3, was completely without reinforcement. With this design, four test results are gained for each type of shear key. Figures 10 and 11 show the reinforcement drawings of the specimens.

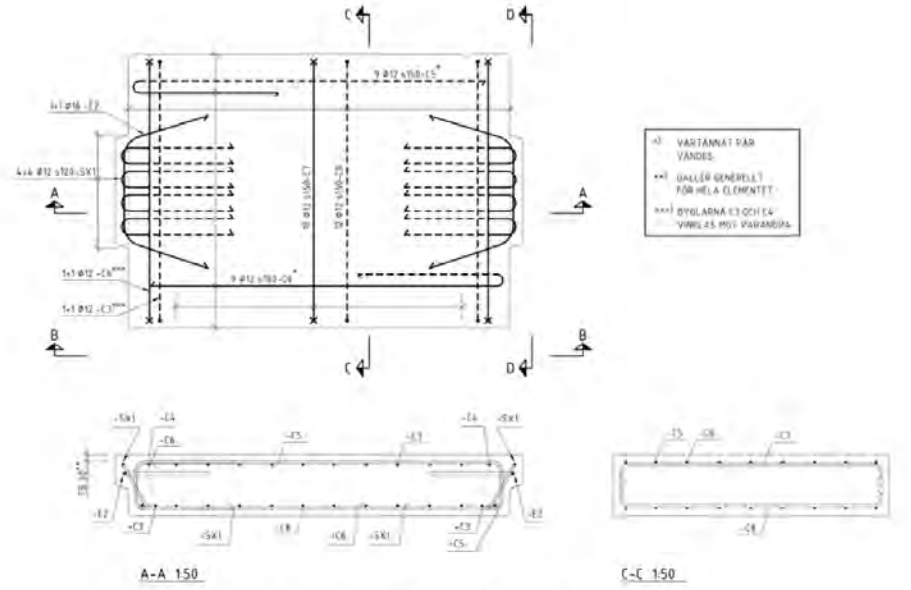

Figure 10 – Reinforcement drawing for specimens of type 1.

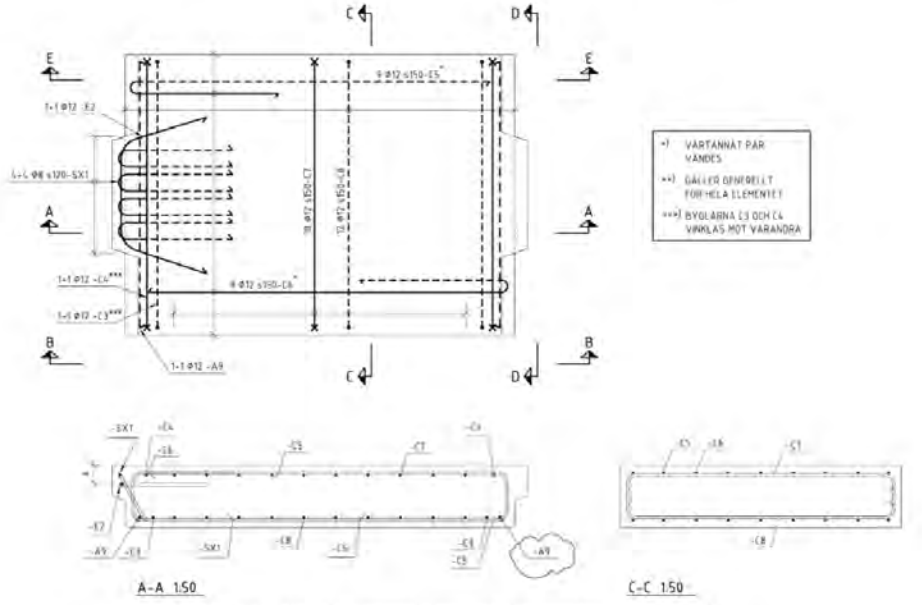

Figure 11 – Reinforcement drawing for specimens of type 2.

3. Results

3.1 Material tests

For each specimen, six cubes were cast out of the same concrete mix. Three of the cubes were used to determine the compressive strength and the other three were used to determine the tensile strength. The test cubes had the dimensions of 150×150×150 mm. The mean values for each specimen are presented in Table 1 below.

Table 1 – Concrete parameters.

Cast date	Test date	Age [days]	δ [kg/m³]	P_c [kN]	f_c [MPa]	P_{ct} [kN]	f_{ct} [MPa]	Specimen type
2010-03-15	2010-06-16	93	2334	1045	46.1	118	2.6	1
2010-03-16	2010-06-11	87	2345	1132	49.7	123	2.8	1
2010-03-18	2010-06-02	76	2372	1082	47.6	103	2.3	2
2010-04-07	2010-06-08	62	2330	967	42.6	94	2.1	2
2010-04-08	2010-06-11	64	2358	1009	44.5	115	2.6	2
2010-04-12	2010-05-31	49	2371	970	42.9	99	2.3	2

P_c = failure load, compressive test f_c = compressive strength
P_{ct} = failure load, splitting test f_{ct} = splitting tensile strength

3.2 Shear key tests

All tests were deformation controlled, with a stroke of 0.02 mm/s. Two different kinds of failures were observed when the reinforced shear keys were tested. Firstly, five of eight reinforced shear keys failed by cracks that activated the reinforcement, giving a ductile behaviour – failure type 1. The shear keys remained as one piece, but with some concrete crushing in the lower parts. Three specimen failed by cracks that were developed outside the reinforcement, resulting in a failure that separated the shear key from the rest of the specimen – failure type 2. This type of failure occurred under lower loads than the previously described failure.

Shear key type 1 – Ø12 reinforced (4 tests)
Two of four shear keys of type 1 resulted in failure type 1. The load-deformation curves from these two tests are shown in Figure 12 with solid lines, together with some photos of the failed shear keys, Figure 13.

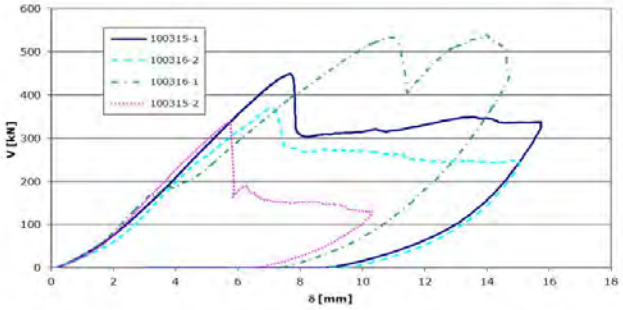

Figure 12 – Load-deformation curve for shear key type 1, failure type 1 (solid) and 2 (dashed).

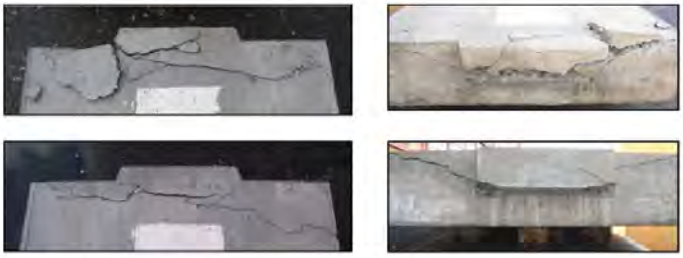

Figure 13 – Photos of shear key type 1 with a failure activating the reinforcement.

The last two specimens failed by cracks that developed outside the reinforcement, resulting in a failure that separated the shear key from the rest of the specimen. The load-time curves from these two tests are shown with dashed lines in Figure 12, together with some photos of the failed shear keys, see Figure 14.

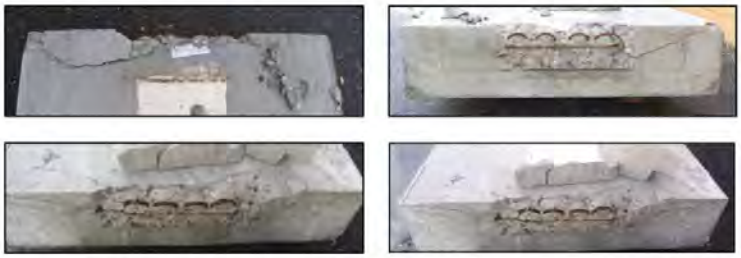

Figure 14 – Photos of shear key type 1 after failure in the concrete covering layer.

Shear key type 2 – Ø8 reinforced (4 tests)
The load-time curves from the tests are shown below together with some photos of the failed shear keys, see Figures 15 and 16.

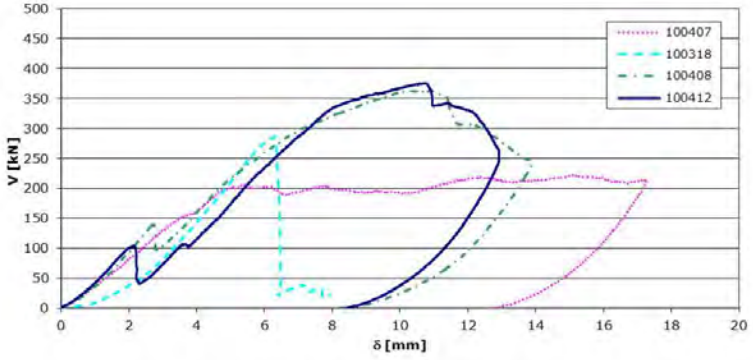

Figure 15 – Load-time curve for shear key type 2.

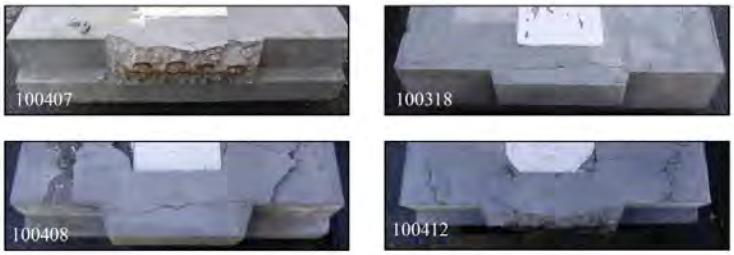

Figure 16 – Photos of shear key type 2 after failure.

In one aspect, the results from these tests reminds of the tests of shear key type 1 – Ø12 reinforced, since three shear keys remains rather unaffected after cracking, and one shear key fail outside the reinforcement. The latter shows a very plastic behaviour before it finally fails in the concrete cover layer.

Shear key type 3 – unreinforced (4 tests)
The load-time curves from the tests are shown below together with some photos of the failed shear keys, see Figures 17 and 18.

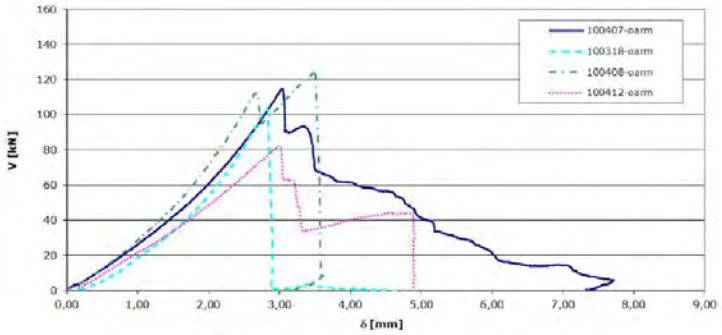

Figure 17 – Load-time curve for shear keys of type 3

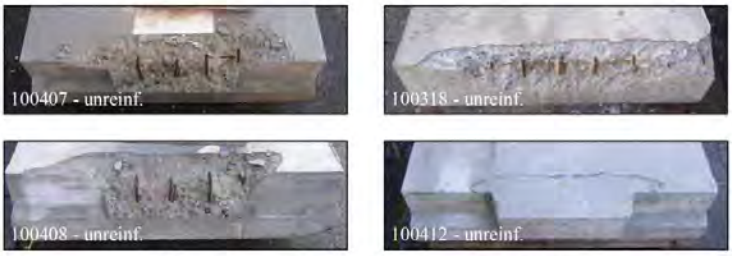

Figure 18 – Photos of shear-keys after failure.

4. Analysis

The strength of the shear keys has been estimated by using four different design models:

1. classical beam linear elastic analysis – shear key type 3 with failure type 2
2. Eurocode 2 – shear key type 1 and 2 with failure type 2 [6]
3. Eurocode 2 – shear key 1 and 2 with failure type 1 [6]
4. force equilibrium model

The material parameters from the test of concrete cubes are used to calculate the shear capacity for each shear key. The results from the design models are presented in Table 2.

1. Shear resistance for shear key type 3 with failure type 2

The shear resistance for failure type 2 in shear key type 3 without reinforcement can be estimated as, according to classic beam analysis and assuming that the shear strength is half the tensile strength [7],

$$V_{Rd.c} = \frac{2}{3} b_w h f_{shear} \approx \frac{1}{3} b_w h f_{ct} \tag{1}$$

where

b_w = 540 mm; the smallest width of the cross-section within the effective height

h = 165 mm; height of shear key

f_{ct} = is the splitting tensile strength of the concrete, see Table 1

2. Shear resistance for shear key type 1 and 2 with failure type 2 [5].

The shear resistance for failure type 2 can also be estimated by using formulas from [5],

$$V_c = b_w d f_v \tag{2}$$

$$f_v = 0.3 \cdot \xi \cdot (1 + 50\rho) f_{ct} \tag{3}$$

$$\rho = A_{s0} / (b_w \cdot d) \leq 0{,}02 \tag{4}$$

$\xi = 1.4$ when d ≤ 0.2 m

d = 140 mm

b_w = 540 mm

b_w the smallest width of the cross-section within the effective height

d effective height

f_v shear strength of the concrete

f_{ct} tensile strength of the concrete

A_{s0} the smallest amount of bending reinforcement in the tensile part of the studied cross-section. This is set to 0, since there is no bending reinforcement in the shear key, only shear reinforcement.

3. Shear resistance for shear key 1 and 2 with failure type 1 [6].
This approach has been used on at least two bridges in Sweden, a bridge over Rokån and a bridge in Norrfors.

According to Eurocode 2 [6] the shear resistance for a section with inclined shear reinforcement is

$$V_{Rd,s} = \frac{A_{sw}}{s} z f_{ywd} (\cot\theta + \cot\alpha)\sin\alpha \tag{5}$$

When shear reinforcement is used locally, with inclined rebars in one line (the –SX rebars), then the equation above can be simplified to

$$V_{Rd,s} = A_{sw} f_{ywd} \sin\alpha \tag{6}$$

where

A_{sw} = is the area of the shear reinforcement

f_{yw} = 500 MPa, is the yield strength of the shear reinforcement

θ = is the angle of the shear crack (~45° observed in the test)

α = 60° is the inclination of the shear reinforcement

4. Force equilibrium model.
This model has been suggested, by Dr. Bo Westerberg (KTH, Stockholm), in order to describe the load carrying capacity in more detail. It is a force equilibrium model that involves both the reinforcement and compressive struts in the concrete, see Figure 19.

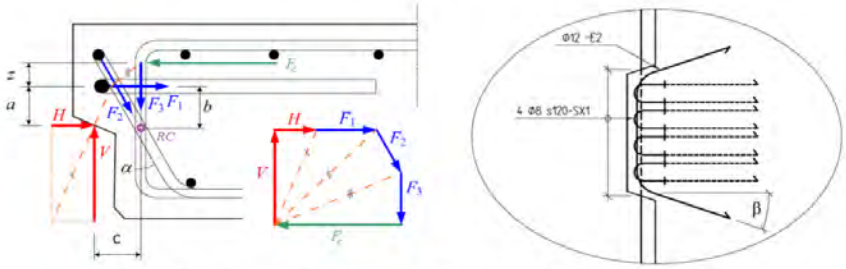

Figure 19 – Illustration of force equilibrium model and the notations.

The horizontal force *H* is believed to have great influence on the load carrying capacity. Without a compressive horizontal force, there is a risk for shear failure of the concrete cover at the edge of the shear key. The load carrying capacity is hard to predict in such a scenario, but it cannot be more than the shear strength of the concrete.

In the laboratory tests, the size of the force *H* is dependent on the shape of the supports, the rigidity of the test-rig etc. In a real bridge, this force will vary along the bridge and will depend on the global load situation as well as the local load situation.

Equilibrium equations:

$$\Sigma F \uparrow: \quad V - F_2 \cos\alpha - F_3 = 0 \tag{7}$$

$$\Sigma F \rightarrow: \quad H - F_c + F_2 \sin\alpha + F_1 = 0 \tag{8}$$

$$\Sigma M_{RC}: \quad V \cdot c + F_1 b + H(b-a) - F_c(b+z) = 0 \tag{9}$$

The load carrying capacity of the shear key can be estimated by using the maximum capacity of each rebar.

$$F_1 \le f_y A_{s1} \cos\beta \tag{10}$$

$$F_2 \le f_y A_{s2} \tag{11}$$

$$F_3 \le f_y A_{s3} \tag{12}$$

giving

$\varnothing_1 = 12$ mm

$$F_{1,\max} = 500 \cdot 2\frac{\pi \cdot 16^2}{4} \cdot \cos 18.5° = 191 \text{ kN}$$

$$F_{2,\max} = 500 \cdot 8\frac{\pi \cdot 12^2}{4} = 452 \text{ kN}$$

$$F_{3,\max} = 500 \cdot 3\frac{\pi \cdot 12^2}{4} = 170 \text{ kN}$$

$\varnothing_2 = 8$ mm

$$F_{1,\max} = 500 \cdot 2\frac{\pi \cdot 12^2}{4} \cdot \cos 18{,}5° = 107 \text{ kN}$$

$$F_{2,\max} = 500 \cdot 8\frac{\pi \cdot 8^2}{4} = 201 \text{ kN}$$

$$F_{3,\max} = 500 \cdot 3\frac{\pi \cdot 12^2}{4} = 170 \text{ kN}$$

As a first assumption the horizontal force, H, is set equal to zero. Then we assume that we are utilizing the shear reinforcement up to 100%. This gives the following result by Equation (7).

$\varnothing_1 = 12$ mm

$$V_{\max} = 452\cos 30° + 170 = 561 \text{ kN}$$

$\varnothing_2 = 8$ mm

$$V_{\max} = 201\cos 30° + 170 = 344 \text{ kN}$$

The moment equilibrium Equation (9) gives:

$\varnothing_1 = 12$ mm

$$F_c = \frac{561 \cdot 66 + 191 \cdot 65}{65 + 20} = 582 \text{ kN}$$

$\varnothing_2 = 8$ mm

$$F_c = \frac{344 \cdot 66 + 107 \cdot 65}{65 + 20} = 349 \text{ kN}$$

Assuming that the compressive strut in the concrete is developed over a height of 30 mm and the width of 540 mm, the compressive stress in the concrete can be calculated as:

$\varnothing_1 = 12$ mm

$\sigma_{Fc} = F_c/(w \cdot h)$

$\sigma_{Fc} = 582/(540 \cdot 30) = 35.9$ MPa

$\varnothing_2 = 8$ mm

$\sigma_{Fc} = F_c/(w \cdot h)$

$\sigma_{Fc} = 353/(540 \cdot 30) = 21.8$ MPa

These compressive stresses are below the compressive strengths that have been measured, and failures caused by concrete crushing could not be observed in the tests. The assumed distribution of forces in the rebars would be a possible solution according to this load model, resulting in yielding in the shear reinforcement. Anyhow, this is only one possible solution for this model, based on theoretical positions of the rebars. This load model should be calibrated to the test results, as should the influence of the horizontal force *H*. For example, frictional forces between the concrete surfaces will influence the result.

5. Test results vs. calculation models

Table 2 – Test results compared to results from calculation models.

Cast date	Test results V_{max} [kN]			Model 1 V_{max} [kN]				Model 2 V_{max} [kN]				Model 3 V_{max} [kN]				Model 4 V_{max} [kN]			
2010-	Ø12	Ø8	-	Ø12	Ø8	-	η^*	Ø12	Ø8	-	η^*	Ø12	Ø8	-	η^*	Ø12	Ø8	-	η^*
03-15	449	-	-	80	-	-	*5.61*	*84*	-	-	*5.36*	392	-	-	*1.15*	561	-	-	*0.80*
03-15	337	-	-	80	-	-	*4.21*	*84*	-	-	*4.03*	392	-	-	*0.86*	561	-	-	*0.60*
03-16	532	-	-	83	-	-	*6.41*	*88*	-	-	*6.07*	392	-	-	*1.36*	561	-	-	*0.95*
03-16	370	-	-	86	-	-	*4.30*	*88*	-	-	*4.22*	392	-	-	*0.94*	561	-	-	*0.66*
03-18	-	285	-	-	68	-	*4.19*	-	*73*	-	*3.88*	-	174	-	*1.64*	-	344	-	*0.83*
03-18	-	-	104	-	-	68	*1.53*	-	-	73	*1.42*	-	-	0	-	-	-	0	-
04-07	-	222	-	-	63	-	*3.52*	-	67	-	*3.30*	-	174	-	*1.28*	-	344	-	*0.65*
04-07	-	-	114	-	-	63	*1.81*	-	-	67	*1.70*	-	-	0	-	-	-	0	-
04-08	-	363	-	-	77	-	*4.71*	-	82	-	*4.42*	-	174	-	*2.09*	-	344	-	*1.06*
04-08	-	-	123	-	-	77	*1.60*	-	-	82	*1.50*	-	-	0	-	-	-	0	-
04-12	-	376	-	-	68	-	*5.53*	-	71	-	*5.30*	-	174	-	*2.16*	-	344	-	*1.09*
04-12	-	-	82	-	-	68	*1.21*	-	-	71	*1.16*	-	-	0	-	-	-	0	-

* η = test result divided by the predicted value for the given calculation model.

According to the result presented in Table 2, calculation model 1 and 2 can be useful to estimate the strength for a shear key without reinforcement. The design values are on the safe side with a safety factor from 1.16 – 1.81. Model 3 gives results that are on safe side except for the failures in the concrete cover for test specimen type 1. With the assumptions made, design model 4 is the same as model 3, except the fact that model 4 makes the vertical reinforcement bars in the slab active. The result is often on the unsafe side, which could indicate that the vertical rebars does not influence the load carrying capacity as much as assumed in the calculations. This model needs to be studied more detailed, calibrated to the test results and maybe modified.

One thing that can be noted is that the shear keys that fail in the concrete covering layer still transfer forces that are far higher than the capacity of the concrete itself. Therefore, the reinforcement must have been activated, and should be included in the design formula in one way or another.

6. Conclusions

The results from the tests have a considerable scatter. Still some interesting points can be noted. Firstly, the tests show that unreinforced concrete can not transfer the design shear forces, caused by the vehicle models in Eurocode, from one element to another. This was an expected result, in line with the result from the calculations. However, in the reality we believe that the shear keys can transfer a higher load since the surrounding elements will deflect together with the loaded element, which probably gives longitudinal compressive forces which would counteract the tensile stresses that occurs due to the shear forces.

Secondly, the load carrying capacity of the previously used shear keys seems to be larger than necessary, especially if we can avoid a failure that is developed by a crack growing through the concrete covering. The shear keys with less amount of reinforcement (Ø8mm) are still strong enough to carry the load. However, we suggest some changes in the shear key reinforcement since we see some potential improvement. Two new reinforcement layouts are presented in Figure 18. In both cases the concrete cover layer has been reduced. In the left case, additional reinforcement have been added (-E8), and in the right case the SX-rebars have been replaced by EX-rebars. The geometry of the EX- and SX- rebars can be seen in Figure 10 and 20. By using stainless steel in some of the rebars in the shear keys, it would be possible to decrease the thickness of the concrete covering layer, and hopefully avoid a failure in the covering layer.

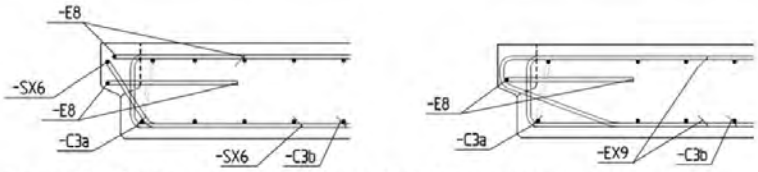

Figure 20 – Illustration of two suggested reinforcement layouts.

REFERENCES

1. Hällmark, R., Collin, P & Nilsson M., "Prefabricated composite bridges," Proceedings, IABSE Symposium, Bangkok, Thailand, Sept. 2009, Vol. 96, pp. 282-283.
2. Hällmark, R., Collin, P & Stoltz A., "Innovative Prefabricated Composite Bridges," Structural Engineering International, 2009, Vol. 19, no:1, pp. 69-78.
3. Collin et al., "International workshop on prefabricated composite bridges", March 4th 2009, Stockholm, ISBN: 1402-1536.
4. EN 1991-2, Eurocode 1 – Actions on structures - Part 2: Traffic Loads on Bridges. CEN, European Committee for Standardization: Brussels, 2005.
5. BBK04, Swedish Concrete Regulations, Boverket, Karlskrona, 2004.
6. EN 1992-1-1, Eurocode 2 – Design of concrete structures, Part 1: General rules and rules for buildings. CEN, European Committee for Standardization: Brussels, 2004.
7. Betonghandboken – Konstruktion, Ch. 3.7:2, AB Svensk Byggtjänst, Stockholm.

Paper IV

The behaviour of a prefabricated composite bridge with dry deck joints – evaluation of field monitoring

Robert Hällmark, Peter Collin and Mikael Möller

Submitted to:
Structural Engineering International, June 2012.

This paper is based on tests planned and evaluated by Hällmark, who also has been the author of this paper. Collin has contributed with his experiences, views and opinions through the whole process. Möller has provided data from earlier tests and has also given his views on the content of the paper.

The behaviour of a prefabricated composite bridge with dry deck joints

Robert Hällmark
M.Sc
Ramböll
Luleå, Sweden

Peter Collin
Professor
LTU/Ramböll
Luleå, Sweden

Mikael Möller
Ph.D
LTU/Areva
Luleå, Sweden

Summary

This paper describes the monitoring of a one span composite bridge in Northern Sweden. The bridge was built in 2000, with prefabricated deck elements connected to steel girders, and the end screens as well as the piers were also prefabricated. The bridge was monitored in both 2001 and 2011, instrumented with equipment measuring the deflections and strains in the steel cross section. The bridge was loaded by a truck in midspan, with a total weight of 25 Tons. When the truck was centred between the girders the results showed a symmetric behaviour, with respects to deflections as well as stresses. For the case with the truck right above one of the steel girders, the anti-symmetric behaviour is studied with means of FE-calculations, taking into account the stiffness of the composite section as well as the end screens and the earth pressure behind them.

Keywords: Composite bridge, prefabrication, deck elements, dry joints, monitoring.

1. Introduction

Composite bridges have the benefit that the steel section can carry the formwork, as well as the wet concrete, without the need of temporary supports. This makes this type of bridge very competitive for water crossings, and for bridges spanning over existing roads, railways etc. Today, a lot of bridges are built in urban areas where congestion often is a growing problem. The total construction cost of a bridge in such an area should not only be based on the cost of material and labour. The cost of the traffic disturbance should also been taken into account. If this is done, solutions with high degree of prefabrication and short assembly times will be benefited. One way of increasing the degree of prefabrication is to use not only prefabricated steel girders, but also prefabricated concrete deck elements. [1]

Starting in the late nineties, a solution with concrete deck elements with dry joints has been developed in Sweden. The joints are totally dry and transfer shear forces by overlapping shear keys, see Figure 1 and Figure 2. Longitudinal compressive forces are transferred by the contact pressure in the concrete surfaces at the transverse joints. In case of tensional forces, the steel section is designed to take the whole load, since there is no reinforcement going through the joints. This type of structure is described more in detail in [2].

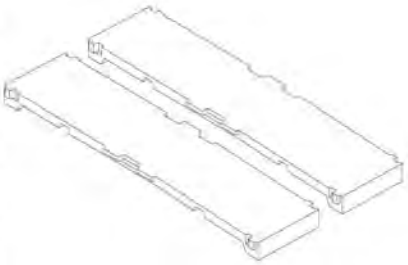

Figure 1 Schematic drawing of two concrete deck elements with dry joints.

THE BEHAVIOUR OF A PREFABRICATED COMPOSITE BRIDGE WITH DRY DECK JOINTS

Starting in the late nineties, a solution with concrete deck elements with dry joints has been developed in Sweden. The joints are totally dry and transfer shear forces by overlapping shear keys, see Figure 1 and Figure 2. Longitudinal compressive forces are transferred by the contact pressure in the concrete surfaces at the transverse joints. In case of tensional forces, the steel section is designed to take the whole load, since there is no reinforcement going through the joints. This type of structure is described more in detail in [2].

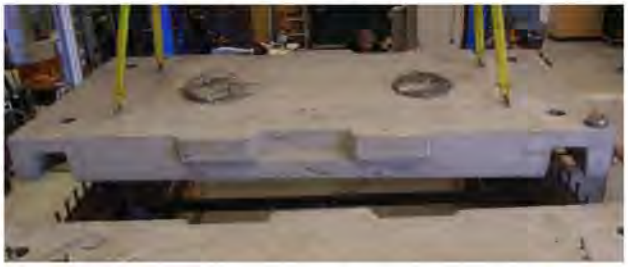

Figure 2 Picture of a dry deck joint in a large scale test specimen.

A bridge deck of this type is well suited for single span bridges with mostly compressive forces in the concrete deck. Nevertheless, laboratory tests indicated that it would not be a problem to use this type of deck on multi span bridges as well, regarding ultimate strength of the shear keys and the shear key fatigue resistance [2, 3]. In such a case, the requirement on the water insulation as well as the pavement should be specified according to the estimated joint openings.

During the development process, questions have been raised whether or not this type of structure behaves as a composite section. In the current paper, a real single span bridge with dry deck joints is studied. The study includes field monitoring done in year 2001 and 2011, as well as an FE-analysis of the bridge. All results are also compared to the design calculations of the bridge, which is based on beam theory.

This paper focuses on the stiffness behaviour of the superstructure and especially the interacting concrete area. In the design stage this area is normally estimated according to [4]. Figure 3 illustrates how the stress is modelled as concentrated into blocks, instead of the real distribution caused by the shear lag phenomenon. Equation 1 shows how the effective flange width is calculated in midspan sections. The equivalent span length, L_e, is set to $0.7 \cdot L_e$.

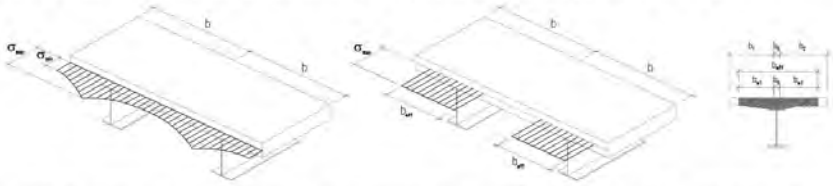

Figure 3 Stress distribution caused by shear lag, and definition of effective flange width, b_{eff}.

$$b_{eff} = b_0 + \Sigma b_{ei} \quad \text{if} \quad b_{ei,max} \le L_e / 8 \quad \text{else} \quad b_{ei} = L_e / 8 \tag{1}$$

There is however reasons to believe that a bridge with dry deck joints will behave a bit different, at least at moderate load levels, than a conventional composite bridge with an in-situ cast concrete deck. The gaps in the joints are kept as small as possible by using match-casting and limited tolerances that are regulated by a control program. Nevertheless, there will always be gaps in the joints that have to be closed before the prefabricated deck elements can transfer compressive forces as good as an in-situ cast deck slab. Thus the formulas for the effective flange width might not be correct in SLS (Serviceability Limit State) for a bridge of this kind.

2. Rokån Bridge

In year 2000 a single span composite bridge, with a prefabricated deck with dry joints, was built in northern Sweden. The bridge was constructed in order to replace an old bridge over the stream Rokån. The project was very successful and the bridge could be replaced with a minimum of traffic disturbance. The road was closed in just 30 h before it was reopened for traffic over the new bridge. [2]

The superstructure is made of two I-girders and has a span length of 16.2 m, see Figure 4 and Figure 5. The bridge has prefabricated back walls connected to the ends of the steel girders. This gives extra rotational stiffness at the end of the girders, which is generally neglected in the design of bridges.

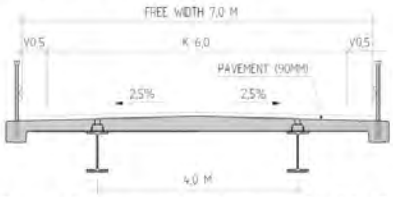

Figure 4 Cross-section drawing of Rokån Bridge.

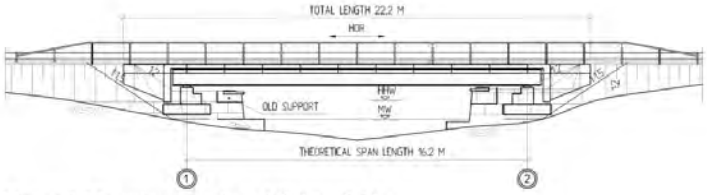

Figure 5 Elevation drawing of Rokån Bridge.

2.1 Steel girders

The bridge consists of two steel I-girders with the dimensions according to Figure 6. Since the bridge length is rather short, each steel girder is made as one piece without any transversal joint. The web and the upper flange are made of S355J2G3 steel and the bottom flange is made of S460M. The real material properties have not been investigated. All material parameters have been taken from [5], see Table 1.

2.2 Concrete deck

The concrete deck consists of 8 deck elements, each with a length of 1.8 m, made of concrete in strength class C30/37. The dimensions of the deck slab are presented in Figure 1. Some of the most important material parameters are listed in Table 1 [6].

The concrete deck elements were all precast in a concrete workshop and transported to the bridge site on trucks and each element had a weight of 9.0 tons. In addition to the deck elements, the back- and the wing-walls were also precast as one unit.

The reinforcement was mainly in grade B500B (fy = 500 MPa), with the exception of the transversal reinforcement at the top surface, which was in grade K600S (fy = 600 MPa). Figure 8 shows the reinforcement drawing for the elements.

Figure 6 Steel section

Table 1 Material parameters

Steel	t [mm]	w [mm]	Material	E [GPa]	ν [-]
Top flange	20	420	S355J2G3	210	0.3
Web	12	750	S355J2G3	210	0.3
Bot. flange	28	500	S460M	210	0.3
Concrete	Area [m²]	e_{CG}* [mm]	Material	E [GPa]	ν [-]
A_1	0.194	0	C30/37	33	0.2
A_2	0.316	-117	C30/37	33	0.2
A_3	0.550	-138	C30/37	33	0.2
$2\cdot(A_2 + A_3)$	1.732	-130	C30/37	33	0.2
A_{total}	2.121	-106	C30/37	33	0.2

* = z-coordinate for the centre of gravity position, with the origin at the upper side of the top flange and with positive values downwards.

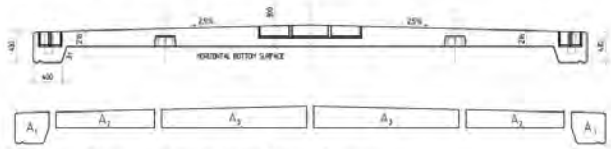

Figure 7 Concrete deck slab dimensions

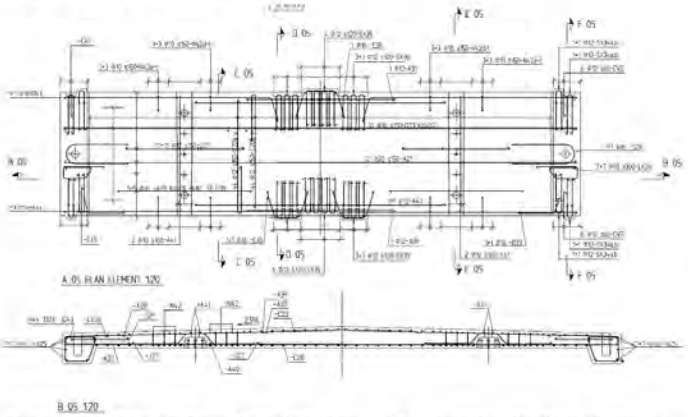

Figure 8 Extraction from the reinforcement drawing for the deck elements.

3. Monitoring

In the spring of 2001, field tests were performed with a loaded truck, measuring global deflections as well as strains in the steel flanges. In the spring of 2011, the bridge was monitored once again in order to study if and how the behaviour had changed after 10 years.

3.1 Test set-up

The same test set-up was used in year 2001 and 2011. The deflections were measured with LVDT-gauges in three positions on each girder, in the middle of the bridge (d_3 and d_4) and at the supports (d_1, d_2, d_5, and d_6), see Figure 9. The steel strains were measured at the bottom of the top flange and at the top of the bottom flange, in three sections. With the origin at midspan, the studied sections were located at x = 0.200 – 0.900 – 7.175 m, see Figure 9.

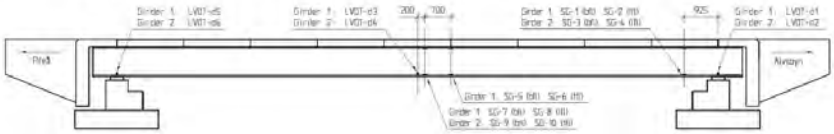

Figure 9 Positions of the measuring devices on Rokån Bridge

The strain gauges were glued to the flanges in the same positions as during the monitoring in year 2001, see Figure 10. The first section was located 0.200 m away from midspan and the second 0.900 m from midspan. The latter position is chosen since it coincides with a deck joint, and the first position is chosen since it is near the middle of an element. Since there are web stiffeners at midspan, the strain gauges are moved 0.200 m, in order to avoid measuring a disturbed longitudinal stress state. The third section that is monitored is located 0.925 m from a support section. This section is monitored in order to get an estimation of the degree of restraint at the end of the steel girder.

Figure 10 Strain gauges at steel flanges.

3.2 Vehicle loads

The loading of the bridge was performed in a similar way in both tests. The following two sections specify the loads and the load positions in detail. In both cases, the axle loads were scaled before the test started. During the measurements the vehicle always moved from left to right in Figure 9.

3.2.1 Test 2011

The bridge was loaded by a truck with three axels, see Figure 11. During each test the vehicle stopped in two positions. First with the front axle in the midspan and second with the bogie centred at the midspan. The vehicle position in the transversal directions was also varied. The vehicle was positioned straight above both girders and also along the bridge centreline.

Load position:
LP 1: Centred along one of the girders, axel 1 at midspan.
LP 2: Centred along one of the girders, bogie centre at midspan.
LP 3: Centred between the girders, axel 1 at midspan.
LP 4: Centred between the girders, bogie centre at midspan.

Figure 11 Truck load and positions that was used in the test performed in 2011 [mm].

3.2.2 Test 2001

The bridge was loaded by a truck with three axels, see Figure 12. During each test the vehicle stopped in three positions. In each position, one of the axles is at midspan. The vehicle position in the transversal directions was also varied. The vehicle was positioned straight above both girders and also along the centreline of the bridge. [7]

Load position:
LP 1: Centred along one of the girders, axel 1 at midspan.
LP 2: Centred along one of the girders, axel 2 at midspan.
LP 3: Centred along one of the girders, axel 3 at midspan.
LP 4: Centred between the girders, axel 1 at midspan.
LP 5: Centred between the girders, axel 2 at midspan.
LP 6: Centred between the girders, axel 2 at midspan.

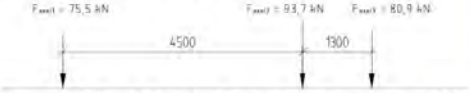

Figure 12 Truck load and positions that was used in the test performed in 2001 [mm].

3.3 Results

In the sections below the results from the latest test are presented in detail, together with more summarized results from the earlier test.

3.3.1 Deflections

The presented deflections are all midspan deflections that have been compensated for the vertical deformations at the supports according to the equations below.

$$d_{G1} = d_3 - 0.5 \cdot (d_1 + d_5) \quad (2)$$

$$d_{G2} = d_4 - 0.5 \cdot (d_2 + d_6) \quad (3)$$

Test 2011 - Load centred above steel girders

In the case with the truck load centred above girder 1 (Test 1) the measured deflections are 3.3 mm when the front load is in midspan and 4.1 mm when the bogie is in midspan, see Figure 13. In the same figure Test 2 is plotted, showing the situation when the same load is centred above the other girder, girder 2. The deflections are in line with the results from Test 1, ±0.1 mm.

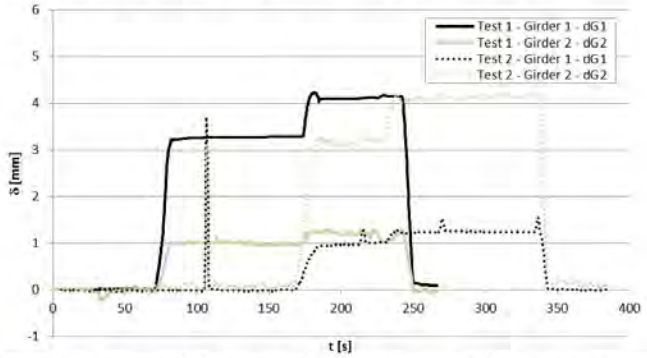

Figure 13 Measured deflections with the truck centred above girder 1 resp. 2.

Test 2011 - Load centred along the centreline between the girders

The results from Test 3, with the centred truck load are presented in Figure 14. The bridge shows a very symmetric behaviour with the same deflection in both girders. The deflections are 2.0 mm when the front axis is in midspan, and 2.6 mm when the bogie is in midspan.

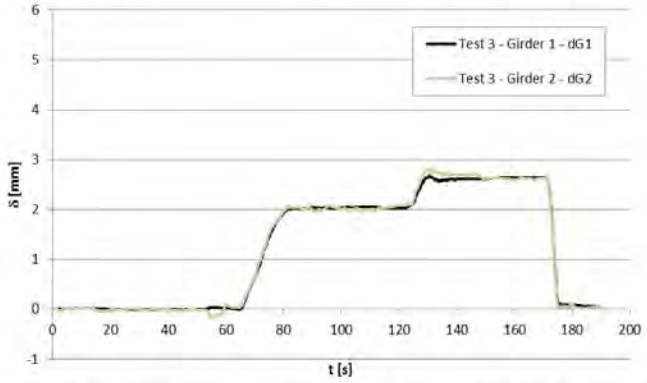

Figure 14 Measured deflections with the truck centred between the girders.

Test 2001 and 2011 – Summarization of the deflections

The deflections measured in 2001 are summarized in Table 2. The deflections measured in 2011 are also presented in the same table as a comparison.

Table 2 Measured deflections at midspan

Year 2001	Test 1			Test 2			Test 3		
	LP1	LP2	LP3	LP1	LP2	LP3	LP4	LP5	LP6
d_{G1} [mm]	3.4	-	4.4	1.3	1.8	1.7	2.3	3.2	3.1
d_{G2} [mm]	1.3	-	1.7	3.3	4.5	4.3	2.3	3.2	3.0

Year 2011	Test 1		Test 2		Test 3	
	LP1	LP2	LP1	LP2	LP3	LP4
d_{G1} [mm]	3.3	4.1	1.0	1.3	2.0	2.6
d_{G2} [mm]	1.0	1.3	3.2	4.1	2.0	2.6

3.3.2 Steel stresses

The measured steel strains have been transformed into stresses assuming $E_{steel} = 210$ GPa.

2011 - Load centred above steel girders

The steel stresses in a section 0.200 m away from midspan are presented graphically in Figure 15. The largest difference between the measured stresses in test 1 and 2 is less than 1 MPa.

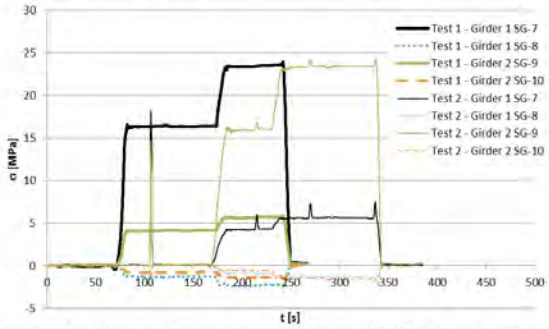

Figure 15 Measured stresses in Test 1 and 2, 0.200 m from midspan.

2011 - Load centred along the centreline between the girders

The results from test 3 with the centred truck load are presented in Figure 16. The presented stresses are measured in a section 0.200 m from midspan.

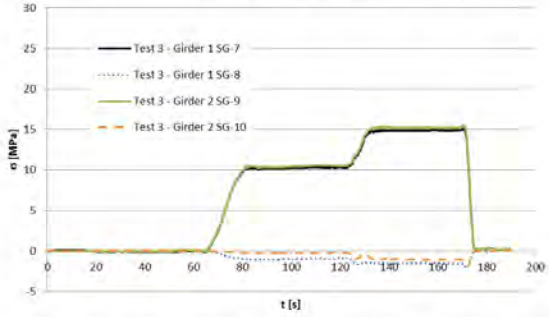

Figure 16 Measured stresses in Test 3, 0.200 m from midspan.

Test 2001 and 2011 – Summarization of the stresses

The stresses measured in 2001 and 2011 are summarized in Table 3 - Table 5 . Unfortunately, the only stresses that have been saved from the test in 2001 are the stresses in the bottom flange at section x = 0.200 m, which is given in [7].

Table 3 Measured stresses in section x = 0.200 m.

Year	Test 1			Test 2			Test 3		
2001	LP1	LP2	LP3	LP1	LP2	LP3	LP4	LP5	LP6
σ_{SG-7} [MPa]	18.2	-	26.6	5.0	7.6	7.4	11.6	17.5	17.0
σ_{SG-8} [MPa]	-	-	-	-	-	-	-	-	-
σ_{SG-9} [MPa]	4.9	-	6.8	17.2	26.3	25.6	11.6	17.5	16.7
σ_{SG-10} [MPa]	-	-	-	-	-	-	-	-	-

Year	Test 1		Test 2		Test 3	
2011	LP1	LP2	LP1	LP2	LP3	LP4
σ_{SG-7} [MPa]	16.3	23.4	4.3	5.6	10.3	14.8
σ_{SG-8} [MPa]	-1.3	-2.4	-0.9	-1.3	-1.0	-1.5
σ_{SG-9} [MPa]	4.1	5.6	16.0	23.3	10.5	15.2
σ_{SG-10} [MPa]	-0.8	-1.4	-0.6	-1.5	-0.3	-1.0

Table 4 Measured stresses in section x = 0.900 m.

Year	Test 1		Test 2		Test 3	
2011	LP1	LP2	LP1	LP2	LP3	LP4
σ_{SG-5} [MPa]	14.7	23.1	3.9	5.5	9.0	14.2
σ_{SG-6} [MPa]	-1.9	-1.5	-0.7	-1.2	-1.0	-0.9

Table 5 Measured stresses in section x = 7.175 m.

Year	Test 1		Test 2		Test 3	
2011	LP1	LP2	LP1	LP2	LP3	LP4
σ_{SG-1} [MPa]	-7.4	-7.2	-1.2	-0.9	-3.9	-3.6
σ_{SG-2} [MPa]	0.8	0.8	0.0	-0.2	0.4	0.1
σ_{SG-3} [MPa]	-1.4	-1.0	-7.0	-6.9	-4.3	-3.9
σ_{SG-4} [MPa]	0.1	-0.1	0.5	0.7	0.4	0.1

4. Analysis

The results from the measurements have been compared to different design models. First a simplified beam-model which is the model this bridge originally was design according to. Second a more detailed FE-analysis including the back walls and the restraint from the soil.

All steel parts are modelled with the material parameters given in Table 1.

4.1 Design models

Beam model

In the simplified beam model the bridge is regarded as simply supported and the girders are separated in the analysis. Due to the symmetry, half of the deck slab is assumed to contribute to the stiffness of each composite girder. The loads are then distributed between the girders depending on the location of the load resultants, in the transverse direction. This gives a load factor of 0.5 when the truck is standing right between the girders and a factor of 1.0 resp. 0.0 when the truck is standing right above one of the girders.

The cross-sectional parameters have been calculated according to [3, 4, 7], taking into consideration shear lag as well as local buckling. There is no reduction of the steel cross-section, but the width of the interacting concrete is reduced from 3.355 m to 2.873 m in the field section. In Figure 17, the interacting part of the concrete are hatched. This figure also presents some of the important cross-sectional parameters.

Steel		Concrete		
Web t	12 mm	n_L	6,4	-
Web h	750 mm	A_{conc}	0.741	m^2
B.flange t	28 mm	I	0.00493	m^4
B.flange w	500 mm	CG_{conc}*	-126	m
T.flange t	20 mm			
T.flange w	420 mm			

Centre of gravity*	0	mm
Area	0.1479	mm^2
I_x	0.01306	mm^4
W_{tf}	29.4233	mm^3
$W_{w,t}$	0.6387	mm^3
$W_{w,b}$	0.0169	mm^3
W_{bf}	0.0164	mm^3

* = origin at the top of the steel upper flange, positive downwards.

Figure 17 Cross-sectional paramteres for the beam model, assuming short term loading.

FE-model

The bridge superstructure has been modelled with shell-elements. The steel-concrete connection was modelled as fully composite, assuming no shear connection deformations.

The bridge has been modelled in three different ways, first without back walls, second with back walls, and third with crushed rocks as backfill behind the back walls. In the last model, the crushed rocks are modelled with an elastic modulus of 50 MPa. The soil is modelled by volumetric elements with a depth of 1.0 m. One side of these elements is attached to the back walls and the other side is locked from longitudinal displacements. The three FE-models are all illustrated in Figure 18.

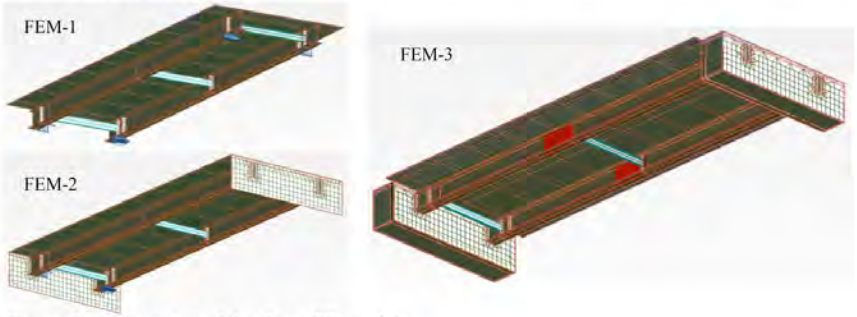

Figure 18 Illustration of the three FE-models.

In a simple design calculation (the beam model) the positive contribution from the edge beams are neglected. The FE-analysis is however done in order to describe the reality as good as possible, the edge beams are therefore included.

4.2 Deflections

If the measured deflections are compared to the theoretical deflections of a simply supported I-girder, the measured deflections are significantly smaller than the calculated deflections, see Table 6. This is quite expected, since the torsional/warping stiffness of the superstructure will distribute a part of the moment to the other girder. The back walls will also give an extra rotational stiffness in the end of the steel girders. These two factors are often neglected in the design of this type of bridge.

Table 6 Test results compared to results from calculation models.

Test – 2001

Load position 1	Test	BM	FEM-1	FEM-2	FEM-3
δ_3 [mm]	3.3	5.4	4.2	4.0	3.4
δ_4 [mm]	1.3	0.0	1.6	1.8	1.0

Load position 2	Test	BM	FEM-1	FEM-2	FEM-3
δ_3 [mm]	4.5	7,1	5.4	5.3	4.5
δ_4 [mm]	1.8	0.0	2.2	2.4	1.3

Load position 3	Test	BM	FEM-1	FEM-2	FEM-3
δ_3 [mm]	4.3	6,5	5.0	4.9	4.2
δ_4 [mm]	1.7	0.0	2.1	2.3	1.2

Load position 4	Test	BM	FEM-1	FEM-2	FEM-3
δ_3 [mm]	2.3	2.7	2.9	2.9	2.1
δ_4 [mm]	2.3	2.7	2.9	2.9	2.1

Load position 5	Test	BM	FEM-1	FEM-2	FEM-3
δ_3 [mm]	3.2	3.5	3.8	3.8	2.8
δ_4 [mm]	3.2	3.5	3.8	3.8	2.8

Load position 6	Test	BM	FEM-1	FEM-2	FEM-3
δ_3 [mm]	3.0	3.3	3.5	3.5	2.6
δ_4 [mm]	3.0	3.3	3.5	3.5	2.6

Test – 2011

Load position 1	Test	BM	FEM-1	FEM-2	FEM-3
δ_3 [mm]	3.3	5.4	4.2	4.0	3.3
δ_4 [mm]	1.0	0.0	1.6	1.8	1.0

Load position 2	Test	BM	FEM-1	FEM-2	FEM-3
δ_3 [mm]	4.1	6.6	5.1	4.9	4.2
δ_4 [mm]	1.2	0.0	2.0	2.2	1.2

Load position 3	Test	BM	FEM-1	FEM-2	FEM-3
δ_3 [mm]	2.0	2.7	2.9	2.9	2.1
δ_4 [mm]	2.0	2.7	2.9	2.9	2.1

Load position 4	Test	BM	FEM-1	FEM-2	FEM-3
δ_3 [mm]	2.7	3.3	3.5	3.5	2.7
δ_4 [mm]	2.7	3.3	3.5	3.5	2.7

The FE-models confirms that the back walls will contribute to the distribution of the deflections, if the bridge is loaded unsymmetrically. However, the effect from the back walls seems to be quite small. If the load is centred above one of the girders, the deflection in the most loaded girder will decrease with about 4% when the back walls are included in the analyses (FEM-1 vs. FEM-2). Torsional- and warping-stiffness of the superstructure itself seems to be the major reason to the distribution of the load, the effect from the cross-beams is negligible.

The results presented in Table 6 shows that the beam model is very conservative, so are also the FE-models that do not include the soil stiffness. FEM-3, which is the only model that includes the soil stiffness, is the model that corresponds best to the reality. The results from 2001 indicate a somewhat stiffer behaviour than the measurements. The results from 2011 are very close to the deformations predicted by FEM-4. Thus, the deflection due to the traffic load is somewhat lower in 2011 than in 2001.

The soil model is quite simple, and the soil properties are a possible source of error. Since no field measurement of the soil properties has been done, tabled values have been used. The relative difference between 2001 and 2011, are believed

4.3 Stresses

The measured stresses have been compared to the calculated stresses according to the beam model as well as the FE-analysis. The measured stresses in the two midspan sections are presented in Table 7 - Table 8.

Table 7 Test results from year 2011 vs. design models in section x = 0.200 m [MPa].

Load position 1		measured	BM	FEM-1	FEM-2	FEM-3
Girder 1 - SG 8	σ_{tfl}	-1.3	0.9	0.4	0.4	1.8
Girder 1 - SG 7	σ_{bfl}	16.3	33.3	23.2	22.4	17.7
Girder 2 - SG 10	σ_{tfl}	-0.8	0.0	0.8	0.8	0.4
Girder 2 - SG 9	σ_{bfl}	4.1	0.0	9.3	10.1	5.0
Load position 2		measured	BM	FEM-1	FEM-2	FEM-3
Girder 1 - SG 8	σ_{tfl}	-2.4	1.2	0.3	0.3	2.4
Girder 1 - SG 7	σ_{bfl}	23.4	43.5	31.2	30.3	24.3
Girder 2 - SG 10	σ_{tfl}	-1.4	0.0	1.0	1.1	0.5
Girder 2 - SG 9	σ_{bfl}	5.6	0.0	12.2	13.1	6.6
Load position 3		measured	BM	FEM-1	FEM-2	FEM-3
Girder 1 - SG 8	σ_{tfl}	-1.0	0.4	0.4	0.6	1.2
Girder 1 - SG 7	σ_{bfl}	10.3	16.6	16.1	16.1	11.4
Girder 2 - SG 10	σ_{tfl}	-0.2	0.4	0.6	0.6	1.2
Girder 2 - SG 9	σ_{bfl}	10.3	16.6	16.1	16.1	11.4
Load position 4		measured	BM	FEM-1	FEM-2	FEM-3
Girder 1 - SG 8	σ_{tfl}	-1.5	0.6	0.7	0.4	1.6
Girder 1 - SG 7	σ_{bfl}	14.8	21.7	21.3	21.3	15.5
Girder 2 - SG 10	σ_{tfl}	-1.1	0.6	0.7	0.7	1.6
Girder 2 - SG 9	σ_{bfl}	15.2	0.6	21.3	21.3	15.5

Table 8 Test results from year 2011 vs. design models in section x = 0.900 m [MPa].

Load position 1		measured	BM	FEM-1	FEM-2	FEM-3
Girder 1 - SG 6	σ_{tfl}	-1.9	0.8	0.0	0.0	1.8
Girder 1 - SG 5	σ_{bfl}	14.8	29.5	20.4	19.6	15.6
Load position 2		measured	BM	FEM-1	FEM-2	FEM-3
Girder 1 - SG 6	σ_{tfl}	-1.5	1.1	0.1	0.1	2.6
Girder 1 - SG 5	σ_{bfl}	23.0	42.0	29.6	28.7	23,5
Load position 3		measured	BM	FEM-1	FEM-2	FEM-3
Girder 1 - SG 6	σ_{tfl}	-1.0	0.4	0.3	0.4	1.1
Girder 1 - SG 5	σ_{bfl}	9.0	14.7	14.7	14.7	10.1
Load position 4		measured	BM	FEM-1	FEM-2	FEM-3
Girder 1 - SG 6	σ_{tfl}	-0.9	0.6	0.6	0.3	1.5
Girder 1 - SG 5	σ_{bfl}	14.2	21.0	20.7	20.8	14.9

As expected, FEM-3 is the model that describes the reality best. The measured stresses are very close to the predicted stresses according to FEM-3, if the support section (x = 7.175) is excluded. The stress distribution in this section is totally different compared to the measured distribution. However, the supports are modelled with no friction at all in the bearings, so all four bearing are free to move in the longitudinal direction. If the supports in one end of the bridge are modelled as fixed or with frictional supports, the stress distribution in FEM-3 will correspond rather well to the observed distribution, as well as to the absolute stress values.

Table 7 and 8 presents stress values in the middle of an element respectively at a joint. When the two sections are compared, no significant differences in the position of the neutral bending axis can be observed. This indicates that the interacting concrete area does not varying over an element in compression.

Figure 19 illustrates the stress situation when the vehicle is standing right above girder 1, with the front axle centred at the midspan (Load position 1).

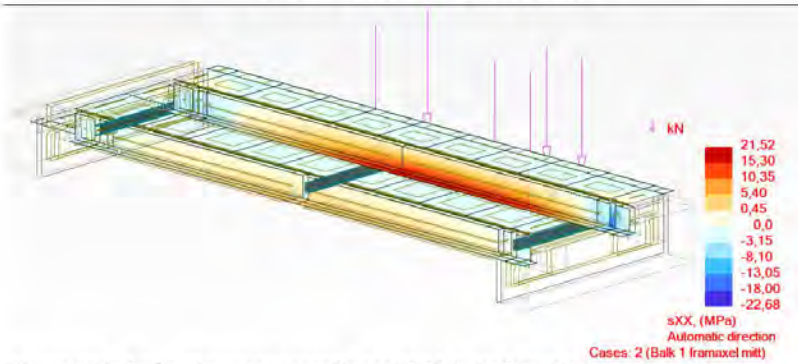

Figure 19 Calculated stresses according to FEM-3, load position 1.

One interesting thing concerning the stresses is the fact that the measured position of the neutral bending axis is positioned a bit lower, compared to the position in the design models. In all design models the neutral bending axis is positioned near the top of the upper flange. In the reality it seems to be positioned about 60-100 mm down from the top of the upper flange in the most loaded girder, and about 140-180 mm in the other girder. If the load is centred between the girders the neutral axis tends to be in the former interval.

The measured steel stresses can be used in order to estimate the interacting concrete area. The difference between the tensional- and the compressive forces in the steel, corresponds to the force taken by the concrete.

$$\Sigma F \rightarrow: \quad F_{steel.comp.} + F_{steel.tens.} + F_{conc.} = 0 \tag{4}$$

Assuming a linear stress distribution over the cross-section, the force in the concrete can be calculated as,

$$F_{conc} = -\left(\sigma_{bfl.m} \cdot t_{bfl} \cdot w_{bfl} + \frac{\sigma_{w.b}}{2} \cdot t_w \left(h_w - e_{neutral} + t_{ifl} \right) + \sigma_{tfl.m} \cdot t_{tfl} \cdot w_{tfl} + \frac{\sigma_{w.t}}{2} \cdot t_w \left(e_{neutral} - t_{tfl} \right) \right) \tag{5}$$

$F_{steel.comp.}$ = compressive normal force in the steel
$F_{steel.tens.}$ = tensile normal force in the steel
F_{conc} = compressive normal force in the concrete
$\sigma_{bfl.m}$ = mean stress in the steel bottom flange
$\sigma_{tfl.m}$ = mean stress in the steel top flange
$\sigma_{w.t}$ = stress in the top of the web
$\sigma_{w.b}$ = stress in the bottom of the web
$e_{neutral}$ = position of neutral bending axis*
e_{conc} = centre of gravity for concrete deck slab*

t_{bfl} = steel bottom flange thickness
w_{bfl} = steel bottom flange width
t_{tfl} = steel top flange thickness
w_{tfl} = steel top flange width
t_w = steel web thickness
h_w = steel web height
n_0 = short term modular ratio E_{steel}/E_{conc}

* = along the z-axis with the origin at the upper side of the steel top flange, positive downwards.

If the measured steel strains are extrapolated up to the centre of gravity for the concrete deck, then the interacting concrete area, $A_{int.conc}$, can be calculated as according to Equation 6.

$$A_{int.conc.} = \frac{F_{conc}}{\frac{\sigma_{tfl}}{n_0} \cdot \left(\frac{e_{neutral} - e_{conc}}{e_{neutral}} \right)} \tag{6}$$

In Table 9 below, the interacting concrete area is presented together with the ratio between the measured interacting concrete area and the interacting concrete area according to [4], n_{ratio}, assuming that the prefabricated concrete deck behaves as a concrete deck cast on site. In the section near the support, x = 7.175 m, no values are presented. Since this section is close to one of the supports, the stress distribution is this section is not linear, and extrapolation of the measured strains is not possible.

Table 9 Interacting concrete area and the n_{ratio}.

		Test 1		Test 2		Test 3		
x = 0.200 m		LP1	LP2	LP1	LP2	LP3	LP4	
Girder 1	$A_{int.conc}$	0.379	0.342	0.225	0.209	0.350	0.343	[m²]
	n_{ratio}	0.51	0.46	0.30	0.28	0.47	0.46	[-]
Girder 2	$A_{int.conc}$	0.237	0.197	0.472	0.409	0.497	0.406	[m²]
	n_{ratio}	0.32	0.27	0.64	0.55	0.67	0.55	[-]
x = 0.900 m								
Girder 1	$A_{int.conc}$	0.305	0.408	0.251	0.219	0.329	0.411	[m²]
	n_{ratio}	0.41	0.55	0.34	0.29	0.44	0.55	[-]

The results from the measurement in 2001 are incomplete, only the steel stresses in the bottom of the webs have been documented. Therefore, it is not possible to estimate the interacting concrete area in an appropriate, since it is impossible to find out the how much of the load that is carried by the steel section respectively the composite section. However, the measured stresses in the bottom of the webs have been compared to FE-analyses and also to the new measurements from 2011, and they all correspond well.

5. Discussion and conclusions

The type of bridge studied in this paper is often designed assuming a simple beam model. The tests show that such a model is very conservative when deflections and steel stresses are calculated. The FE-models show that the torsional/warping stiffness of the superstructure will distribute the force between the steel girders, even if the load is acting straight over one of the girders. The back walls seem to have a similar load distribution effect, but not that significant. It is also obvious that the soil behind the retaining wall will affect the bridge quite a lot, and the FE-model that includes the soil (FEM-3) is the model that describes the reality best.

The tests show that the interacting concrete area is a lot smaller than the effective flange width for a concrete deck in a composite bridge, according to [4]. This conclusion is supported by test on other bridges of same type [9]. The major reason why the interacting concrete area is a lot smaller is believed to be explained by the dry joints. These joints will always give a small gap that has to be closed before the concrete can transfer compressive forces over the joints. If there are small gaps in the joints, when the in-situ cast channels are injected, these gaps will be permanent. This means that the in-situ cast concrete alone will transfer the compressive forces over the joint, until the load is big enough to close the joints.

The significant difference, regarding the position of the neutral bending axis, between the most loaded girder and the other girder, indicate that there are gaps in the joints that are closing when the load increases. For an increasing load, the neutral bending axis is moving upwards towards the theoretical position for an in-situ cast deck slab. In ULS (Ultimate Limit State), a bridge deck of this kind can be treated as an in-situ cast deck. In SLS and FLS (Fatigue Limit State) the bridge designer should be careful not to underestimate the extra load effects on the steel, due to the partial composite action.

In the SLS and FLS, the effective width of the concrete can be reduced in order to compensate for the gap effects. For the bridge presented in this paper, a reduction factor of ~0.5 seems to be a good estimation in case of moderate loading. In the ULS, it is still reasonable to use the effective flange width according to [4] for single span bridge, since the joints will close when the load is increased. This phenomenon has been seen in large scale laboratory tests, and also by FE-models simulating gaps in the deck joints.

During the tests in 2011 a heavy transport vehicle, ~200 ton, crossed the bridge along the centreline, see Figure 20. This vehicle gave steel stresses that were more than 3 times higher than the stresses for the test vehicle in the same position, and about 2 times higher than the highest stress for the test vehicle (~50 MPa in the bottom of the web). Also for this higher load, the stress distribution in the steel section was almost the same, with a neutral bending axis in the web ~100 mm below the top flange.

Figure 20 Heavy transport vehicle that crossed the bridge during the measurements.

Concerning the long-term effect, it can be noted that the passive girder had a relatively larger deflection, compared to the active girder, in 2001 than in 2011. This might indicate that there were initial gaps in the joint, back in 2001, which have been closed or at least partly closed due to abrasion of irregularities at the concrete surfaces in the dry joints. Since no measurements of the absolute vertical position of the steel girders have been done in 2001 and 2012, this indication is hard to verify.

In all models the potential stiffness contribution from the pavement and the rails, have been neglected. Their contribution is believed to be rather low and the measurements do not indicate that the total stiffness is significantly underestimated. Another possible source of error in the FE-modelling is the soil model, since it is based on tabled values and not on field test.

References

[1] Hällmark, P. White, H. & Collin, P. (2012). "Prefabricated Bridge Construction across Europe and America," ASCE – Practice Periodical on Structural Design and Construction, 2009, Vol. 17, no:3

[2] Hällmark, R., Collin, P. & Stoltz, A., "Innovative Prefabricated Composite Bridges," Structural Engineering International, 2009, Vol. 19, no:1, pp. 69-78.

[3] Hällmark, R., Collin, P. & Nilsson, M., "Concrete shear keys in prefabricated bridges with dry deck joints," Nordic Concrete Research, 2011, Vol. 44, no:2, pp. 109-122.

[4] EN 1994-2. (2005), *"Eurocode 4 – Design of composite steel and concrete structures – Part 2: General rules and rules for bridges"*, CEN, European Committee for Standardization, Brussels, Belgium.

[5] EN 1993-1-1. (2005), *"Eurocode 3 – Design of steel structures – Part 1-1: General rules and rules for buildings"*, CEN, European Committee for Standardization, Brussels, Belgium.

[6] EN 1992-1-1. (2005), *"Eurocode 2 – Design of concrete structures – Part 1-1: General rules and rules for buildings"*, CEN, European Committee for Standardization, Brussels, Belgium.

[7] Collin, P., & Möller, M., *"Utvärdering av belastningsprov - Bro över Rokån"*, Technical Report 01:01, Luleå University of Technology, Division of Steel Structures, 2001 (in Swedish).

[8] EN 1993-1-5. (2006), *"Eurocode 3 – Design of steel structures – Part 1-5: Plated structural elements"*, CEN, European Committee for Standardization, Brussels, Belgium.

[9] Collin, P., Johansson, B. & Pétursson, H. (1998). *"Samverkansbroar med elementbyggda farbanor"*. Technical Report. Swedish Institute of Steel Construction, Publication 165, 1998. ISBN: 91 7127 022 1 (in Swedish).

Paper V

Large scale tests of a composite bridge with a prefabricated concrete deck with dry deck joints

Robert Hällmark, Peter Collin and Martin Nilsson

Submitted to:
Bridge Engineering, August 2012.

This paper is based on tests planned and evaluated by Hällmark, who also has been the author of this paper. Collin and Nilsson have contributed with their experiences, views and opinions.

Large scale tests of a composite bridge with a prefabricated concrete deck with dry deck joints

Robert Hällmark
M.Sc
Ramböll
Luleå, Sweden

Peter Collin
Professor
LTU/Ramböll
Luleå, Sweden

Martin Nilsson
Ph.D
LTU
Luleå, Sweden

Summary

This paper describes large scale tests of a composite bridge with prefabricated deck elements, with dry joints in between the elements. The work carried out is a part the European R&D project ELEM (RFCS-CT-2008-00039). The bridge type has been used for three single span bridges in Sweden, and has contributed to minimizing the construction time as well as the disturbances for the traffic. In the tests the behaviour at midspan and the behaviour over an internal support of a continuous bridge were studied, and the results are analyzed by FEM and discussed. Conclusions for the design of this type of bridges such bridges are drawn, with respect to the global analysis as well as the cross section capacity.

Keywords: Composite bridge, prefabrication, deck elements, dry joints, laboratory test.

1. Introduction

In order to make steel-concrete composite bridges even more competitive, the degree of prefabrication can be increased. Using prefabricated concrete deck elements is one way of doing this. Bridges with prefabricated deck elements have been built worldwide for many decades, but are still rare exceptions, and different countries have developed their own ways of implementing the prefabrication techniques. In [1,2,3,4] some global experiences from the use of prefabricated concrete deck elements are presented.

This paper is limited to a prefabricated concrete deck system that has been developed in Sweden, starting in the late nineties. In this deck system the transversal joints are totally dry, and no pre-stressing tendons are used. Shear forces are transferred from one element to another by overlapping concrete tongues, shear keys. These are designed as a series of male-female connections, see Figure 1. This type of bridge deck is described more in detail in [5,6]. The behaviour and strength of this kind of connections have been tested, and discussed in [7].

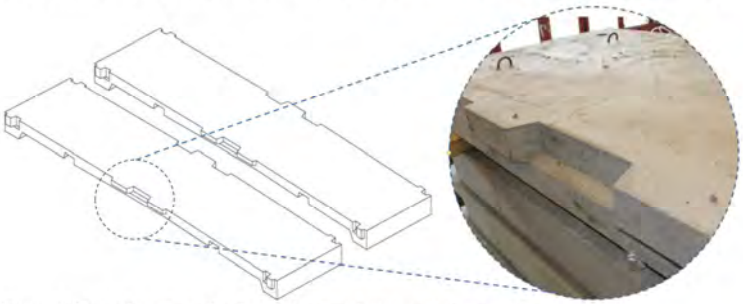

Figure 1 Shear keys in a dry deck joint in a large scale test specimen.

In order to study the behaviour of a composite bridge with this type of deck, large scale laboratory tests were performed in the summer of year 2011. The tests were focused on the behaviour with respect to shear-lag, composite action, joint openings and static capacity of the shear keys. However, this paper is limited to the study of the shear-lag and composite action.

2. Laboratory tests

The specimen and the test set-up were planned in a way which made it possible to perform tests simulating both a load situation in the field area of a continuous bridge, and a load situation at an internal support. The test specimen was designed with a real deck element, from a single span bridge over the river Rokån in Sweden, as model. The geometry of the bridge deck element is presented in Figure 2.

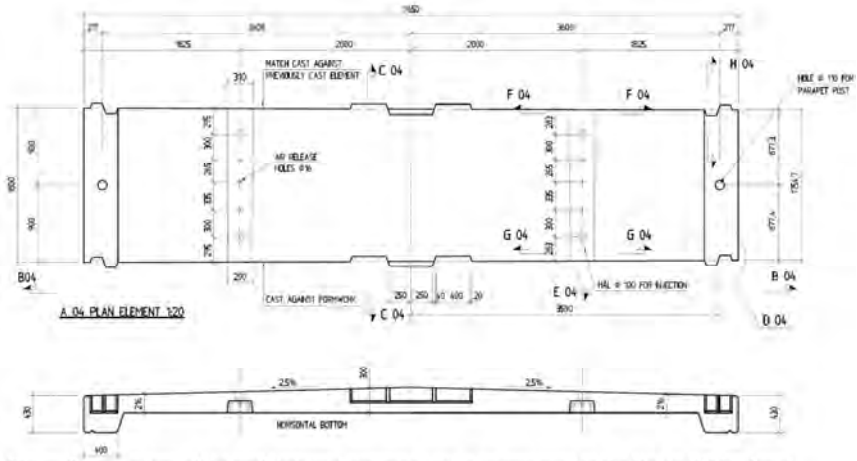

Figure 2 Dimensions of the prefabricated concrete deck elements used in the Rokån Bridge [mm].

Since several different tests were performed on one specimen, all load situations had to be kept below the failure load resulting in non-destructive testing. Only the last test was destructive, when a shear key was loaded until a final failure.

As a complement to these non-destructive tests, destructive tests have been performed by RWTH (Rheinisch Westfaelische Technische Hochschule), in Aachen, on similar specimens. In the last section of this paper, the results from the Swedish and the German tests are compared and discussed.

2.1 Test specimen

The test specimen consisted of two steel I-girders with the dimensions presented in Figure 4, and four prefabricated concrete deck elements on top of that. Composite action was achieved by shear studs, Ø22 – 185 mm. Figure 3 shows a drawing of the specimen.

Steel grade:
S355K2 + N (EN 10025-2:2004)

Measured steel dimensions

Girder		Left	Right
$w_{top.fl}$	[mm]	299	301
$t_{top.fl}$	[mm]	20.2	20.2
h_{web}	[mm]	760	760
t_{web}	[mm]	11.9	12.0
$w_{bot.fl}$	[mm]	300	300
$t_{bot.fl}$	[mm]	20.2	20.2

Figure 3 Steel girder dimensions [mm].

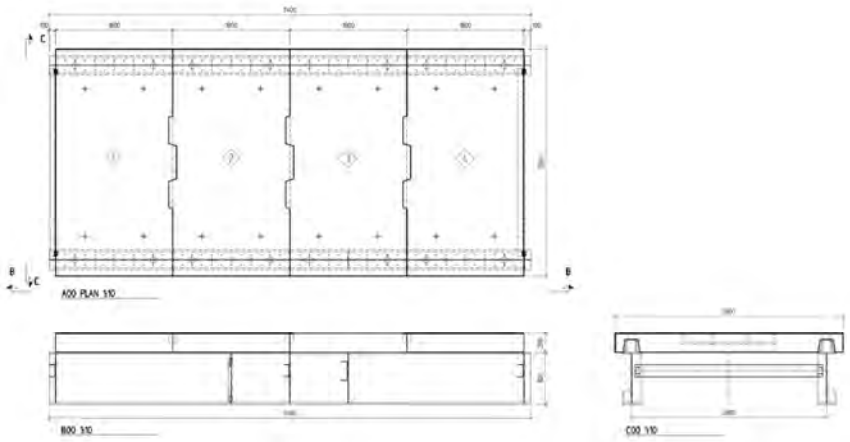

Figure 4 Drawings of the test specimen [mm].

The dimension of each concrete element was 1.8 x 3.5 x 0.29. The height (0.290 m) and the length (1.8 m) of the tested elements are the same as the size of prefabricated elements previously used in real single span bridges. Full height was used in order to get real dimensions of the shear keys, and to avoid discussions about how scale factors affect the results. The length of the deck elements is generally governed by the distance between the parapet posts, which means 1.8-2.0 m in Sweden. The parapet post distance is governing the length of prefabricated elements, due to the benefits gained in both the production and the design stage by using the same position of the post on each element. The width of the concrete deck elements in the test bridge is 3.5 m and the distance between the steel girders is 3.0 m. Generally the distance between the girders is somewhere between 4-7 m in Sweden, depending on the total width of the bridge. This means that the specimen has been scaled down in the transversal direction, and that only the internal part of deck slab is considered. Due to size limitations of the test set-up, the cantilevering parts of the deck slab are missing. Figure 5 and Figure 6 show some drawings of the concrete elements.

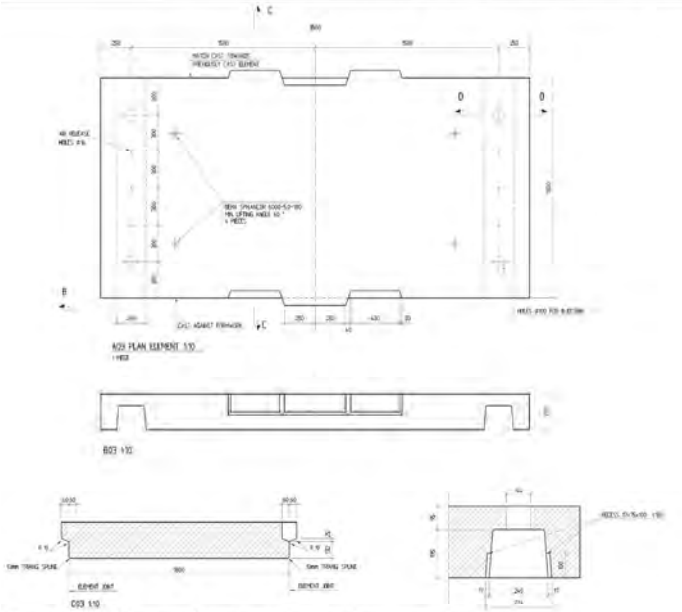

Figure 5 Prefabricated concrete element dimensions [mm].

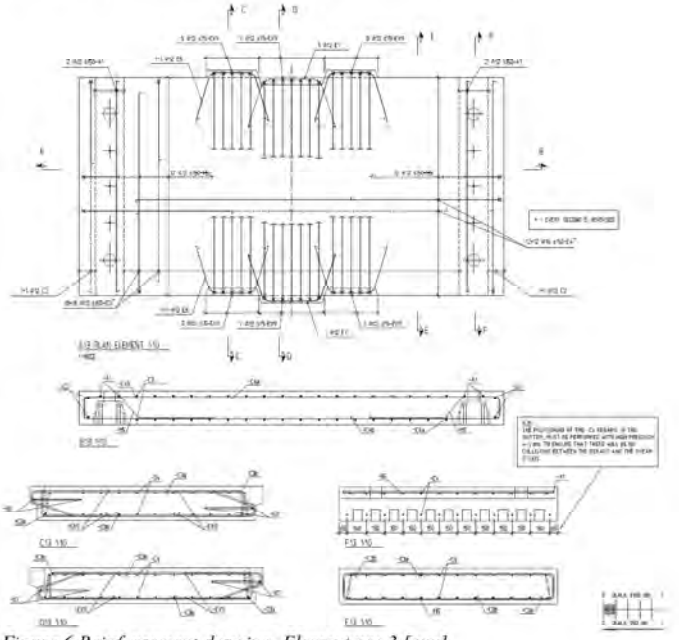

Figure 6 Reinforcement drawing, Element no: 3 [mm].

The ordered concrete strength class was C35/45. For each element three test cubes were cast, 100x100x100 mm. The compressive strength of these cubes was tested at the same time as the large scale tests were running. Self-Compacting Concrete (SCC) was used to cast the channels on top of the steel girders, in order to get composite action. Six test cubes were cast. Three of them were tested after 12 days, when the large scale tests started. The remaining cubes were tested after 28 days. Table 1 and Table 2 show the concrete recipe respectively the specification of the SCC properties, and the tested characteristics of the fresh SCC concrete. Table 3 shows the properties of the hardened concrete.

Table 1 Concrete mix recipe for the elements

***C35/45** (SS-EN 106-1 / SS1370003)*		
VCT	0.38	-
Cement	420	kg
Aggregate 0 - 4	412	kg
Aggregate 0 - 4 sand	412	kg
Aggregate 4 - 16	500	kg
Aggregate 4 - 16 crushed	500	kg
Sikament VS-1	0.9	% of powder
Air	4.0	%
Water	160	kg

Table 2 Specification of the SCC for the in-situ cast channels, and the measured properties.

***C35/45** SCC*	Specification	Measured properties
VCT	< 0.4 -	
Air	> 4.0 %	
t_{500}	3-4 sec	5.5 sec
slump flow	720±30 mm	620 mm

Table 3 Concrete properties – hardened concrete

	Cast date	Test date	Age [days]	δ [kg/m³]	P_c [kN]	$f_{c,cyl}$* [MPa]	P_{ct} [kN]	f_{ct}** [MPa]	E*** [GPa]
Element 1	2011-03-31	2011-06-13	74	2295	592	45.9	-	-	34.7
Element 2	2011-04-05	2011-06-13	69	2282	622	47.6	-	-	35.1
Element 3	2011-04-05	2011-06-13	69	2319	629	47.9	-	-	35.2
Element 4	2011-04-06	2011-06-13	68	2331	620	47.3	-	-	35.1
SCC-channel	2011-05-20	2011-06-17	28	2353	1224	42.0	-	-	33.8
SCC-channel	2011-05-20	2011-06-01	12	2359	1175	40.5	134	3.0	33.5

* = Calculated value according to Equation 1, Betonghandboken 11.11:10 [8]
** = Calculated value according to Equation 2, EN 1992-1-1 (3.3) [9]
*** = Calculated value according to Equation 3 (f_{cm} in MPa), EN 1992-1-1Table 3.1 [9]

$$f_{c,cyl} = f_{c,cube}(0.84 - 0.0012 \cdot f_{c,cube}) \quad (1)$$

$$f_{ct} = 0.9 \cdot 0.9 \cdot f_{ct,sp} \quad (2)$$

$$E = 22 \cdot (f_{cm,cyl}/10)^{0.3} \quad (3)$$

All elements were produced by a concrete workshop specialized on prefabricated elements. In order to assure the accuracy of fit in this kind of joints match-casting of the joints are necessary.The precision of the match-cast joints was measured with a feeler gauge before the channels were cast, and composite action achieved. In Figure 7, the results from the measurements are presented.

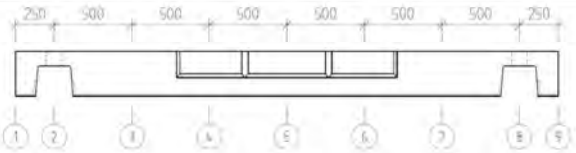

	[mm]	1	2	3	4	5	6	7	8	9
JOINT 1-2	TOP	0.60	0.50	0.50	0.50	0.40	0.40	0.50	0.50	0.50
	BOTTOM	0.25	-	>0.15	>0.15	>0.15	>0.15	>0.15	-	0.25
JOINT 2-3	TOP	0.40	0.40	0.40	0.50	0.40	0.40	0.40	0.40	0.40
	BOTTOM	0.25	-	>0.15	>0.15	>0.15	>0.15	>0.15	-	0.25
JOINT 3-4	TOP	0.25	0.25	0.25	0.20	0.25	0.25	0.20	0.30	0.30
	BOTTOM	0.25	-	>0.15	>0.15	>0.15	>0.15	>0.15	-	0.25

Figure 7 Results from feeler gauge measurements.

2.2 Test set-up

Throughout the paper, the x-axis is defined with its origin in the joint between element 2 and 3, and is defined as positive in the direction of increasing element numbers.

Test set-up no: 1

Figure 8 shows a schematic sketch of the load situation in the first test set-up, with an internal support at x = 0.000 m. Two things are of special interest under this load situation. Firstly, will the bridge girders behave as a composite section regarding deflections and stresses? Secondly, how much of the forces will enter the very short concrete slabs and how will they be distributed due to shear-lag?

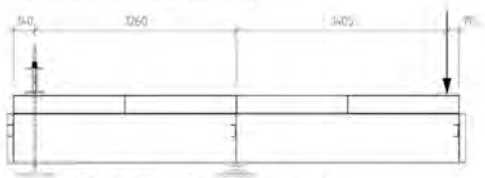

Figure 8 Illustration of test set-up no: 1

Test set-up no: 2

Figure 9 shows a schematic sketch of the second test set-up. This set-up was used to study whether or not a bridge of this kind behaves as an ordinary composite bridge in the field sections. It was also checked if the behaviour will change after a couple of large load cycles. This was done in order to find out if the irregularities in the dry joints will be smoothened by local concrete crushing, resulting in a better fit after a couple of large load cycles. Another thing that was studied was the shear-lag effect, in order to find out if a bridge of this type behaves as a conventional composite bridge, regarding to shear-lag in the field sections.

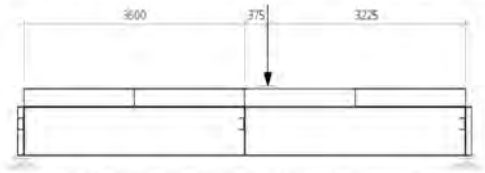

Figure 9 Schematic illustration of test set-up no: 2.

The load was applied in two different ways. First as a point load, 350x350 mm, acting in the centreline of the bridge, and then as two point loads acting straight above the steel girders. The latter was achieved by using a load distribution beam as shown in Figure 10.

The hydraulic jack that was used in all tests had a maximum capacity of 700 kN. During the static tests it was deformation controlled with a stroke rate of 0.02-0.03 mm/s during the loading sequence, and 0.05 mm/s during unloading. In the case of cyclic loading the jack was load controlled with a frequency of 0.0333 Hz.

Figure 10 Two point loads straight above the steel girders.

2.3 Measurement devices

During the tests 6 channels were used to measure the deflections and 9 channels were used for steel strain measurements. In total there were 51 channels measuring concrete strains, reinforcement strains, joint openings etc.

Deflections

Deflections were measured in the middle and at the end of the girders. The equipment used was six LVDT's (Linear Variable Differential Transformer), named LU1-LU6. The LVDT's were mounted vertically, and measured the deflection on top of the low stiffeners. Figure 11 shows a plan over the deflection measurements, and Figure 12 shows a picture of how the deflections were measured.

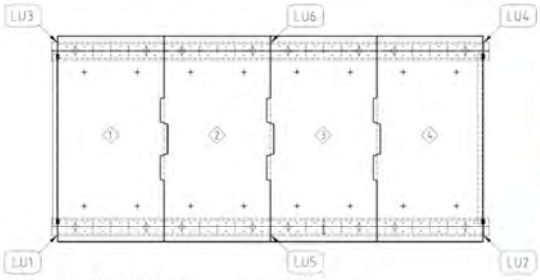

Figure 11 Deflection measurement plan

Figure 12 Picture of one LVDT

Steel strains

In order to study in which extent the concrete is interacting with the steel, nine strain gauges were attached to one of the steel girders. By measuring the steel strains in the top respectively the bottom of the web, the position of the neutral bending axis can be calculated and the area of interacting concrete can then be estimated. In order to get a third reference point, an extra strain gauge was used in the middle of the web. The strain gauges were all located over the length of Element 3. The position of the strain gauges is presented in Figure 13.

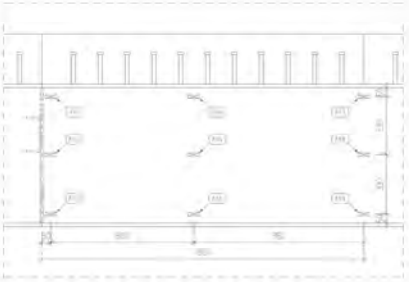

Figure 13 Installation scheme for the steel strain gauges

2.4 Test schedule

The test schedule is presented in Table 4 below.

Table 4 Test schedule

Test no:	*Type of load situation*	*Force*	*Number of cycles*
Test 1	Set-up 1 - one point load	100 kN	-
Test 2	Set-up 1 - one point load	280 kN	-
Test 3	Set-up 1 - two point loads	310 kN	-
Test 4	Set-up 1 - two point loads	430 kN	-
Test 5	Set-up 1 - two point loads	5-250 kN	50 cycles
Test 6	Set-up 1 - one point load	250 kN	-
Test 7	Set-up 1 - two point loads	400 kN	-
Test 8	Set-up 1 - two point loads	5-250 kN	50 cycles
Test 9	Set-up 2 - two point loads	500 kN	-
Test 10	Set-up 2 - two point loads	5-450 kN	100 cycles
Test 11	Set-up 2 - one point loads	300 kN	-
Test 12	Set-up 2 - one point loads	450 kN	-
Test 13	Set-up 2 - one point loads	5-400 kN	100 cycles

3. Results

In the sections below the results from the deflections measurements and the steel strain measurements are presented.

3.1 Deflections

The deflections that are presented are the deflections caused by pure bending, which means that the support settlements have been taken into consideration in the case of a simply supported beam, test set-up no:2 (Test 9-13). In test set-up no:1 (Test 1-8) the support settlements have been taken into consideration as well as the rotation due to the settlements in the negative support, see Equation 4 - 7.

$$LU2_{bend} = LU2 - LU5 + (LU1-LU5) \quad (4)$$

$$LU4_{bend} = LU4 - LU6 + (LU3-LU6) \quad (5)$$

$$LU5_{bend} = LU5 - (LU1 + LU2)/2 \quad (6)$$

$$LU6_{bend} = LU6 - (LU3 + LU4)/2 \quad (7)$$

The vertical deformations from Test 1-8, $LU2_{bend}$ and $LU4_{bend}$, are all plotted in the same load-deformation diagram see Figure 14. The vertical deformations from Test 9-13, $LU5_{bend}$ and $LU6_{bend}$, are shown in Figure 15.

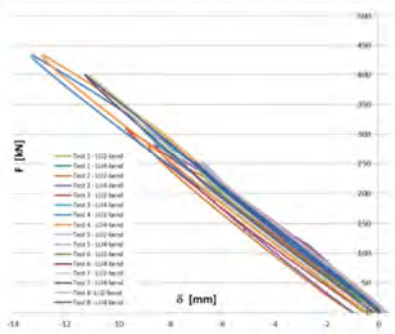

Figure 14 Load deformation diagram for test 1-8, $LU2_{bend}$ and $LU4_{bend}$.

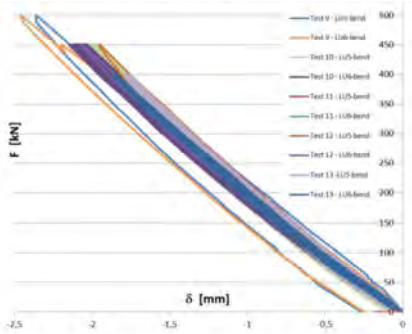

Figure 15 Load deformation diagram for test 9-13, $LU5_{bend}$ and $LU6_{bend}$.

3.2 Steel strains

The steel strains have been measured at three points in three sections. All strains have been transformed into stresses according to Hooke's law, assuming E_{steel} = 210 GPa.

$$\sigma = E \cdot \varepsilon \tag{8}$$

The first section is located 0.050 m from the internal support, which means 0.050 m from the joint between Element 2 and 3. The second section is located 0.850 m from the internal support, which means 0.050 m from the middle of Element 3. The third and last section is located 1.800 m from the internal support, which means right at the joint between Element 3 and 4. An illustration of the location of the steel strain gauges (FS1-9) is presented in Figure 13. The results from the measurements are summarised below by Figure 16 - Figure 21.

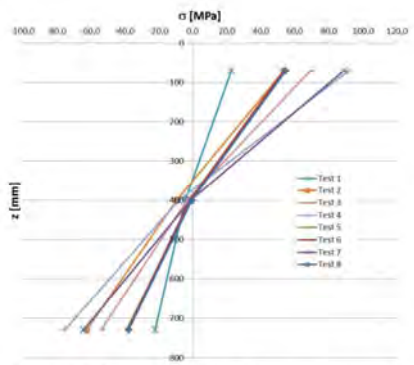

Figure 16 Longitudinal steel stresses measured in section x = 0.050 m, test set-up 1.

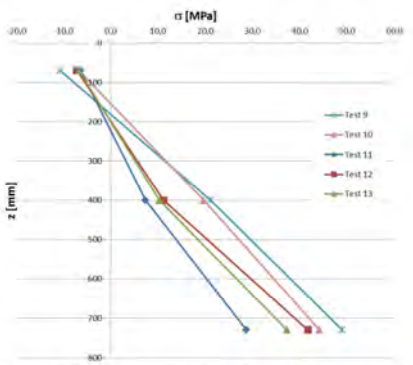

Figure 17 Longitudinal steel stresses measured in section x = 0.050 m, test set-up 2.

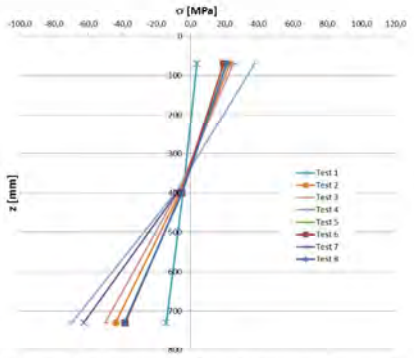

Figure 18 Longitudinal steel stresses measured in section x = 0.850 m, test set-up 1.

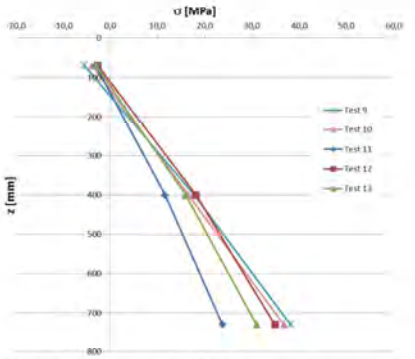

Figure 19 Longitudinal steel stresses measured in section x = 0.850 m, test set-up 2.

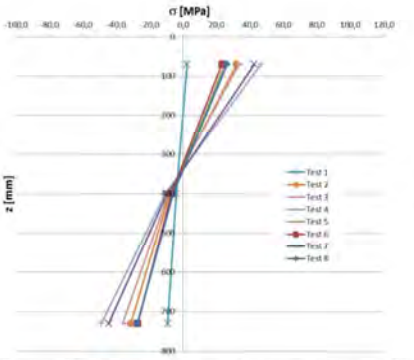

Figure 20 Longitudinal steel stresses measured in section x = 1.800 m, test set-up 1.

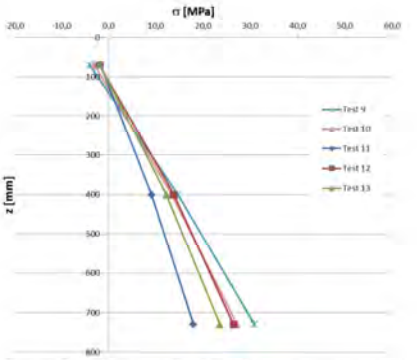

Figure 21 Longitudinal steel stresses measured in section x = 1.800 m, test set-up 2.

4. Analysis

In Sweden, the general way of performing global analyses on composite bridges is so far by using beam models. The analyses in this section have been made with focus on how the behaviour of this type of bridge section best can be described with ordinary beam models. Different design assumptions have been made, resulting in four different beam models. These models have also been compared to the test results. FE-analyses have also been made in order to see if more advance modelling agrees better with the test results.

In all models, the steel parts are modelled with E = 210 GPa, and the concrete elements are modelled with E = 35.0 GPa, which corresponds to the tested material parameters.

4.1 Design models

Beam models

The beam models have been developed in line with [9] and the general way to design composite bridges in Sweden. One of the questions raised is in which extent the concrete will interact with the steel. The test results have been compared to four different beam-models, with varying width of the interacting concrete, see Figure 22.

BM-1

In the first model, the beam is modelled as the steel cross-section only. This gives a reference value of how the bridges would behave if there was no interaction at all, between steel and concrete.

BM-2

The second model assumes that the concrete interacts with the steel over the full width of the deck, and that there are no joints in the deck. This gives a reference value of how the bridges would behave if the studied part is a conventional composite cross-section under negative bending moment, and with no shear-lag. Generally a field section.

BM-3

The third model includes the shear-lag in the concrete deck. The distance between the points of contra flexure for the bending moment, L_e, is the length of the test bridge for positive moments, and the distance between the outmost shear studs within one element, in case of negative bending moments. The latter gives a large reduction of the width of the interacting concrete.

BM-4

In this model only the in-situ cast concrete is taken into account.

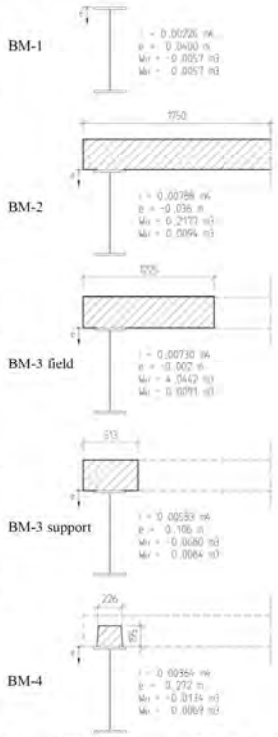

Figure 22 Illustration of the four beam models.

FE-models

All finite element calculations have been done in Autodesk Robot, and all materials are modelled as linear elastic. The steel and the concrete are modelled with shell elements. Rigid elements are used to model the eccentricity between the concrete deck slab and the top flange. The general model is presented in Figure 23 - Figure 24. FEM-1 is mainly interesting for test set-up 1 and FEM-2 and 3 are of interest for test set-up 2.

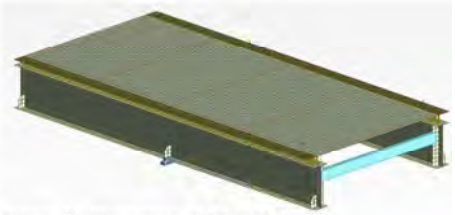

Figure 23 Illustration of FE-models.

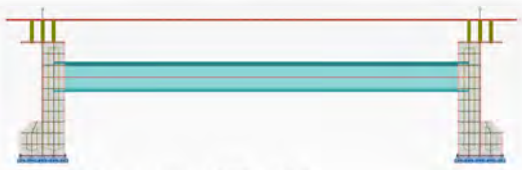

Figure 24 Cross-section of FE-models.

FEM-1
In this model, the concrete deck elements are modelled with no connections at all in the dry joints. The elements are allowed to deform independently freely in all. This model is mainly used to study the global behaviour at an internal support, and to calculate the steel stress distribution.

FEM-2
This model is similar to FEM-1, but the deck slab is modelled as one continuous slab without any joints, and is most interesting for test set-up 2. This is a model that should be equal to the case with an in-situ cast deck slab in compression.

FEM-3
FEM-3 is similar to FEM-2, but the joints are modelled non-linear with initial gaps of 0.4 mm, which close under the deflection. The initial gap width was chosen based on feeler gauge measurements. The in-situ cast channels are however modelled with no gap.

4.2 Deflections

The deflections are studied in order to find out in which extent the prefabricated concrete deck are influencing the stiffness, and in order to get a better understanding for how a bridge of this type should be modelled in a global analysis.

The measured deflections are compared to the calculated deflections according to the four beam models, and to the deflections achieved from the FE-models. The calculataed deflections for the beam models are results of the deflections caused by bending and support rotations, but also due to shear deformations in the web. For test set-up 1 and 2, this extra deformation is calculated according to Equation 9 and Figure 25.

$$\delta_{Shear} = L \cdot \frac{V}{A_w \cdot G} \tag{9}$$

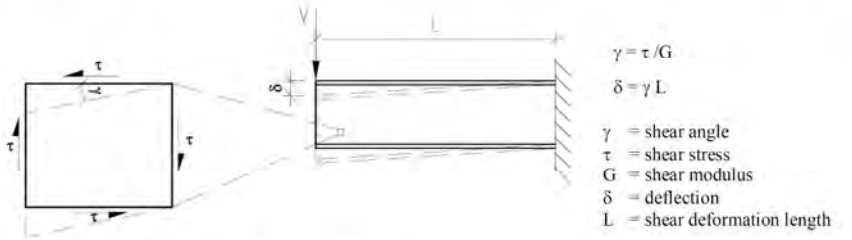

Figure 25 Shear deformation denominations.

The measured deflections were not truly elastic. In general, the results indicate a linear behaviour in the loading and unloading sequence, but a part of the deformation is remaining. Test 2 and test 6 are used to illustrate the differences in deflection during the first large load cycle in comparison to the deflections when a similar load is repeated, see Figure 26.

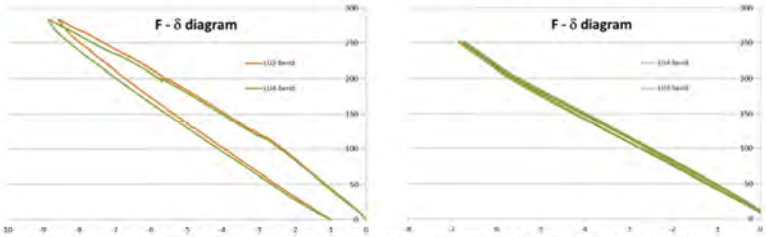

Figure 26 Load-deformation diagram for test 2 (left) and test 6 (right), $LU2_{bend}$ and $LU4_{bend}$.

Since the calculation models assume a concrete stiffness that corresponds to short term loading and a linear elastic behaviour, the elastic deformations are presented separately in Table 5 and Table 7.

Test set-up 1

Table 5 Test set-up 1, vertical deflections at x = 3,600 m, measured vs. calculated [mm].

	Load	LU2		LU4		BM-1	BM-2	BM-3	BM-4	FEM-1	FEM-2	FEM-3
	F [kN]	δ	δ_{el}	δ	δ_{el}	δ	δ	δ	δ	δ	δ	δ
Test 1	100	-2.7	-2.3	-2.5	-2.3	-3.1	-1.1	-1.7	-2.0	-2.6	-	-
Test 2	280	-8.8	-7.8	-8.6	-7.6	-8.8	-3.0	-4.7	-5.7	-7.3	-	-
Test 3	310	-9.7	-9.2	-9.1	-8.8	-9.7	-3.3	-5.2	-6.3	-8.1	-	-
Test 4	430	-13.3	-12.8	-12.9	-12.4	-13.5	-4.6	-7.2	-8.8	-11.2	-	-
Test 5	5-250	-7.0	-7.0	-7.1	-7.1	-7.9	-2.7	-4.2	-5.1	-6.5	-	-
Test 6	250	-7.1	-7.0	-6.9	-6.9	-7.9	-2.7	-4.2	-5.1	-6.5	-	-
Test 7	400	-11.1	-10.9	-11.3	-11.1	-12.6	-4.3	-6.7	-8.2	-10.4	-	-
Test 8	5-250	-7.3	-7.3	-7.1	-7.1	-7.9	-2.7	-4.2	-5.1	-6.5	-	-

The extra deflection caused by shear is included in the presented deflections for the beam models. The first test is excluded throughout the analysis due to large permanent deformations.

The first beam model, BM-1, gives the level of the maximum deflection that can occur, since it is based on the assumption of no composite action. The deflections predicted by BM-1 are all in the range of 7-15 % larger than the measured deflections.

The other beam models are all far too stiff, BM-2 and BM-3 predict deflections that are 40-65% smaller than the measured values. Even BM-4 is too stiff, although only the concrete channel is taken into account. In an ordinary composite bridge, this would be an indication that the concrete is cracked and should be replaced by the stiffness of the reinforced section. However, the measure concrete stresses were in this case very small, and there were no visual signs of cracking. In the comparison of the effective width, later in this paper, the interacting widths have been calculated for both concrete and reinforcement.

FEM-1 indicates a bit stiffer behaviour than the test results. The measured deflections are 3-10% larger than those predicted by the model.

The measured deflections are all very small since the specimen is very stiff. The longitudinal strains in the pre-stressed rebars that act as a negative support are almost of the same magnitude, resulting in a rotation of the whole specimen around the internal support. The measured deflections have therefore been separated in deflections caused by pure bending and

deflections caused by rotation. This mathematical operation, which is based on an assumption of linear behaviour along the girder, adds an extra source of error to the measured deflections.

Besides the comparison between the measured values and the different design models, the measured deflections have been used to calculate the corresponding moment of inertia and the theoretical interacting concrete width, $b_{eff,conc}$, assuming that the deck slab interact evenly over its thickness see Equation 10-11, Figure 27 and Table 6. The corresponding value has also been calculated for a cracked section, $b_{eff,reinf}$. However, the concrete stresses are low and no signs of cracking have been observed.

$$\delta_{bend} = \delta_{measured} - \delta_{shear} \tag{10}$$

$$I = -\frac{Fa^2 L_2}{4E\delta_{bend}} \cdot \left(1 - \frac{a}{3L_2}\right) - \frac{FaL_2 L_1}{6E\delta_{bend}} \tag{11}$$

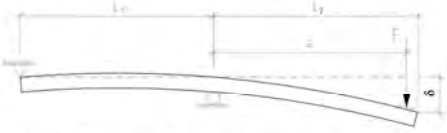

Figure 27 Schematic deformation figure and denominations for test set-up 1.

Table 6 Calculated moment of inertia and effective concrete width for test set-up 1.

	Test set-up	F [kN]	L_1 [m]	L_2 [m]	L [m]	a [m]	δ_{bend} [mm]	I_{calc} [m^4]	$b_{eff,conc}$ [mm]	$b_{eff,reinf}$ [mm]
Test 1	1	100	3.260	3.600	-	3.405	-2.1	**0.003204**	**74**	**-**
Test 2	1	280	3.260	3.600	-	3.405	-7.1	**0.002605**	**24**	**830**
Test 3	1	310	3.260	3.600	-	3.405	-8.3	**0.002466**	**14**	**480**
Test 4	1	430	3.260	3.600	-	3.405	-11.6	**0.002435**	**12**	**404**
Test 5	1	250	3.260	3.600	-	3.405	-6.5	**0.002528**	**19**	**634**
Test 6	1	250	3.260	3.600	-	3.405	-6.4	**0.002570**	**22**	**740**
Test 7	1	400	3.260	3.600	-	3.405	-10.0	**0.002622**	**26**	**875**
Test 8	1	250	3.260	3.600	-	3.405	-6.6	**0.002491**	**16**	**542**

Test set-up 2

Table 7 Test set-up 2, vertical deformations at x = 0,000 m, measured vs. calculated [mm].

	Load	LU5		LU6		BM-1	BM-2	BM-3	BM-4	FEM-1	FEM-2	FEM-3
	F [kN]	δ	δ_{el}	δ	δ_{el}	δ	δ	δ	δ	δ	δ	δ
Test 9	500	-2.4	-2.1	-2.5	-2.2	-4.7	-1.8	-1.9	-3.1	-	-1.6	-1.9
Test 10	5-450	-2.1	-2.0	-2.1	-2.1	-4.2	-1.6	-1.7	-2.8	-	-1.4	-1.8
Test 11	300	-1.4	-1.3	-1.4	-1.4	-2.8	-1.1	-1.1	-1.9	-	-0.9	-1.2
Test 12	450	-2.0	-1.9	-2.1	-2.1	-4.2	-1.6	-1.7	-2.8	-	-1.4	-1.7
Test 13	5-400	-1.8	-1.6	-1.9	-1.8	-3.7	-1.4	-1.5	-2.5	-	-1.2	-1.5

Among the studied beam models, the measured deflections are best described by BM-3. This gives deflections that are ~15% smaller than the measured values. However, the measured deflections are very small, which means that the influence of small gaps in the joints can be quite high. This effect is believed to decrease when the load and the deformations are increasing. FEM-3 is used to study how the gaps will influence the deflections.

FEM-2, which represents an in-situ cast slab with full interaction between steel and concrete, gives deflections that are ~20% smaller than the measured values. This indicates that the joints will decrease the overall stiffness, resulting in larger deformations. In FEM-3, the joints are modelled with small gaps. This means that the specimen must deflect before the deck elements are transferring longitudinal forces over the joints. When the joints are modelled with a gap width of 0.4 mm, the deflections in midspan will be 10-13 % smaller than the measured values.

It is obvious that the joints will influence the global stiffness. However, in the tests the percental influence of the joints is believed to be unproportionately big, since the allowed stresses in a real bridge are a lot higher. The stress levels in the bottom flanges, in test set-up 2, are always < 60 MPa. A gap will decrease the stiffness up to the point when it is closed, from that on the stress will be distributed over the composite section, even near the joints. Due to the rather low load, the influence from the joints gaps on the stiffness will be quite high.

The corresponding moment of inertia and the interacting concrete width, $b_{eff,conc}$, have been calculated for the measured deflections, Equation 12 and Figure 28.

$$I = -\frac{F(L-a)\cdot L^2}{96E\delta}\cdot\left(3-\frac{4(L-a)^2}{L^2}\right) \quad \text{for} \quad a \geq -\frac{L}{2} \tag{12}$$

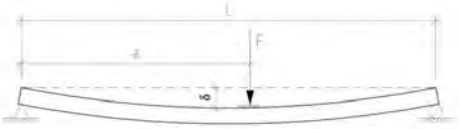

Figure 28 Schematic deformation figure and denominations for test set-up 2.

Table 8 Calculated moment of inertia and effective concrete width for test set-up 2.

	Test set-up	F [kN]	L_1 [m]	L_2 [m]	L [m]	a [m]	δ_{bend} [mm]	I_{calc} [m⁴]	$b_{eff,conc}$ [mm]
Test 9	2	500	-	-	7.200	3.975	-1.5	**0.005919**	**541**
Test 10	2	450	-	-	7.200	3.975	-1.5	**0.005552**	**437**
Test 11	2	300	-	-	7.200	3.975	-1.0	**0.005427**	**407**
Test 12	2	450	-	-	7.200	3.975	-1.4	**0.005730**	**485**
Test 13	2	400	-	-	7.200	3.975	-1.2	**0.005881**	**529**

The effective concrete width is about two times larger than the width of the concrete channel. This is actually almost the area that is derived if it is assumed that L_e is the distance between the outmost shear studs within an element, L_e = 1.5 m.

4.3 Steel stresses

When the measured steel stresses are compared to the design models, there is good agreement in some sections and worse in others.

Test set-up 1

One thing that can be noted is that the measured steel stress distribution is non-linear in the sections near the open joints. The linear stress distribution seems to be disturbed near the top of the steel girders. This is however quite expected, since a part of the stresses in the steel will enter and leave the concrete elements within a distance of 1.5 m. At the joints the steel section has to carry the whole load, and the forces that were carried by the concrete a few decimetres away will not be distributed over the whole section. The stresses will instead be concentrated around the upper flange, since they will starts to enter the concrete again after just 300 mm, which is the longitudinal distance between the neighbouring studs in two elements. This effect can be seen in Figure 16 - Figure 21 which present the measured stresses, and is also obvious in the results from the FE-analyses. Figure 29 presents the stress distribution, according to the FE-analyses, within the web plate for Test 4. The support, in x = 0.000 m, gives a disturbed stress state also in the bottom of the web. Section x = 1.800 m should give a more representative stress distribution for the general case near an open joint.

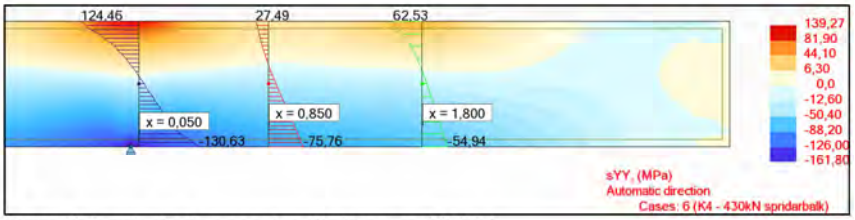

Figure 29 Longitudinal stresses in web-plates, test 4 FEM-1.

Figure 29 also shows that the neutral bending axis is only shifted slightly upwards in the middle of the element, indicating that the contribution to the stiffness from the concrete is very limited. This is in line with the result from the tests. In Figure 30 - Figure 32 the stresses in the web plate is plotted from z = 0.070 – 0.730 m, for Test 4, which means between the measured points, for all design models together with the measured values. The beam models fail to describe the stress distributions within the web, since they are all linear. However, BM-4 gives a rather good estimation of the stress distribution over the composite section.

The stresses predicted by FEM-1 are quite close to the measured stresses. The only section where the FE-model fails to describe the stress state is near the support. The FE-model indicates higher stresses near the bottom of the web, due to the singularity point at the support. In the reality load distribution steel plates (70x300x300 mm) are used at the supports, see Figure 33. These plates will probably interact with the bottom flange and decrease the longitudinal stresses locally, which can explain the lower stresses in the bottom of the web.

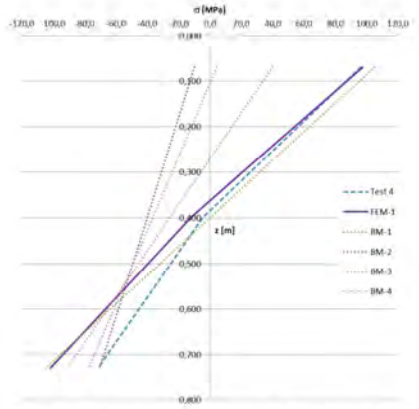

Figure 30 Longitudinal stresses in the web plate, x = 0.050 m, Test 4.

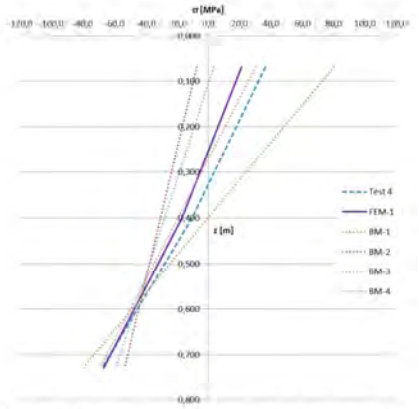

Figure 31 Longitudinal stresses in the web plate, x = 0.850 m, Test 4.

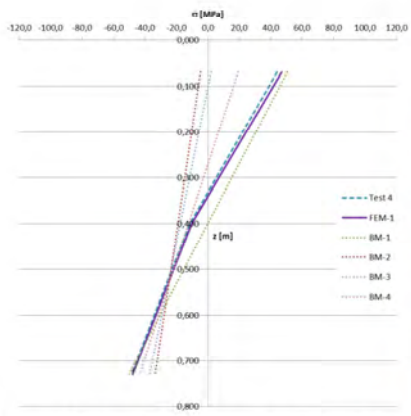

Figure 32 Longitudinal stresses in the web plate, x = 1.800 m, Test 4.

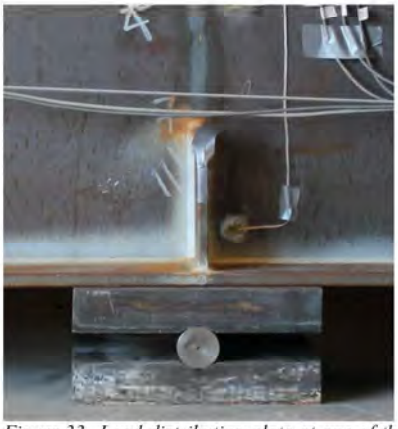

Figure 33 Load distributing plate at one of the supports.

The FE-results have also been used in order to estimate the effective width of the interacting concrete area in the middle between two joints. This has been done by assuming a linear strain distribution from the neutral bending axis and up to the centre of the concrete deck slab. This is a simplification, since it has been noted that the stress distribution is not perfectly linear. At a joint the interacting concrete area are zero, and the FE-model indicates that the effective width is increasing from the outmost row of studs to a maximum in the middle of an element.

If the steel stresses from the FE-model are extrapolated up to the centre of gravity for the concrete deck, then the interacting concrete area, $A_{int,conc}$, can be calculated according to Equation 13. The normal force in the deck slab is taken from the FE-analyses.

$$A_{int,conc.} = \frac{F_{conc}}{\frac{\sigma_{ff}}{n_0} \cdot \left(\frac{e_{neutral} - e_{conc}}{e_{neutral}} \right)} \qquad (13)$$

F_{conc} = normal force in the concrete
σ_{ff} = stress at the upper side of the steel top flange
$e_{neutral}$ = position of neutral bending axis*
e_{conc} = centre of gravity for concrete deck slab*
n_0 = short term modular ratio E_{steel}/E_{conc}
* = along the z-axis with the origin at the upper side of the steel top flange, positive downwards.

FEM-1 - Test 4

$$A_{int,conc.} = \frac{475 \cdot 10^3}{\frac{27.5 \cdot 10^6}{6.0} \cdot \left(\frac{0.270 + 0.145}{0.270} \right)} = 0.0674 \text{ m}^2 \text{ and } h_{conc} = 0.290 \text{ m} \Rightarrow b_{eff,conc} = 0.232 \text{ m}$$

The calculated effective concrete width is almost the same as the mean width of the concrete channels, 0.225 m. However, this calculation is based on the assumption that the longitudinal concrete stress is distributed over the full height of the concrete deck. The FE-model as well as the measurements indicates that the forces that enter the concrete are not distributed evenly over the section. The effective width should be even less, in order to take the uneven vertical distribution into consideration. And the mean value of the effective width over the length of an element will be ~100 mm, assuming a linear longitudinal distribution from the joints to the middle of an element.

Test set-up 2

Also in this case it is obvious that the interacting concrete area is strongly influenced by the joint gaps, see Figure 37 and Figure 38. FEM-3 is the model that comes closest to the measured values. It describes the measured stress state rather well in the first two sections, x = 0.050 and x = 0.850 m, but underestimates the influence from the concrete in section x = 1.800 m, see Figure 34 - Figure 36. It would be possible to adjust the gaps individually in the model, trying to get closer to the measured stress distribution. However, if the model is calibrated for a better description of the stress state, it will become a bit stiffer and then describe the deflections worse. To find the exact FE-model is a bit out of scope for this study, since the aim is to find a reasonable design model for this type of bridge, and a non-linear FE-model that simulates closing gaps is not the model that this study is looking for.

It can be noted that FEM-2 and BM-3 gives similar results, which indicates that the shear-lag model, in [9], works very well on an in-situ cast superstructure of this type. If the effective concrete width is calculated out of the FE-model, see Equation 13, it results in $b_{eff.conc}$ = 1.25 m. This can be compared to BM-3, which gives $b_{eff.conc}$ = 1.23 m

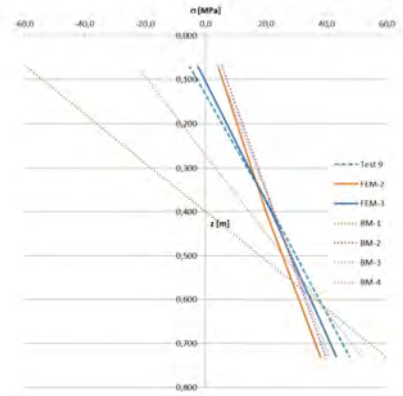

Figure 34 Longitudinal stresses in the web plate, x = 0.050 m, Test 9.

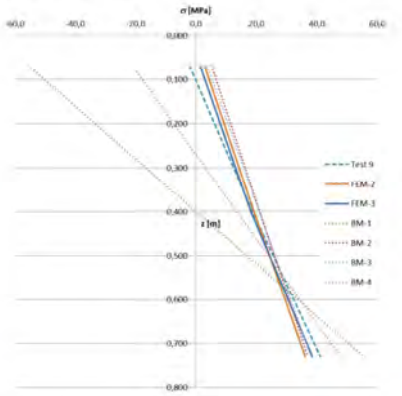

Figure 35 Longitudinal stresses in the web plate, x = 0.850 m, Test 9.

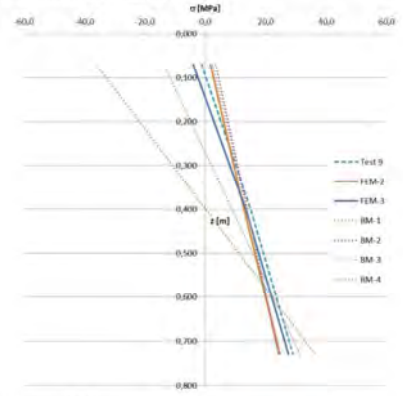

Figure 36 Longitudinal stresses in the web plate, x = 1.800 m, Test 9.

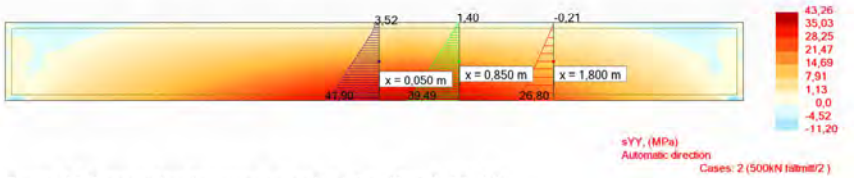

Figure 37 Longitudinal stresses in web-plates, Test 9 FEM-2.

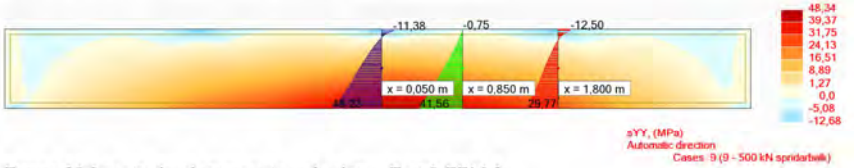

Figure 38 Longitudinal stresses in web-plates, Test 9 FEM-3.

In comparison to test set-up 1, the measured stress state is almost linear, especially in a section near the middle of an element, x = 0.850 m. A beam model can therefore be adjusted to fit the measured stress state quite good. In Table 9, the adapted interacting concrete widths are presented for section x = 0.850 m. Figure 39 and Figure 40 show the correspondence between the measured stresses and the adjusted beam model. In the cases with two point loads acting directly above the steel girders, Test 9 and 10, the correspondence are really good. In the case with a point load between the elements, Test 11 - 13, the stress distribution within the web are non-linear. In these cases, the beam model still describes the stress state pretty well.

Table 9 Effective concrete width for the beam model, adapted from the stress measurements.

	F [kN]	x = 0.050 m $b_{eff,conc}$ [mm]	x = 0.850 m $b_{eff,conc}$ [mm]	x = 1.800 m $b_{eff,conc}$ [mm]
Test 9	500	400	500	450
Test 10	450	380	450	450
Test 11	300	300	450	450
Test 12	450	320	480	450
Test 13	400	320	470	450

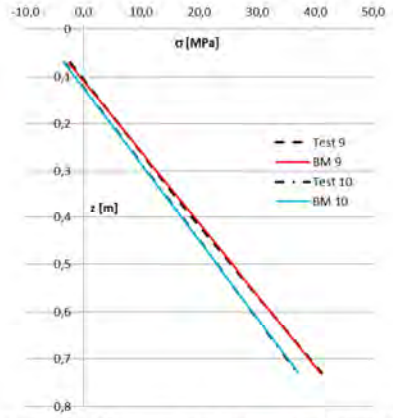

Figure 39 Measured steel stresses for Test 9-10 vs. adapted beam model, x = 0.850 m.

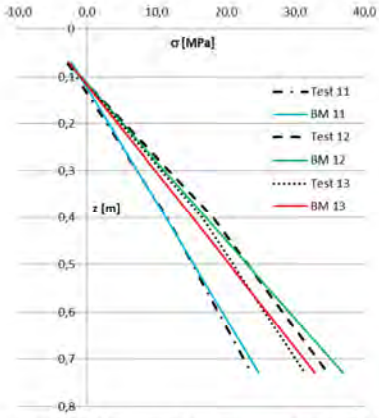

Figure 40 Measured steel stresses for Test 11-13 vs. adapted beam model, x = 0.850 m.

5. Discussion and conclusions

The deflections measured in both test set-ups indicate a lower stiffness than expected. In areas with negative bending moment, the effect of the interacting concrete seems to be negligible. In case of positive bending moments, the interacting concrete area is limited to a width that is about two times larger than the width of the concrete channel.

Based on the former observation, in the global analysis of a multi-span bridge of this type it would be reasonable to model the support areas with the stiffness of the steel-section only. This was also the suggested model before the tests were performed. The latter observation was more unexpected, since it indicates that the effective width of the compressed concrete is a lot smaller compared to an in-situ cast concrete deck. Single span bridges of this kind, have been designed with the assumption that the deck behaves as in-situ cast concrete. The results from these tests, together with results from field monitoring of a single span bridge indicate that this assumption should be revised, at least in the in the SLS and FLS, since the dry joints have a significant influence on the stiffness and the local stress distribution for moderate loads.

At the load levels used in the tests, the width of the interacting concrete is best described by assuming that L_e is equal to the maximum longitudinal distance of the shear studs within a single element (1.5 m). This observation is also supported by the test results from RWTH [11]. The suggested model for the global analysis is most suitable for SLS and FLS. It is reasonable to believe that the influence of the joint gaps will decrease under an increasing load. This has been validated by performing calculations with increasing loads in FEM-3, and also by test performed in Aachen by RWTH. These tests indicate that the composite section of a bridge of this type has an ultimate limit capacity in line with the capacity for a composite section, according to [10], with an in-situ cast deck slab. The tests in Aachen show that this is valid even for joint gaps as large as 5 mm. This should be compared to 0.4 mm gaps, which has been the allowed mean tolerance in the first three bridges, in Sweden, constructed with this type of deck. The results from these tests will be published in the final report from the RFCS-project ELEM, that will be available in the late 2012. [11]

The FE-models as well as the measured data indicates that the vertical stress distribution is non-linear, especially near an open joint. Stress concentrations can be expected in the top of the steel girder. This should be kept in mind, in the design of this kind for bridges especially in the case of fatigue loading. However, if the suggested methods below are followed the design should be on safe side.

The recommendations below are based on the available test data from only two different tests, by LTU and RWTH, and further tests can give grounds for a revision of the recommendations.

When the resistance of a cross-section is checked it is suggested to design the steel section to carry the whole load if the top fibre of the steel girder is in tension. For an in-situ cast section the resistance for the steel-section plus the longitudinal reinforcement is normally used. This is generally the case in areas with hogging moments. However, pre-stressing forces can be used to keep the deck in compression also in areas of hogging moments. If the top fibre of the steel girder is in compression, composite action can be assumed. It is however suggested that different effective concrete widths are used in SLS and ULS. In ULS it is reasonable to use the effective concrete width according to [10], which is used on continuous deck slabs, since the influence of the joint gaps will be reduced under an increasing load. The plastic capacity in these sections will not be affected by small initial joint gaps (< 0.5 mm). In SLS and FLS the effective concrete width should be reduced in comparison to [10]. It is suggested that the

distance between the points of contra flexure for the bending moment, L_e, is reduced to the distance between the outmost shear studs within one element.

Two possible reasons to why the interacting concrete area, in compression, is limited to an area about twice as wide as the concrete channel have been discussed. In the first reason, it is assumed that there are joint gaps that make the forces in the concrete to enter and leave the element within a length of the maximum distance between the shear studs within the element. This assumption gives results close to the measured values. The other explanation is that the in-situ cast channel and the concrete paste that leaks out and fills the joint gaps near the channel might make the initial gap more or less permanent outside this area. This part of the concrete will carry the total load until it is compressed up to the size of the gap, then the other concrete part will start to contribute to the load carrying capacity. None of these two explanations can be rejected by the test results.

References

[1] Hällmark, P. White, H. & Collin, P. (2012). Prefabricated Bridge Construction across Europe and America, *ASCE – Practice Periodical on Structural Design and Construction*, 2009, Vol. 17, no:3.

[2] Ralls et al. (2005) Prefabricated Bridge Elements and Systems in Japan and Europe, *FHWA Publication no: FHWA-PL-05-003*, pp 64, Office of Engineering, Bridge Division, Washington DC, USA.

[3] Gordon S & May I (2007) Precast deck systems for steel-concrete composite bridges, *Prodeedings of the ICE – Bridge Engineering*, *Vol* 160(1): 25-35.

[4] Collin, P., Johansson, B. & Pétursson, H. (1998). *Samverkansbroar med elementbyggda farbanor*. Technical Report. Swedish Institute of Steel Construction, Publication 165, 1998. ISBN: 91 7127 022 1 (in Swedish).

[5] Hällmark, R., Collin, P. & Stoltz, A., "Innovative Prefabricated Composite Bridges," *Structural Engineering International*, 2009, Vol. 19, no:1, pp. 69-78.

[6] Stoltz A (2001) *Effektivare samverkansbroar – Prefabricerade farbanor med torra fogar*, Licentiate Thesis 2001:41, Luleå, Sweden, pp 188 (in Swedish).

[7] Hällmark, P. Nilsson, M. & Collin, P. (2011). Concrete shear keys in prefabricated bridges with dry deck joints, *Nordic Concrete Research*, 2011, Vol. 22, no:2, pp 109-122.

[8] *Betonghandboken – Konstruktion / The Concrete Handbook* (1964), Svensk Byggtjänst, Stockholm.

[9] EN 1992-1-1. (2005), *Eurocode 2 – Design of concrete structures – Part 1-1: General rules and rules for buildings*, CEN, European Committee for Standardization, Brussels, Belgium.

[10] EN 1994-2. (2005), *Eurocode 4 – Design of composite steel and concrete structures – Part 2: General rules and rules for bridges*, CEN, European Committee for Standardization, Brussels, Belgium.

[11] Möller F, Hällmark R, Seidl G et al. (2012) *Final Report – ELEM - Composite Bridges with Prefabricated Decks*, RFSR-CT-2008-00039, Technical report No: 6.